THE CCRUSH STUDY:

CHARACTERIZATION OF COARSE AND FINE PARTICULATE MATTER IN

NORTHEASTERN COLORADO

by

NICHOLAS STEVEN CLEMENTS

B.S., University of Colorado at Boulder, 2009

M.S., University of Colorado at Boulder, 2010

A thesis submitted to the

Faculty of the Graduate School of the

University of Colorado in partial fulfillment

Of the requirement for the degree of

Doctor of Philosophy

Department of Mechanical Engineering

2013

This thesis entitled

The CCRUSH Study:

Characterization of Coarse and Fine Particulate Matter in Northeastern Colorado

written by Nicholas Steven Clements

has been approved for the Department of Mechanical Engineering

_____

Dr. Michael P. Hannigan, chair

_____

Dr. Shelly L. Miller, co-chair

Date: _____

The final copy of this thesis has been examined by the signatories, and we find that both the content and the form meet acceptable presentation standards of scholarly work in the above mentioned discipline.

ABSTRACT

Clements, Nicholas Steven (Ph.D., Mechanical Engineering)

THE CCRUSH STUDY: CHARACTERIZATION OF COARSE AND FINE PARTICULATE

MATTER IN NORTHEASTERN COLORADO

Thesis directed by Professors Michael P. Hannigan, Shelly L. Miller, and Jana B. Milford

Particulate matter in the troposphere adversely impacts human health when inhaled and alters climate through cloud formation processes and by absorbing/scattering light. Particles smaller than 2.5 μm in diameter (fine particulate matter; $PM_{2.5}$), are typically emitted from combustion-related sources and can form and grow through secondary processing in the atmosphere. Coarse particles ($PM_{10-2.5}$), ranging 2.5 to 10 μm, are typically generated through abrasive processes, such as erosion of road surfaces, entrained via resuspension, and settle quickly out of the atmosphere due to their large size. After deciding against regulating $PM_{10-2.5}$ in 2006 citing, among other reasons, mixed results from epidemiological studies of the pollutant and lack of knowledge on health impacts in rural areas, the United States Environmental Protection Agency (US EPA) funded a series of studies that investigated the ambient composition, toxicology, and epidemiology of $PM_{10-2.5}$. One such study, The Colorado Coarse Rural-Urban Sources and Health (CCRUSH) study, aimed to characterize the composition, sources, and health effects of $PM_{10-2.5}$ in semi-arid northeastern Colorado and consisted of two field campaigns and an epidemiological study. Summarized here are the results from the two field campaigns, the first of which included over three years of continuous $PM_{10-2.5}$ and $PM_{2.5}$ mass concentration monitoring at multiple sites in urban-Denver and rural-Greeley, Colorado. This data set was used to characterize the spatiotemporal variability of $PM_{10-2.5}$ and $PM_{2.5}$. During the second year of continuous monitoring, $PM_{10-2.5}$ and $PM_{2.5}$ filter samples were collected for compositional analyses that included: elemental composition, bulk elemental and

organic carbon concentrations, water-soluble organic carbon concentrations, UV-vis absorbance, fluorescence spectroscopy, and endotoxin content. Elemental composition was used to understand enrichment of trace elements in atmospheric particles and to identify sources via positive matrix factorization (PMF). The organic fraction of both particulate size ranges was explored with a variety of bulk characterization techniques commonly utilized in analysis of soil and aquatic natural organic matter. To date, the CCRUSH study is one of the largest research efforts devoted to understanding $PM_{10-2.5}$ and provides the US EPA with vital information that will be used in future policy making decisions regarding the regulation of this pollutant.

ACKNOWLEDGEMENTS

TABLE OF CONTENTS

LIST OF TABLES

LIST OF FIGURES

CHAPTER 1

INTRODUCTION

1.1 RESEARCH MOTIVATION

Atmospheric particulate matter adversely impacts human health through inhalation and deposition in the respiratory tract (Brunekreef and Forsberg, 2005). In their seminal paper on the effects of air pollution on mortality, Dockery et al. (1993) observed a strong linear trend between mortality and ambient concentrations of particles with aerodynamic diameters less than 2.5 μm. These fine particles, or $PM_{2.5}$, are generally emitted through combustion processes and undergo significant physical and chemical changes in the atmosphere including formation processes like nucleation, growth through condensation and coagulation, and oxidation. Atmospheric particulate mass distributions typically exhibit a peak between 0.1 and 1 μm, classified as the accumulation peak, which the $PM_{2.5}$ fraction includes (Seinfeld and Pandis, 2006).

Another peak in ambient particulate mass distributions is commonly observed between 2.5 and 10 μm, and is categorized as the coarse particulate mode. Coarse particulate matter, or $PM_{10-2.5}$, is thought to be derived primarily from abrasive processes, like vehicles grinding road materials, and is entrained into the atmosphere through resuspension (Harrison et al., 2012). $PM_{10-2.5}$ is commonly dominated by inorganic crustal material derived from geogenic and road dusts, though separation of the two source factors is difficult. Recent advances in isotopic ratio analysis and the use of ternary diagrams may improve our understanding of these two sources (e.g. Gueguen et al., 2012). Vehicular emissions of brake and tire wear are also commonly found in urban coarse mode aerosols (Pakbin et al., 2011; Amato et al., 2013). $PM_{10-2.5}$ and $PM_{2.5}$ contain bioaerosols that include bacteria, fungi, and pollen, but the contribution of bioaerosols to the mass of particles in the atmosphere is still under heavy investigation (Bowers

et al., 2013; Despres et al., 2012). $PM_{10-2.5}$ can also contain soil-related organic matter like leaf litter and humic substances (Edgerton et al., 2009; Cheung et al., 2012), but the coarse organic fraction has yet to be well characterized compositionally and source dynamics are still understudied. A recent study comparing modeled to measured concentrations of $PM_{10-2.5}$ in the western United States highlights the poor understanding of this pollutant; of 50 sites considered, mass concentration time series from all but one site were poorly captured and underestimated by the model (Li et al., 2013).

In the United States, the Environmental Protection Agency (EPA) maintains a list of National Ambient Air Quality Standards for six classes of air pollution harmful to the public health and environment including CO, lead, NO_2, O_3, particulate matter, and SO_2. Under the particulate matter classification, fine particulates and concentrations of particles less than 10 µm, or PM_{10} which includes both coarse and fine size fractions, are currently regulated (US EPA, 2013). In 2006, the EPA proposed to regulate $PM_{10-2.5}$ (US EPA, 2006a), though the proposal was rejected due in part to lack of consensus in the epidemiological literature about the public health impact of $PM_{10-2.5}$. In particular, the EPA cited lack of understanding of the health effects in rural areas as a limitation of the knowledge base at the time (US EPA, 2006b). Following the rejection of the proposed rule, the EPA funded multiple studies with a wide scope to broaden the scientific understanding of $PM_{10-2.5}$. Funded studies included field campaigns (e.g. Pakbin et al., 2011; Clements et al, 2012), toxicological studies (e.g. Brook et al. 2013), and an epidemiological campaign.

The Colorado Coarse Rural-Urban Sources and Health (CCRUSH) study was funded by the EPA and included two field campaigns aimed at collecting ambient mass concentration and composition data for understanding differences in urban and rural $PM_{10-2.5}$ and for use in an epidemiological study. The data generated by the CCRUSH study will provide valuable information to the EPA about future regulation and monitoring of $PM_{10-2.5}$.

1.2 THE COLORADO COARSE RURAL-URBAN SOURCES AND HEALTH STUDY

The CCRUSH study is composed of three main parts: (1) three years of continuous mass concentration monitoring at multiple sites in urban Denver and comparatively rural Greeley, Colorado, (2) a year of filter sample collection for compositional analysis, and (3) collection of public health data to be coupled with continuous mass concentrations in an epidemiological study. Results from parts 1 and 2 are included in this dissertation. Discussion of the epidemiological results is outside the scope of this dissertation. Four monitoring sites, two in Denver and two in Greeley, formed the core set of CCRUSH monitoring sites. Alsup Elementary (ALS) was a traffic-influenced urban site located in Commerce City, a suburb northeast of Denver. Edison Elementary (EDI) was an urban residential site east of downtown Denver. CCRUSH study monitoring sites in Greeley were located at Maplewood Elementary and McAuliffe Elementary, schools located near the town center and in the suburban fringe, respectively. At each CCRUSH site, a dichotomous (simultaneous $PM_{10-2.5}$ and $PM_{2.5}$ collection) continuous mass concentration monitor and a dichotomous filter sampler were placed on site rooftops. Continuous sampling began in January 2009 and continued through April 2012, and filter sampling took place from February 2010 to March 2011. Continuous mass concentration data were used to understand spatial and temporal patterns of $PM_{10-2.5}$ and $PM_{2.5}$. Filter samples were used in a suite of compositional analyses including: elemental composition, bulk organic carbon characterization, and endotoxin content. The following five chapters detail the results from these two field campaigns.

1.3 THESIS ORGANIZATION

The next five chapters of this dissertation are manuscripts at various stages of submission, review, and publication. Chapters 2, 3, and 4 detail the results from the continuous monitoring portion of the CCRUSH study. Chapters 2 and 4 characterize the spatiotemporal trends observed in $PM_{10-2.5}$ and $PM_{2.5}$ concentrations and explore how meteorological parameters drive temporal variability. In Chapter 3, errors introduced when using collocated PM_{10} and $PM_{2.5}$ monitors to estimate $PM_{10-2.5}$ through subtraction are assessed for monitors with and without correction for semivolatile losses. Chapters 5 and 6 discuss the composition and source analyses produced from the filter sampling campaign. Chapter 5 details the elemental composition analysis and inorganic source identification. Chapter 6 explores the organic fraction of $PM_{10-2.5}$ and $PM_{2.5}$ using techniques commonly used to understand bulk properties of complex mixtures of organic matter in aquatic and soil environments. Chapter 7 summarizes the CCRUSH study results and suggests future research directions. Chapter 2 is currently published (Clements et al., 2012) and Chapters 3 and 5 are in the midst of the review process. Chapters 4 and 6 have yet to be submitted to a peer-reviewed research publication and should be considered drafts of manuscripts that are we plan to be submitted for peer review.

The following five chapters were produced in collaboration with a many other scientists and students and as such I was not the sole contributor to the contents there within. Coauthors are listed at the beginning of each chapter. My role in the study included maintaining continuous monitors, managing filter collection, and performing much of the data analysis. Ricardo Piedrahita performed much of the data analysis for Chapter 2, including the nonparametric regression analysis, and Prof. Jana Milford, Jenny Eav, and Mingjie Xie were integral in data analysis and sour ce apportionment of the elemental composition data included in Chapter 5.

1.4 REFERENCES

Amato, F., Shaap, M., Denier van der Gon, H.A.C., Pandolfi, M., Alastuey, A., Keuken, M., Querol, X. 2013. Short-term variability of mineral dust, metals and carbon emission from road dust resuspension. Atmospheric Environment 74, 134-140.

Bowers, R.M., Clements, N., Emerson, J.B., Wiedinmyer, C., Hannigan, M.P., Fierer, N. 2013. Seasonal Variability in Bacterial and Fungal Diversity of the Near-Surface Atmosphere. Environmental Science and Technology. Advanced online publication.

Brook, R.D., Bard, R.L., Kaplan, M.J., Yalavarthi, S., Morishita, M., Dvonch, J.T., Wang, L., Yang, H.-Y., Spino, C., Mukherjee, B., Oral, E.A., Sun, Q., Brook, J.R., Harkema, J., Rajagopalan, S. 2013. The effect of acute exposures to coarse particulate matter air pollution in a rural location on circulating endothelial progenitor cells: results from a randomized controlled study. Inhalation Toxicology 25(10), 587-592.

Brunekreef, B., Forsberg, B. 2005. Epidemiological evidence of effects of coarse airborne particles on health. European Respiratory Jounral 26, 309-318.

Cheung, K., Olson, M.R., Shelton, B., Schauer, J.J., Sioutas, C. 2012. Seasonal and spatial variations of individual organic compounds of coarse particulate matter in the Los Angeles Basin. Atmospheric Environment 59, 1-10.

Clements, N., Piedrahita, R., Ortega, J., Peel, J.L., Hannigan, M.P., Miller, S.L., Milford, J.B. 2012. Characterization and Nonparametric Regression of Rural and Urban Coarse Particulate Matter Mass Concentrations in Northeastern Colorado. Aerosol Science and Technology 46(1), 108-123.

Despres, V.R., Huffman, J.A., Burrows, S.M., Hoose, C., Safatov, A.S., Buryak, G., Frohlich-Nowoisky, J., Elbert, W., Andreae, M.O., Poschl, U., Jaenicke, R. 2012. Primary biological aerosol particles in the atmosphere: a review. Tellus B 64, 15598.

Dockery, D.W., Pope, A. III, Xu, X., Spengler, J.D., Ware, J.H., Fay, M.E., Ferris, B.G. Jr.,
Speizer, F.E. 1993. An Association between Air Pollution and Mortality in Six U.S. Cities.
The New England Journal of Medicine 329(24), 1753-1759.

Edgerton, E.S., Casuccio, G.S., Saylor, R.D., Lersch, T.L., Hartsell, B.E., Jansen, J.J., Hansen,
D.A. 2009. Measurements of OC and EC in Coarse Particulate Matter in the
Southeastern United States. Journal of the Air and Waste Management Association 59,
78-90.

Gueguen, F., Stille, P., Dietze, V., Giere, R. 2012. Chemical and isotopic properties and origin
of coarse airborne particles collected by passive samples in industrial, urban, and rural
environments. Atmospheric Environment 62, 631-645.

Harrison, R.M., Jones, A.M., Gietl, J., Yin, J., Green, D.C. 2012. Estimation of the Contributions
of Brake Dust, Tire Wear, and Resuspension to Nonexhaust Traffic Particles Derived
from Atmospheric Measurements. Environmental Science and Technology 46, 6523-
6529.

Li, R., Wiedinmyer, C., Baker, K.R., Hannigan, M.P. 2013. Characterization of coarse particulate
matter in the western United States: a comparison between observation and modeling.
Atmospheric Chemistry and Physics 13, 1311-1327.

Pakbin, P., Ning, Z., Shafer, M.M., Schauer, J.J., Sioutas, C. 2011. Seasonal and Spatial
Coarse Particle Elemental Concentrations in the Los Angeles Area. Aerosol Science and
Technology 45(8), 949-963.

Seinfeld, J.H., Spyros, P.N., 2006. Atmospheric Chemistry and Physics - From Air Pollution to
Climate Change, 2nd Edition, John Wily & Sons.

US EPA. 2006. 40 CFR Parts 53 and 58: Revisions to Ambient Air Monitoring Regulations;
Proposed Rule. Federal Register, Vol. 71, No. 10, Part III.

US EPA. 2006. 40 CFR Part 50: National Ambient Air Quality Standards for Particulate Matter,
Vol. 71 No. 200.

U.S. EPA. 2013. National Ambient Air Quality Standards (NAAQS).

http://www.epa.gov/air/criteria.html. Accessed November 4, 2013.

CHAPTER 2

CHARACTERIZATION AND NONPARAMETRIC REGRESSION OF RURAL AND URBAN

COARSE PARTICULATE MATTER MASS CONCENTRATIONS IN NORTHEASTERN

COLORADO

Nicholas Clements[a], Ricardo Piedrahita[a], John Ortega[b], Jennifer L. Peel[c], Michael P. Hannigan[a], Shelly L. Miller[a], Jana B. Milford[a]

[a]Department of Mechanical Engineering, College of Engineering and Applied Science, University of Colorado at Boulder, Boulder, CO, 80309-0427

[b]Atmospheric Chemistry Division, National Center of Atmospheric Research, Boulder, CO, 80301

[c]Department of Environmental and Radiological Health Sciences, Colorado State University, Fort Collins, CO, 80523

2.0 ABSTRACT

The Colorado Coarse Rural Urban Sources and Health study (CCRUSH) is an ongoing study of the relationship between coarse particulate mass concentrations ($PM_{10-2.5}$, particulate matter with diameter between 2.5 and 10µm) and selected health effects. For two urban monitoring sites in Denver, CO and two comparatively rural sites in Greeley, CO, hourly mass concentrations of $PM_{10-2.5}$ and fine particulate matter ($PM_{2.5}$, diameter less than 2.5 µm) are being measured using dichotomous tapered element oscillating microbalances (TEOMs) with Filter Dynamics Measurement Systems (FDMS). This paper presents air quality results from just over a year of $PM_{2.5}$ and $PM_{10-2.5}$ measurements. Average $PM_{2.5}$ concentrations ranged from 7.7 to 9.2 µg m^{-3} across the four sites, with higher concentrations in Denver than Greeley. Average $PM_{10-2.5}$ concentrations ranged from 9.0 to 15.5 µg m^{-3}, with the highest values at the site in northeast Denver. Temporal variability in $PM_{10-2.5}$ was higher than that in $PM_{2.5}$ concentrations at all four sites. The two Greeley sites displayed moderate spatial correlation for $PM_{2.5}$ and high correlation for $PM_{10-2.5}$, whereas the two Denver sites showed lower spatial correlation for both PM sizes. $PM_{10-2.5}$ concentrations in Denver were highest with winds from the direction of the city's urban core. $PM_{10-2.5}$ concentrations in Greeley were moderately elevated with winds from the southwest to the northwest, coming from Denver and other large Front Range communities. Wind speed regressions for $PM_{10-2.5}$ at the Denver sites primarily exhibited resuspension effects, while $PM_{10-2.5}$ concentrations in Greeley showed relatively complex wind speed dependence.

2.1 INTRODUCTION

Coarse particulate matter in the size range from 2.5 to 10 microns ($PM_{10-2.5}$) is believed to be important for human health because particles in this size range are capable of penetrating to the thoracic region of the lungs when inhaled (Chan and Lippmann, 1980). Size resolved and chemically speciated data indicate that compared to particulate matter less than 2.5 microns in diameter ($PM_{2.5}$), $PM_{10-2.5}$ is more likely to contain crustal elements such as aluminum, iron, and calcium, but may also contain ions, transition metals, organic and biological material (e.g., Milford and Davidson, 1985; 1987; Boreson, et al., 2004; Hueglin et al., 2005). $PM_{10-2.5}$ is commonly derived from abrasive mechanical processes, including construction and agricultural activities, resuspended road dust, vegetative debris, and sea spray (Patterson and Gillette, 1977; Duce et al, 1976), with emissions from many of these processes depending strongly on wind speed (Harrison et al., 2001). $PM_{10-2.5}$ is also produced from incomplete combustion of solid fuels such as coal and biomass (U.S. EPA, 1995).

Brunekreef and Forsberg (2005) reviewed nearly 60 studies that evaluated health effects of short-term exposure to $PM_{10-2.5}$ and concluded that for some endpoints, including chronic obstructive pulmonary disease, asthma, and respiratory admissions, $PM_{10-2.5}$ could have as strong or a stronger effect than $PM_{2.5}$. Short-term increases in $PM_{10-2.5}$ have also been positively associated with mortality in several studies (e.g., Castillejos et al., 2000; Mar et al., 2000; Ostro et al., 2000; Villeneuve et al., 2003; Zanobetti and Schwartz, 2009). In a recent review of studies of the health effects associated with short-term exposure to ambient $PM_{10-2.5}$, the U.S. Environmental Protection Agency (EPA) concluded that existing evidence is suggestive of a causal relationship between exposures and mortality, cardiovascular effects, and respiratory effects (U.S. EPA, 2009). EPA also recognized several critical uncertainties in epidemiology studies of $PM_{10-2.5}$ impacts, including relatively high exposure error compared to $PM_{2.5}$, due to greater expected spatial variability in $PM_{10-2.5}$ concentrations, and limitations in characterization

of spatial distributions. Many epidemiologic studies published to date have used differences between PM_{10} and $PM_{2.5}$ concentrations measured at co-located monitors and in some cases monitors located at different sites within the same county to estimate $PM_{10-2.5}$, which contributes further uncertainty in exposure estimation. Furthermore, epidemiologic studies of $PM_{10-2.5}$ have mostly focused on urban areas, where large populations result in greater power for detecting statistically significant effects. Because sources of $PM_{10-2.5}$ may be different in urban compared to rural regions, the associations with health effects may also be different in smaller communities or rural areas.

Because of their size, coarse particles are removed from the atmosphere more quickly than fine particles. As a consequence of both deposition velocity and the intermittent nature of many source processes, concentrations of $PM_{10-2.5}$ are expected to be more spatially and temporally variable than $PM_{2.5}$ concentrations. Wilson et al. (2005) reviewed prior studies and found that reported correlation coefficients between sites within several cities ranged from 0.14 – 0.60 for 24-h average $PM_{10-2.5}$ concentrations; these values are generally lower than those observed for $PM_{2.5}$ or PM_{10}. Chen et al. (2007) found an average correlation coefficient of 0.75 between 24-h average $PM_{10-2.5}$ concentrations measured on about 70 days at a central monitor in Chapel Hill, NC and monitors placed at residences within about a 60 km radius. With a year of weekly monitoring at 10 sites across the Los Angeles basin, Pakbin et al. (2010) found pair-wise correlations ranging from 0.04 for 24-h average $PM_{10-2.5}$ concentrations from an industrial site in Long Beach and concentrations at two suburban monitors located about 30 and 70 km away, to 0.80 for $PM_{10-2.5}$ concentrations at a pair of coastal sites located within a few kilometers of each other.

Most studies of seasonal variability in $PM_{10-2.5}$ concentrations have observed the highest concentrations in summer, but exceptions occur due to specific source activity patterns (Thornburg et al., 2009; Pakbin et al., 2010). Harrison et al. (2001) measured $PM_{10-2.5}$ continuously at five sites in England over a three-year period. They observed higher $PM_{10-2.5}$

concentrations on weekdays than on weekends, and found the fraction of PM_{10} contributed by $PM_{10-2.5}$ was highest in the spring and summer. Moore et al. (2010) reported correlation coefficients of 0.1 – 0.4 for continuous hourly $PM_{10-2.5}$ concentrations measured at three sites across the Los Angeles basin. In their study, the most pronounced diurnal variation in $PM_{10-2.5}$ concentrations was observed at a site near Riverside, CA, with less diurnal variability in concentrations measured near downtown Los Angeles and at a desert location about 110 km NW of downtown. Daytime or evening maxima were observed at all three locations.

This paper presents just over a year of mass concentration data from continuous $PM_{10-2.5}$ and $PM_{2.5}$ sampling conducted in Denver and Greeley, Colorado, as part of the Colorado Coarse Rural Urban Sources and Health (CCRUSH) study. CCRUSH is a multi-year study of the relationship between $PM_{10-2.5}$ mass concentrations and adverse health effects, including cardiopulmonary emergency department visits and adverse birth outcomes. Denver and Greeley were selected for the study to allow comparison of the composition and relative health effects of coarse PM in urban and rural communities. For two sites in Denver and two sites in Greeley, continuous hourly mass concentrations of $PM_{10-2.5}$ and $PM_{2.5}$ were measured using dichotomous tapered element oscillating microbalances (TEOMs). Sampling began in January 2009 and will continue for three years. At the end of the sampling period, the mass concentration data will be analyzed with local data on birth outcomes and emergency department visits to assess and compare associations between the two communities.

This paper examines spatial and temporal variations in hourly and 24-h average concentration values for $PM_{10-2.5}$ and $PM_{2.5}$. The paper also examines the influence of hourly wind speed and wind direction on the mass concentrations. Nonparametric regression (NPR; Henry et al., 2002, 2009; Yu et al., 2004; Kim and Hopke, 2004) was used to characterize the wind speed and wind direction relationships, and help understand differences in mass concentrations across sampling locations.

2.2 METHODS

2.2.1 Sampling Locations

 Continuous particulate mass concentrations were measured at two locations in Denver and two in Greeley, CO. Greeley has a population of 92,625 (U.S. Census, 2009b) and an area of 77.7 km^2, and is located within Weld County. Weld County has a population of 254,759 (U.S. Census, 2009a) and an area of 10,417 km^2. Agriculture and oil and gas extraction are among the county's leading economic activities. In contrast, the City and County of Denver has a population of 610,345 (U.S. Census, 2009c) and an area of 401.3 km^2, with a highly mixed economy (the urban area of Denver-Aurora has a population of 1.98 million and an area of 1291.9 km^2). 'Urban area' above is defined as consisting of core census block groups or blocks that have a population density of at least 1000 people per square mile (386 people/km^2) and surrounding census blocks that have an overall density of at least 500 people per square mile (193 people/km^2; US Census, 2000). Denver is transected by major interstate highways and experiences much greater traffic volumes than Greeley. Correspondingly, $PM_{10-2.5}$ concentrations in Denver are expected to be dominated by resuspended urban road dust, while agricultural activities (e.g., feedlots, soil preparation, and ditch burning) are expected to be relatively important sources in Greeley.

 Monitors were located on the roofs of two elementary schools in Denver: Alsup and Edison, which are 11.1 km apart. Monitors were located in Greeley on the roof of Maplewood elementary school and in the HVAC system enclosure at McAuliffe elementary school. The two Greeley schools are 4.5 km apart. The city of Greeley is roughly 80 km northeast of Denver. Table 2.1 includes site descriptions, sampling periods, and completeness statistics for the CCRUSH data sets considered.

Table 2.1 Monitoring site descriptions, sampling periods, and completeness statistics for the CCRUSH Study

Monitoring Site (Abbreviation)	Edison (EDI)	Alsup (ALS)	Maplewood (MAP)	McAuliffe (MCA)
Coordinates	39.76 N, 105.04 W	39.83 N, 104.94 W	40.42 N, 104.71 W	40.43 N, 104.77 W
Elevation (m)	1584	1560	1433	1454
Inlet Height (m)	9	6	9	10.5
Location Description	Urban-Residential	Industrial-Residential	Residential	Residential
Start Date/Time	1/8/2009 12:00	1/16/2009 15:00	1/16/2009 18:00	1/1/2009 3:00
End Date/Time	1/8/2010 10:00	2/5/2010 15:00	10/16/2009 16:00	6/19/2009 10:00
Number of Hourly Observations	8759	9241	6551	4064
PM$_{2.5}$ No. Usable Hourly Samples (% completeness)	7182 (82.0%)	8050 (87.1%)	5550 (84.7%)	3963 (97.5%)
PM$_{10-2.5}$ No. Usable Hourly Samples (% completeness)	7182 (82.0%)	7910 (85.6%)	5550 (84.7%)	3963 (97.5%)

2.2.2 Particulate Matter Monitoring Methods

Tapered element oscillating microbalance (TEOM), model 1405-DF (ThermoFisher Scientific, Waltham, MA), ambient PM monitors were located at each site. Three monitors (Alsup, Edison, and Maplewood) were located outside on roofs and housed in enclosures (Complete Outdoor Enclosure for TEOM Series 1405, ThermoFisher Scientific, Waltham, MA) designed to maintain appropriate instrument conditions. At extreme high and low ambient temperatures the enclosures failed to maintain appropriate instrument operating conditions, which resulted in data removal. The monitor located at McAuliffe was located just below the roof in a HVAC system crawl space and was equipped with an in-house designed foam

enclosure equipped with a commercial air conditioner/heater unit set to maintain a temperature of 21.1°C.

The TEOM 1405-DF is equipped with a Filter Dynamic Measurement System (FDMS) to correct for semi-volatile species evaporation from mass measurement filter surfaces. After a 16.7 lpm PM_{10} impactor inlet removes particles larger than 10 μm from the sample stream, a round-nozzle virtual impactor is used to separate the $PM_{2.5}$ and $PM_{10-2.5}$ size fractions into dual measurement channels. Virtual impactors separate size fractions using particle inertia similar to a traditional inertial impactor. By replacing the impaction surface with a vertical collection probe with a low flow rate, virtual impactors separate larger particles that have sufficient inertia to impact the "virtual surface" of the cross-section of the collection probe inlet. Flow through the collection probe is referred to as the minor flow. The major flow, containing small particles, diverts away from the collection probe and has a collection efficiency that is less than unity due to a fraction of the smaller particles penetrating into the collection probe. This fraction is defined by the ratio of minor to inlet flow rates. Virtual impactor design and flow characteristics are described in detail elsewhere (Loo and Cork, 1988; Marple and Chien, 1980). The TEOM 1405-DF uses a 2.5 μm cutpoint virtual impactor with inlet, major ($PM_{2.5}$), and minor ($PM_{10-2.5}$) volumetric flow rates of 16.7, 15, and 1.67 lpm, respectively. Mass concentration corrections for penetration of $PM_{2.5}$ mass into the $PM_{10-2.5}$ channel are described in the data processing section below. The mass measurements are made by dual vertical oscillating tapered glass elements, one for each PM channel, with Pallflex TX-40 TEOM filters placed on the ends. Particulate mass is deposited as aerosol passes through the filter, which changes the natural oscillating frequency of the tapered glass element. The frequency change is related to filter mass change by simple vibration theory. The ambient mass concentrations are calculated by the change in mass and volumetric air flow rates.

With the FDMS system, the instrument operates by sampling in two modes that alternate every six minutes. In the "Base" measurement mode, the sample stream is held at 30°C, with

15

the aerosol passing directly to the mass measurement filter. The effect of water is reduced in the TEOM 1405-DF by the use of a Nafion™ membrane diffusion dryer in each particulate channel. In the Base mode, mass can be either lost or gained from the filter, depending on the amount of semi-volatile material present. In the "Reference" mode, after the dryer, the sample is diverted through the cooled FDMS filter, a 47mm Pallflex TX-40 filter held at $4^{o}C$. This filter removes particles and semi-volatile material that will condense at $4^{o}C$ or below. This filtered air stream is then directed through the TEOM filter and the mass change on the filter recorded. Reference mode values are commonly negative due to mass loss from the TEOM filter, but adsorption or absorption of organic gases may also occur, resulting in mass gain (Green et al., 2009). The mass change during the Reference mode due to evaporation and gas-phase sampling artifacts is assumed to be equal to the artifact contribution to the mass change that occurred during the previous Base measurement. The time series of Reference mass concentrations are thus subtracted from the Base measurements, correcting for sampling artifacts and approximating the true aerosol mass concentration. This provides a total mass concentration for each 12-minute time step, with the first 6 minutes providing the Base and the second 6 minutes the Reference concentration. The instruments were operated at flow rates prescribed by the manufacturer: 1.67 lpm ($PM_{10-2.5}$), 3 lpm ($PM_{2.5}$), and 12 lpm (bypass). For this study, TEOMs were set up to record the raw mass concentration data (Base and Reference) for the $PM_{2.5}$ and $PM_{10-2.5}$ channels, along with ambient temperature, relative humidity, and various instrument conditions, at 6 minute intervals. Raw mass concentration data are not smoothed by between-measurement averaging for unmeasured channels and do not include a correction for the penetration of $PM_{2.5}$ mass into the $PM_{10-2.5}$ channel from the virtual impactor separation. This correction was made during subsequent data processing. Flow control was set to active and actual flow rates were used to calculate mass concentrations.

TEOM instrument maintenance was performed monthly at each site and consists of changing TEOM and FDMS filters; cleaning the PM_{10} inlet, virtual impactor, and FDMS valve;

16

checking for seal leaks in the mass transducer, FDMS valve and FDMS filter holder; flow audit and calibration; and an instrument leak check. Operators ensured the instrument was operating properly before leaving the site. Other regular maintenance was performed as needed and included exchanging Nafion diffusion dryers, pump maintenance, and replacing mass transducer, FDMS valve and FDMS filter holder seals. Ball valves were installed between the virtual impactor and diffusion dryers to increase ease of access to sample lines for flow audits, which were performed at a higher frequency than prescribed by the manufacturer. A single external filter on the bypass flow line was used to extend pump life.

To assure the highest quality data were used for analysis, extensive quality assurance protocols were developed. Upon arriving at a monitoring site, an instrument status log, maintenance log, comment log, and flow audit/leak check log were completed. The status log was filled out before and after maintenance to assure the instrument conditions did not change due to operator intervention. The TEOM data were downloaded manually each month prior to instrument maintenance. The discrete section of data from the last site visit to the current visit was downloaded via the available USB port on the front of the instrument. This process closed the previous section of data before the operator interfered with instrument operation. Using the ePort software provided by Thermo Scientific, the entire TEOM database was also downloaded. Data were transferred from a field laptop or flash drive to a desktop computer immediately upon arriving back at the University of Colorado.

Discrete data sections downloaded via USB flash drive were processed by a code developed in-house. Log files for each data section were created that specified data filenames, whether maintenance occurred, whether to output hourly averages, saved data interval, number of hours to remove after maintenance occurred, and number of hours to shift the time stamp into Mountain Standard Time (MST). Rows were flagged as missing data if the status code reported the following errors: power failure, database failure, FDMS valve failure, mass transducer failures, any channel flow deviating from the set flow rate (lpm) by more by than 10%, either

17

channel reading filter loading above 90%, or heater tube temperatures (°C) deviating from set temperature by more than 2%. Instrument problems were flagged as well and included: vacuum pressures above 40.5 kPa, cooler temperatures deviating more than $0.5^{\circ}C$ from the specified set point, or if channel relative humidity was above 98%. Data corresponding to instrument problem flags were inspected manually.

Equations 1 – 3 were applied to the 6-minute mass concentration data to correct for $PM_{2.5}$ mass depositing in the $PM_{10\text{-}2.5}$ channel due to the virtual impactor. In the following equations, Q represents the volumetric flow rate through the indicated channel. PM represents the mass concentration, with the $TEOM$ label indicating raw TEOM data. It was assumed that both Base and Reference channels followed the same correction, i.e., that semi-volatile mass loss was proportional to the amount of total mass in each channel.

$$\frac{Q_{PM\,10-2.5}}{Q_{Total}} = \frac{1.67lpm}{16.67lpm} = 0.1$$

(1)

$$PM_{10-2.5Base} = PM_{10-2.5Base}(TEOM) - \frac{Q_{PM\,10-2.5}}{Q_{Total}}\left(PM_{2.5Base}(TEOM)\right)$$

(2)

$$PM_{10-2.5Ref} = PM_{10-2.5Ref}(TEOM) - \frac{Q_{PM\,10-2.5}}{Q_{Total}}\left(PM_{2.5Ref}(TEOM)\right)$$

(3)

The hourly average and standard error (i.e., the standard deviation divided by the square root of the number of measurements in the hour) of all downloaded variables were calculated and exported, excluding data flagged as missing. Logs used to process data were accessed to compile full data sets, filling in missing sections of data between discrete data sets with missing data flags or combining same-hour measurements with a weighted average based on the number of measurements made in that hour in each separate data set. Three scenarios were identified that required further data processing: major events of mass loss from filter surfaces, instances of highly variable noise due to temperature aliasing from rapid or oscillating changes of enclosure temperature or other sources, or instances of elevated standard error when a non-

removal status code had been triggered. The mass loss incidents were identified if the calculated mass concentration was less than the 1st percentile of the time series and the standard error of the measurement was above the 95th percentile. Incidents of induced highly variable noise were identified if the calculated concentration was below the 1st percentile and the subsequent measurement was greater than the 99th percentile or vice versa. The third scenario was triggered when a non-zero status code was recorded and the calculated hourly mass concentration standard error was above the 95th percentile. Each occurrence of one of these three scenarios was assessed manually to determine if data should be removed for final hourly average data sets. Data were then filtered for hours with less than 75% completeness. Daily averages were calculated from cleaned hourly average data sets; days missing more than 75% of completed hours were also removed.

The data set reported in this paper has been labeled Phase 1, and results from cutting off the currently validated results when instruments were updated to a new version of the TEOM 1405-DF firmware. This update required exchanging a physical flash card; after the update instrument settings were unintentionally reset to defaults. The start and end dates and completeness statistics for each site's Phase 1 data are listed in Table 2.1. Sampling began on different dates at each site, and completeness varies by site based on instrument maintenance issues.

The TEOM 1405-DF is a relatively new instrument and correspondingly posed numerous challenges in our effort to produce continuous time series of mass concentration data. Through collaboration with Thermo Scientific, solutions were found for most problems, but they nonetheless led to substantial gaps in our time series. Denver and Greeley experience significant seasonal temperature variations. The air heating and cooling systems incorporated into the Thermo Scientific TEOM 1405-DF enclosures were unable to adequately condition the space within the enclosures when ambient temperatures were very high or low. Numerous measurements from midday throughout the summer were suspect and hence flagged for

19

removal due to large hourly variability associated with increased TEOM mass transducer temperatures. This high measurement variability mostly originated in the Reference channel, where hourly standard errors sometimes exceeded 500 µg m^{-3}. Cold temperature extremes were less of an issue, though the operating temperatures of the FDMS systems occasionally dropped below 4°C. These changes in FDMS operating temperature were not accompanied by significant increases in variability of mass concentration measurements, so corresponding data were not removed. A further problem with the HVAC systems occurred at Alsup and Maplewood, where insulation near the blowers peeled off and either shredded or blocked the blowers.

Malfunction of the Nafion dryer assemblies and pumps also lead to gaps in the time series. Dryer assemblies had to be replaced every 7-10 months and the pumps rebuilt every 12 months, in each case about six months earlier than the manufacturer's maintenance recommendations. Premature pump failure may be partly due to low ambient atmospheric pressures in Colorado, which are typically about 85.1 kPa. In addition, the bypass flow controller of the TEOM installed at McAuliffe failed when the inlet system did not adequately dispose of water vapor in the bypass line, resulting in condensation when the air was cooled in the enclosure.

Finally, a significant gap in the McAuliffe dataset occurred due to seal leaks within the FDMS valve system that were not detected through the leak check process. The problem was only identified upon later inspection of the data. In response, we modified our monthly maintenance protocol to include disassembling the FDMS valve to verify that no seals failed, and to process and examine data on-site to verify the absence of leaks.

2.2.3 Meteorological Data

To assist with analysis of PM mass concentration data, hourly meteorological data (temperature, RH, wind speed and direction) were obtained from stations located at or near

each of the monitoring sites. Mass concentration data from Edison were related to meteorological data from the Carriage site (39.75 N, 105.03 W), located 1.65 km to the southeast and operated by the CDPHE. Meteorological data for Alsup was collected from a CDPHE-operated meteorological station co-located with our instrument. Meteorological data for Greeley were obtained from the National Oceanic and Atmospheric Administration's (NOAA) Weld County Airport station (40.26 N, 104.38 W), located 6.7 km west and 10.9 km west of Maplewood and McAuliffe monitoring sites, respectively Wind roses of data used for site-specific wind speed and direction regressions from Carriage, Alsup, and the Weld County Airport are shown in the Supplemental Information (Figures 2.S1-4). Vector averaged wind speed was used in the data analyses.

2.2.4 Data Analysis and Nonparametric Regression

The results section presents standard descriptive statistics for $PM_{2.5}$ and $PM_{10-2.5}$ mass concentrations, along with the coefficient of divergence (COD), which is a measure of uniformity. Results of nonparametric regression of concentrations versus wind speed and direction are also presented. All data analyses used concentration data that were error code filtered. No negative data filtering or replacement was performed in any of the analyses, except when calculating the COD.

The coefficient of divergence (Wilson et al., 2005) for a set of measurements, *X*, is defined by:

$$COD = \sqrt{\frac{1}{n}\sum_{i=1}^{n}\left(\frac{X_{ij} - X_{ih}}{X_{ij} + X_{ih}}\right)^2}$$

(4)

where *i* is the sample, and *j* and *h* index different measurement sites. A COD value near 0 represents perfect uniformity, and a value of 1 represents total heterogeneity. The COD loses

meaning when negative values are included, so in calculating this statistic negative values in the dataset were replaced with zeros.

The data set used in the NPR was different than that used in the other analyses, as it required wind data and mass concentrations for each hour, both of which had missing data. Additionally, any data point with a corresponding wind speed value below 1m s^{-1} was excluded from the NPR analysis. Exclusion of these periods with relatively calm winds sharply reduced the number of observations used in the NPR analyses compared to the full sets of hourly mass concentration data.

Nonparametric regression was used to estimate the expected concentration C_i from each wind direction or wind speed i by including all observations using weighting kernels, giving less weight to observations far from the point at which the estimate is being calculated and vice-versa. The Gaussian kernel:

$$K_1(x) = (2\pi)^{-\frac{1}{2}} e^{(-0.5x^2)}, \quad -\infty < x < \infty, \quad x = \frac{\theta - W_i}{\Delta\theta}$$

(5)

was used for the wind direction regressions and the Epanechnikov kernel:

$$K_2(x) = 0.75(1 - x^2), \quad -1 < x < 1$$

(6)

was used for wind speed regressions (Henry et al., 2002). In the kernels, θ is the wind direction or speed for which the estimate is made, W_i is the wind speed or wind direction value at time i, and $\Delta\theta$ is the smoothing parameter. The concentration $C(\theta)$ at a given wind speed or direction is then estimated by the Nadaraya-Watson estimator, defined as:

$$C(\theta) = \frac{\sum_{i=1}^{n} K\left(\frac{\theta - W_i}{\Delta\theta}\right) C_i}{\sum_{i=1}^{n} K\left(\frac{\theta - W_i}{\Delta\theta}\right)}$$

(7)

where K references the appropriate kernel. In this work, the optimal value of the smoothing parameter was found for each data set and meteorological variable by cross validation.

22

Smoothing parameters were then averaged over all sites for each size fraction and meteorological variable, to allow for more direct comparison of the results. The resulting smoothing parameters are 23.13 degrees for $PM_{2.5}$ with wind direction; 10.88 degrees for $PM_{10-2.5}$ with wind direction; 0.55 m s^{-1} for $PM_{2.5}$ with wind speed; and 1.2 m s^{-1} for $PM_{10-2.5}$ with wind speed. Ninety-five percent confidence intervals of the regression estimates were calculated as described in Henry et al. (2002).

2.2.5 Comparison with Other PM Datasets

As part of this study, comparisons were made to $PM_{2.5}$ and $PM_{10-2.5}$ data from other studies and locations. These comparisons are complicated by the use of different instruments and measurement methods. Federal reference methods (FRMs) and federal equivalence methods (FEMs) for PM have been discussed previously (U.S. EPA, 2004; 2009). The FRM for $PM_{10-2.5}$ is calculated as the numeric difference between concurrent and co-located PM_{10} and $PM_{2.5}$ concentrations as measured by FRM low-volume filter samplers of the same make and model (U.S. EPA, 2009). The TEOM 1400AB and 1405 have been designated as FEM methods for PM_{10}. The TEOM 1405-DF has been designated as an FEM method for $PM_{2.5}$, but not (to date) as an FEM for $PM_{10-2.5}$ (U.S. EPA, 2010).

As described above, the TEOM 1405-DF has been designed to minimize sampling artifacts, both positive and negative. Positive artifacts are a result of excess mass collection typically caused by gas-phase adsorption onto the collection media. Negative artifacts are a result of reduced mass collection typically caused by semi-volatile species that were in the particle phase but shift to the gas-phase after collection due to collection temperatures that are higher than ambient or pressures that are slightly less than ambient. For example, when $PM_{2.5}$ concentrations were measured by a pair of TEOMs, one operated at 50°C and the other operated at 30°C, the TEOM held at a higher temperature yielded consistently lower concentrations, as at the higher temperature the sensor collected less semi-volatile and

condensable mass (Zhu et al., 2006; Grover et al., 2005). The TEOM 1405-DF operates at 30°C and also utilizes an FDMS which adjusts for filter adsorption artifacts. Results from previous studies generally show that for $PM_{2.5}$, the TEOM FDMS measures higher concentrations compared to the FRM, especially as the ambient temperature increases (Grover et al., 2005; Schwab et al., 2006; Zhu et al., 2006) as the FRM does not adjust for adsorption artifacts (Solomon and Sioutas, 2008). In the end, it is important to remember that comparison across studies that have used different measurement techniques will have slight biases associated with the technique differences. Thus, the $PM_{10-2.5}$ data discussed below should be viewed as only roughly comparable across studies.

2.3 RESULTS AND DISCUSSION

2.3.1 Summary Statistics and Spatial Trends

Table 2.2 presents summary statistics for the 24-h average $PM_{2.5}$ and $PM_{10-2.5}$ concentrations measured at the four study sites. Average $PM_{2.5}$ concentrations ranged from 7.7 to 9.2 µg m^{-3} across the four sites. Average concentrations of $PM_{2.5}$ were somewhat higher at the two Denver sites than at the two sites in Greeley. Average $PM_{10-2.5}$ concentrations ranged from 9.0 to 15.5 µg m^{-3}. $PM_{10-2.5}$ concentrations were sharply higher at the Alsup site in northeast Denver than at the other three locations. Temporal variability in $PM_{10-2.5}$ concentrations was higher than that in $PM_{2.5}$ concentrations, with COV values for 24-h average $PM_{10-2.5}$ ranging from 0.6 to 0.8 and those for $PM_{2.5}$ all near 0.5. Across the four sites, 95th percentile 24-h average concentrations ranged from 14.7 to 17.9 µg m^{-3} for $PM_{2.5}$ and from 18.9 to 36.0 µg m^{-3} for $PM_{10-2.5}$.

Table 2.2 Summary Statistics for 24-h Average $PM_{2.5}$ and $PM_{10-2.5}$ Concentrations

$PM_{2.5}$	Edison	Alsup	Maplewood	McAuliffe
N (days)	299	328	211	158
Mean (µg m^{-3})	8.7	9.2	7.7	8.6
Median (µg m^{-3})	7.6	8.2	7.0	7.8
St. Dev. (µg m^{-3})	4.6	4.7	3.8	4.0
COV	0.5	0.5	0.5	0.5
5th % (µg m^{-3})	2.8	4.0	3.3	4.3
95th % (µg m^{-3})	17.9	17.7	14.7	15.0
COD				
Edison	0.00	0.21	0.27	0.23
Alsup	-	0.00	0.24	0.17
Maplewood	-	-	0.00	0.13
McAuliffe	-	-	-	0.00
Pearson's R				
Edison	1.00	0.64	0.35	0.44
Alsup	-	1.00	0.48	0.60
Maplewood	-	-	1.00	0.82
McAuliffe	-	-	-	1.00

Table 2.2 (*continued*) Summary Statistics for 24-h Average $PM_{2.5}$ and $PM_{10-2.5}$ Concentrations

$PM_{10-2.5}$	Edison	Alsup	Maplewood	McAuliffe
N (days)	299	323	211	158
Mean ($\mu g\ m^{-3}$)	9.0	15.5	9.6	9.8
Median ($\mu g\ m^{-3}$)	8.0	13.3	8.2	7.7
St. Dev. ($\mu g\ m^{-3}$)	5.4	11.4	7.7	7.8
COV	0.6	0.7	0.8	0.8
5th % ($\mu g\ m^{-3}$)	2.1	1.7	1.5	1.5
95th % ($\mu g\ m^{-3}$)	18.9	36.0	21.4	24.6
COD				
Edison	0.00	0.30	0.25	0.23
Alsup	-	0.00	0.31	0.31
Maplewood	-	-	0.00	0.15
McAuliffe	-	-	-	0.00
Pearson's R				
Edison	1.00	0.70	0.69	0.72
Alsup	-	1.00	0.66	0.68
Maplewood	-	-	1.00	0.97
McAuliffe	-	-	-	1.00

The two Greeley sites, which are separated by a distance of 4.5 km, had the highest spatial correlation for 24-h average concentrations of both $PM_{2.5}$ and $PM_{10-2.5}$, with Pearson's R values of 0.82 for $PM_{2.5}$ and 0.97 for $PM_{10-2.5}$. Concentrations measured at the two Denver sites, separated by a distance of 11.1 km, showed lower correlation. For the Denver sites the Pearson's R values were 0.64 for $PM_{2.5}$ and 0.70 for $PM_{10-2.5}$. The COD was calculated among all site pairs. The pair of Greeley sites displayed the most homogeneous 24-h average $PM_{2.5}$ and $PM_{10-2.5}$ concentrations (COD=0.13 for $PM_{2.5}$ and 0.15 for $PM_{10-2.5}$), while the pair of Edison and Alsup was somewhat more heterogeneous (COD=0.21 for $PM_{2.5}$ and 0.30 for $PM_{10-2.5}$). The heterogeneity of $PM_{10-2.5}$ concentrations in Denver is influenced by the relatively high concentrations at Alsup. A point source close to Alsup appears to contribute to the elevated concentrations seen there, as discussed below in the Nonparametric Regression Results section.

The finding of lower correlation and higher COD values for $PM_{2.5}$ and $PM_{10-2.5}$ in Denver than in Greeley is consistent with expectations, as the Denver monitors are separated by a

greater distance and are located in more sharply contrasting neighborhoods. The finding of higher correlation for $PM_{10-2.5}$ than for $PM_{2.5}$ in both communities is unexpected, as prior studies have generally observed the opposite. The relatively low correlations for $PM_{2.5}$ found in our study may be partly due to noise in the $PM_{2.5}$ channel. In comparison, the $PM_{10-2.5}$ channel is quite stable.

2.3.2 Temporal Patterns

Table 2.3 compares median concentrations of $PM_{2.5}$ and $PM_{10-2.5}$ between weekends and weekdays at each site, as well as between day (6 am – 6 pm) and night (6 pm – 6 am). Significance of differences was assessed using the Kruskal-Wallis test. For $PM_{2.5}$, weekend concentrations were higher than weekday concentrations at all four sites, though the difference is not statistically significant at Edison and Alsup. This result was surprising, as traffic and industrial activity leading to emissions of $PM_{2.5}$ and its precursors are expected to be higher on weekdays than weekends. In contrast to the current study, the Denver Aerosol Sources and Health study (DASH; Vedal et al., 2009), which performed daily $PM_{2.5}$ filter sampling for 4.5 years at Palmer Elementary School in Denver, found a significantly higher weekday median (7.1 µg m^{-3}) than weekend median (6.5 µg m^{-3}) (unpublished statistics). We do not yet have an explanation for the discrepancy.

In contrast to $PM_{2.5}$, concentrations of $PM_{10-2.5}$ followed the expected pattern, with weekday concentrations found to be uniformly significantly higher than weekend concentrations. Likewise, Harrison et al. (2001) reported higher $PM_{10-2.5}$ concentrations on weekdays than weekends for two sites in London and across all seasons. As Table 2.3 also shows, daytime concentrations of $PM_{2.5}$ were higher than nighttime concentrations at Edison and McAuliffe, whereas the opposite was true for Alsup. Maplewood shows no statistically significant difference between day and night concentrations, though the nighttime median is slightly larger. Daytime

27

concentrations of $PM_{10-2.5}$ were significantly higher than nighttime concentrations at all four sampling sites. The diurnal patterns underlying these results are discussed below.

Table 2.3 Comparison of Median 1-h Average Concentrations by Weekday/Weekend and Day/Night

$PM_{2.5}$	Edison	Alsup	Maplewood	McAuliffe
Weekday ($\mu g\ m^{-3}$)	6.28	7.67	6.48	6.75
Weekend ($\mu g\ m^{-3}$)	6.73	7.71	7.29	7.13
p-value	0.051	0.284	0.001*	0.014*
Day ($\mu g\ m^{-3}$)	6.63	7.48	6.79	7.47
Night ($\mu g\ m^{-3}$)	5.88	7.83	6.99	6.59
p-value	0.001*	0.011*	0.701	0.000*
$PM_{10-2.5}$	Edison	Alsup	Maplewood	McAuliffe
Weekday ($\mu g\ m^{-3}$)	8.26	11.77	6.24	6.31
Weekend ($\mu g\ m^{-3}$)	5.68	7.30	4.95	4.19
p-value	0.000*	0.000*	0.000*	0.000*
Day ($\mu g\ m^{-3}$)	8.32	12.03	6.87	6.86
Night ($\mu g\ m^{-3}$)	5.24	8.66	5.19	4.79
p-value	0.000*	0.000*	0.000*	0.000*

* Statistically significant at the 0.05 level

Figure 2.1 shows median hourly concentrations of $PM_{2.5}$ and $PM_{10-2.5}$ for each monitoring location. Across all four locations, median hourly average concentrations of $PM_{2.5}$ were less variable as a function of time of day than median $PM_{10-2.5}$ concentrations. $PM_{2.5}$ concentrations at all sites generally increased in the morning from about 6 am to 10 am, decreased during the afternoon, and then increased again in the evening. Relatively high $PM_{2.5}$ concentrations in the morning hours are likely due to temperature inversions in addition to source activity. The Alsup

28

site showed the strongest peak in $PM_{2.5}$ concentrations. This peak occurred at 7 am, slightly earlier than the morning peaks at the other sites.

$PM_{10\text{-}2.5}$ concentrations at Alsup peaked at about 8 am and then declined until about 2 am. For both $PM_{2.5}$ and $PM_{10\text{-}2.5}$, the relatively pronounced morning peaks at Alsup appear to reflect the influence of relatively heavy industrial activity and traffic at this particular location. At Edison, $PM_{10\text{-}2.5}$ concentrations peak at 11 am and then decline relatively steadily until 4 am. The $PM_{10\text{-}2.5}$ concentrations at the two Greeley sites were higher during the daytime hours than at night, but do not exhibit the afternoon decrease seen for $PM_{10\text{-}2.5}$ in Denver and for $PM_{2.5}$ at all locations. This suggests the strength of $PM_{10\text{-}2.5}$ sources affecting the Greeley monitors increases in the afternoon, roughly compensating for the enhanced dilution that occurs as the mixing layer grows. The finding that $PM_{10\text{-}2.5}$ exhibits relatively strong diurnal variability compared to $PM_{2.5}$ is consistent with the shorter residence time of $PM_{10\text{-}2.5}$ in the atmosphere. Harrison et al. (2001) and Moore et al. (2010) similarly found elevated $PM_{10\text{-}2.5}$ concentrations during daytime hours, at monitoring sites in London and the Los Angeles area, respectively.

Figure 2.1 Median mass concentrations ($\mu g\ m^{-3}$) by time of day at the four monitoring sites for (a) $PM_{2.5}$ and (b) $PM_{10\text{-}2.5}$
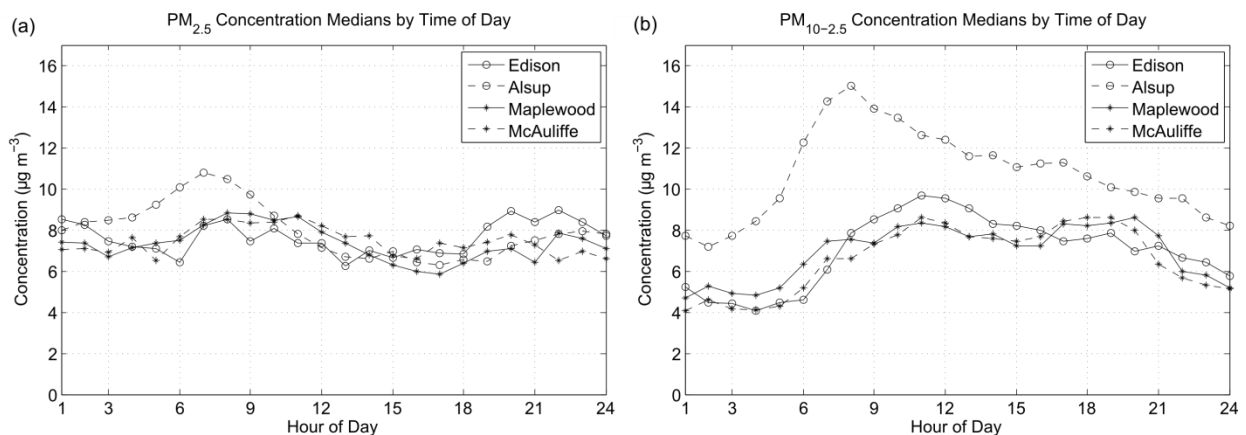
Figure 2.2 shows that the median concentrations of $PM_{2.5}$ and $PM_{10-2.5}$ plotted by month. In each size regime, the four sites showed similar monthly patterns. $PM_{2.5}$ concentrations showed relatively little monthly variation compared to concentrations of $PM_{10-2.5}$. The highest median concentrations of $PM_{10-2.5}$ were measured during July, August and September as well as select winter months. This is consistent with the expectation that $PM_{10-2.5}$ is partly derived from resuspension processes that are enhanced under dry and windy conditions. Additional seasonal analysis will be performed when the three-year time series of concentrations is complete.

Figure 2.2 Monthly median mass concentrations (μg m^{-3}) at the four monitoring sites for (a) $PM_{2.5}$ and (b) $PM_{10-2.5}$
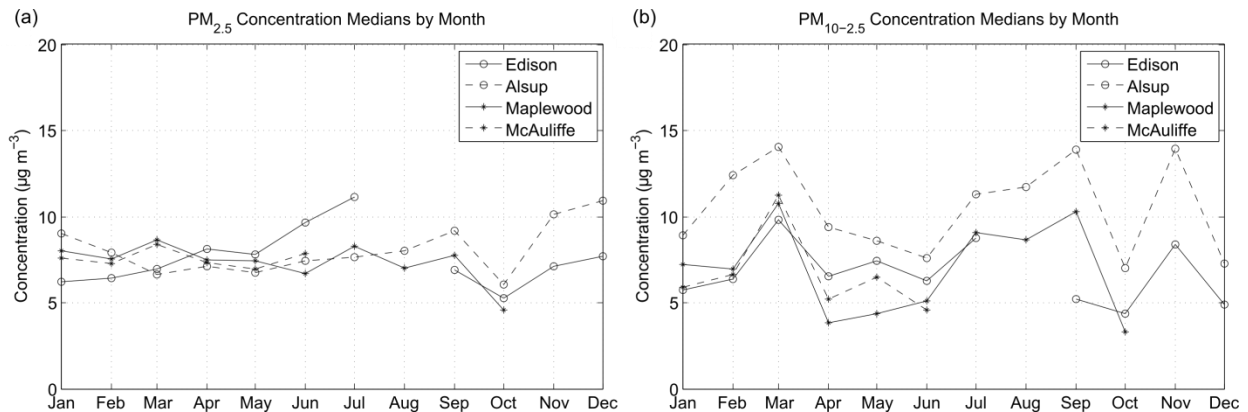
2.3.3 Nonparametric Regression Results

Nonparametric regression results showing relationships of hourly $PM_{2.5}$ and $PM_{10-2.5}$ concentrations with wind speed and wind direction are presented for each site in Figures 2.3– 6. In each figure, the top panels show scatter plots of concentration versus wind direction and wind speed, and the bottom panels show the NPR results. The dark center line represents the values predicted by the regression ($C(\theta)$; where θ is wind direction or speed), and the lighter lines are the 95% confidence intervals based on the assumption that predicted values are means of normal distributions at each θ value. Wind direction data are arranged clockwise from north at

zero degrees. Note that the hourly average concentrations shown in these figures reach sharply higher values than the 24-h average concentration summarized in Table 2.4. As reflected in the wider confidence limits for high wind speeds in some cases, limited data density influenced the curve shapes in these regions.

The NPR results for the Edison site (Figure 2.3) show higher concentration estimates for both size fractions when the wind is from the northeast. Estimated $PM_{2.5}$ concentrations at Alsup peak with winds from the southwest (Figure 2.4a). Estimated $PM_{10-2.5}$ concentrations at Alsup are markedly higher with winds from the west (Figure 2.4b). The wind direction NPR results for both pollutants at both Denver sites point towards the more densely populated, highly travelled, and industrialized core of the city as a significant source area. There are no known major point sources near the Edison site, but the westerly peak in the NPR results for $PM_{10-2.5}$ at Alsup is likely influenced by a sand and gravel operation 1 km west of the monitor and a major interstate-highway junction (I-76, I-270, I-25, and US-36) just west of that.

The Maplewood and McAuliffe sites have similar NPR results (Figures 2.5 and 2.6). The NPR results show that $PM_{2.5}$ concentrations are highest with southerly winds (Figures 2.5a and 2.6a). The NPR results for $PM_{10-2.5}$ for both Greeley sites show peaks corresponding to winds from the west and southwest (Figures 2.5b and 2.6b). A third peak corresponding to winds from the northwest is more pronounced in the results for Maplewood than those for McAuliffe. The predicted value centered on this peak is influenced by multiple data points with concentrations exceeding 100 µg m^{-3}. When these values are omitted from the NPR, the third peak is no longer apparent for either Maplewood or McAuliffe. We have no basis for excluding these data points; the northwesterly influence appears to be a real effect in the data sets. The densely populated portion of Colorado's Northern Front Range extends from metropolitan Denver, which is south-southwest of Greeley, to Fort Collins, which is northwest of Greeley. Emissions from these source areas may account for the peaks in Figures 2.5b and 2.6b. We are

not aware of nearby point sources that are south, southwest, or northwest of the Greeley

monitoring sites.

Figure 2.3 Nonparametric regression results for (a) $PM_{2.5}$ (n = 4028) and (b) $PM_{10-2.5}$ (n = 4028) mass concentrations (µg m^{-3}) at Edison, showing relationships with wind direction (degrees clockwise from north) and wind speed (m s^{-1})
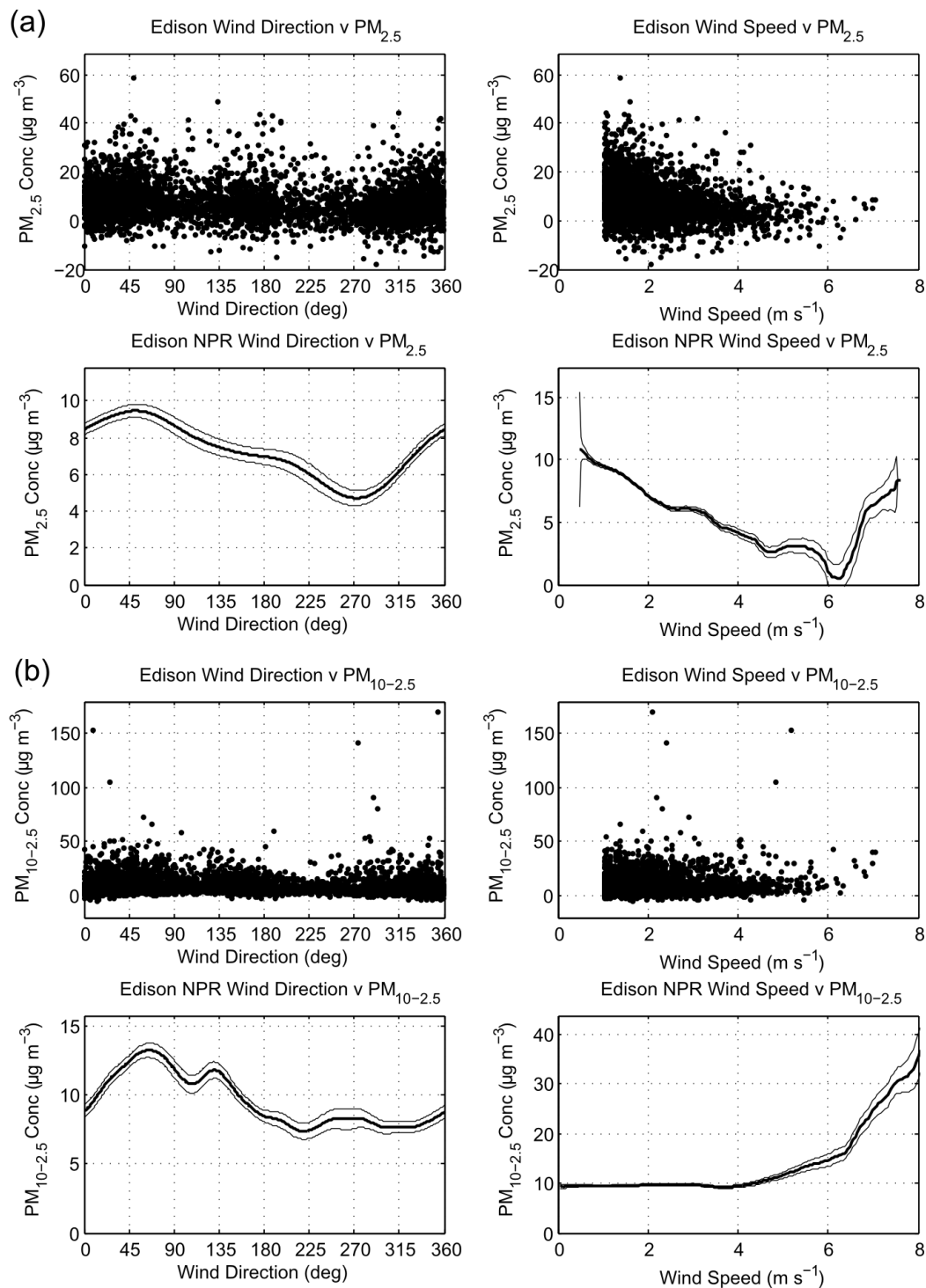
Figure 2.4 Nonparametric regression results for (a) PM$_{2.5}$ (n = 7626) and (b) PM$_{10\text{-}2.5}$ (n = 7496) mass concentrations (μg m^{-3}) at Alsup, showing relationships with wind direction (degrees clockwise from north) and wind speed (m s^{-1})
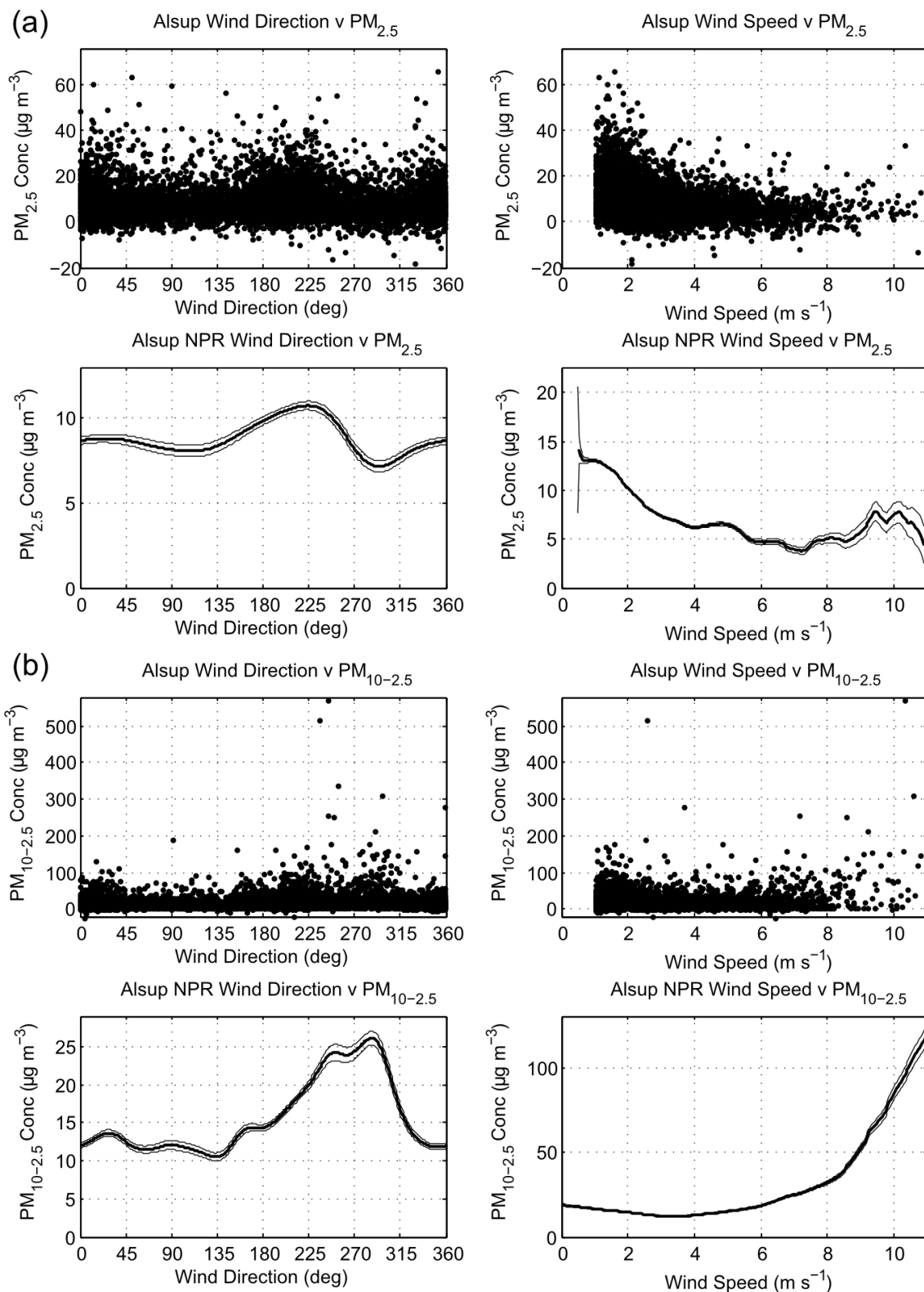
Figure 2.5 Nonparametric regression results for (a) $PM_{2.5}$ (n = 2930) and (b) $PM_{10\text{-}2.5}$ (n = 2930) mass concentrations (µg m^{-3}) at Maplewood, showing relationships with wind direction (degrees clockwise from north) and wind speed (m s^{-1})
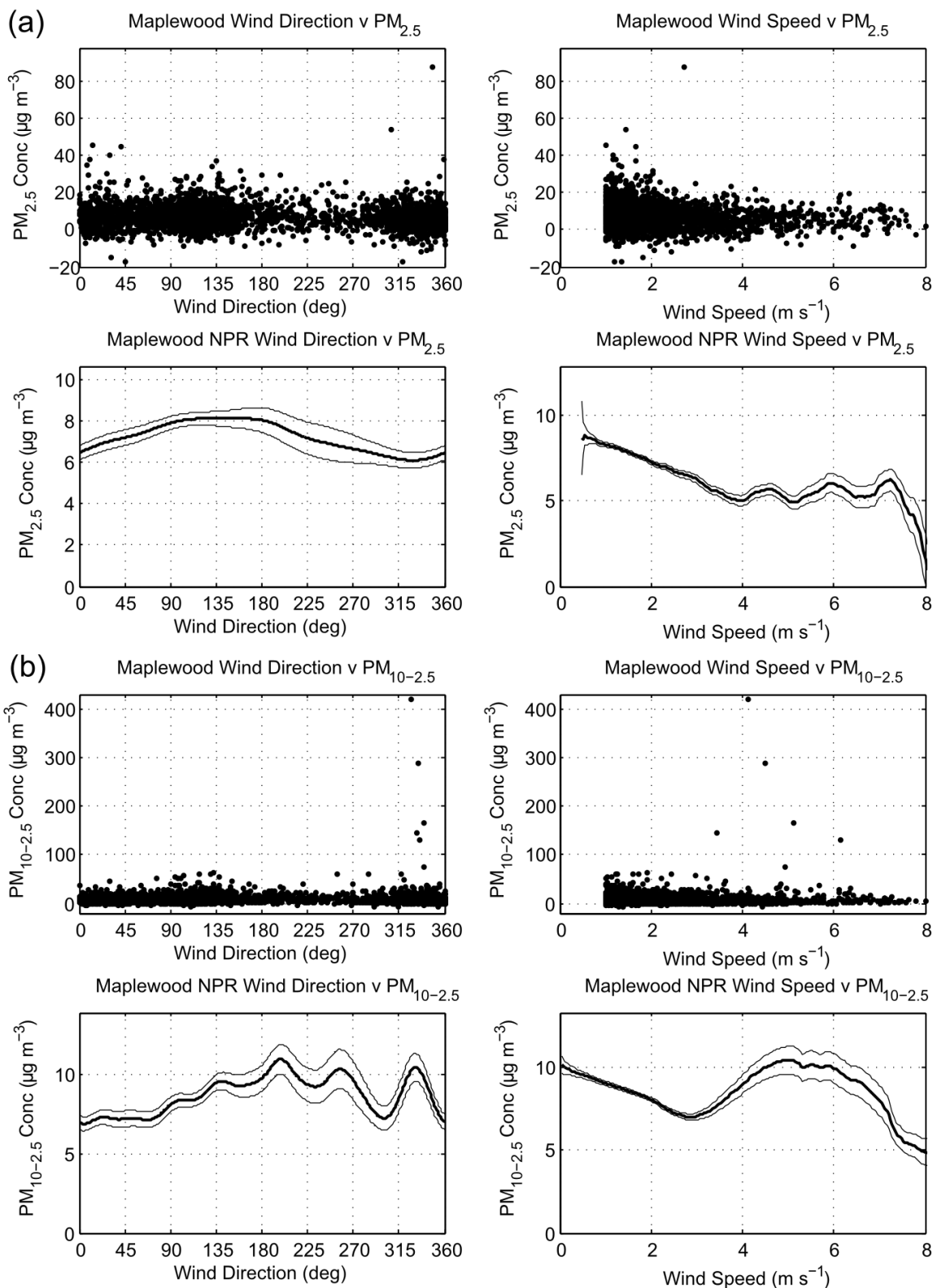
Figure 2.6 Nonparametric regression results for (a) $PM_{2.5}$ (n = 2262) and (b) $PM_{10-2.5}$ (n = 2262) mass concentrations (µg m^{-3}) at McAuliffe, showing relationships with wind direction (degrees clockwise from north) and wind speed (m s^{-1})
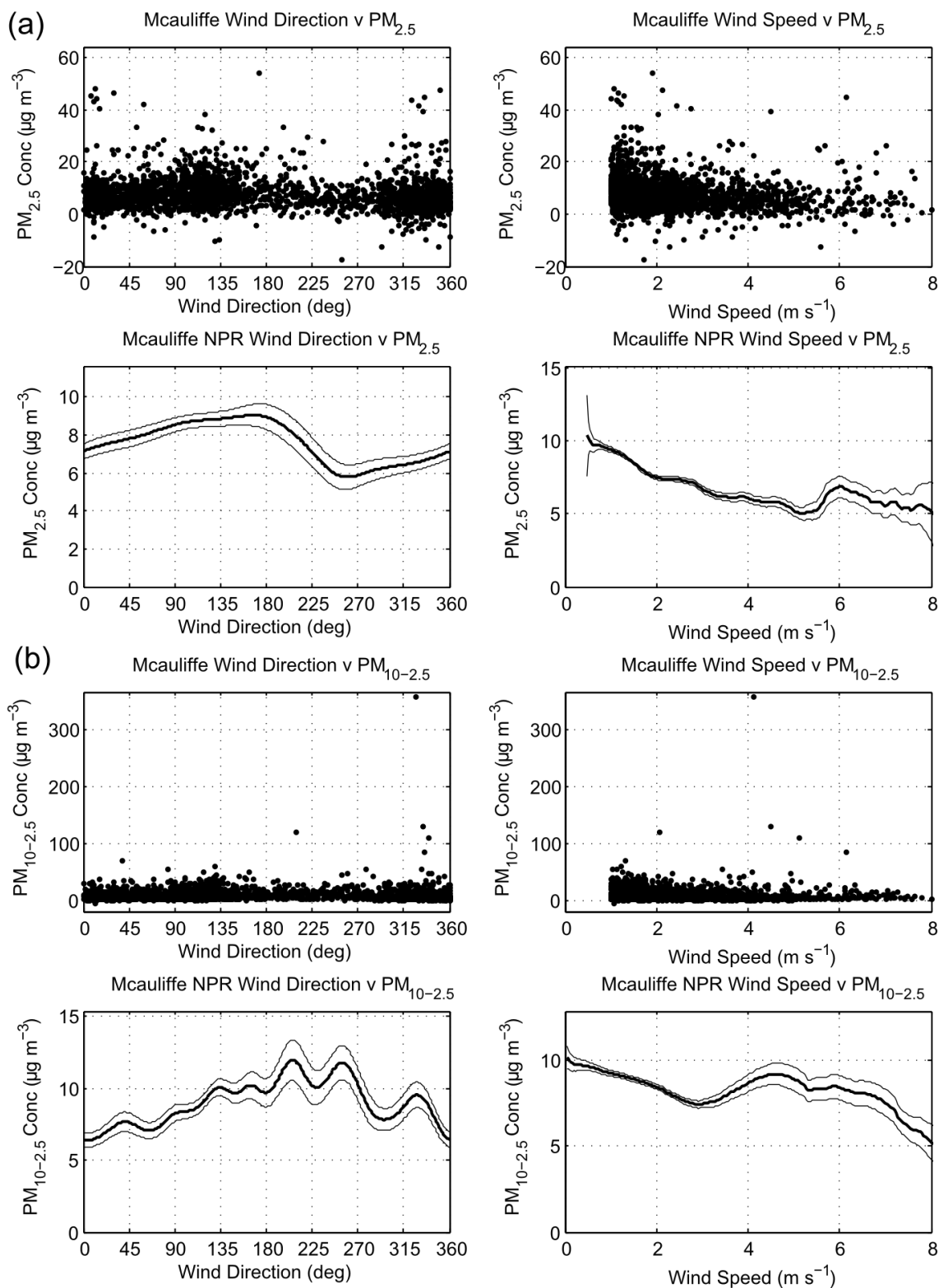
Across all four sites, the NPR results for $PM_{2.5}$ dependence on wind speed show a general dilution effect with increasing wind speed. NPR results for Edison and Alsup show increased $PM_{2.5}$ concentrations with wind speeds above $6 - 7$ m s^{-1}. This could be due to resuspension processes or uncertainty associated with low data density. Additional data in this wind speed range will help interpreting this relationship.

Results for $PM_{10-2.5}$ are more complicated than those for $PM_{2.5}$. The $PM_{10-2.5}$ wind speed regressions for the two Denver sites (Figures 2.3b and 2.4b) suggest resuspension effects, with concentrations increasing with wind speeds up to 8 m s^{-1} at Edison and 10 m s^{-1} at Alsup. The $PM_{10-2.5}$ concentrations at the two Greeley sites (Figures 2.5b and 2.6b) show relatively complex wind speed dependence. They decrease for wind speeds up to about 3 m s^{-1}, increase with wind speeds between 3 and 5 m s^{-1}, and then decrease again at higher wind speeds. In comparison, Harrison et al. (2001) found a U-shaped curve for the wind speed dependence of $PM_{10-2.5}$ mass concentration measurements taken near a roadway in Birmingham Hodge Hill, England, suggesting dilution at wind speeds below about 4 m s^{-1} and resuspension at higher wind speeds. Moore et al. (2010) found positive correlation between $PM_{10-2.5}$ concentration and wind speed for three Los Angeles area sites during the dry seasons, but negligible or negative correlation in winter. Once additional data are available, seasonal analysis and consideration of additional meteorological variables related to resuspension could assist in interpreting the relationship between wind speed and $PM_{10-2.5}$ concentrations at our monitoring sites.

2.3.4 Comparison of 24-h Average Mass Concentrations and Spatial Correlation with other Locations

The State of Colorado (CDPHE) reports mass concentrations of $PM_{2.5}$ and PM_{10} from two urban monitoring sites in Denver: the CAMP site at 2105 Broadway (lat. 39.75, long. -104.99) and the Denver Municipal Animal Shelter (DMAS) site at 678 S. Jason Street (lat. 39.70, long. -105.00). Each site houses a TEOM 1400a equipped with a FDMS unit (Series

8500 FDMS, Thermo Scientific) for continuous $PM_{2.5}$ monitoring and a TEOM 1400AB without a FDMS unit for PM_{10} monitoring. We obtained data from 1/1/2009 to 2/28/2010 for these monitoring sites from CDPHE and estimated $PM_{10-2.5}$ concentrations by subtraction. Descriptive statistics for both size ranges were calculated for comparison with results from the four CCRUSH TEOM sites. For the given time period, the mean 24-h average $PM_{2.5}$ concentration at CAMP was 8.3 µg m^{-3}, with a 95th percentile value of 16.6 µg m^{-3} and COV of 0.5. The mean $PM_{2.5}$ concentration at DMAS was 11.1 µg m^{-3}, with a 95th percentile value of 19.6 µg m^{-3} and COV of 0.4. The mean $PM_{2.5}$ concentration at CAMP thus falls within the range observed at our four monitoring sites, while the concentration at DMAS is about 20 – 40% higher than the mean concentrations we observed. The Pearson's R correlation coefficient for 24-h average $PM_{2.5}$ concentrations at the two CDPHE monitors, separated by 5.1 km, was 0.82. Correlation coefficients for 24-h average $PM_{2.5}$ concentrations at the CDPHE monitors paired with our Denver monitors ranged from 0.69 between Alsup and DMAS (14.7 km apart) to 0.87 between Edison and DMAS (8.8 km apart).

The mean 24-h average $PM_{10-2.5}$ concentration at CAMP was 15.7 µg m^{-3}, with a 95th percentile value of 27.5 µg m^{-3} and COV of 0.4. The mean $PM_{10-2.5}$ concentration at DMAS was 12.9 µg m^{-3}, with a 95th percentile value of 28.4 µg m^{-3} and COV of 0.7. $PM_{10-2.5}$ concentrations at the CDPHE sites are thus comparable to those we observed at Alsup, and higher than those observed at our other study sites. The Pearson's R correlation coefficient for 24-h average $PM_{10-2.5}$ concentrations at the two CDPHE monitors was 0.61. Correlation coefficients for $PM_{10-2.5}$ concentrations at the CDPHE monitors paired with our Denver monitors range from 0.60 between Alsup and CAMP (9.7 km apart) to 0.83 between Edison and DMAS (8.8 km apart).

U.S. EPA (2009) presents distributions of 24-h average $PM_{2.5}$ and $PM_{10-2.5}$ mass concentrations measured from 2005 – 2007 from FRM monitors across the country that report to the agency's Air Quality System. For $PM_{2.5}$, the national mean 24-h average concentration was 12 □g m^{-3} and the 5th and 95th percentile values were 4 □g m^{-3} and 28 □g m^{-3}, based on

nearly 350,000 observations. For Denver, U.S. EPA (2009) reports a mean 24-h average $PM_{2.5}$

concentration during 2005 – 2007 of 9 $\Box$g m^{-3} and 5th and 95th percentile values of 3 $\Box$g m^{-3} and

18 $\Box$g m^{-3}, respectively, based on 4192 observations. Results from the CDPHE monitors

discussed above and from the TEOM sampling conducted in this study during 2009 – 2010

show similar mean $PM_{2.5}$ concentrations to those EPA reports for Denver, but with greater

variability.

For $PM_{10-2.5}$, U.S. EPA (2009) reported concentrations estimated from co-located

monitors using low-volume FRM filter samplers from 2005 to 2007. The national mean 24-h

average $PM_{10-2.5}$ concentration was 13 $\Box$g m^{-3}, with 5th and 95th percentile values of 1 $\Box$g m^{-3} and

33 $\Box$g m^{-3}, respectively, based on just over 12,000 observations. For $PM_{10-2.5}$ in Denver, EPA

reported a mean concentration of 20 $\Box$g m^{-3} with 5th and 95th percentile values of 4 and 42 $\Box$g

m^{-3}, based on 353 observations. In comparison to the values U.S. EPA (2009) reports for

Denver, the results from the CDPHE monitoring discussed above and results from our study

suggest lower mean $PM_{10-2.5}$ concentrations. Differences could be due to differences in

sampling methods and monitoring locations or changes in pollutant levels over time.

As mentioned in the introduction, concentrations of $PM_{10-2.5}$ have generally been

expected to be more variable than those of $PM_{2.5}$. Results from this study indicate that 24-h

average $PM_{10-2.5}$ concentrations are somewhat more temporally variable than those for $PM_{2.5}$,

with coefficients of variation ranging from 0.6-0.8 for $PM_{10-2.5}$ and near 0.5 for $PM_{2.5}$. Data from

CDPHE show a comparatively low COV for $PM_{10-2.5}$ concentrations at CAMP. For both size

classes, spatial correlation was relatively strong for the two monitors in Greeley, compared to

the monitors located in Denver. The correlation coefficient of 0.97 for $PM_{10-2.5}$ concentrations

from the two Greeley locations, which are located 4.5 km apart, is also relatively high compared

to correlation coefficients reported for pairs of $PM_{10-2.5}$ monitors in other cities, including those

with similar separation distances (Wilson et al., 2005; Pabkin et al., 2010; U.S. EPA, 2009). The

high correlation of $PM_{10-2.5}$ for the Greeley monitors suggests the impact of regional sources

and/or meteorological influences, rather than local sources.

2.4 ACKOWLEDGEMENTS

2.5 REFERENCES

Boreson, J., Dillner, A.M., Peccia, J. 2004. Correlating Bioaerosol Load with PM2.5 and PM10cf

Concentrations: A Comparison between Natural Desert and Urban-Fringe Aerosols,

Atmos. Environ. 38:6029-2041.

Brunekreef, B., Forsberg, B. 2005. Epidemiological Evidence of Effects of Coarse Airborne

Particles on Health. *Eur. Respir. J.* 26:309 -318.

Castillejos, M., Borja-Aburto, V.H., Dockery, D., Gold, D.R., and Loomis, D. 2000. Airborne

Coarse Particles and Mortality. *Inhal. Toxicol.* 12:61-72.

http://informahealthcare.com/doi/abs/10.1080/089583700196392.

Chan, T.L., Lippmann, M. 1980. Experimental Measurements and Empirical Modelling of the

Regional Deposition of Inhaled Particles in Humans. *Am. Ind. Hyg. Assoc. J.* 41:399-

409.

Chen, F., Williams, R., Svendsen, E., Yeatts, K., Creason, J., Scott, J., Terrell, D., Case, M.

2007. Coarse Particulate Matter Concentrations from Residential Outdoor Sites

Associated with the North Carolina Asthma and Children's Environment Studies (NC-

ACES). *Atmos. Environ.* 41:1200-1208.

Duce, R.A., Hoffman, G.L., Ray, B.J., Fletcher, I.S., Wallace, G.T., Fasching, J.L., Piotrowicz,

S.R., Walsh, P.r., Hoffman, E.J., Miller, J.M., Heffter, J.L., Trace metals in the marine

atmosphere: sources and fluxes, in H.L. Windom and R.A. Duce eds., Marine Pollutant

Transfer, D.C. Heath, Lexington, MA, 1976, pp. 77-119.

Green, D. Fuller, G.W., and Baker, T. 2009. Development and Validation of the Volatile

Correction Model for PM10 – an Empirical Method for Adjusting TEOM Measurements

for their Loss of Volatile Particulate Matter. *Atmos. Environ.* 43:2132-2141.

Grover, B.D., Kleinman, M., Eatough, N.L., Eatough, D.J., Hopke, P.K., Long, R.W., Wilson,

W.E., Meyer, M.B., and Ambs, J.L. 2005. Measurement of Total PM$_{2.5}$ Mass (Nonvolatile

Plus Semivolatile) with the Filter Dynamic Measurement System Tapered Element
Oscillating Microbalance Monitor. *J. Geophys. Res.* 110, D07S03,
doi:10.1029/2004JD004995.

Harrison, R.M., Yin, J., Mark, D., Stedman, J., Appleby, R.S., Booker, J., Moorcroft, S. 2001.
Studies of the Coarse Particle (2.5 – 10 ☐m) Component in UK Urban Atmospheres.
Atmos. Environ. 35:3667-3679.

Henry, R.C., Chang, Y., Spiegelman, C.H. 2002. Locating Nearby Sources of Air Pollution by
Nonparametric Regression of Atmospheric Concentrations on Wind Direction. *Atmos.
Environ.* 36:2237-2244.

Henry, R., Norris, G.A., Vedantham, R., Turner, J.R. 2009. Source Region Identification Using
Kernel Smoothing. *Environ. Sci. Technol.* 43:4090-4097.

Kim, E., Hopke, P.H. 2004. Comparison between Conditional Probability Function and
Nonparametric Regression for Fine Particle Source Directions. *Atmos. Environ.*,
38:4667–4673.

Hueglin, C., Gehrig, R., Baltensperger, U., Gysel, M., Monn, C., Vonmont, H. 2005. Chemical
Characterization of PM2.5, PM10 and Coarse Particles at Urban, Near-city and Rural
Sites in Switzerland. *Atmos. Environ.* 39:637-651.

Loo, B.W., Cork, C.P. 1988. Development of High Efficiency Virtual Impactors. *Aerosol Sci.
Technol.* 9:167-176.

Mar, T.F., Norris, G.A., Koenig, J.Q., Larson, T.V. 2000. Associations between Air Pollution and
Mortality in Phoenix, 1995-1997. *Environ. Health Perspect.* 108:347-353.

Marple, V.A., Chien, C.M. 1980. Virtual Impactors: A Theoretical Study. *Environ. Sci. Technol.*
14:976-985.

Milford, J.B., Davidson, C.I. 1985. The Sizes of Particulate Trace Elements in the Atmosphere –
A Review, *J. Air Poll. Control Assoc.* 35:1249-1260.

Milford, J.B., Davidson, C.I. 1987. The Sizes of Particulate Sulfate and Nitrate in the

    Atmosphere – A Review, *J. Air Poll. Control Assoc.* 37:125-134.

Moore, K.F., Verma, V., Cruz Minguillon, M., Sioutas, C. 2010. Inter- and Intra-Community

    Variability in Continuous Coarse Particulate Matter (PM10-2.5) Concentrations in the Los

    Angeles Area. *Aerosol Sci. Technol.* 44:526-540.

Ostro, B.D., Broadwin, R., Lipsett, M.J. 2000. Coarse and Fine Particles and Daily Mortality in

    the Coachella Valley, California: A Follow-Up Study. *J Expo. Anal. Environ. Epidemiol.*

    10:412-419.

Pakbin, P., Hudda, N., Cheung, K.L., Moore, K.F., Sioutas, C. 2010. Spatial and Temporal

    Variability of Coarse (PM10-2.5) Particulate Matter Concentrations in the Los Angeles

    Area. *Aerosol Sci. Technol.* 44:514-525.

Patterson, E., Gillette, D. 1977. Commonalities in Measured Size Distributions for Aerosols

    Having a Soil-Derived Component. *J. Geophys. Res.* 82:2074.

Schwab, J.J., Felton, H.D., Rattigan, O.V., Demerjian, K.L. 2006. New York State Urban and

    Rural Measurements of Continuous PM2.5 Mass by FDMS, TEOM, and BAM. *J. Air

    Waste Manage. Assoc.* 56:372-383.Solomon, P.A., Sioutas, C. (2008). Continuous and

    Semicontinuous Monitoring Techniques for Particulate Matter Mass and Chemical

    Components: A Synthesis of Findings from EPA's Particulate Matter Supersites Program

    and Related Studies. *J. Air Waste Manage. Assoc.* 58:164-195.

Solomon, P.A., Sioutas, C. 2008. Continuous and Semicontinuous Monitoring Techniques for

    Particulate Matter Mass and Chemical Components: A Synthesis of Findings from EPA's

    Particulate Matter Supersites Program and Related Studies. *J. Air & Waste Manage.

    Assoc.* 58:164-195.

Thornburg, J., Rodes, C.E., Lawless, P.A., Williams, R. 2009. Spatial and Temporal Variability

    of Outdoor Coarse Particulate Matter Mass Concentrations Measured with a New

Coarse Particle Sampler During the Detroit Exposure and Aerosol Research Study. *Atmos. Environ.* 43:4251-4258.

U.S. Census. 2000. United States Census 2000, Urban and Rural Classification. http://www.census.gov/geo/www/ua/ua_2k.html, accessed December 27, 2010.

U.S. Census. 2009a. Table 1. Annual Estimates of the Resident Population for Counties of Colorado: April 1, 2000 to July 1, 2009. 2009 Population Estimates. United States Census Bureau, Population Division. http://www.census.gov/popest/counties/counties.html, accessed December 27, 2010.

U.S. Census. 2009b. Table 4. Annual Estimates of the Resident Population for Incorporated Places in Colorado: April 1, 2000 to July 1, 2009. 2009 Population Estimates. United States Census Bureau, Population Division. http://www.census.gov/popest/cities/SUB-EST2009-states.html, accessed December 27, 2010.

U.S. Census. 2009c. Table 1. Annual Estimates of the Resident Population for Incorporated Places Over 100,000, Ranked by July 1, 2009 Population: April 1, 2000 to July 1, 2009. 2009 Population Estimates. United States Census Bureau, Population Division. http://www.census.gov/popest/cities/SUB-EST2009.html, accessed December 27, 2010.

U.S. EPA. 1995. AP 42 Fifth Edition: Compilation of Air Pollutant Emission Factors, Vol. 1: Stationary Point and Area Sources. U.S. Environmental Protection Agency, Office of Air Quality Planning and Standards, Research Triangle Park, NC.

U.S. EPA. 2004. Air Quality Criteria for Particulate Matter. EPA/600/P-99/002aF-bF. U.S. Environmental Protection Agency. Research Triangle Park, NC.

U.S. EPA. 2009. Integrated Science Assessment for Particulate Matter. EPA/600/R-08/139F. U.S. Environmental Protection Agency, Washington, DC.

U.S. EPA. 2010. http://www.epa.gov/ttn/amtic/files/ambient/criteria/reference-equivalent-methods-list.pdf, accessed December 29, 2010.

Vedal, S., Hannigan, M.P., Dutton, S.J., Miller, S.L., Milford, J.B., Rabinovitch, N., Kim, S.-Y., Sheppard, L. 2009.The Denver Aerosol Sources and Health (DASH) Study: Overview and Early Findings. *Atmos. Environ.* 43:1666-1673.

Villeneuve, P.J., Burnett, R.T., Shi, Y., Krewski, D., Goldberg, M.S., Hertzman, C., Chen, Y., Brook, J. 2003. A Time-Series Study of Air Pollution, Socioeconomic Status, and Mortality in Vancouver, Canada. *J. Expo. Anal. Environ. Epidemiol.* 13:427-435.

Wilson, J.G., Kingham, S., Pearce, J., Sturman, A.P. 2005. A Review of Intraurban Variations in Particulate Air Pollution: Implications for Epidemiological Research. *Atmos. Environ.* 39:6444-6462.

Yu, K.N., Cheung, Y.P., Cheung, T., Henry, R.C. 2004. Identifying the Impact of Large Urban Airports on Local Air Quality by Nonparametric Regression. *Atmos. Environ.* 38:4501-4507.

Zanobetti, A., Schwartz, J. 2009. The Effect of Fine and Coarse Particulate Air Pollution on Mortality: A National Analysis. *Environ. Health Perspect.*117, 898-903.

Zhu, K., Zhang, J., Lioy, P.J. 2006. Evaluation and Comparison of Continuous Fine Particulate Matter Monitors for Measurement of Ambient Aerosols. *J. Air and Waste Manage. Assoc.* 57:1499-1506.

2.6 SUPPLEMENTAL INFORMATION

Figure 2.S1 Wind rose for data used in the Edison wind regressions
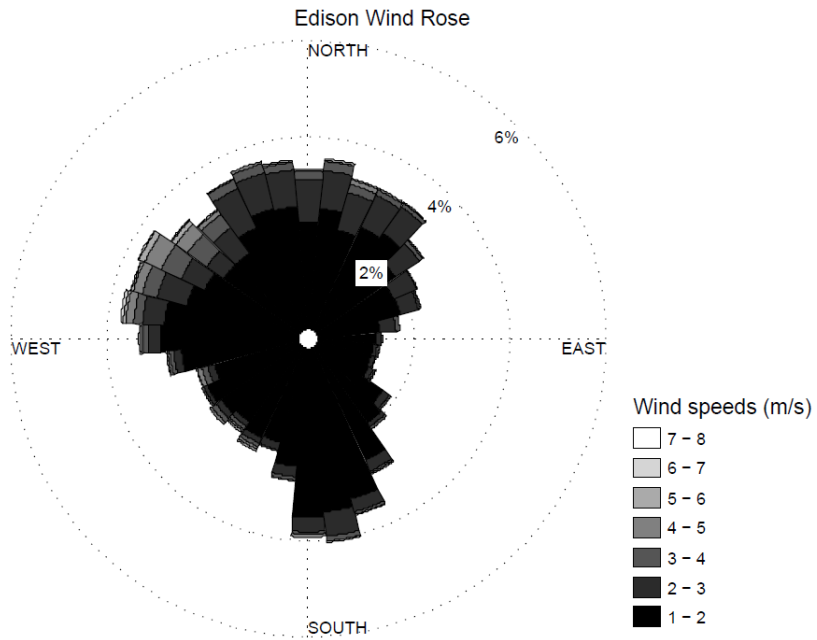
Figure 2.S2 Wind rose for data used in the Alsup wind regressions
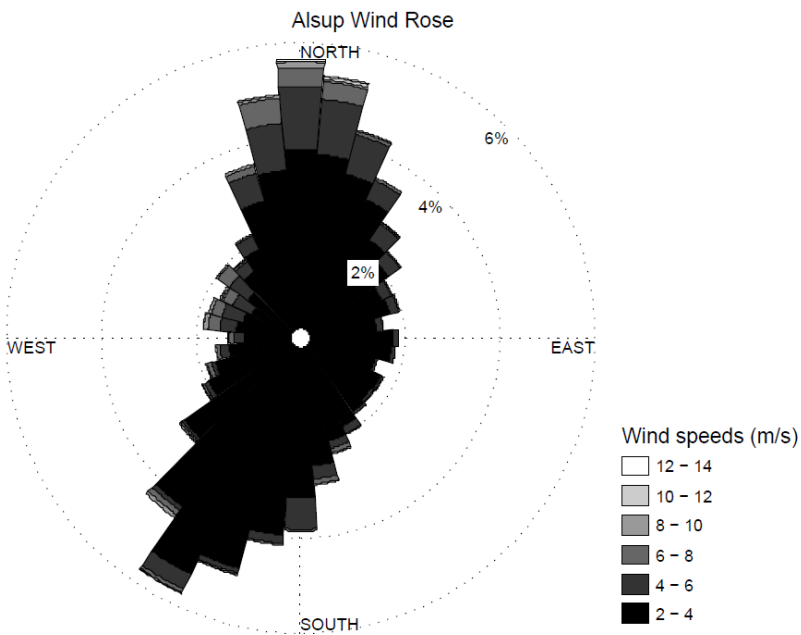
Figure 2.S3 Wind rose for data used in the Maplewood wind regressions

Maplewood Wind Rose
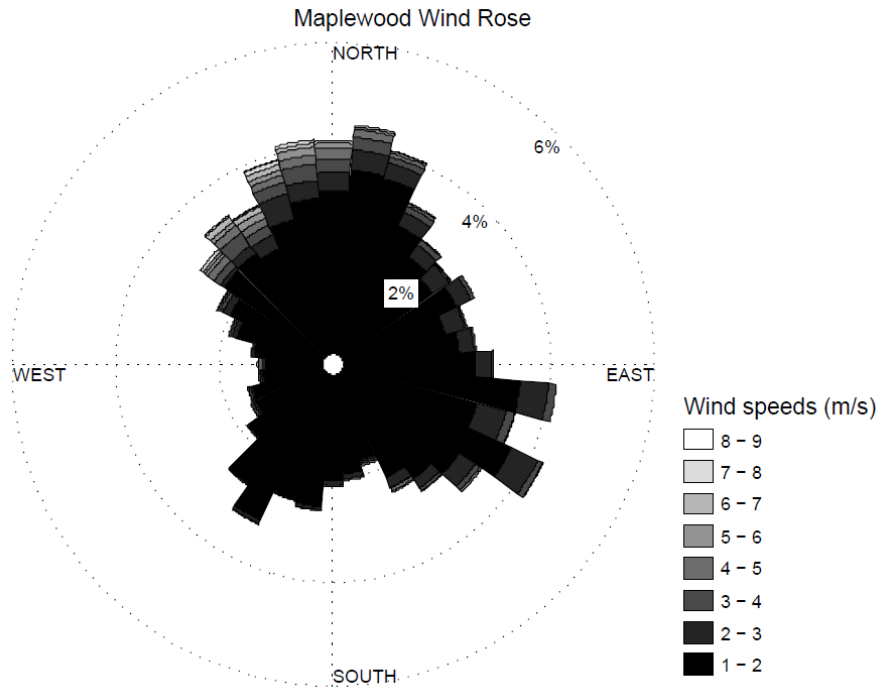
Figure 2.S4 Wind rose for data used in the McAuliffe wind regressions

Mcauliffe Wind Rose
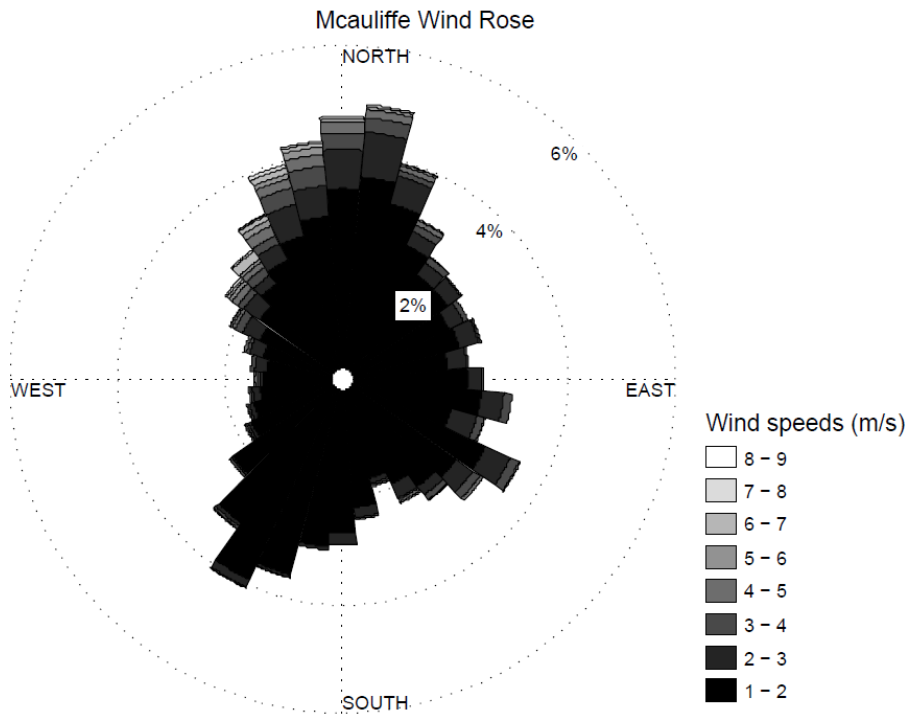
CHAPTER 3

ERRORS IN COARSE PARTICULATE MATTER (PM$_{10\text{-}2.5}$) MASS CONCENTRATIONS AND SPATIOTEMPORAL CHARACTERISTICS WHEN USING SUBTRACTION ESTIMATION METHODS

Nicholas Clements[a], Jana B. Milford[a], Shelly L. Miller[a], William Navidi[b], Jennifer L. Peel[c], Michael P. Hannigan[a]

[a]Department of Mechanical Engineering, College of Engineering and Applied Science, University of Colorado at Boulder, Boulder, CO, 80309-0427

[b]Department of Applied Mathematics and Statistics, Colorado School of Mines, Golden, CO, 80401

[c]Department of Environmental and Radiological Health Sciences, Colorado State University, Fort Collins, CO, 80523

3.0 ABSTRACT

In studies of coarse particulate matter ($PM_{10-2.5}$), mass concentrations are often estimated through the subtraction of $PM_{2.5}$ from collocated PM_{10} tapered element oscillating microbalance (TEOM) measurements. Though all field instruments have yet to be updated, the Filter Dynamic Measurement System (FDMS) was introduced to account for the loss of semi-volatile material from heated TEOM filters. To assess errors in $PM_{10-2.5}$ estimation when using the possible combinations of PM_{10} and $PM_{2.5}$ TEOM units with and without FDMS, data from three monitoring sites of the Colorado Coarse Rural-Urban Sources and Health (CCRUSH) study were used to simulate four possible subtraction methods for estimating $PM_{10-2.5}$ mass concentrations. Assuming all mass is accounted for using collocated TEOMs with FDMS, the three other subtraction methods were assessed for biases in absolute mass concentration, temporal variability, spatial correlation, and homogeneity. Results show collocated units without FDMS closely estimate actual $PM_{10-2.5}$ mass and spatial characteristics due to the very low $PM_{10-2.5}$ semi-volatile concentrations in Colorado. Estimation using either a $PM_{2.5}$ or PM_{10} monitor without FDMS introduced absolute biases of 2.4 µg/m^3 (25%) to -2.3 µg/m^3 (-24%), respectively. Such errors are directly related to the unmeasured semi-volatile mass and alter measures of spatiotemporal variability and homogeneity; all of which have implications for the regulatory and epidemiology communities concerned about $PM_{10-2.5}$. Two monitoring sites operated by the state of Colorado were considered for inclusion in the CCRUSH acute health effects study, but concentrations were biased due to sampling with an FDMS-equipped $PM_{2.5}$ TEOM and PM_{10} TEOM not corrected for semi-volatile mass loss. A regression-based model was developed for removing the error in these measurements by estimating the semi-volatile concentration of $PM_{2.5}$ from total $PM_{2.5}$ concentrations. By estimating non-volatile $PM_{2.5}$ concentrations from this relationship, $PM_{10-2.5}$ was calculated as the difference between non-volatile PM_{10} and $PM_{2.5}$ concentrations.

3.1 INTRODUCTION

Coarse particulate matter ($PM_{10-2.5}$) consists of aerosols with aerodynamic diameter between 2.5 and 10 μm and is linked to multiple adverse health effects (US EPA, 2004). Typically emitted from mechanical abrasion or resuspension processes, $PM_{10-2.5}$ is generally composed of a mixture of road-wear material and soil derived minerals, soil organic matter, brake and tire wear, and biological particles (Almeida et al., 2006, Simoneit et al., 2004, Harrison et al., 2012). Biological particles include bacteria, fungi, pollen, and plant detritus (Polymenakou et al., 2008; Boreson et al., 2004; Puxbaum and Tenze-Kunit, 2003). Salt particles may also be present near oceans or during winter in areas where roads are salted (Wang and Shooter, 2005; Kumar et al., 2012). Inorganic ions are commonly present in low concentrations in $PM_{10-2.5}$, except in large urban areas such as Los Angeles (Lee et al., 2008; Cheung et al., 2011). Local sources may vary widely, with urban, suburban, continental background, desert, and forest samples having distinctly different $PM_{10-2.5}$ compositions (Malm et al., 2007; Lagudu et al., 2011; Sillanpaa et al., 2006).

Although fewer investigators have specifically examined coarse particles compared to the fine particulate fraction, epidemiological studies have provided evidence that increased coarse particle concentrations are associated with adverse health effects. In their 2005 review of the epidemiological evidence related to coarse particles, Brunekreef and Forsberg concluded there was inconsistent evidence of a relationship between $PM_{10-2.5}$ and mortality, but for COPD, asthma, and respiratory illness hospital admissions, relative risks were generally higher for $PM_{10-2.5}$ than $PM_{2.5}$. Recently, Malig and Ostro (2009) limited the case deaths in their model to those living in a zip code within 20 km of pollution monitors, due to the spatial heterogeneity of $PM_{10-2.5}$ in California, and observed a significant positive association between both all-cause and cardiovascular mortality and increased $PM_{10-2.5}$ concentrations. Using 47 locations throughout the United States, Zanobetti and Schwartz (2009) observed an increased relative risk for all-

cause, stroke-related, and respiratory-related mortality associated with increased $PM_{10-2.5}$ concentrations, with respiratory illness mortality having the largest relative risk. Meister et al. (2012) also observed a significant relationship between increased $PM_{10-2.5}$ concentrations and mortality using eight years of data from Stockholm, Sweden. Two recent studies of $PM_{10-2.5}$ health effects in Hong Kong demonstrated a positive association for respiratory disease hospitalizations and no relationship for cardiovascular disease hospitalizations (Qiu et al., 2012; Qiu et al. 2013). In many studies of $PM_{10-2.5}$ health effects, $PM_{2.5}$ concentrations are subtracted from PM_{10} concentrations in order to estimate $PM_{10-2.5}$ concentrations indirectly (Chen et al., 2005; Lin et al., 2005; Lipsett et al., 2006; Kan et al., 2007; Host et al., 2008; Peng et al., 2008; Perez et al., 2008; Tecer et al., 2008; Malig and Ostro, 2009, Zanobetti and Schwartz, 2009; Chang et al. 2011; Meister et al., 2012; Qiu et al., 2013). Biases in mean estimates and inflated measurement variability due to some differencing approaches need to be considered prior to the use of these measurements to characterize the air quality or to estimate population exposure in epidemiological studies (Goldman et al., 2011).

The tapered element oscillating microbalance (TEOM) is a semi-continuous monitor that measures particulate mass concentrations. TEOMs are commonly used throughout the United States, allowing quick reporting of pollution episodes, providing high temporal resolution (hourly) measurements, and reducing the time and effort required to reach a point measurement compared to the gravimetric method. During the measurement, TEOM filters are heated to 30°C (or 50°C, depending on instrument model), resulting in evaporation of semi-volatile species such as ammonium nitrate and various organic molecules. To quantify the loss of semi-volatile mass, a self-referencing module called the Filter Dynamic Measurement System (FDMS) was introduced to the TEOM system, though many units deployed in the United States have yet to be updated. Previous studies have quantified the bias inherent in uncorrected TEOM measurements and compared them to other measurement methods. For example, Green and Fuller (2006) compared PM_{10} and $PM_{2.5}$ measurements from a TEOM without semi-volatile

mass-loss correction and from a Partisol sampler, which collects particulate mass on a filter for gravimetric analysis. The study addressed the influence of the US EPA's TEOM correction factor in estimating unmeasured semi-volatile mass, 1.03 times the raw mass concentration plus 3 µg/m^3, on reported PM_{10} and $PM_{2.5}$ mass concentrations, and also addressed how the use of standard temperature and pressure for reporting mass concentrations biases results compared to values reported at actual temperature and pressure. They found the TEOM, with the EPA's correction factor removed and reporting actual flow conditions, underestimated mass concentrations by about 40% compared to the Partisol. The study also recommended that the US EPA correction factor be removed due to being too simplistic to account for spatial and temporal changes in particulate composition. A method for correcting PM_{10} TEOM concentrations without FDMS units installed using nearby TEOMs with FDMS units has been proposed for use in the United Kingdom air pollution monitoring network (Green et al., 2009). Because $PM_{10-2.5}$ is commonly estimated through the subtraction method, different combinations of PM_{10} and $PM_{2.5}$ TEOMs that have and have not been updated for semi-volatile loss correction are possible. Each possible combination involves a different inherent error.

To assess these errors, monitoring data from two cities in Colorado were used. The Colorado Coarse Rural-Urban Sources and Health (CCRUSH) study aims to characterize ambient $PM_{10-2.5}$ in urban and rural environments in semi-arid Colorado (Clements et al., 2012). Planned analyses include using the CCRUSH mass concentration data in an epidemiological study to assess $PM_{10-2.5}$ health effects. Mass concentration data were collected by dichotomous TEOMs, with semi-volatile mass loss correction, located at three monitoring sites for approximately three years. Data from two sites in Denver, operated by the Colorado Department of Public Health and Environment (CDPHE), will also be included in the CCRUSH health study. The CDPHE sites use collocated TEOMs to estimate $PM_{10-2.5}$ through subtraction of semi-volatile loss-corrected $PM_{2.5}$ from uncorrected PM_{10} concentrations. To explore the biases introduced by this subtraction method and other possible TEOM configurations, all

combinations of collocated TEOMs with and without correction for evaporative mass loss were simulated with data from the CCRUSH sites. Errors in absolute concentrations, data distributions, and spatiotemporal variability measures were reported and discussed for all TEOM combinations. A model was developed for each CDPHE site to remove the error from $PM_{10-2.5}$ estimations, a correction which makes the CDPHE data suitable for use in a future epidemiological study.

3.2 METHODS AND DATA ANALYSIS

Three of the four CCRUSH monitoring locations are included in this analysis, the details of which have been published previously (Clements et al., 2012). Briefly, two urban monitors were located near or in the city of Denver. Alsup Elementary School (ALS) is a traffic-influenced, industrial-residential site northeast of downtown Denver in the suburb of Commerce City. ALS is also an EPA AQS Chemical Speciation Network site for $PM_{2.5}$ in Denver (AQS Site ID: 080010006). Edison Elementary School (EDI) is an urban background site located 4.5 km northwest of downtown Denver and 3 km west of I-25. Maplewood Elementary School (MAP) is a rural-residential site located in Greeley, an agricultural community approximately 75 km north-northeast of Denver. The other CCRUSH monitoring site in Greeley, McAuliffe Elementary, is not included in this analysis as it was taken offline early in the campaign due to TEOM instrument issues. Denver and Greeley were selected for this study to examine contrast in sources, composition, and potentially in the health impacts of $PM_{10-2.5}$ in urban and rural environments.

The CDPHE monitoring sites included in this analysis are CAMP (AQS Site ID: 080310002), located in downtown Denver, and DMAS (AQS Site ID: 080310025), located along I-25, 5 km south of downtown Denver. DMAS is also part of the US EPA NCore Multipollutant Monitoring Network. Data from these sites were provided by CDPHE and collected throughout the duration of the CCRUSH sampling campaign. Table 3.1 summarizes all monitoring site locations, including start/end dates and completeness statistics. Figure 3.S1 of the supplemental information is a regional map of the CCRUSH and CDPHE monitoring sites.

Table 3.1 Monitoring site details

Site	ALS (CCRUSH)	EDI (CCRUSH)	MAP (CCRUSH)	CAMP (CDPHE)	DMAS (CDPHE)
Coordinates	39.83N/ 104.94W	39.76N/ 105.04W	40.42N/ 104.71W	39.75N/ 104.99W	39.70N/ 105.00W
Inlet Height (m)	6	9	9	6	5
Location Description	Industrial-residential	Urban-residential	Rural-residential	Urban-roadside	Urban-roadside
Start Date/Time	1/16/2009 16:00	1/8/2009 13:00	1/16/2009 18:00	11/20/2010 1:00	1/1/2009 1:00
End Date/Time	9/29/2011 10:00	3/1/2012 10:00	2/2/2012 12:00	4/30/2012 24:00	4/30/2012 24:00
No. of PM$_{2.5}$ Daily Samples (% Completeness)	755 (76.5%)	747 (65.0%)	822 (73.9%)	505 (95.6%)	1097 (90.2%)
No. of PM$_{10-2.5}$ Daily Samples (% Completeness)	755 (76.5%)	747 (65.0%)	822 (73.9%)	474 (89.8%)	961 (79.0%)
No. of PM$_{10}$ Daily Samples (% Completeness)	755 (76.5%)	747 (65.0%)	822 (73.9%)	492 (93.2%)	1034 (85.0%)
Median (IQR) Daily Semi-Volatile PM$_{2.5}$ Mass Conc. (µg/m^3)	2.08(1.55)	1.81(1.67)	2.22(1.62)	NA	NA
Median (IQR) Daily Semi-Volatile PM$_{10-2.5}$ Mass Conc. (µg/m^3)	0.16(0.35)	0.01(0.27)	0.05(0.38)	NA	NA

All CCRUSH monitoring sites were equipped with a TEOM 1405-DF (Thermo Scientific) for roughly three years starting in January, 2009. The TEOM 1405-DF is dichotomous and is equipped with an FDMS to quantify the mass of evaporated semi-volatile species. All instruments were housed in temperature-controlled TEOM enclosures and kept on site rooftops. The TEOM measures aerosol mass concentration by continuously sampling particles onto a TEOM TX-40 filter placed at the end of an oscillating glass tube (the tapered element). By monitoring changes in the oscillating frequency of the tapered element, the deposited mass can be calculated. Figure 3.1 is a schematic of the TEOM 1405-DF configuration. Particles are continuously sampled through a 16.7 L/min PM$_{10}$ inlet, and are subsequently separated using a 2.5 µm cut-point virtual impactor. The PM$_{2.5}$ and PM$_{10-2.5}$ sampling channels then pass the aerosol through Nafion membrane diffusion driers to remove particulate-bound water. Following

the driers, aerosol enters the FDMS, which either directs the samples through heater tubes (30°C) and onto TEOM filters, or redirects the sample through a chilled (4°C) 47 mm TX-40 filter to remove particles and condensable gases. This cleaned air stream is then directed through the heater tubes and TEOM filters to allow for quantification of the mass loss of material that is volatile at 30°C. These two modes of FDMS operation will be referred to as base and reference measurements, with base measurements representing the non-volatile particulate mass and reference measurements representing the semi-volatile mass. Total mass concentrations were calculated by adding the evaporated semi-volatile mass to the non-volatile base measurement. The FDMS valve switches flow direction every six minutes, giving one base, reference, and total mass concentration measurement for each twelve minute interval.

Figure 3.1 TEOM 1405-DF Instrument Configuration
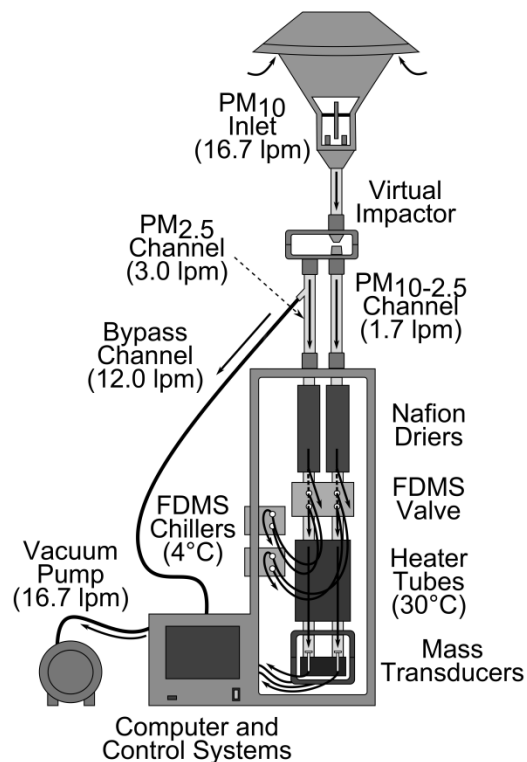
A TEOM data logging scheme specific to the CCRUSH study was developed prior to deploying the instruments. Raw base and reference mass concentration data, ambient temperature and relative humidity, and instrument parameters relevant for diagnostics were stored on each instrument at six minute intervals. Raw base and reference data contained no interpolated concentrations. Data were downloaded from each TEOM unit once per month. Data processing software corrected the raw $PM_{10-2.5}$ base and reference measurements for the 10% of $PM_{2.5}$ mass that penetrates into the $PM_{10-2.5}$ channel due to the virtual impactor, and calculates the total PM mass for each channel by subtracting the negative reference values (due to measuring mass loss) from the base concentrations (Clements et al., 2012). Twelve-minute mass concentration and six-minute meteorological and instrument condition data were then averaged on an hourly basis, and data points associated with instrument issues or hours with less than 75% completeness were replaced with missing value designators. Daily averages were then calculated with the hourly average data and days with less than 75% completeness were censored. PM_{10} concentrations were calculated by adding $PM_{10-2.5}$ and $PM_{2.5}$ mass concentrations. All mass concentrations are reported using actual volume conditions. It is noted that the TEOM 1405-DF instruments used in the CCRUSH study were received prior to the instrument being designated as a US EPA $PM_{2.5}$ FEM sampler, and the $PM_{10-2.5}$ and PM_{10} channels of the TEOM 1405-DF have yet to receive equivalency designation. CCRUSH TEOM maintenance followed similar protocols to those of the CDPHE sites.

In this study, CCRUSH PM_{10} and $PM_{2.5}$ mass concentration data were used to simulate all possible combinations of collocated PM_{10} and $PM_{2.5}$ TEOMs, with or without FDMS units, to calculate $PM_{10-2.5}$ through subtraction. The four TEOM subtraction method combinations are shown below in eqs 1-4, where the FDMS subscript denotes the total mass concentration and no subscript denotes base mass concentrations, representing a TEOM without an FDMS. The equivalent nonvolatile (NV) and semi-volatile (SV) contributions to the estimated $PM_{10-2.5}$ mass for each case are also shown. For each monitoring site, $PM_{10-2.5}$ concentrations were estimated

57

using the same hourly or daily averaged data for each subtraction case. See Table 3.1 for the

start and end dates of monitoring at each site.

$$Case\ 1: PM_{10-2.5} = PM_{10,FDMS} - PM_{2.5,FDMS} = PM_{10-2.5}NV + PM_{10-2.5}SV \tag{1}$$

$$Case\ 2: PM_{10-2.5} = PM_{10,FDMS} - PM_{2.5} = PM_{10-2.5}NV + PM_{10}SV \tag{2}$$

$$Case\ 3: PM_{10-2.5} = PM_{10} - PM_{2.5,FDMS} = PM_{10-2.5}NV - PM_{2.5}SV \tag{3}$$

$$Case\ 4: PM_{10-2.5} = PM_{10} - PM_{2.5} = PM_{10-2.5}NV \tag{4}$$

Case 1 is equal to $PM_{10-2.5}$ concentrations reported by the TEOM 1405-DF, as it accounts for

both nonvolatile and semi-volatile mass. Calculating the differences between Case 1 and Cases

2-4 provided the theoretical mean bias introduced by each subtraction method: Case 2

overestimates $PM_{10-2.5}$ by the mass concentration of semi-volatile $PM_{2.5}$; Case 3 underestimates

$PM_{10-2.5}$ by the mass concentration of semi-volatile PM_{10}; and Case 4 underestimates $PM_{10-2.5}$ by

the mass concentration of semi-volatile $PM_{10-2.5}$.

To assess spatial correlation and homogeneity between sites in Denver and Greeley,

Pearson's correlation coefficient (ρ) and the concordance correlation coefficient (CCC, eq 5)

were used, respectively. The CCC is the ratio of two times the covariance of time series 1 and 2

(σ_{12}) divided by the sum of the variance of each time series (σ_1^2 and σ_2^2) and the squared

difference in means (μ_1 and μ_2). In a pair-wise comparison, the CCC simultaneously quantifies

correlation and deviation from the concordance, or 1:1 line. Unlike the coefficient of divergence

(COD), which is typically used to assess spatial homogeneity in air quality studies, the CCC has

the advantage of being directly comparable to correlation through a penalization factor (C_b, Lin,

1989). This measure of homogeneity considers both differences in spatiotemporal trends and

measurement magnitude and is a more intuitive summary statistic for homogeneity compared to

the COD.

$$CCC = \frac{2\sigma_{12}}{\sigma_1^2 + \sigma_2^2 + (\mu_1 - \mu_2)^2} = \rho C_b \tag{5}$$

CDPHE sites CAMP and DMAS are each equipped with collocated PM_{10} and $PM_{2.5}$ TEOM monitors that operated throughout the period of the CCRUSH study. All CDPHE TEOMs operated at 30°C. PM_{10} monitors at both sites lack an FDMS, while both $PM_{2.5}$ monitors are equipped with FDMS units. The EPA correction factor for TEOMs without FDMS units was not used to adjust CDPHE PM_{10} mass concentrations. Quality reviewed hourly average data was received from the CDPHE, and daily averages were calculated and censored for days with less than 75% completeness. This scenario is simulated by Case 3, so comparisons between CCRUSH Case 3 data and CDPHE estimated $PM_{10-2.5}$ are important for understanding errors in measurement magnitude. The CDPHE data was corrected using a model that predicts $PM_{2.5}$ semi-volatile concentrations, which were used to calculate non-volatile $PM_{2.5}$ concentrations. Case 4-estimated $PM_{10-2.5}$ concentrations were then calculated using non-volatile PM_{10} and $PM_{2.5}$ concentrations.

3.3 RESULTS

3.3.1 Mass Concentration Biases

Data distributions of all sites and cases for hourly and daily mass concentration averages are shown as box plots in Figure 3.2. Of the CCRUSH sites, $PM_{10-2.5}$ concentrations at ALS were on average highest, likely because of two nearby sources: a gravel and sand operation and a major highway intersection. The other CCRUSH site in Denver, residential-EDI, had the lowest $PM_{10-2.5}$ concentrations. EDI had no significant point sources nearby with the highest concentrations on days when the wind was from the east and northeast, the general direction of downtown Denver and the intersection of four major highways (Clements et al., 2012). Both CDPHE sites exhibited distributions similar in magnitude to the traffic and industrially influenced ALS and were affected by nearby roads as emission sources. Comparing distributions of Case 3 data to CDPHE site data, the bias caused by underestimating $PM_{10-2.5}$ by the PM_{10} semi-volatile mass concentration is shown most obviously by all 5th percentile values being negative. In the case of the CCRUSH hourly data, the percentage of negative values was on average 2.7% for Case 1 and 18.5% for Case 3.

For daily average values, summary statistics for each case and site are listed in Table 3.2. Case 1 is considered the "base case" as it accounts for all particulate mass. Table 3.2 also lists the absolute differences between Cases 2-4 and Case 1 medians, 5th percentiles, and 95th percentiles. Differences between medians followed the theoretical trends expressed in eqs 1-4. Case 2 overestimated $PM_{10-2.5}$ mass concentrations by 2.07-2.53 µg/m^3, or 25%, whereas Case 3 underestimated $PM_{10-2.5}$ mass concentrations by 1.96-2.51 µg/m^3, or 24%. Case 4 closely matched Case 1 values due to the low concentrations of semi-volatile material measured in the coarse fraction, which were on average less than 0.1 µg/m^3.

Figure 3.2 Site-wise box plots of average PM$_{10-2.5}$ concentrations for each subtraction case (whiskers are 5th and 95th percentiles, hr – hourly averages, dy – daily averages)
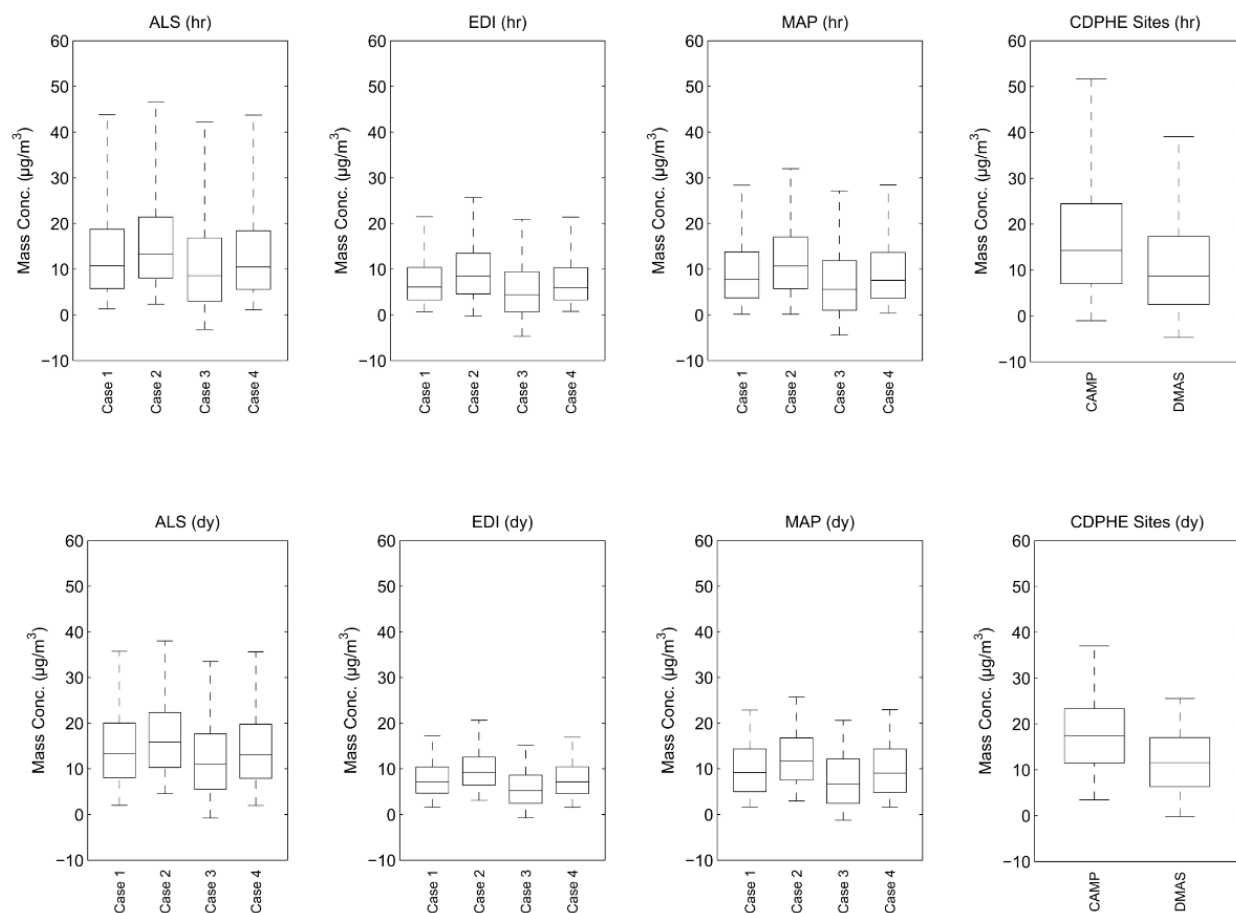
Differences in the 5th and 95th percentiles were considered to determine effects of subtraction method on extreme values. Low value extremes showed the largest relative changes, with percent differences for Case 2 and 3 ranging from -175% (MAP Case 3) to 126% (ALS Case 2). Case 3 5th percentiles were on average underestimated by 2.66 µg/m^3. For 95th percentiles, Case 2 resulted in the largest biases, increasing values by 2.85 µg/m^3, or 13%. Extreme values of Case 4 distributions were similar to Case 1, with much lower differences than Case 2 or 3.

Table 3.2 Statistical summary of $PM_{10-2.5}$ estimation methods (daily average data)

ALS	Case 1	Case 2	Case 3	Case 4
Mean (St. Dev.) ($\mu g/m^3$)	15.30(10.36)	17.61(10.26)	12.78(10.65)	15.10(10.34)
Median (IQR) ($\mu g/m^3$)	13.37(11.97)	15.87(12.03)	11.06(12.08)	13.05(11.82)
5th Percentile ($\mu g/m^3$)	2.02	4.58	-0.77	1.96
95th Percentile ($\mu g/m^3$)	35.74	38.00	33.52	35.65
COV	0.68	0.58	0.83	0.68
Diff. from Case 1 Median($\mu g/m^3$)	-	2.50	-2.31	-0.32
Diff. from Case 1 5th Percentile($\mu g/m^3$)	-	2.56	-2.79	-0.06
Diff. from Case 1 95th Percentile($\mu g/m^3$)	-	2.26	-2.22	-0.09
EDI	**Case 1**	**Case 2**	**Case 3**	**Case 4**
Mean (St. Dev.) ($\mu g/m^3$)	8.02(4.85)	10.07(5.23)	5.94(5.19)	8.00(4.84)
Median (IQR) ($\mu g/m^3$)	7.17(5.76)	9.24(6.17)	5.21(6.18)	7.11(5.85)
5th Percentile ($\mu g/m^3$)	1.61	3.09	-0.72	1.58
95th Percentile ($\mu g/m^3$)	17.20	20.66	15.16	16.94
COV	0.61	0.52	0.87	0.61
Diff. from Case 1 Median($\mu g/m^3$)	-	2.07	-1.96	-0.06
Diff. from Case 1 5th Percentile($\mu g/m^3$)	-	1.48	-2.33	-0.03
Diff. from Case 1 95th Percentile($\mu g/m^3$)	-	3.46	-2.04	-0.26
MAP	**Case 1**	**Case 2**	**Case 3**	**Case 4**
Mean (St. Dev.) ($\mu g/m^3$)	10.34(7.11)	12.73(7.35)	7.90(7.35)	10.29(7.13)
Median (IQR) ($\mu g/m^3$)	9.17(9.37)	11.70(9.24)	6.66(9.69)	9.06(9.53)
5th Percentile ($\mu g/m^3$)	1.63	2.97	-1.23	1.59
95th Percentile ($\mu g/m^3$)	22.89	25.73	20.61	22.94
COV	0.69	0.58	0.93	0.69
Diff. from Case 1 Median($\mu g/m^3$)	-	2.53	-2.51	-0.11
Diff. from Case 1 5th Percentile($\mu g/m^3$)	-	1.34	-2.86	-0.04
Diff. from Case 1 95th Percentile($\mu g/m^3$)	-	2.84	-2.28	0.05

The coefficient of variation (COV), or the ratio of standard deviation to the mean, is a

measure of temporal variability. Case 2 tended to underestimate the COV due to positive biases

in the mean, Case 3 tended to overestimate COV due to negative biases in the mean, and Case 4 gave approximately the same COV values as Case 1. Case 3 COVs differed from Case 1 the most, due to both increases in distribution widths, and decreases in means. Due to CDPHE sites being estimated with Case 3, it is likely that COVs for CAMP and DMAS (0.60 and 0.70, respectively) are overestimates of the temporal variability at those sites. This overestimation was assessed with corrected CDPHE data.

3.3.2 Biases in Spatial Comparisons

Biases in estimates of correlation and homogeneity statistics were considered because of their importance in estimating pollutant spatial variability and for exposure assessment in epidemiological studies. Correlation coefficients (ρ) and CCCs between daily averages of all sites and subtraction methods are shown in Figure 3.3. Also displayed are ratios of all summary statistics to the Case 1 statistic for each pairwise site comparison (green and blue markers) and can be visually compared to the red line, indicating unity. Generally, correlation (blue markers) decreases compared to the Case 1 correlation for all site and case comparisons, while homogeneity (green markers) has a more intricate relationship with each site and case. Among case pairs for the same site (diagonal plots in Figure 3.3), comparing Case 2 to Case 3 shows the largest decrease in estimated correlation and CCC. Other pairs of cases have similar decreases, the magnitudes of which depend on the mean $PM_{10-2.5}$ concentrations considered.

Comparisons of homogeneity become fairly complex due to the biases introduced by each subtraction case causing different effects on the CCC. Comparing EDI Case 2 against ALS Case 3 increases the CCC value due to the smaller difference in means compared to using Case 1 concentrations. In contrast, comparing ALS Case 2 against EDI Case 3 decreases the CCC because of the larger difference between means of the two time series. This effect is most obvious in comparisons between Case 2 and 3 of the same site where one data set is biased

high and the other low, respectively. Spatial statistics involving the EDI site are most affected by

subtraction method biases because at this site $PM_{10-2.5}$ mean concentrations are the lowest.

Figure 3.3 Spatial summary statistics and ratios of each spatial statistic over the Case 1 vs. Case 1 statistic for daily $PM_{10-2.5}$ averages of all combinations of sites and subtraction cases
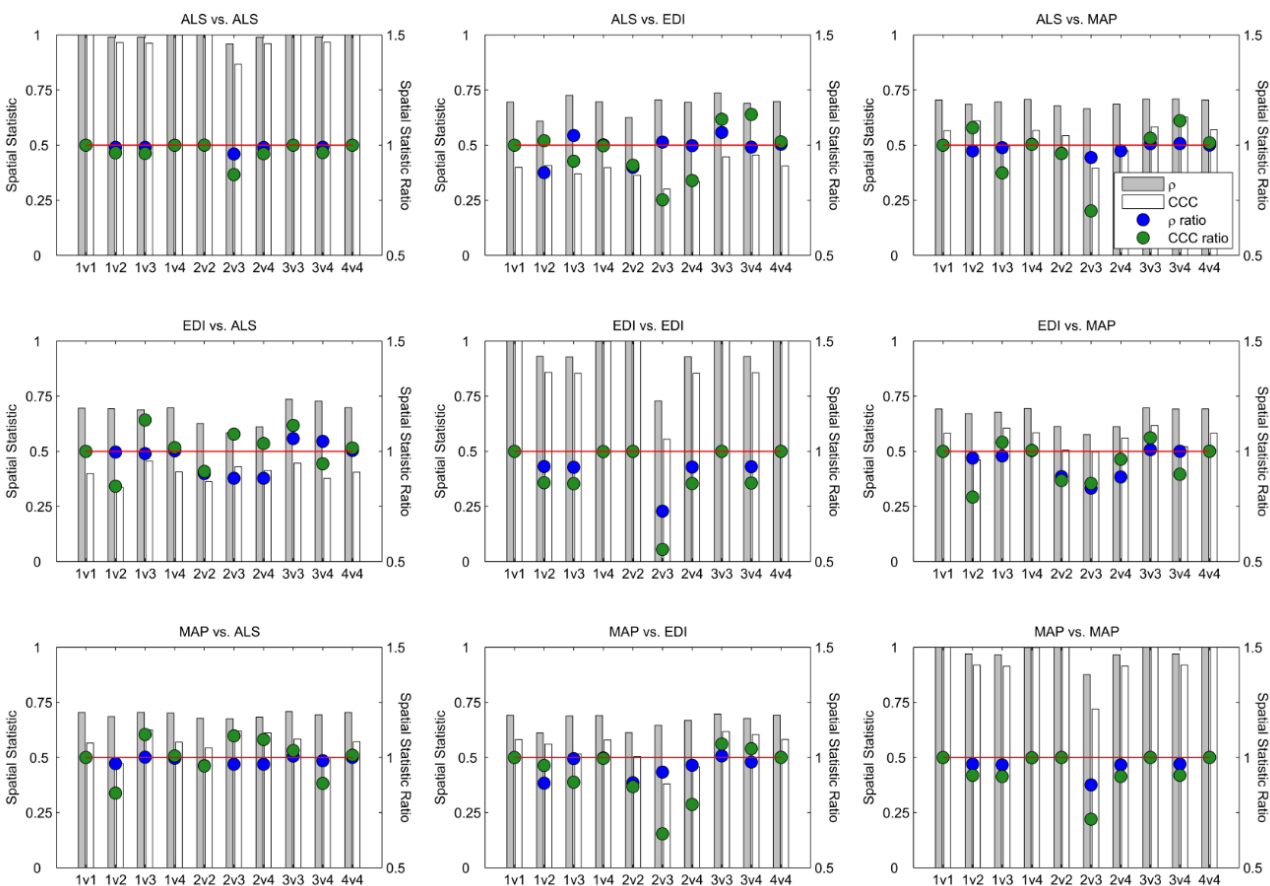
3.3.3 Error Correction Model

For monitoring in the United Kingdom, Green et al. (2009) proposed a method for

correcting PM_{10} concentrations measured by a TEOM without FDMS to make them equivalent

to measurements made with an FDMS-equipped TEOM, which had previously been deemed

equivalent to the EU's gravimetric reference method. The correction entailed using the

reference channel from one FDMS-equipped TEOM to estimate semi-volatile mass

concentrations for the region. The correction is applied in two steps. First, base TEOM measurements made by instruments operating at 50°C (TEOM$_{original}$) are corrected to be comparable to base measurements made by instruments operating at 30°C with a linear regression-derived relationship. Second, due to the uniformity and high spatial correlation of reference concentrations at several sites in the United Kingdom, it was determined that a reference channel measurement from an FDMS-equipped TEOM up to 200 km away (FDMS$_{regional}$) can be used to estimate a semi-volatile mass concentration to add to the previously corrected base PM$_{10}$ concentrations. Using their Volatile Correction Model, corrected PM$_{10}$ TEOM concentrations (TEOM$_{corrected}$) in the United Kingdom were estimated as:

$$TEOM_{corrected} = TEOM_{original} - 1.87 FDMS_{regional} \qquad (6)$$

A somewhat different approach was used in this study to estimate semi-volatile concentrations and correct for errors in the CDPHE PM$_{10-2.5}$ concentrations. This was largely because daily averaged semi-volatile concentrations were not as spatially correlated in Colorado (ρ=0.26-0.53) compared to the United Kingdom (ρ=0.86-0.99). To reiterate, CDPHE PM$_{10-2.5}$ concentrations are the result of subtracting FDMS-corrected PM$_{2.5}$ measurements from uncorrected PM$_{10}$ measurements, which is simulated as Case 3 in the analysis above and theoretically underestimates PM$_{10-2.5}$ concentrations by the semi-volatile concentration of the PM$_{10}$ fraction. For much of the time period of the CCRUSH study, CDPHE archived only the total FDMS-corrected PM$_{2.5}$, without retaining the separate measurements for the base and reference channels. However, at both CDPHE sites, PM$_{2.5}$ base and reference concentrations were recorded from October 2011 to July 2012. This data set allowed development of a least-squares linear regression model estimating PM$_{2.5}$ semi-volatile concentrations from total PM$_{2.5}$ mass concentrations. This model was then applied to the time series of CDPHE concentrations that corresponded to the CCRUSH campaign, approximating CDPHE PM$_{2.5}$ semi-volatile concentrations throughout that period. These concentrations were subtracted from measured total PM$_{2.5}$ concentrations, providing non-volatile concentrations. Non-volatile PM$_{2.5}$

concentrations were then subtracted from the corresponding measurements of non-volatile PM_{10}, providing $PM_{10-2.5}$ concentrations estimated according to Case 4, which was shown above to closely approximate Case 1 concentrations.

This corrective model depends on the observed relationship between $PM_{2.5}$ semi-volatile and total mass concentrations. Figures 3.4a and 3.4b, respectively, show scatter plots and linear regression lines of $PM_{2.5}$ semi-volatile versus total concentration for CAMP and DMAS data collected from October 2011 to July 2012. Marker color represents ambient temperature, scaling from blue for cold temperatures (<0°C), to green and yellow for moderate temperatures (>0°C and <15°C), and to orange and red for warm temperatures (>15°C). Missing temperature data is denoted with no marker color. Slopes for both CAMP and DMAS regressions were 0.25, but site-specific regressions were used to perform data corrections due to large differences in intercept terms, -0.53 for CAMP and 0.15 for DMAS. Correlation (ρ) values for each comparison are high, 0.72 and 0.80, suggesting a strong linear trend. A corrective model similar to Green et al. (2009), where regional $PM_{2.5}$ semi-volatile concentrations were used to estimate concentrations at the CDPHE sites, was also tested, but this spatial-relationship-based model had increased variance of the residuals and a decreased coefficient of determination (R^2) compared to the regression between $PM_{2.5}$ semi-volatile and total mass concentrations. Scatterplots of predicted and measured semi-volatile concentrations are plotted in Figures 3.4c and 3.4d, showing that during the period from October 2011 – June 2012, models for both CAMP and DMAS underpredict concentrations at high values (> 7.5 µg/m^3) and overpredict concentrations at low values (< 2 µg/m^3) of semi-volatile $PM_{2.5}$.

Figure 3.4 (a,b) Scatter plots and linear regressions between daily average $PM_{2.5}$ semi-volatile and total mass concentrations from CAMP and DMAS for data from October 2011 to July 2012 (c,d) Scatter plots of predicted and measured $PM_{2.5}$ semi-volatile concentrations from CAMP and DMAS for data from October 2011 to July 2012
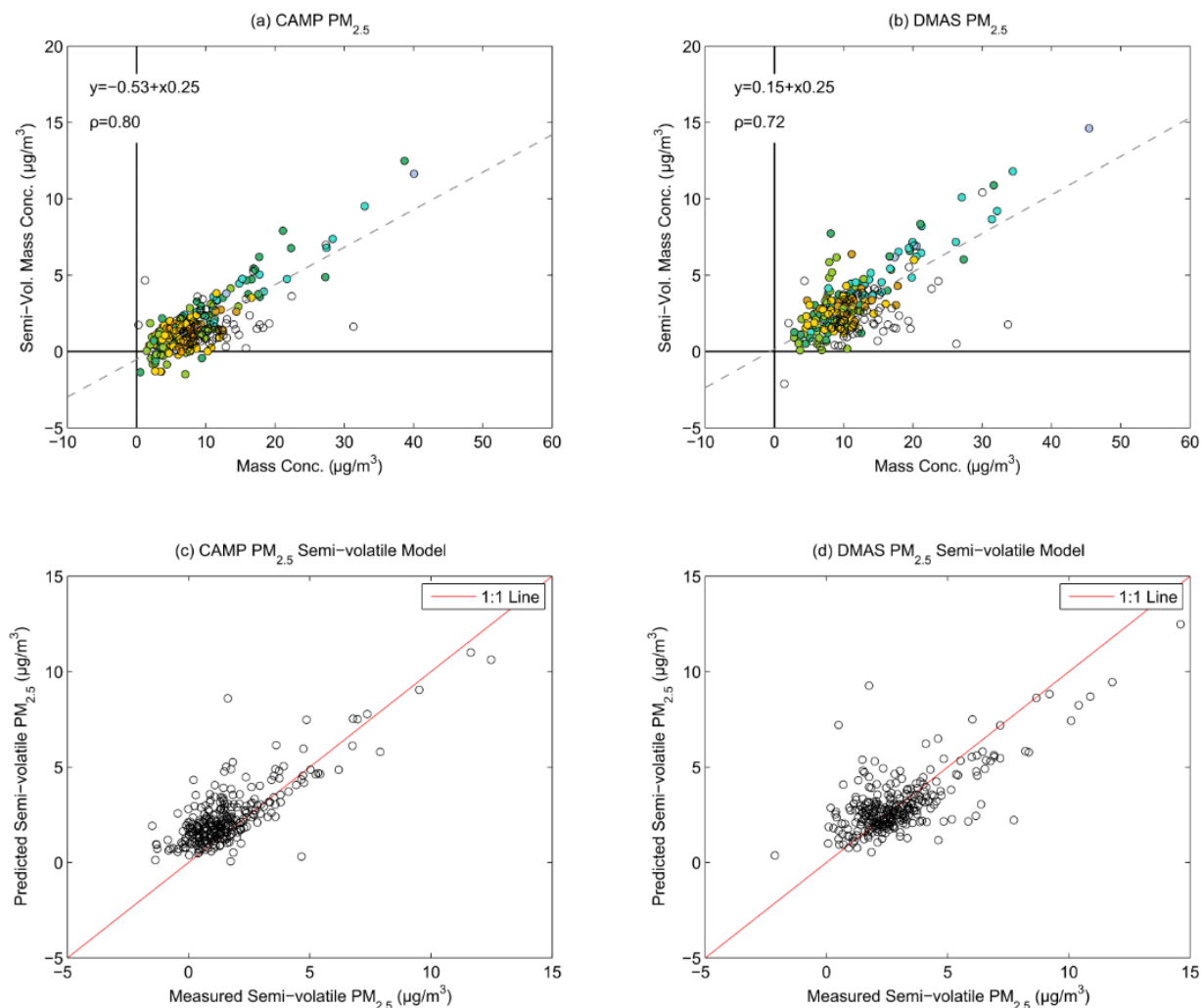
An assumption of the CAMP and DMAS correction models is that the derived relationships using CAMP and DMAS site data from October 2011 to July 2012 (290 days) applies throughout the CCRUSH monitoring period beginning in 2009. This assumption was tested by assessing the same model estimating semi-volatile $PM_{2.5}$ from total $PM_{2.5}$ concentrations, but derived using all available data from the CCRUSH site ALS, shown in Figure 3.8a. This ALS model was then compared to bootstrapped models derived from random 10

month sections of the three-year ALS time series to explore the variability in model parameters

when using a shortened data set. ALS was chosen due to similarities between it and both

CDPHE sites, and because the CDPHE only recently began recording $PM_{2.5}$ semi-volatile

concentrations. Segments of 290 days were randomly sampled 1000 times and the model

described above was performed for each bootstrapped segment. The distributions of regression

model intercept (β_0), slope (β_1), R^2, and the variance of the residuals for all bootstrapped sample

sets are shown in Figure 3.5. Distributions of bootstrapped model intercepts, slopes, and R^2

tend to be bimodal with mean±standard deviation of 0.10±0.20 µg/m^3, 0.25±0.02, and

0.64±0.09, respectively.

Figure 3.5 Distributions of regression intercept (β_0), regression slope (β_1), coefficient of determination (R^2), and variance of the model residuals for 1000 bootstrapped regressions of 10 month segments of the ALS $PM_{2.5}$ time series
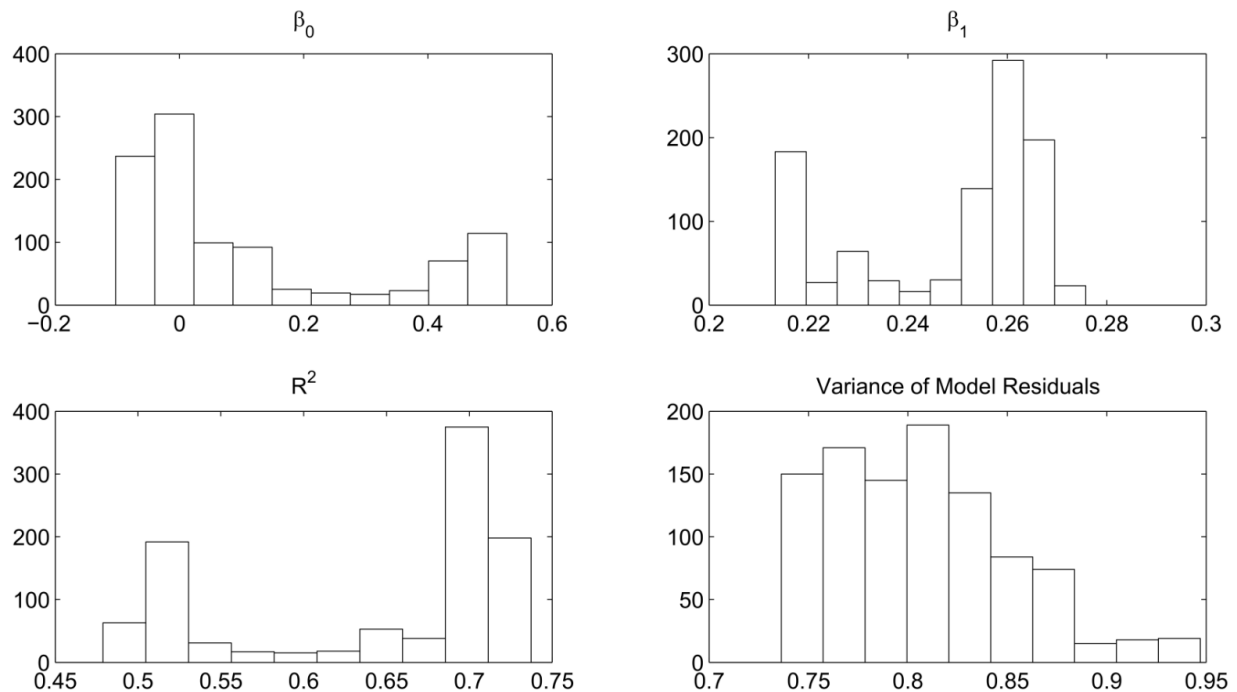
To explore what drove the observed bimodality, 50 bootstrapped regression lines were

plotted and classified by their R^2 value, as shown in Figure 3.6. Regression models found in the

lower mode of R^2 values ($R^2 < 0.64$) also tended to have increased intercepts and decreased slopes. Further analysis shows this set of bootstrapped samples contained fewer samples from the higher range of PM$_{2.5}$ values (> 10 µg/m^3), which tended to occur during cold periods. The full ALS model lies between regression parameter distribution modes and is similar to the median bootstrapped parameters, with original and bootstrap median intercepts of 0.06 and 0.01, and slopes of 0.25 and 0.26, respectively. After observing little variability in bootstrapped model parameters and the similarity between the full model and the bootstrapped model parameters, it was determined that a 290-day period is enough data to develop a well-defined model predicting PM$_{2.5}$ semi-volatile concentrations from total mass concentrations.

Comparing the 95% confidence intervals for estimated values in the original model to the distribution of regression lines in Figure 3.6 shows the original model underestimates the variability suggested by the bootstrapping exercise, which is instead indicative of variability in the possible 290-day models during the CCRUSH campaign time period. This suggests uncertainties in model estimates that are derived solely from a single regression are underestimates, as there is an added uncertainty in model parameters due to using a 290-day data set to derive the regression.

Figure 3.6 Full model (±95% confidence intervals) and bootstrapped regression lines, with red lines representing regressions with R^2 greater than 0.64 and blue representing lines with correlation less than 0.64
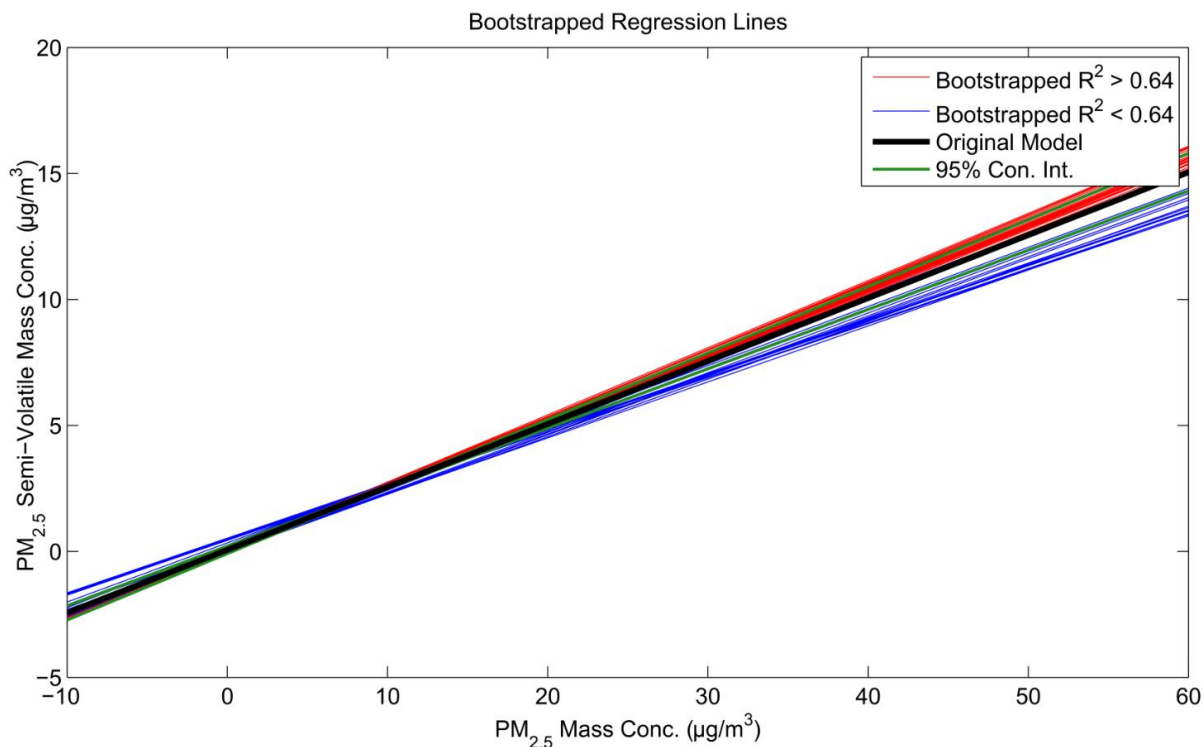
Using the regression relationships developed separately for CAMP and DMAS, $PM_{2.5}$ semi-volatile concentrations were estimated for the CCRUSH time period from total $PM_{2.5}$ concentrations reported for that period. The estimated semi-volatile concentrations were then subtracted from the reported $PM_{2.5}$ concentrations at each site, giving non-volatile $PM_{2.5}$. Non-volatile $PM_{2.5}$ was then subtracted from the non-volatile PM_{10} measured at each site, giving $PM_{10-2.5}$ concentrations estimated by Case 4. Figure 3.7 compares distributions of $PM_{10-2.5}$ concentrations estimated using Case 3 and Case 4. Case 4 CAMP and DMAS means are, respectively, 1.40 and 2.66 μg/m^3 higher than means of values estimated using Case 3, and 5th percentile values are no longer negative. COVs decreased to 0.56 for CAMP and DMAS. Correlations between CCRUSH Denver sites and CDPHE sites were increased by 0-6%.

Figure 3.7 Box plots of CAMP and DMAS $PM_{10\text{-}2.5}$ concentrations using Case 3 (uncorrected) and Case 4 (corrected) estimations

CDPHE $PM_{10-2.5}$ Correction Comparison
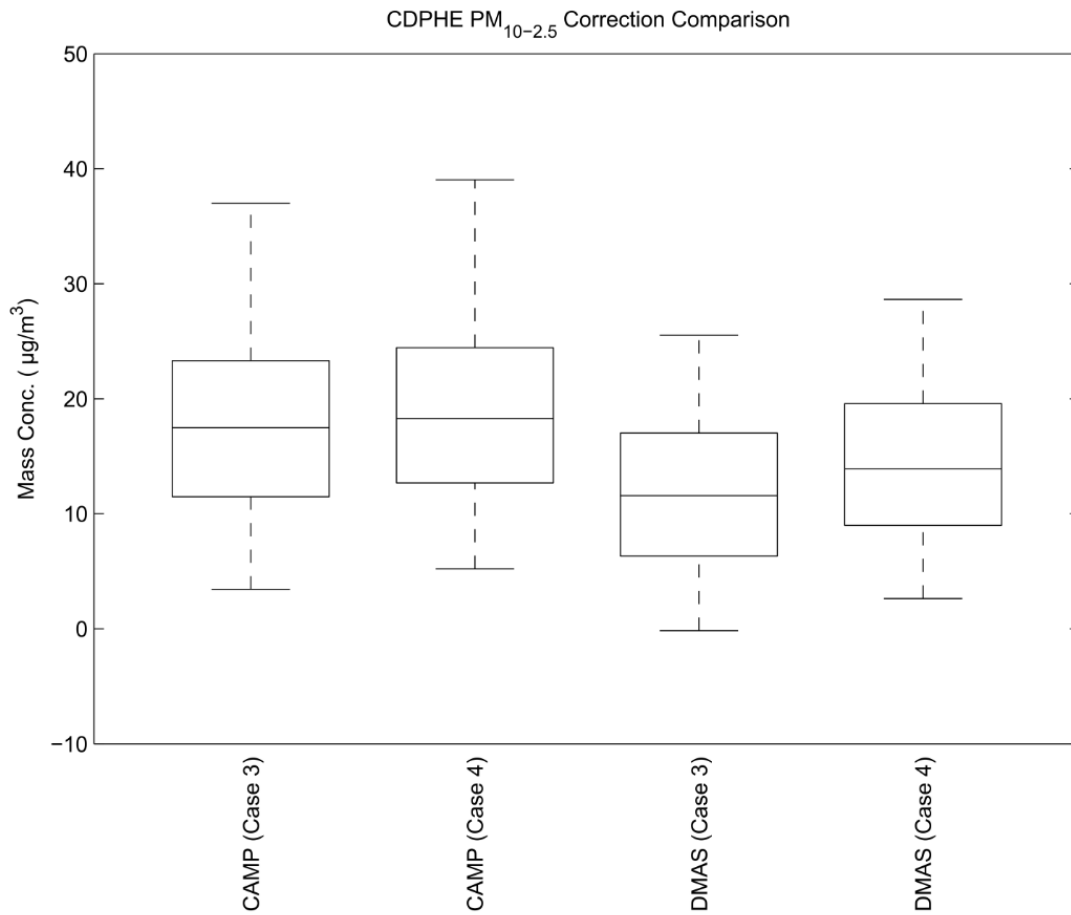
3.4 DISCUSSION

This analysis first addressed possible errors in $PM_{10-2.5}$ estimation when using a

combination of measurements from TEOMs equipped and not equipped with FDMS. Median

daily average $PM_{10-2.5}$ concentrations at the three CCRUSH sites were on average biased by 2.4

$\mu g/m^3$ (25%) to -2.3 $\mu g/m^3$ (-24%) for Case 2 and 3 estimations. In 2006, the EPA proposed a

24-hour average $PM_{10-2.5}$ National Ambient Air Quality Standard (NAAQS) that would replace

the current PM_{10} standard. This proposed $PM_{10-2.5}$ NAAQS was to be evaluated as the mean of

the 98th percentile daily average over three years (US EPA, 2006). Although not adopted at the

time, such an assessment of compliance with the standard would be significantly affected by the

extreme value biases like those seen in this analysis, with 95th percentiles biased by 2.85 to -

2.18 $\mu g/m^3$ for Case 2 and 3, respectively. Case 4 concentrations closely estimated mean and

extreme values of Case 1 concentrations due to the low concentrations of $PM_{10-2.5}$ semi-volatile

material in Colorado, which were on average less than 0.1 $\mu g/m^3$. Estimation of $PM_{10-2.5}$ mass

concentration using non-volatile (or base) PM_{10} and $PM_{2.5}$ concentrations from collocated

monitors may be a low-cost option for monitoring $PM_{10-2.5}$ in areas with low $PM_{10-2.5}$ semi-volatile

mass concentrations, though equivalency testing of this method is out of the scope of this study.

Such concentrations can be downloaded from all TEOM units.

Errors in the Case 2-4 $PM_{10-2.5}$ time series can be viewed as having two components.

One is the mean absolute bias discussed above that is related to the average mass of the

unmeasured semi-volatile fraction. The second component is the added variability of the semi-

volatile fraction time series. Because $PM_{2.5}$ and PM_{10} semi-volatile concentrations tended to be

normally distributed and uncorrelated with $PM_{10-2.5}$ concentrations ($0.01 < \rho < 0.14$), the variability

added to the $PM_{10-2.5}$ time series with the above subtraction methods can be viewed as

classical-type error as discussed in the Goldman et al. (2011) study. In the study, classical-type

error is defined as measurements that vary randomly around the true value. Differences in

correlations discussed in the *Biases in Spatial Comparisons* section above were due to the addition of this type of error. The COV of biased data is affected by both the absolute mean bias and the increased variability associated with classical error, typically leading to an overestimation of temporal variability. Averaged across sites, the ratio of the standard deviation of Cases 2-4 to Case 1 is 1.03, 1.04, and 1.00, respectively, showing Case 2 and 3 have only slight increases in variability due to this added measurement error. Like the COV, homogeneity estimates between sites using biased data will be affected by both the absolute mean bias and increased variability, resulting in both increases and decreases in the CCC depending on the site pair and bias direction (positive or negative). As shown by Goldman et al. (2011), adding classical-type measurement error to a data set has a significant attenuation effect on estimations of pollutant relative risk from time series epidemiological studies, both on a per-unit measurement and an IQR increase in concentrations basis. This suggests that if historical health studies utilized Case 2-4 estimated $PM_{10-2.5}$ concentrations, they may have underestimated the relative risk of health effects of $PM_{10-2.5}$.

The relative influence of the estimation error is site dependent due to larger differences in mean $PM_{10-2.5}$ concentrations between sites compared to the differences in mean semi-volatile concentrations between sites. For example, the standard deviation of 24-hour averaged urban-influenced ALS $PM_{2.5}$ semi-volatile concentrations is 1.49 $\mu g/m^3$, about 10% of the average ALS $PM_{10-2.5}$ concentration. For the more residential site, EDI, this ratio is 24%, explaining why differences in correlation estimates were largest for EDI and smallest for ALS; the random variability of the semi-volatile concentrations included in the biased time series is more significant for a site with a smaller mean $PM_{10-2.5}$ concentration. Areas with a high fractional contribution of semi-volatile material to the fine particulate mode and comparatively low $PM_{10-2.5}$ mass concentrations will be most affected by the errors addressed in this analysis.

PM$_{2.5}$ semi-volatile concentrations tended to scale with total concentrations at a similar rate across all sites in Colorado as shown in Figures 3.4a and 3.4b above and Figure 3.8 below.

Regression slopes ranged from 0.25 to 0.29. The three sites near heavy traffic (ALS, CAMP, DMAS) had regression slopes of 0.25, while EDI and MAP, an urban background site and a rural site, had slightly increased slopes. Intercepts differed between regressions, ranging from - 0.53 for DMAS to 0.15 for CAMP. Days of high total (> 25 µg/m^3) and semi-volatile (> 7 µg/m^3) PM$_{2.5}$ concentrations are associated with days with temperatures less than 0°C at all sites. This trend is likely due to stagnant air masses that occur frequently during the winter and spring in the Front Range region of Colorado, though further analysis is required to test this hypothesis. Additional analyses of this data set will include understanding the spatiotemporal trends of the PM$_{2.5}$ semi-volatile fraction, and how meteorological conditions relate to changes in semi-volatile concentrations.

Figure 3.8 Scatter plots and linear regressions between daily average PM$_{2.5}$ semi-volatile and total mass concentrations for ALS, EDI, MAP and all CCRUSH sites for data from the entire CCRUSH campaign
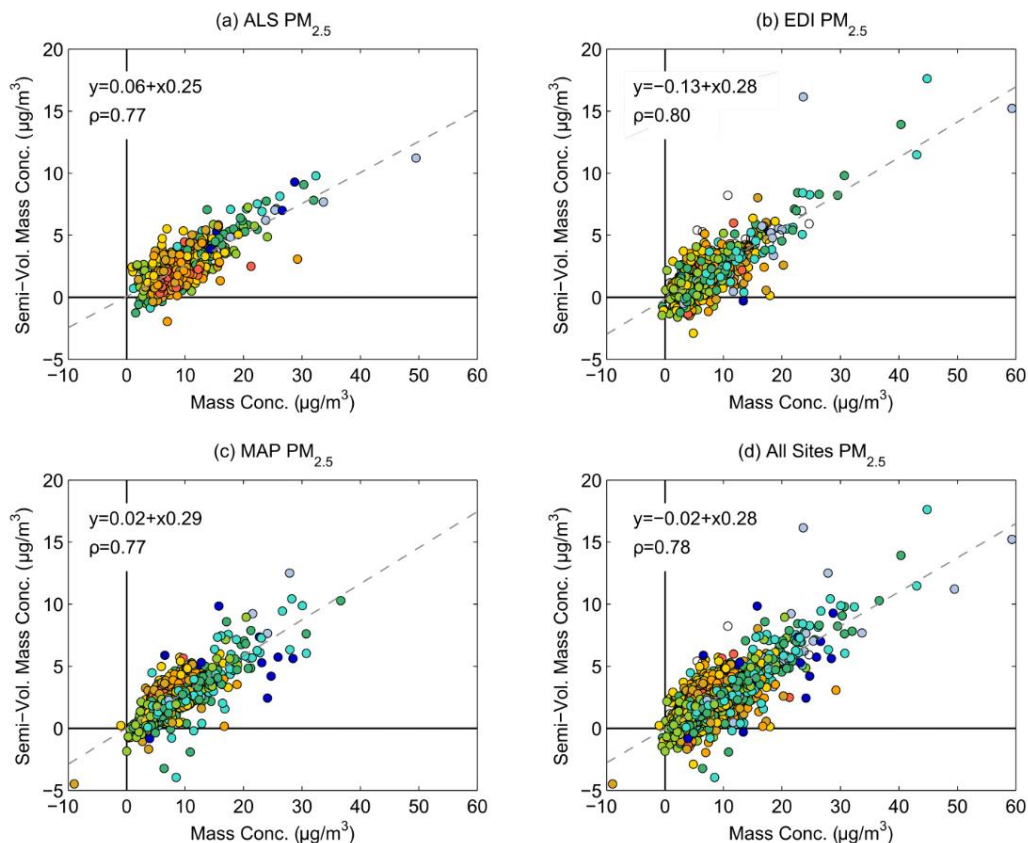
Two models were developed, one for each CDPHE site in Denver, to correct known

errors in $PM_{10-2.5}$ concentrations that arise from using the subtraction method of estimation with

collocated FDMS-equipped $PM_{2.5}$ TEOMs and PM_{10} TEOMs without semi-volatile mass loss

correction. Each model was based on the linear regression relationship between daily averaged

$PM_{2.5}$ semi-volatile and total mass concentrations. After estimating $PM_{2.5}$ semi-volatile

concentrations for each site throughout the CCRUSH campaign, $PM_{2.5}$ non-volatile mass

concentrations were calculated and subtracted from collocated PM_{10} non-volatile mass

concentration measurements. This allowed estimation of $PM_{10-2.5}$ using Case 4, which subtracts

non-volatile $PM_{2.5}$ from non-volatile PM_{10} and closely estimates unbiased Case 1

concentrations. After the correction, CAMP and DMAS $PM_{10-2.5}$ concentrations were on average

increased by 1.40 and 2.66 $\mu g/m^3$, or 9.1% and 22.2%, respectively, and showed a slight

increase in spatial correlation estimates and a decrease in temporal variability estimates.

In summary, collocated PM_{10} and $PM_{2.5}$ TEOM units that quantify semi-volatile mass loss

from filter surfaces are recommended for monitoring $PM_{10-2.5}$, though in areas with low semi-

volatile mass concentrations in the coarse fraction, non-volatile mass concentrations may be

used as a close estimate of the actual mass concentrations. Estimating $PM_{10-2.5}$ concentrations

using collocated TEOMs with a mixture of FDMS-equipped and non-FDMS-equipped units

introduces errors in the resultant mass concentration estimations. These errors are directly

related to the unmeasured semi-volatile fraction and were shown to affect estimates of spatial

and temporal variability, and bias median concentrations by up to 25% in Colorado. These

results are impactful for both the regulatory community concerned over using high-quality data

to assess air quality standards and the epidemiological community which is actively researching

links between coarse particulate matter and negative public health effects.

To correct for such biases in $PM_{10-2.5}$ data collected by the CDPHE at two sites in Denver

during the CCRUSH campaign, two regression models were developed to quantify the

unmeasured semi-volatile fraction at each site, leading to $PM_{10-2.5}$ concentration estimations

based on the non-volatile fraction of PM_{10} and $PM_{2.5}$. The US EPA implemented a TEOM correction factor with the same goal, but their correction model is not representative of the true relationship between $PM_{2.5}$ total and semi-volatile fractions at specific sites due to spatial variability in the relationship. Site specific semi-volatile correction models are recommended where collocated non-volatile PM_{10} and $PM_{2.5}$ concentrations are not available. Other correction models, such as using spatial relationships to predict semi-volatile concentrations, are also recommended to be considered, but were not applicable in the present study.

3.5 ACKNOWLEDGEMENTS

3.6 REFERENCES

Almeida, S.M., Pio, C.A., Freitas, M.C., Reis, M.A., and Trancoso, M.A. 2006. Source apportionment of atmospheric urban aerosol based on weekdays/weekend variability: evaluation of road re-suspended dust contribution. *Atmospheric Environment*. 40:2058-2067.

Boreson, J., Dillner, A.M., and Peccia, J. 2004. Correlating bioaerosol load with PM2.5 and PM10cf concentrations: a comparison between natural desert and urban-fringe aerosols. *Atmospheric Environment*. 38:6029-6041.

Brunekreef, B., and Forsberg, B. 2005. Epidemiological evidence of effects of coarse airborne particles on health. *European Respiratory Journal.* 26:309-318.

Chang, H.H., Peng, R.D., and Dominici, F. 2011. Estimating the acute health effects of coarse particulate matter accounting for exposure measurement error. *Biostatistics*. 12(4):637-652.

Chen, Y., Yang, Q., Krewski, D., Burnett, R.T., Shi, Y., and McGrail, K.M. 2005. The effect of coarse ambient particulate matter on first, second, and overall hospital admissions for respiratory disease among the elderly. *Inhalation Toxicology*. 17:649-655.

Cheung, K., Daher, N., Kam, W., Shafer, M.M., Ning, Z., Shauer, J.J., and Sioutas, C. 2011. Spatial and temporal variation of chemical composition and mass closure of ambient coarse particulate matter ($PM_{10-2.5}$) in the Los Angeles area. *Atmospheric Environment.* 45:2651-2662.

Clements, N., Piedrahita, R., Ortega, J., Peel, J.L., Hannigan, M., Miller, S.L., and Milford, J.B. 2012. Characterization and nonparametric regression of rural and urban coarse particulate matter mass concentrations in northeastern Colorado. *Aerosol Science and Technology*. 46(1):108-123.

Goldman, G.T., Mulholland, J.A., Russell, A.G., Strickland, M.J., Klein, M., Waller, L.A., Tolbert, P.E. 2011. Impact of exposure measurement error in air pollution epidemiology: effect of error type in time-series studies. *Environmental Health*, 10:61.

Green, D., and Fuller, G.W. 2006. The implications of tapered element oscillating microbalance (TEOM) software configuration on particulate matter measurements in the UK and Europe. *Atmospheric Environment.* 40:5608-5616.

Green, D.C., Fuller, G.W., and Baker, T. 2009. Development and validation of the volatile correction model for PM_{10} – An empirical method for adjusting TEOM measurements for their loss of volatile particulate matter. *Atmospheric Environment.* 43:2132-2141.

Harrison, R.M., Jones, A.M., Gietl, J., Yin, J., and Green, D.C. 2012. Estimation of the contributions of brake dust, tire wear, and resuspension to nonexhaust traffic particles derived from atmospheric measurements. *Environmental Science and Technology.* 46:6523-6529.

Host, S., Larrieu, S., Pascal, L., Blanchard, M., Declercq, C., Fabre, P., Jusot, J.-F., Chardon, B., Le Tertre, A., Wagner, V., Prouvost, H., and Lefranc, A. 2008. Short-term associations between fine and coarse particles and hospital admissions for cardiorespiratory diseases in six French cities. 65:544-551.

Kan, H., London, S.J., Chen, G., Zhang, Y., Song, G., Zhao, N., Jiang, L., and Chen, B. 2007. Differentiating the effects of fine and coarse particles on daily mortality in Shanghai, China. *Environment International.* 33:376-384.

Kumar, P., Hopke, P.K., Raja, S., Casuccio, G., Lersch, T.L., and West, R.R. 2012. Characterization and heterogeneity of coarse particles across an urban area. *Atmospheric Environment.* 46:449-459.

Lagudu, U.R.K., Raja, S., Hopke, P.K., Chalupa, D.C., Utell, M.J., Casuccio, G., Lersch, T.L., and West, R.R. 2011. Heterogeneity of coarse particles in an urban area. *Environmental Science and Technology.* 45:3288-3296.

Lee, T., Yu, X.-Y., Ayres, B., Kreidenweis, S.M., Malm, W.C., and Collett, J.L.Jr. 2008. Observations of fine and coarse particle nitrate at several rural locations in the United States. *Atmospheric Environment.* 42:2720-2732.

Lin, L.I.-K. 1989. A concordance correlation coefficient to evaluate reproducibility. *Biometrics.* 45(1):255-268.

Lin, M., Stieb, D.M., and Chen, Y. 2005. Coarse particulate matter and hospitalizations for respiratory infections in children younger than 15 years in Toronto: A case-crossover analysis. *Pediatrics.* 116:e235-e240.

Lipsett, M.J., Tsai, F.C., Roger, L., Woo, M., and Ostro, B.D. 2006. Coarse particles and heart rate variability among older adults with coronary artery disease in the Coachella Valley, California. *Environmental Health Perspectives.* 114:1215-1220.

Malig, B.J., and Ostro, B.D. 2009. Coarse particles and mortality: evidence from a multi-city study in California. *Occupational and Environmental Medicine.* 66(12):832-839.

Malm, W.C., Pitchford, M.L., McDade, C., and Ashbaugh, L.L. 2007. Coarse particle speciation at selected locations in the rural continental United States. *Atmospheric Environment.* 41:2225-2239.

Meister, K., Johansson, C., and Forsberg, B. 2012. Estimated short-term effects of coarse particles on daily mortality in Stockholm, Sweden. *Environmental Health Perspectives.* 120:431-436.

Peng, R.D., Chang, H.H., Bell, M.L., McDermott, A., Zeger, S.L., Samet, J.M., and Dominici, F. 2008. Coarse particulate matter air pollution and hospital admissions for cardiovascular and respiratory diseases among Medicare patients. *JAMA.* 299(18):2172-2179.

Perez, L., Tobias, A., Querol, X., Kunzli, N., Pey, J., Alastuey, A., Viana, M., Valero, N., Gonzalez-Cabre, M., and Sunyer, J. 2008. Coarse particles from Saharan dust and daily mortality. *Epidemiology.* 19(6):800-807.

Polymenakou, P.N., Mandalakis, M., Stephanou, E.G., and Tselepides, A. 2008. Particle size distribution of airborne microorganisms and pathogens during an intense African dust event in the eastern Mediterranean. *Environmental Health Perspectives*. 116:292-296.

Puxbaum, H., and Tenze-Kunit, M. 2003. Size distribution and seasonal variation of atmospheric cellulose. *Atmospheric Environment*. 37:3693-3699.

Qiu, H., Yu, I.T-S., Tian, L., Wang, X., Tse, L.A., Tam, W., and Wong, T.W. 2012. Effects of coarse particulate matter on emergency hospital admissions for respiratory diseases: A time-series analysis in Hong Kong. *Environmental Health Perspectives*. 120:572-576.

Qiu, H., Yu, I.T.-S. Wang, X., Tian, L., Tse, L.A., and Wong, T.W. 2013. Differential effects of fine and coarse particles on daily emergency cardiovascular hospitalizations in Hong Kong. *Atmospheric Environment*. 64:296-302.

Sillanpaa, M., Hillamo, R., Saarikoski, S., Frey, A., Pennanen, A., Makkonen, U., Spolnik, Z., Van Grieken, R., Branis, M., Brunekreef, B., Chalbot, M.-C., Kuhlbusch, T., Sunyer, J., Kerminen, V.-M., Kulmala, M., and Salonen, R.O. 2006. Chemical composition and mass closure of particulate matter at six urban sites in Europe. *Atmospheric Environment*. 40:S212-S223.

Simoneit, B.R.T., Elias, V.O., Kobayashi, M., Kawamura, K., Rushdi, A.I., Medeiros, P.M., Rogge, W.F., and Didyk, B.M. 2004. Sugars – dominant water-soluble organic compounds in soils and characterization as tracers in atmospheric particulate matter. *Environmental Science and Technology*. 38:5939-5949.

Tecer, L.H., Alagha, O., Karaca, F., Tuncel, G., and Eldes, N. 2008. Particulate matter ($PM_{2.5}$, $PM_{10-2.5}$, and PM_{10}) and children's hospital admissions for asthma and respiratory diseases: A bidirectional case-crossover study. *Journal of Toxicology and Environmental Health, Part A: Current Issues*. 71(8):512-520.

US EPA. 2004. *US EPA Air Quality Criteria for Particulate Matter (Final Report, Oct, 2004)*. U.S. Environmental Protection Agency, Washington, DC, EPA 600/P-99/002aF-bF.

US EPA. 2006. 40 CFR Parts 53 and 58: Revisions to Ambient Air Monitoring Regulations; Proposed Rule. Federal Register, Vol. 71, No. 10, Part III.

Wang, H., and Shooter, D. 2005. Source apportionment of fine and coarse atmospheric particles in Auckland, New Zealand. *Science of the Total Environment*. 340:189-198.

Zanobetti, A., and Schwartz, J. 2009. The effect of fine and coarse particulate air pollution on mortality: A national analysis. *Environmental Health Perspectives*. 117:898-903.

3.7 SUPPLEMENTAL INFORMATION

Figure 3.S1 Regional map of the CCRUSH and CDPHE monitoring sites
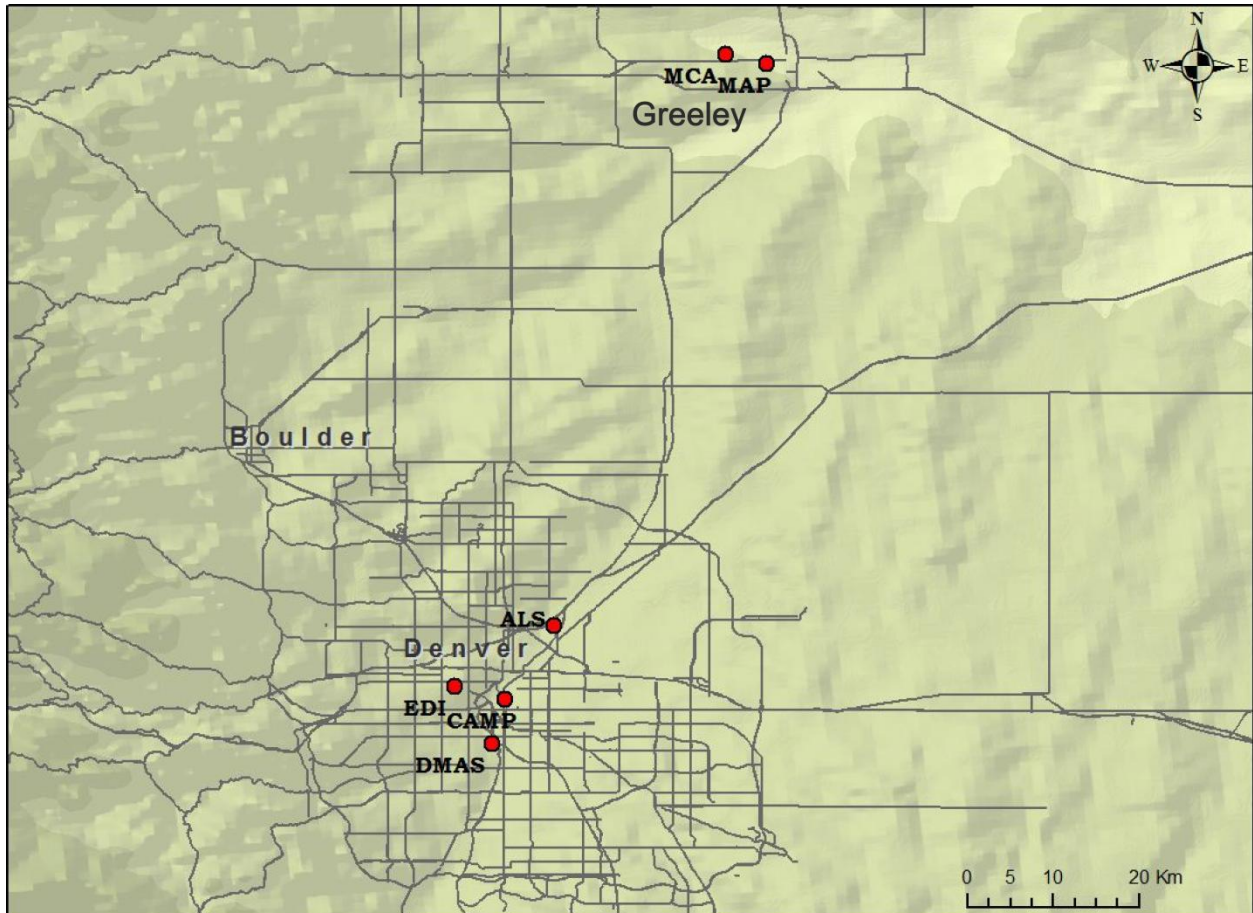
CHAPTER 4

SPATIOTEMPORAL AND METEOROLOGICAL TRENDS OF TOTAL AND SEMIVOLATILE PM$_{10\text{-}2.5}$ AND PM$_{2.5}$ MASS CONCENTRATIONS IN NORTHEASTERN COLORADO

Nicholas Clements[a], Jana B. Milford[a], Shelly L. Miller[a], Jennifer L. Peel[b], Michael P. Hannigan[a]

[a]Department of Mechanical Engineering, College of Engineering and Applied Science,

University of Colorado at Boulder, Boulder, CO, 80309-0427

[b]Department of Environmental and Radiological Health Sciences, Colorado State University,

Fort Collins, CO, 80523

4.0 ABSTRACT

Coarse ($PM_{10-2.5}$) and fine ($PM_{2.5}$) particulate matter in the atmosphere adversely affect human health and influence climate. While $PM_{2.5}$ is a relatively well-studied air pollutant, less is known about the sources and fate of $PM_{10-2.5}$. The Colorado Coarse Rural-Urban Sources and Health (CCRUSH) study measured $PM_{10-2.5}$ and $PM_{2.5}$, as well as the semivolatile (SV) fraction of each size regime ($PM_{2.5}$-SV, $PM_{10-2.5}$-SV), in urban (Denver, CO) and comparatively rural (Greeley, CO) environments for three years. $PM_{10-2.5}$ concentrations in Greeley were comparable to the urban-residential site in Denver, though traffic influenced sites in Denver had greatly elevated $PM_{10-2.5}$ concentrations. $PM_{10-2.5}$ tended to peak in March and throughout the summer and fall. $PM_{2.5}$ and $PM_{2.5}$-SV concentrations peaked in winter during periodic inversions. Diurnal peaks in $PM_{10-2.5}$ and $PM_{2.5}$ corresponded to the morning peak of traffic activity. $PM_{2.5}$-SV concentrations did not appear to be affected by anthropogenic activity, and negligible semivolatile material was observed in the coarse mode. Using moving correlation analysis, periods were identified for each site when either regional meteorology and/or local sources were the dominant driving factors in temporal variability of $PM_{10-2.5}$. For example, correlations between $PM_{10-2.5}$ and traffic counts peaked in winter at the two Denver sites located near interstate highways (DMAS and ALS). Nonparametric regression analysis focused on understanding spatial and temporal trends in the importance of local sources and resuspension at each site. Sites located near highways appeared to be most influenced by resuspension. Relative humidity and soil moisture appeared to inhibit resuspension at high levels and enhance resuspension at low levels. Overall it was shown that shifts in meteorological conditions (RH, soil moisture, and wind speed) and traffic drove the temporal variability of $PM_{10-2.5}$ in Colorado, the effects of which were enhanced when sites were near emission sources.

85

4.1 INTRODUCTION

Suspended ambient particulate matter (PM) in the troposphere is a complex mixture of inorganic and organic components with particle aerodynamic diameters ranging from a few nanometers to tens of micrometers. PM has been linked to multiple detrimental public health outcomes and plays an integral role in climatic processes, such as cloud formation and the solar radiation budget (US EPA, 2004; Wang et al., 2011; Stevens and Feingold, 2009; Kim and Ramanathan, 2008). Particle size reflects emission sources and composition, with fine particulate matter ($PM_{2.5}$, aerodynamic diameters less than 2.5 μm) being derived primarily from combustion and industrial sources or produced secondarily through atmospheric processing (Seinfeld and Pandis, 2006). Currently, the secondary formation of organic aerosols is a system under much investigation (e.g. Pohlker et al., 2012; Zaveri et al., 2012; Iinuma et al., 2013).

In contrast, coarse particulate matter ($PM_{10-2.5}$, aerodynamic diameters between 2.5 and 10 μm) is typically emitted from abrasive mechanical processes and resuspension, and can contain geogenic and road dust, brake and tire wear particles, heavy element-rich particles emitted from various industrial processes, sea-salt near coasts, road-salt in snowy regions, microbiological organisms, and soil organic matter (Kavouras et al., 2007; Harrison et al., 2012; Pakbin et al., 2011; Hwang et al., 2008; Cheung et al., 2012; Kumar et al., 2012; Clements et al., 2013a; Huffman et al., 2012; Huang et al., 2013). Due to the short atmospheric lifetime of $PM_{10-2.5}$ and the wide range of possible local sources, $PM_{10-2.5}$ composition is typically heterogeneous across ecological regions and within urban areas (Malm et al., 2007; Pakbin et al., 2011; Lagudu et al., 2011). $PM_{10-2.5}$ is poorly modeled using the Community Multiscale Air Quality (CMAQ) modeling system, suggesting both sources and transport of this pollutant are not well understood (Li et al., 2013a).

In their 2005 review of the epidemiological literature on the health risks of $PM_{2.5}$ and $PM_{10-2.5}$, Brunekreef and Forsberg concluded both fractions are harmful to human health. $PM_{2.5}$

consistently showed a significant relationship with mortality after adjustment for confounding pollutants. $PM_{10-2.5}$ showed inconsistent relationships with risk of mortality, and after adjustment for $PM_{2.5}$ the associations became null in the three studies that addressed confounding pollutants. The reviewers concluded that $PM_{10-2.5}$ may have a stronger short-term effect than $PM_{2.5}$ for some endpoints, like asthma and respiratory hospital admissions. Multiple $PM_{10-2.5}$ epidemiological studies conducted since 2005, that take confounding by $PM_{2.5}$ into account, confirmed the relationship between $PM_{10-2.5}$ and respiratory illness and asthma (Stafoggia et al., 2013; Malig et al., 2013; Qiu et al., 2012). Significant risks between mortality and $PM_{10-2.5}$ were also recently reported in studies using multi-pollutant epidemiological models (Meister et al., 2012; Perez et al., 2012; Malig and Ostro, 2009; Zanobetti and Schwartz, 2009). As highlighted by Wilson et al. (2005), epidemiological studies focusing on $PM_{10-2.5}$ must address the issue of spatial heterogeneity for proper exposure assessment, though few studies addressed the issue in their experimental design (e.g. Malig et al., 2013; Malig and Ostro, 2009).

Denver, Colorado's notorious 'Brown Cloud' was the subject of multiple monitoring campaigns in the 1970's and 1980's that were used to guide policy decisions for reducing air pollution in the region. Such studies provided a small set of supramicron particle composition data prior to the present analysis of $PM_{10-2.5}$ in Colorado. Countess et al. (1980) measured wintertime $PM_{15-3.5}$ (particulate matter with diameters between 15 and 3.5 μm), showing that crustal material contributed 60-80% of the observed mass, with smaller contributions from organic matter, inorganic ions, and lead salts. Source apportionment efforts based on elemental composition in both 1986 and 2013 identified soils and street salt as components of supramicron particles in Denver (Lewist et al., 1986; Clements et al., 2013a). Vehicle wear and catalysts were identified as $PM_{10-2.5}$ sources only in 2013. Vehicle wear, which includes both brake and tire wear particles, has been identified as a $PM_{10-2.5}$ emission source in urban areas and near roads (e.g. Pakbin et al., 2011; Harrison et al., 2012; Amato et al., 2013).

PM$_{2.5}$ was recently characterized in the Denver region by the Denver Aerosol Sources and Health (DASH) study, which collected daily PM$_{2.5}$ filter samples for five years at an elementary school near the urban core of Denver, and a subsequent year-long campaign collected PM$_{2.5}$ samples at four spatially distributed sites in Denver every sixth day. PM$_{2.5}$ mass concentrations averaged 7.95 µg/m^3, of which 12% was nitrate and 39% was organic carbon (Dutton et al., 2009). Strong seasonality in many PM$_{2.5}$ components were also measured, showing nitrate, EC, methoxyphenols, middle PAHs, methyl-PAHs, and hopanes peaked in the winter. Organic carbon, odd n-alkanes, and even n-alkanoic acids peaked in summer due to increased emissions and/or photochemical processing (Dutton et al., 2010b).

The Colorado Coarse Rural-Urban Sources and Health (CCRUSH) study aimed to compare the mass concentrations and composition of PM$_{10-2.5}$ in two distinctly different cities, urban Denver and comparatively rural Greeley, Colorado. To accomplish this goal, continuous PM$_{10-2.5}$ and PM$_{2.5}$ mass concentrations were collected for roughly three years (Jan. 2009 - Apr. 2012) and a year of PM$_{10-2.5}$ and PM$_{2.5}$ filter samples (Feb. 2010 - Mar. 2011) were collected every sixth day for compositional analyses. The continuous particulate monitor used in the CCRUSH study, the tapered element oscillating microbalance (TEOM) model 1405-DF, is a semi-continuous ambient particulate sampler that is dichotomous, measuring PM$_{10-2.5}$ and PM$_{2.5}$ directly with the inclusion of a virtual impactor (VI) after the PM$_{10}$ inlet. The TEOM 1405-DF also quantifies the loss of semivolatile (SV) material from heated collection filters, providing total and semivolatile mass concentrations on an hourly-average basis. 'Semivolatile,' in the context of the TEOM instrument measurements, is defined as any particulate bound substance that will evaporate at temperatures up to 30°C. Ammonium nitrate and semivolatile organic matter were shown to explain the majority of PM$_{2.5}$ semivolatile material, as measured by TEOMs, in Fresno, California, United States, Paris, France, and Beijing, China (Grover et al., 2006; Favez et al., 2007; Sciare et al., 2007).

This study explored the factors that drove temporal and spatial variability of $PM_{10-2.5}$ and $PM_{2.5}$ total and semivolatile concentrations in northeastern Colorado. Temporal variability was assessed on multiple timescales, and diurnal patterns on weekdays and weekends revealed the impact of anthropogenic activites on mass concentrations. Moving correlation and nonparametric regression analyses were used to explore the complex relationships between meteorological variables and $PM_{10-2.5}$ mass concentrations. A focus was placed on understanding the dynamics between $PM_{10-2.5}$ concentrations, traffic, wind conditions, relative humidity, and soil moisture.

4.2 MATERIALS AND METHODS

4.2.1 Monitoring Sites

The CCRUSH monitoring campaign, running from 1/1/2009 to 4/30/2012, took place at four elementary schools, two located in Denver and two in Greeley. Data from two additional pollutant monitoring sites operated by the Colorado Department of Public Health and Environment (CDPHE), CAMP and DMAS, were included to provide additional insights into regional health effects and pollutant concentration trends. Detailed descriptions of CCRUSH and CDPHE monitoring sites can be found in previous publications from the CCRUSH study (Clements et al., 2012; Clements et al., 2013a; Clements et al., 2013b). Table 4.1 contains a description of the CCRUSH monitoring sites.

Table 4.1 Summary of the CCRUSH and CDPHE particulate monitoring sites

Monitoring Site	ALS (CCRUSH)	EDI (CCRUSH)	CAMP (CDPHE)	DMAS (CDPHE)	MAP (CCRUSH)	MCA (CCRUSH)
City	Denver	Denver	Denver	Denver	Greeley	Greeley
Coordinates	39.83N 104.94W	39.76N 105.04W	39.75N 104.99W	39.70N 105.00W	40.42N 104.71W	40.43N 104.77W
Start Date	1/26/2009	1/8/2009	11/20/2010	1/1/2009	1/16/2009	1/1/2009
End Date	9/29/2011	3/1/2012	4/30/2012	4/30/2012	2/2/2012	6/19/2009
Site Description	Industrial-Residential	Urban-Residential	Urban-Roadside	Urban-Roadside	Rural-Residential	Rural-Residential
Inlet Height (m)	6	9	6	5	9	10.5

Denver is the largest city in Colorado and in 2011 had an estimated metropolitan-area population of 2,599,504, about half of the state population (U.S. Census Bureau, 2012). In contrast, the much smaller community of Greeley, with a population of 95,357, is located 75 km north-northeast of Denver in Weld County (U.S. Census Bureau, 2012). As of 2007, Weld County contained 2.1 million acres dedicated to farming and raising livestock (U.S. Department

of Agriculture (USDA), 2007). For reference, Figure 4.S1 is a regional map of the CCRUSH, CDPHE, and meteorological sites included in this analysis.

The two CCRUSH monitors in Denver were located at Alsup Elementary School (ALS) and Edison Elementary School (EDI). ALS was a residential-industrial site northeast of the urban core of Denver and about 4.5 km east of the intersection of four major roadways (I-25, I-270, I-76, and US-36). Interstate-76 is located a half kilometer away from ALS and runs diagonally from west to north of the site. To the west of the site, between I-76 and ALS, is a gravel/concrete operation. EDI was an urban site located in a residential area west of the urban core of Denver. EDI is surrounded by gridded neighborhoods and notably tall deciduous trees, providing a slight vegetative canopy to the area. The CDPHE sites CAMP and DMAS are located in downtown Denver and 5 km south of downtown Denver, respectively. CAMP (AQS Site ID: 080310002) is a stand-alone building containing monitoring capabilities for multiple pollutants, including $PM_{2.5}$, PM_{10}, CO, NO_X, and SO_2. DMAS (AQS Site ID: 080310025) was part of the EPA NCore Multipollutant Monitoring Network and was located on the rooftop of the Denver Municipal Animal Shelter directly west of I-25. DMAS also has monitoring capabilities for multiple pollutants, including $PM_{2.5}$, PM_{10}, CO, and NO_Y.

The two CCRUSH sites in Greeley were located in residential areas, with McAuliffe Elementary School (MCA) located on the west side of town in the suburban fringe and Maplewood Elementary (MAP) located nearer to the town center. The two major roadways near Greeley, US-85 and US-34, had an order of magnitude less traffic per hour than the interstates in Denver (Table 4.S1) and are located 2.7 km east and 3.1 km south of MAP, respectively.

4.2.2 Particulate Matter Monitoring

A TEOM 1405-DF semi-continuous particulate monitor was operated at each CCRUSH site for three years, with the exception of MCA, where the TEOM was only operated for only six months before being shut down due to a leak in the instrument's Filter Dynamic Measurement

System (FDMS) linear-valve seals. The TEOM quantifies particulate concentrations by measuring changes in the oscillating frequency of a tapered glass element with a TEOM filter placed on its end as particles are deposited on the filter. Oscillating frequency is converted to deposited mass via a calibration coefficient and first principles. Reported mass concentrations are based on actual sample flow rates (Thermo Scientific, 2009). All monitors were placed in temperature controlled shelters on elementary school rooftops with the exception of MCA, where the monitor was placed in an attic with inlet tubing running through the ceiling onto the rooftop. At monthly intervals, all TEOM monitors were thoroughly cleaned and inspected, TEOM (TEOM TX40, Thermo Scientific) and FDMS (47mm TX40, Thermo Scientific) filters were changed, and flow rates were calibrated. Data was downloaded during each monthly visit and processed on-site to further identify possible instrument issues. Sites were visited every one to two weeks for general instrument inspection, performing flow audits, and to observe and log instrument conditions. All TEOM 1405-DF instruments were operated and maintained according to the manufacturer's specifications.

TEOM data processing details were presented in prior publications from the CCRUSH study (Clements et al., 2012; Clements et al., 2013b). Briefly, raw mass concentrations, which contain no interpolated values, were downloaded and corrected for the deposition of $PM_{2.5}$ in the $PM_{10-2.5}$ channel due to the VI. The TEOM 1405-DF quantifies concentrations of semi-volatile species with the use of the FDMS, which consists of a linear valve that diverts the sample flow to chilled FDMS filters (4°C), cleaning the sample stream. At six-minute intervals the FDMS valve changes position, switching between depositing sample particles on TEOM filters and flowing clean air across TEOM filters. TEOM filter mass change measured during the particle depositing mode measures the non-volatile particulate mass, and the mass change when clean air is flowing through collection filters measures the loss of semivolatile mass due to the heated TEOM filters (30°C). Summing the two fractions gives the total particulate mass concentration. Hourly and daily averages of $PM_{2.5}$ and $PM_{10-2.5}$ total, non-volatile, and semi-volatile mass

concentrations were calculated from the raw six-minute data for the whole CCRUSH data set. Hourly and daily averages missing more than 25% of the data from the specified time interval were censored due to lack of completeness.

Quality checked hourly-average PM_{10} and $PM_{2.5}$ total mass concentration data were provided by the CDPHE for the CAMP and DMAS monitoring sites. At both CDPHE sites, a PM_{10} TEOM without FDMS and a $PM_{2.5}$ TEOM with FDMS were collocated on site rooftops. CDPHE $PM_{10-2.5}$ concentrations were estimated by subtracting $PM_{2.5}$ from PM_{10} mass concentrations. PM_{10} concentrations, and subsequently $PM_{10-2.5}$ concentrations, were not available from CAMP from 1/1/2009 to 11/19/2010 due to a data logging issue with the TEOM. Due to the errors that are introduced by the subtraction-method when using a combination of TEOMs with and without semi-volatile mass loss correction, daily average CDPHE data containing this error were corrected following the methods of Clements et al. (2013b). This correction estimated the semivolatile fraction of $PM_{2.5}$ ($PM_{2.5}$-SV) from total $PM_{2.5}$ concentrations for the CAMP and DMAS time series using linear regression. Nine months of $PM_{2.5}$-SV and $PM_{2.5}$ data collected at each site from October 2011 through July 2012 were used to develop the correction models at each site. Modeled $PM_{2.5}$-SV concentrations were subtracted from total $PM_{2.5}$ concentrations, yielding nonvolatile $PM_{2.5}$ concentrations that were then subtracted from measurements from the collocated PM_{10} TEOM monitor to estimate $PM_{10-2.5}$. Due to the very low concentrations of $PM_{10-2.5}$ SVM in Colorado, this correction method was shown to closely estimate true $PM_{10-2.5}$ concentrations. Hourly averaged $PM_{10-2.5}$ concentrations could not be corrected due to the low coefficients of determination for the $PM_{2.5}$-SV vs. $PM_{2.5}$ linear regression relationships at CAMP and DMAS. Uncorrected CDPHE $PM_{10-2.5}$ hourly mass concentrations may be biased by up to 30%, on average. Such errors were shown to affect both spatial and temporal summary statistics (Clements et al., 2013b). CDPHE site data on the hourly average scale will be used sparingly in this analysis due to this uncertainty.

4.2.3 Meteorological, Gas-Phase Pollutant, and Traffic Count Data

Ambient temperature and relative humidity data were collected by each TEOM throughout the CCRUSH campaign. Meteorological data collected by the CDPHE include ambient temperature and wind conditions from CAMP; temperature, and wind conditions from DMAS; wind conditions from ALS; wind conditions from Carriage (CRG), a site 1.75 km southeast of EDI; and ambient temperature from the Greeley Weld County Tower site (GRET). CRG wind condition data will be considered for comparisons with EDI pollutant data as was done in Clements et al. (2012). Ambient temperature, relative humidity, and wind condition data sets were downloaded from the National Climatic Data Center (NCDC) for the Greeley Airport (GREA) site operated by NOAA (Site #: 24051/GXY). Soil moisture and temperature data were downloaded for the Nunn #1 site (NUN, SCAN Site #: 2017) located in Weld County and operated by the United States Department of Agriculture's National Resources Conservation Service. Soil moisture and temperature data is compared to air pollutant data collected in Greeley. From this set of meteorological variables, hourly and daily arithmetic averages were calculated for ambient temperature, relative humidity, soil moisture, and soil temperature, and vector averages were calculated for wind conditions.

CDPHE-monitored gas-phase pollutant concentrations were also provided with the particulate concentration data. Gas-phase pollutant data was provided from CAMP (NO, SO_2, CO), DMAS (O_3, NO, SO_2, CO), GRET (O_3, CO) and a site 1.5 km northwest of ALS located on the northwest side of I-76, WBY (O_3, NO, SO_2, CO). A summary of the monitoring capabilities of the meteorological and gaseous pollutant monitoring sites can be found in Table 4.S1. Hourly vehicle count data was downloaded from the Colorado Department of Transportation Data Explorer for I-25, I-70, I-76, and I-270 in Denver, and CO-257 and US-85 in Greeley. Traffic count site details and distances to nearest CCRUSH monitoring sites can be found in Table 4.S2 of the supplemental information.

4.2.4 Data Analysis

Multiple summary statistics were used to describe spatial and temporal variability in air pollutant time series. The coefficient of variability (COV), or the ratio of a time series standard deviation over the mean, is used to compare temporal variability. Pearson's correlation coefficient (ρ) summarizes the strength of linear trends, and is indicative of time series having similar temporal trends. The concordance correlation coefficient (CCC) accounts for correlation as well as divergence from the concordance, or 1:1 line, and is a measure of reproducibility (Lin, 1989). The CCC is useful in quantifying the spatial homogeneity of a pollutant, and can be compared to ρ directly through a bias correction factor (C_b), as shown in equation 1, where for time series from sites j and h, σ_j^2 and σ_h^2 are time series variances, σ_{jh} is the covariance, and μ_j and μ_h are time series means. A more common measure of spatial homogeneity, the coefficient of divergence (COD, equation 2), is also considered for comparison with other studies. In calculating the COD, X_{ij} and X_{ih} represent measurement i from monitoring sites j and h, respectively, and n is the total number of data points considered.

$$CCC = \frac{2\sigma_{jh}}{\sigma_j^2+\sigma_h^2+(\mu_j-\mu_h)^2} = \rho C_b \tag{1}$$

$$COD = \sqrt{\frac{1}{n}\sum_{i=1}^{n}\left(\frac{X_{ij}-X_{ih}}{X_{ij}+X_{ih}}\right)^2} \tag{2}$$

We focussed our analysis on the CCC instead of the COD because the CCC is directly comparable to correlation and the deviation from correlation can be explained by differences in mean values between the sites considered. Such comparisons are not possible with the COD as it follows a different range (0 to 1 for homogenously to heterogeneously distributed concentrations, respectively) and has no direct comparison with correlation. Bootstrap analyses comparing the two summary statistics over a range of simulated added variability showed the COD was also more sensitive to slight changes in time series variability than the CCC. This is because the COD is based on differences between individual measurements, while the CCC is

95

based on mean differences. A summary of regional heterogeneity is also possible through the use of the Overall Concordance Correlation Coefficient (OCCC, Barnhart et al., 2002).

Moving correlation analysis was performed using hourly averages of all site pairs for each particulate pollutant and between all relevant meteorological variables and each pollutant to assess temporal variability in linearity of such relationships. In the analysis, Pearson's correlation coefficient is computed for all data points falling within a moving window. A sensitivity analysis was performed to determine optimal window size, with a thirty-day moving window chosen to reflect general shifts in both mass concentrations and meteorological factors.

Nonparametric regression (NPR) was used to estimate trends between pollutant concentrations and meteorological conditions using the methods described in Clements et al. (2012). In short, the Nadaraya-Watson estimator is used to calculate weighted average concentrations within a moving window, the width of which is defined by the smoothing parameter ($\Delta\theta$). A Gaussian kernel was applied to all meteorological NPRs. Wind speed and direction regressions excluded 'calm' conditions, approximated as hours with wind speeds below 0.5 m/s. An optimal smoothing parameter for each meteorological variable and pollutant type was determined via leave-one-out cross validation (Henry et al., 2002). To perform leave-one-out cross validation, for each meteorological observation considered in the regression (W_j, j = 1...n), the jth concentration was estimated with the nonparametric regression, leaving out the jth observation as shown in equation 3. The optimal smoothing parameter minimized the sum of the squared errors ($V(\Delta\theta)$) between the observed (C_j) and the 'leave-one-out' estimated concentrations ($\bar{C}_j$), as shown in equation 4.

$$\bar{C}_j(W_j, \Delta\theta) = \frac{\sum_{i \neq j} K\left(\frac{W_j - W_i}{\Delta\theta}\right) C_i}{\sum_{i \neq j} K\left(\frac{W_j - W_i}{\Delta\theta}\right)} \tag{3}$$

$$V(\Delta\theta) = \sum_{j=1}^{n} \left(C_j - \bar{C}_j(W_j, \Delta\theta)\right)^2 \tag{4}$$

For each meteorological variable and pollutant pair considered, the optimal smoothing parameters from all sites were averaged together and this average smoothing parameter was used to assess final NPR relationships. Smoothing parameters used in this analysis for $PM_{10-2.5}$ were: 0.32 m/s for wind speed, 9.3° for wind direction, 3.25% for relative humidity, and 0.30% for soil moisture (MAP only). Smoothing parameters used in this analysis for $PM_{2.5}$ were: 0.24 m/s for wind speed, 6.7° for wind direction, 1.65% for relative humidity, and 0.30% for soil moisture (MAP only). Confidence intervals of regression lines were calculated using methods of Henry et al. (2002) and presented as dashed lines in all NPR figures. Due to the large size of the data sets considered, confidence intervals were often indiscernible from the trend line.

Gaussian-kernel smoothing was used for presentation of particulate matter data, meteorological data, and the moving correlation time series. A sensitivity analysis on smoothing parameters for each time series was performed and smoothing parameters that maintained seasonal trends and peaks but removed higher frequency variability were selected for use. Smoothing parameters implemented for each plot are included in plot captions.

4.3 RESULTS AND DISCUSSION

4.3.1 Summary Statistics

A statistical summary of the daily average CCRUSH and CDPHE particulate matter concentration data set is presented in Table 4.2. The highest mean $PM_{2.5}$ concentrations were measured at DMAS (10.15 µg/m^3) and ALS (9.02 µg/m^3). Both of these sites were located in semi-industrial parts of Denver and were less than 0.5 km from busy interstate highways. The lowest average $PM_{2.5}$ mass concentrations were measured east of downtown Denver at the residential EDI site. The average Denver $PM_{2.5}$ mass concentration over the whole CCRUSH campaign was 8.74 µg/m^3, which is similar to the average $PM_{2.5}$ concentration measured in Greeley. Peak $PM_{2.5}$ mass concentration values were similar at all sites; 95th percentiles ranged from 15.43 µg/m^3 at MCA to 18.18 µg/m^3 at DMAS.

Average $PM_{10-2.5}$ concentrations did not follow the same spatial pattern as $PM_{2.5}$. Instead, average $PM_{10-2.5}$ concentrations in Denver at CAMP (18.57 µg/m^3), ALS (15.30 µg/m^3), and DMAS (14.60 µg/m^3) were elevated substantially above concentrations measured at EDI (8.02 µg/m^3). As mentioned above, ALS and DMAS were located near major roadways, which likely contributed to the relatively high concentrations measured at those sites via emissions of road dust and vehicle wear particles. Though CAMP was roughly the same distance from the nearest major roadway as EDI, downtown traffic on nearby roads within 20 m of all sides of the CAMP site was a likely local $PM_{10-2.5}$ source. In Greeley, the average $PM_{10-2.5}$ concentration at MAP was 10.34 µg/m^3, falling between the concentrations measured at the traffic-influenced sites in Denver and the residential site, EDI. $PM_{10-2.5}$ 95th percentiles were roughly double those measured for $PM_{2.5}$, with traffic influenced sites having the highest peak concentrations. It should be noted that in nearly all statistical comparisons, Greeley particulate pollutant concentrations fall between those measured at EDI and the other traffic-influenced Denver sites. Within the context of $PM_{10-2.5}$ concentrations measured in the western United States as reported

98

by Li et al. (2013), Denver and Greeley concentrations were generally below the average measured across 50 sites (17.25 µg/m^3) and were similar to $PM_{10-2.5}$ concentrations in other urban environments including Seattle, WA (9.0 and 14.8 µg/m^3), Spokane, WA (15.9 µg/m^3), Salt Lake City, UT (11.1 and 12.7 µg/m^3), and multiple cities in California (e.g. San Diego, Sacramento, Anaheim, and Fresno; Li et al., 2013). Sites located in the arid-southwest (Arizona, New Mexico, and Texas) tended to have increased $PM_{10-2.5}$ concentrations compared to the rest of the western United States.

The COV was used to compare temporal variability of daily averages for each particulate size regime. $PM_{10-2.5}$ was more temporally variable (higher COV) than $PM_{2.5}$ at all sites except CAMP and EDI. The most temporally variable $PM_{10-2.5}$ concentrations were measured at ALS and MAP, with COVs of 0.68 and 0.69, respectively. Hourly $PM_{10-2.5}$ COVs were calculated for comparison with other sites in the western United States, which tended to be above 1.00 (Li et al., 2013). EDI, CAMP, and MAP had the lowest hourly COVs, at 0.96, 1.09, and 1.10, respectively. ALS and DMAS hourly COVs were much higher at 1.20 and 1.34, respectively. As shown in later sections, ALS and DMAS appear to be heavily affected by local sources, which drive the temporal variability at these sites higher than sites lacking local sources.

Table 4.2 Summary statistics of daily average particulate pollutant concentrations during the CCRUSH campaign (SV - semivolatile fraction)

Monitoring Site	ALS				EDI			
Particulate Fraction	$PM_{2.5}$ Total	$PM_{2.5}$ SV	$PM_{10-2.5}$ Total	$PM_{10-2.5}$ SV	$PM_{2.5}$ Total	$PM_{2.5}$ SV	$PM_{10-2.5}$ Total	$PM_{10-2.5}$ SV
Mean (St. Dev., µg/m^3)	9.02 (4.64)	2.32 (1.50)	15.30 (10.36)	0.20 (0.30)	7.66 (5.33)	2.05 (1.91)	8.02 (4.85)	0.02 (0.25)
Median (µg/m^3)	8.07	2.08	13.37	0.16	6.55	1.81	7.17	0.01
5th/95th Percentile (µg/m^3)	3.90/ 16.90	0.50/ 5.29	2.02/ 35.74	-0.20/ 0.72	2.14/ 16.92	-0.28/ 5.16	1.61/ 17.20	-0.35/ 0.44
COV	0.51	0.65	0.68	1.53	0.67	0.93	0.61	13.18
N (% Completeness)	755 (76%)				747 (65%)			
Monitoring Site	CAMP				DMAS			
Particulate Fraction	$PM_{2.5}$ Total	$PM_{2.5}$ SV[a]	$PM_{10-2.5}$ Total[b]	$PM_{10-2.5}$ SV[c]	$PM_{2.5}$ Total	$PM_{2.5}$ SV[a]	$PM_{10-2.5}$ Total[b]	$PM_{10-2.5}$ SV[c]
Mean (St. Dev., µg/m^3)	8.11 (5.08)	1.46 (1.25)	18.57 (10.46)	-	10.15 (4.51)	2.72 (1.14)	14.60 (8.20)	-
Median (µg/m^3)	7.09	1.21	17.47	-	9.30	2.50	13.89	-
5th/95th Percentile (µg/m^3)	2.91/ 17.64	0.18/ 3.80	3.44/ 37.00	-	4.95/ 18.18	1.40/ 4.74	2.62/ 28.63	-
COV	0.63	0.86	0.60	-	0.44	0.42	0.56	-
N (% Completeness)	505 (96%)	505 (96%)	448 (85%)	-	1097 (90%)	1097 (90%)	980 (81%)	-
Monitoring Site	MAP				MCA			
Particulate Fraction	$PM_{2.5}$ Total	$PM_{2.5}$ SV	$PM_{10-2.5}$ Total	$PM_{10-2.5}$ SV[d]	$PM_{2.5}$ Total	$PM_{2.5}$ SV	$PM_{10-2.5}$ Total	$PM_{10-2.5}$ SV
Mean (St. Dev., µg/m^3)	8.15 (4.79)	2.39 (1.80)	10.34 (7.11)	0.05 (0.38)	8.68 (4.29)	2.58 (1.54)	9.87 (7.74)	-0.06 (0.24)
Median (µg/m^3)	7.13	2.22	9.17	0.05	7.71	2.22	7.76	-0.05
5th/95th Percentile (µg/m^3)	2.60/ 17.64	0.10/ 5.41	1.63/ 22.89	-0.54/ 0.62	4.45/ 15.43	0.75/ 4.87	1.69/ 23.97	-0.39/ 0.29
COV	0.59	0.75	0.69	7.68	0.49	0.60	0.78	4.19
N (% Completeness)	822 ($PM_{10-2.5}$ SV: 788) (74%, $PM_{10-2.5}$ SV: 71%)				168 (99%)			

[a] Estimated using the regression models presented in Clements et al. (2013b)
[b] Corrected subtraction-method errors using the method of Clements et al. (2013b)
[c] $PM_{10-2.5}$ semivolatile concentrations were not measured at the CDPHE monitoring sites
[d] MAP $PM_{10-2.5}$ semivolatile concentrations were not available from 8/13/2009 to 9/18/2009, $PM_{10-2.5}$ base concentrations were used to estimate total $PM_{10-2.5}$ for this period

Semivolatile concentrations were measured in both particle size regimes, though

significant concentrations were measured exclusively in the $PM_{2.5}$ range. Average measured

PM$_{2.5}$ semivolatile concentrations (PM$_{2.5}$-SV) varied less between monitoring sites than did the

total PM$_{2.5}$ mass concentrations, differing by just 0.53 µg/m^3 between the minimum (EDI, 2.05

µg/m^3) and maximum (MCA, 2.58 µg/m^3) mean concentrations. PM$_{2.5}$ at the more rural MAP site

contained 29% semivolatile material on average, similar to percentages at both ALS (26%) and

EDI (27%). For comparison, PM$_{2.5}$ at a background site in Paris was found to be 23% and 18%

semivolatile material in winter and summer, respectively, using TEOM instruments (Favez et al.,

2007). The contribution of PM$_{10-2.5}$ semivolatile material to the total coarse particulate mass at

was the highest at ALS (1%), though the high level of instrument noise for this channel suggests

PM$_{10-2.5}$-SV concentrations were typically below instrument detection limits.

An interesting trend observed in Clements et al., (2013b) was that PM$_{2.5}$-SV

concentrations tended to vary linearly with total PM$_{2.5}$ concentrations at a similar rate at all sites,

with linear regression slopes ranging from 0.25 to 0.29 for ALS, EDI and MAP. Because

semivolatile concentrations were not measured at CAMP and DMAS for much of the study

period, PM$_{2.5}$-SV values shown in Table 4.2 for these sites were estimated via linear regression

with total PM$_{2.5}$ concentrations using the methods of Clements et al., 2013b. From these

predicted concentrations, DMAS was expected to have the highest PM$_{2.5}$-SV concentrations.

Experimental observations of the semi-volatile fraction at the CDPHE sites began in 2011 and

were considered when building the corrective models. Daily mean (±st.dev.) CAMP and DMAS

PM$_{2.5}$-SV concentrations measured from October 2011 to July 2012 were 1.62 (±1.79) and 2.95

(±2.08) µg/m^3, respectively, which are very similar to averages predicted for the CCRUSH

campaign.

The temporal variability of PM$_{2.5}$-SV concentrations was typically higher than for total

PM$_{2.5}$, though signal noise and detection limits may have been an issue at low semivolatile

concentrations. It is suspected that the measured response of PM$_{10-2.5}$-SV was largely

instrument noise and any measurable signal was below detection limits. For the semi-volatile

measurements, detection limits are not published by the instrument manufacturer and were not

assessed in this study. The largest semivolatile concentrations in the coarse size range were measured at ALS, averaging (st.dev.) just 0.20 (±0.30) µg/m^3. Low semivolatile concentrations in the coarse particle size range suggest that ammonium nitrate and semi-volatile organic matter are not found in large concentrations in the coarse mode in Colorado. Gas-phase nitric acid may still partition to the coarse mode via heterogeneous reactions with dust-related minerals (Usher et al., 2003), but the reaction product compounds are not volatile at 30°C. The slight signal in PM$_{10-2.5}$-SV at traffic-influenced ALS may be in part due to semivolatile PAHs, which have been measured at traffic sites in the coarse mode in California (Cheung et al., 2012). Semivolatile organic species have also been identified in the coarse mode during haze events in China (Wang et al., 2009).

4.3.2 Time Series Overview – Particulate Matter and Meteorology

The Front Range of Colorado consists of a series of cities and towns oriented north-south along the I-25 corridor, located at the far western edge of the Great Plains where the Rocky Mountains rise quickly to topographical prominence. Since the Denver 'Brown Cloud' episodes of the 1970's and 1980's, relationships between local meteorology and air pollutants have been well studied, though local meteorological impacts on PM$_{10-2.5}$ concentrations were not well characterized prior to the CCRUSH study.

Due to the semi-arid nature of the region and geographical location, Colorado experiences four distinct seasons characterized by cold, snowy winters; windy springs; hot summers; and a short fall characterized by a drastic cooling in ambient temperatures (Ray et al., 2008). Air mass movement in the region follows a mountain-valley flow pattern. The topographic features influencing this flow are the Rocky Mountains to the west and south and the Cheyenne Plateau to the north. The valley drains out the South Platte River valley, flowing from the south northwards through Denver towards Greeley (Haagenson,1979). Nighttime down-slope flow tends to transport air pollution generated and aged in Denver during the day towards Weld

county communities to the north. Persistent inversions are also common in wintertime and result in elevated pollution levels locally. The up-slope/down-slope flow pattern is sometimes interrupted by synoptic-scale meteorological events, such as low pressure systems in the south driving wind east to west in the spring, sometimes causing snowstorms (Neff, 1997). During summer and fall, afternoon thunderstorms are a common occurrence and are the result of daytime up-slope flow driving moisture upwards toward the Front Range where it accumulates (Toth and Johnson, 1985).

Smoothed ($\Delta\theta$ = 7 hours) time series of the meteorological conditions measured during the CCRUSH campaign are displayed in Figure 4.1. City-based values in Figure 4.1 are averages of values from all monitoring sites with meteorological data in each city. Average temperatures were similar in both cities and ranged from 22.1°C in summer to 1.6°C in winter. Relative humidity was typically higher in Greeley than Denver, with averages of 57.5% and 47.9%, respectively, and typically reached a minimum in March. Average wind speeds were about 1 m/s higher in Greeley (3.0 m/s) than Denver (2.0 m/s), and Greeley wind speeds were twice as variable with a standard deviation of 2.7 m/s versus 1.2 m/s in Denver. Peak wind speeds (95th percentiles) in Greeley were roughly twice those in Denver, measuring 8.8 and 4.2 m/s, respectively, suggesting Greeley tends to be influenced by strong gusts of wind more frequently than Denver. Average wind speeds were lowest during the summer, and spring was typically the windiest season. Large year-to-year differences were seen for relative humidity in general and for wind speed in winter and spring. Seasonal hodographs for ALS and MAP (Figures 4.S2 and 4.S3) clearly show the daily patterns of mountain valley flow along the South Platte River basin. In Denver, wind flow is typically from the southwest at night, transitioning to up-valley flow from the northeast during the day. In Greeley, down-slope flow runs from the northwest at night followed by flow from the southeast during the day. Seasonal wind roses are presented for ALS and MAP in the supplemental information (Figures 4.S4 and 4.S5).

Figure 4.1 Smoothed (Δθ=7 hours) time series of hourly average (a) Denver temperature (°C), (b) Greeley temperature (°C), (c) Denver relative humidity (%), (d) Greeley relative humidity (%), (e) Denver wind speed (m/s), and (f) Greeley wind speed (m/s)
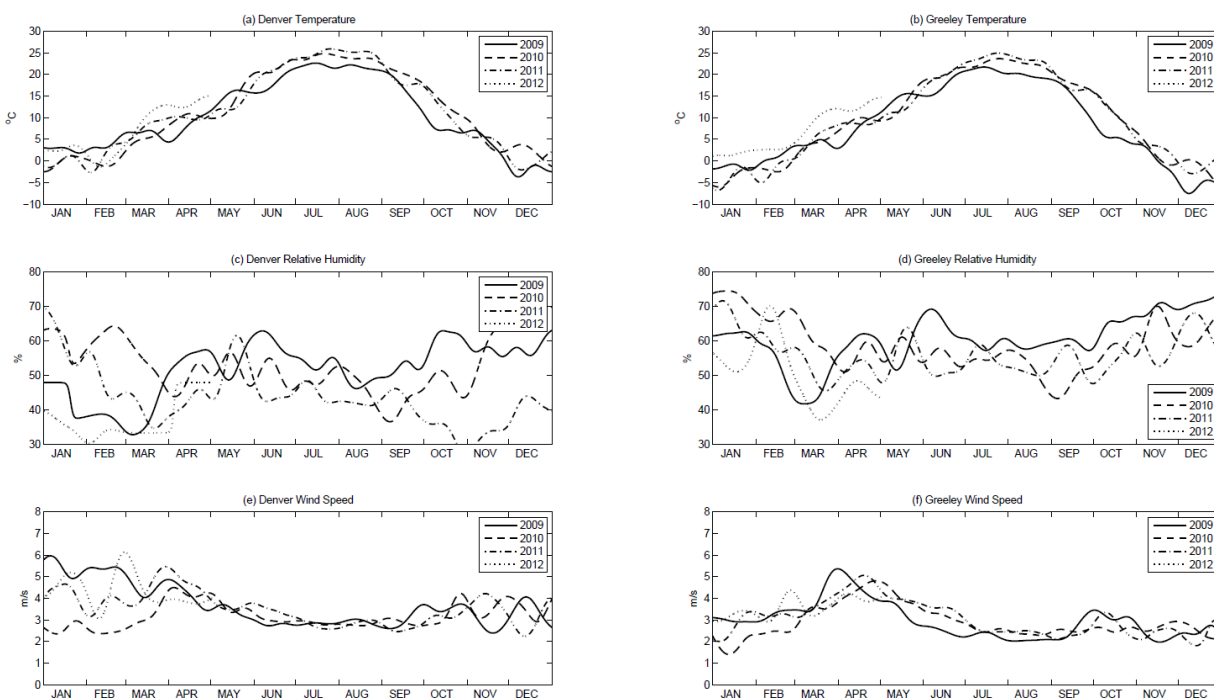
The smoothed (Δθ=7 hours) $PM_{10-2.5}$, $PM_{2.5}$, and $PM_{2.5}$-SV mass concentration time series are presented in Figure 4.2. $PM_{2.5}$ concentrations tended to increase at all sites simultaneously during the winter. The majority of wintertime $PM_{2.5}$ peaks appear to be episodic inversions, identified by simultaneous increases in CO and NO with peaks in both $PM_{2.5}$ and $PM_{2.5}$-SV. Wintertime inversions did not affect $PM_{10-2.5}$ to the same extent as they influence well-mixed pollutants, as $PM_{10-2.5}$ concentrations decreased during many of the periods of peaking $PM_{2.5}$. Calm winds and stable atmospheric conditions during inversions would inhibit turbulent resuspension and atmospheric dispersion, explaining $PM_{10-2.5}$ concentration decreases during these periods.

At first glance, temporal trends in $PM_{10-2.5}$ are less obvious than those for $PM_{2.5}$ due to the highly temporally variable nature of the pollutant and its sources. As noted above, Figure 4.2 shows the large differences in $PM_{10-2.5}$ mass concentrations between sites compared to $PM_{2.5}$.

The highest $PM_{10-2.5}$ concentrations were measured at CAMP during the summer and fall of 2011, though this monitoring site only operated through the second half of the CCRUSH study. There were no significant differences in year-to-year average particulate concentrations and very little differences in year-to-year COVs.

Figure 4.2 Smoothed ($\Delta\theta$=7 hours) time series of hourly average (a) $PM_{10-2.5}$ mass concentrations, (b) $PM_{2.5}$ mass concentrations, (c) $PM_{2.5}$-SV mass concentrations, and (d) gas-phase pollutant concentrations
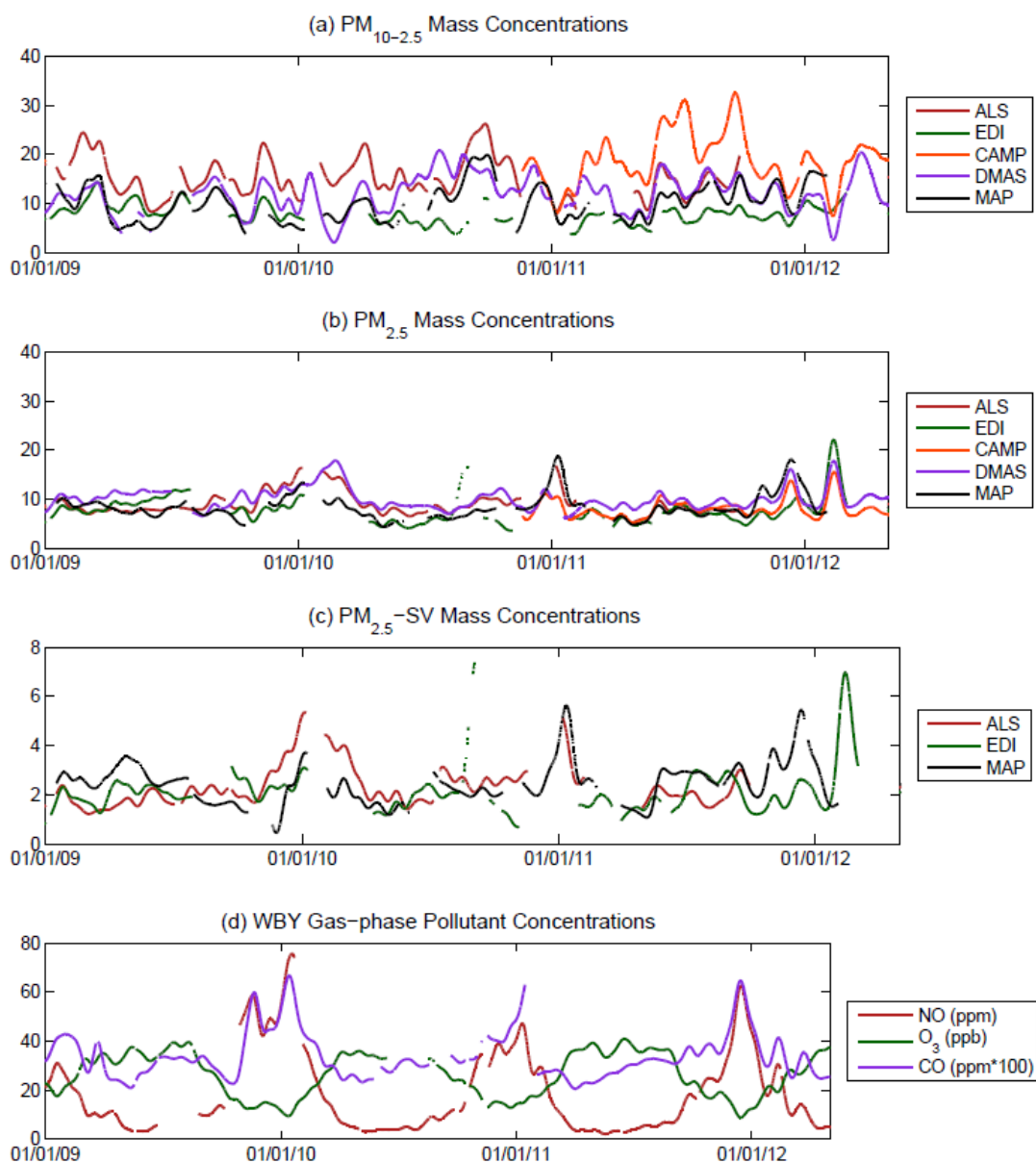
Particulate matter spatial variability and homogeneity were assessed using Pearson's

correlation coefficient (ρ) and the concordance correlation coefficient (CCC), respectively.

Comparisons between each monitoring site for daily averaged $PM_{2.5}$, $PM_{2.5}$-SV, and $PM_{10-2.5}$ are

presented in Table 4.3. In Table 4.3, correlation values are below the diagonal and above the

diagonal are CCCs for each comparison. Bias correction factors (C_b) are listed in parentheses

for comparisons between sites for the same pollutant. Within Denver, $PM_{2.5}$ tended to be more

correlated across sites than $PM_{10-2.5}$, with correlation coefficients ranging from 0.65 for the ALS-

EDI comparison to a value of 0.92 between CAMP and DMAS. $PM_{10-2.5}$ correlation coefficients

within Denver ranged from 0.59 (ALS-CAMP) to 0.79 (CAMP-DMAS). Correlations for $PM_{10-2.5}$

between MAP and the Denver sites were larger than those for $PM_{2.5}$ and, with the exception of

CAMP, were comparable to correlation values found between sites within Denver. High regional

correlations for $PM_{10-2.5}$ suggest regional shifts in meteorology are important drivers of temporal

variability for this pollutant. Correlations within Greeley were also high; the correlation

coefficients for $PM_{2.5}$ and $PM_{10-2.5}$ between MAP and MCA over six months of monitoring were

0.82 and 0.98, respectively (Clements et al., 2012).

$PM_{10-2.5}$ concentrations in Colorado tended to be more spatially correlated than observed

in previous studies using continuous monitors in Los Angeles, CA and the United Kingdom

(Moore et al., 2010; Liu and Harrison, 2011). Of all site comparisons from the western United

States described in Li et al. (2013) that utilized continuous monitors, only the four sites in El

Paso, TX had a range of correlation values ($0.49 < \rho < 0.76$) comparable to those observed in

Colorado. Other regions in the western US showing considerable spatial correlation of $PM_{10-2.5}$

concentrations included Albuquerque, NM ($\rho = 0.53$), three sites in North Dakota ($0.46 < \rho < 0.60$),

and three sites in northern Idaho/northeastern Washington ($0.48 < \rho < 0.61$; Li et al., 2013).

Spatial correlation values derived from filter samples, typically collected weekly or biweekly, or

passive samplers assess other time scales and thus are difficult to compare directly to

continuous data. Using 24-hour $PM_{10-2.5}$ filter samples collected at 10 sites throughout the Los Angeles metropolitan area, Pakbin et al. (2010) showed moderate to high correlation between urban Los Angeles sites ($0.48<\rho<0.80$) and lower correlations when compared to an industrial shipping site ($0.04<\rho<0.25$), and semi-rural sites in Riverside, California ($0.04<\rho<0.48$). Overall, spatial correlation of $PM_{10-2.5}$ seems to be strongly related to spatial variability in topography and meteorological conditions as well as to the proximity of local sources such as roadways.

The CCC represents correlation that has been penalized according to the mean difference in concentrations between two sites. Due to the larger differences in concentrations between sites, $PM_{10-2.5}$ tended to have lower CCC and C_b values (more heterogeneous) than $PM_{2.5}$ for comparisons within Denver. Regional CCCs were larger for $PM_{10-2.5}$ than $PM_{2.5}$ because of the low correlations found for $PM_{2.5}$ comparisons with MAP. Low to no correlation was found between $PM_{2.5}$ and $PM_{10-2.5}$ for all site pairs. C_b values show a distinct difference between homogenous $PM_{2.5}$ and the more heterogeneously distributed $PM_{10-2.5}$. $PM_{2.5}$ and $PM_{2.5}$-SV C_b values were all above 0.90, while C_b values for $PM_{10-2.5}$ comparisons within Denver ranged from 0.33 to 0.94. Classification of homogeneity based on the CCC and C_b will require additional studies utilizing the summary statistic, but based on results from the CCRUSH study, an approximate threshold for heterogeneity would be a measured C_b in the range between 0.70 and 0.90.

CODs for all site and particle size comparisons are available in Table 4.S3 for comparison with other studies. $PM_{2.5}$ CODs within Denver ranged from 0.15 to 0.27, and $PM_{10-2.5}$ CODs ranged from 0.23 to 0.47. For all comparisons within Denver, $PM_{2.5}$ CODs were lower than the associated $PM_{10-2.5}$ COD. $PM_{2.5}$ CODs across cities were slightly higher than within Denver and were comparable to within-Denver values for $PM_{10-2.5}$. Similar conclusions can be drawn from both the CCC and COD analyses: $PM_{2.5}$ is more homogenous than $PM_{10-2.5}$ in Denver but with comparisons between cities, the two fractions are similarly heterogeneous.

Table 4.3 Correlation (ρ, below the diagonal) and CCC (above the diagonal) values for spatial comparisons with daily averaged $PM_{2.5}$, $PM_{10-2.5}$, and $PM_{2.5}$-SV

ρ\CCC (C_b)		$PM_{2.5}$					$PM_{10-2.5}$					$PM_{2.5}$-SV		
		ALS	EDI	CAMP	DMAS	MAP	ALS	EDI	CAMP	DMAS	MAP	ALS	EDI	MAP
$PM_{2.5}$	ALS	1.00	0.62 (0.96)	0.82 (0.98)	0.71 (0.96)	0.56 (0.92)	0.10	0.28	-0.01	0.08	0.03	0.16	0.09	0.06
	EDI	0.65	1.00	0.72 (0.96)	0.66 (0.85)	0.34 (0.99)	-0.04	0.22	-0.08	-0.07	-0.06	0.12	0.25	0.08
	CAMP	0.83	0.75	1.00	0.86 (0.94)	0.37 (0.94)	0.12	0.26	0.05	0.05	0.07	0.12	0.22	0.11
	DMAS	0.74	0.78	0.92	1.00	0.37 (0.94)	0.03	0.21	0.01	-0.01	-0.05	0.08	0.11	0.04
	MAP	0.61	0.34	0.39	0.41	1.00	0.05	0.20	-0.01	0.06	0.14	0.13	0.05	0.22
$PM_{10-2.5}$	ALS	0.17	-0.10	0.19	0.06	0.11	1.00	0.40 (0.57)	0.38 (0.65)	0.68 (0.94)	0.57 (0.80)	-0.02	-0.03	-0.01
	EDI	0.28	0.22	0.26	0.24	0.20	0.70	1.00	0.20 (0.33)	0.43 (0.62)	0.58 (0.84)	-0.02	0.00	0.01
	CAMP	-0.03	-0.18	0.13	0.02	-0.02	0.59	0.62	1.00	0.66 (0.83)	0.28 (0.60)	-0.01	-0.02	0.00
	DMAS	0.13	-0.12	0.08	-0.02	0.09	0.72	0.70	0.79	1.00	0.60 (0.90)	-0.01	-0.03	0.00
	MAP	0.04	-0.08	0.09	-0.06	0.16	0.70	0.69	0.47	0.67	1.00	-0.04	-0.03	0.00
$PM_{2.5}$-SV	ALS	0.77	0.50	0.54	0.53	0.47	-0.14	-0.08	-0.16	-0.14	-0.20	1.00	0.53 (0.99)	0.37 (0.99)
	EDI	0.45	0.80	0.61	0.59	0.21	-0.24	0.01	-0.20	-0.19	-0.14	0.53	1.00	0.25 (0.96)
	MAP	0.30	0.25	0.28	0.23	0.77	-0.07	0.03	-0.01	0.00	0.01	0.37	0.26	1.00

Using nonparametric regression with wind direction, Clements et al. (2012) identified a concrete and gravel operation point source less than 0.5 km west of ALS that influences $PM_{10-2.5}$ concentrations measured at that site. Interstate-76, a line source for $PM_{10-2.5}$, is also located nearby, about 0.5 km away in the general direction of the gravel operation. The wind direction window in which concentrations were most affected by the gravel operation and traffic-related emissions was from 225 to 315 degrees, where average concentrations were over 25 μg/m^3, compared to all other wind directions for which concentrations averaged about 13 μg/m^3. To determine how spatial correlations are affected by nearby point sources, hourly data collected while wind was coming from the location of the gravel pit and I-76 (225°-315°) were removed

from the ALS time series and spatial correlations were computed using daily averages based on the censored hourly time series.

Spatial correlations for $PM_{10-2.5}$ ALS comparisons increased by 2% to 8% and homogeneity (CCC) decreased by 4% for the comparison with CAMP and increased by 11% to 19% for the other site comparisons after removing data affected by local sources. Comparisons with EDI and MAP were most affected. The large increase in CCC observed for the EDI and MAP comparisons (19% and 15%, respectively) was due to the decrease in mean ALS $PM_{10-2.5}$ concentrations from 15.30 µg/m^3 to 14.38 µg/m^3 after the adjustment. Homogeneity estimates with CAMP and DMAS are less affected due to the CDPHE sites having similar concentrations to ALS. After the adjustment, 2993 hourly measurements were removed. After censoring for 75% completeness when calculating daily averages, one daily average was removed due to a reduction in completeness. As shown in the seasonal wind rose for ALS in Figure 4.S4, wind does not typically blow from the direction of the gravel pit, and wind speeds from that direction were typically less than 5 m/s. It is likely that spatial correlations would be more affected if the local sources were oriented north-northeast or south of the site, the typical wind directions due to the mountain valley wind flow effects of the Front Range.

Hourly average data was used to assess temporal shifts in spatial correlations that may be related to general shifts in local source importance and meteorological factors. Moving correlation analysis was performed between all pairs of monitoring sites with a thirty-day window for $PM_{10-2.5}$ and $PM_{2.5}$. Figure 4.3 shows the smoothed (Δθ=4 hours) annual correlation relationships between ALS $PM_{10-2.5}$ and $PM_{10-2.5}$ measured at EDI, MAP, and DMAS. CAMP and MCA were excluded because the time series were too short to assess annual trends. Commonly during the year, spatial correlations peaked between March and June, followed by a period of decrease in correlation throughout the summer, increasing again in the fall. This pattern was seen both within Denver and between sites in different cities, as shown for MAP $PM_{10-2.5}$ comparisons in Figure 4.S6. The shift in $PM_{10-2.5}$ spatial correlations between spring and

summer/fall is likely due to shifts in regional meteorological conditions and the importance of local $PM_{10-2.5}$ source emissions during this time.

Moving correlation analysis was also performed using $PM_{2.5}$ concentrations. ALS tended to be poorly correlated with other sites in Denver in summer and early fall months, though correlations during the rest of the year showed less consistent trends year-to-year than those observed for $PM_{10-2.5}$ (Figure 4.S7). Moving $PM_{2.5}$ correlations between Denver and Greeley sites were consistently low throughout the study.

Figure 4.3 Annual moving correlation plot for hourly average $PM_{10-2.5}$ spatial comparisons between ALS and (a) EDI, (b) MAP, and (c) DMAS (Gaussian kernel smoothed, Δθ=4 hours)
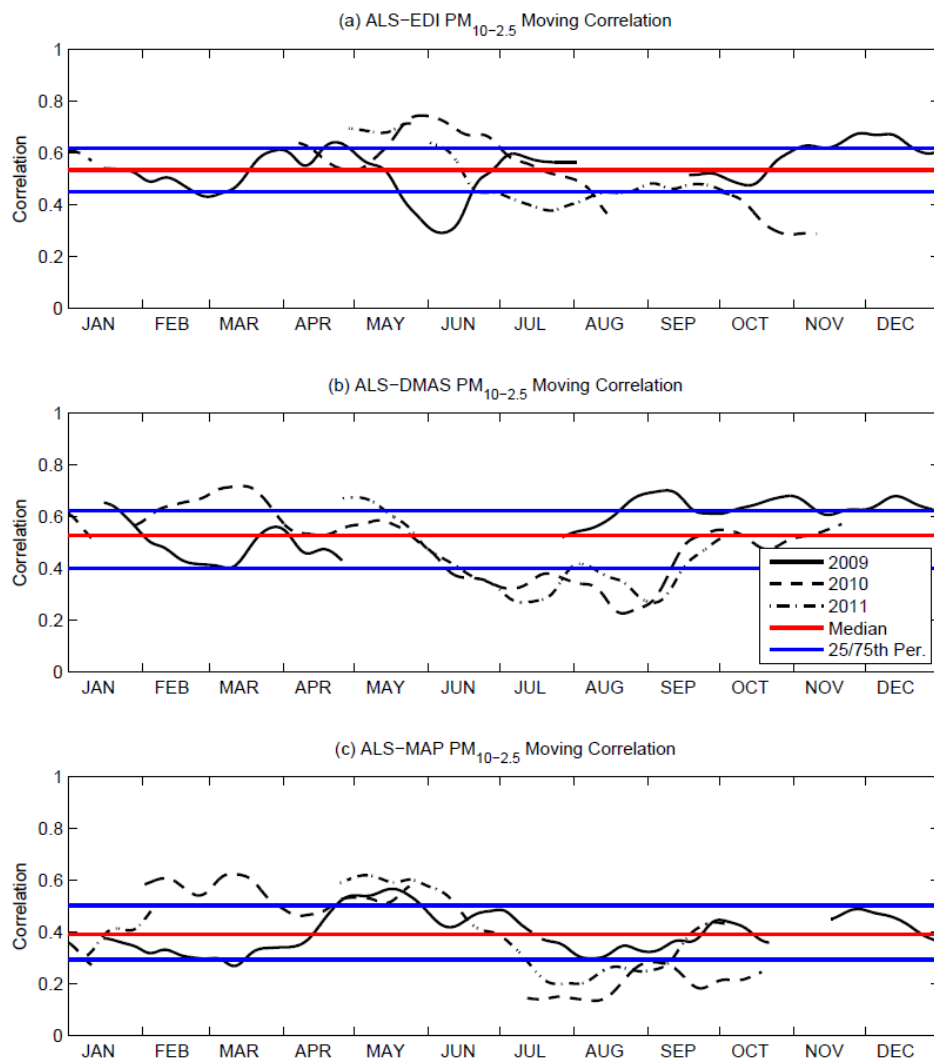
Because the CCRUSH sampling campaign spanned several years and collected data at the hourly average time resolution, temporal trends can be observed on multiple timescales. To assess seasonal shifts in concentrations, monthly medians of daily average particulate mass concentrations ($PM_{10-2.5}$, $PM_{2.5}$, and $PM_{2.5}$-SV) and gaseous pollutant concentrations (CO, NO, O_3) were calculated and are presented in Figure 4.4. $PM_{10-2.5}$ tended to peak in March, followed by a decrease in concentrations as spring progressed. The March $PM_{10-2.5}$ peak may be due to a decrease in regional RH, which is usually near its minimum in March. Concentrations peaked again starting at the beginning of summer, lasting until the end of fall. Across all sites, the month of September had the first or second highest median $PM_{10-2.5}$ concentrations. The exception was EDI, which had only slight peaks in March, September, and November. $PM_{10-2.5}$ in Greeley tended to increase throughout the summer, peaking distinctly in September and decreasing into the winter. Traffic influenced sites in Denver tended to vary together seasonally, peaking broadly over the summer and fall.

The annual pattern of $PM_{2.5}$ showed a peak in winter followed by a smaller peak in the middle of summer. Compared to the seasonal variability found in the coarse range, fine mode aerosol masses were relatively unvarying. $PM_{2.5}$-SV concentrations followed the trend of total fine PM, peaking in summer and winter. As expected, O_3 concentrations also peaked in summer, while CO and NO peaked in winter. $PM_{2.5}$ nonvolatile concentrations ($PM_{2.5}$ - $PM_{2.5}$-SV, not pictured) tended to peak only in winter, which suggests production of semivolatile material, likely semivolatile secondary organic matter, was driving the summertime peak in $PM_{2.5}$. Two recent source apportionment studies in Denver, Colorado found significant contributions to the $PM_{2.5}$ fraction from a light n-alkane/PAH factor during summer, which would contribute to the semivolatile fraction measured by the TEOM during this time (Xie et al., 2013). The summertime $PM_{2.5}$-SV peak was more pronounced at rural-MAP, possibly due to regional agricultural

biogenic VOC emissions, while the wintertime peak driven by nitrate formation was most

significant at traffic-influenced ALS.

Figure 4.4 Monthly median of daily average pollutant concentrations: (a) $PM_{10-2.5}$, (b) $PM_{2.5}$, (c) gas-phase pollutants (CO, NO, O_3), and (d) $PM_{2.5}$-SV
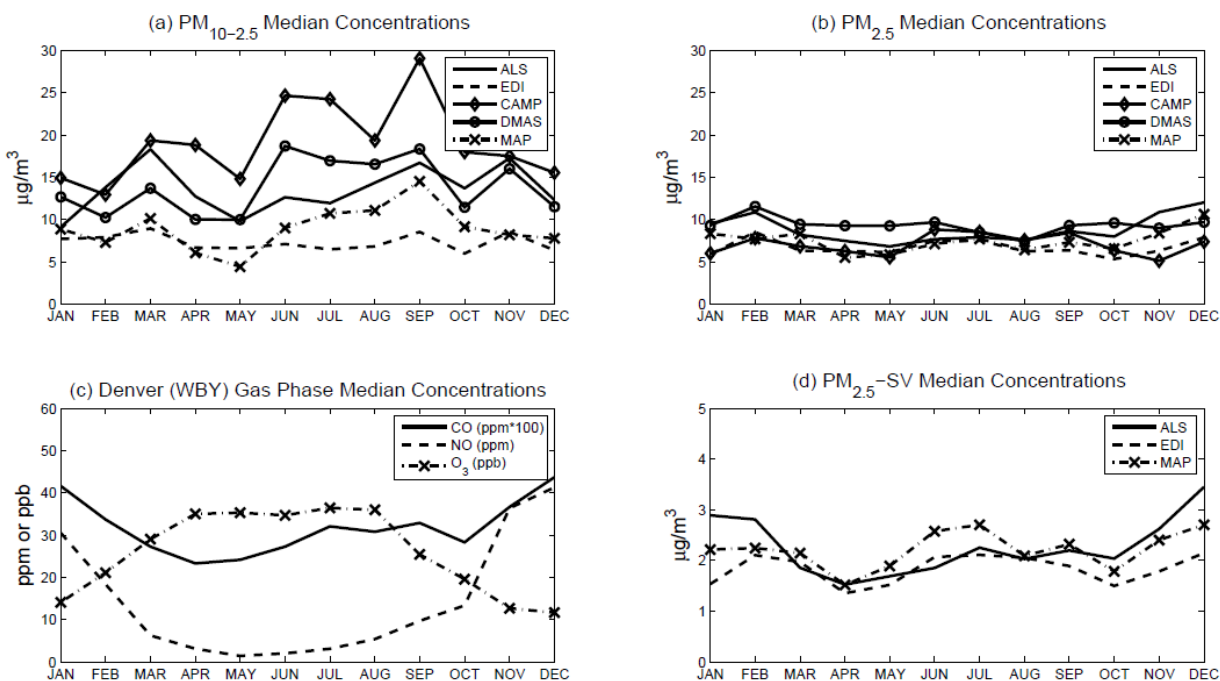
Assessing seasonal changes in $PM_{10-2.5}$ as a fraction of PM_{10} shows the increase in

$PM_{2.5}$ concentrations observed during winter, causing a decrease in $PM_{10-2.5}/PM_{10}$ ratios at all

sites (Figure 4.S8). Maximum monthly median $PM_{10-2.5}/PM_{10}$ ratios tended to occur in the fall at

all sites, simultaneously with peaking $PM_{10-2.5}$ concentrations. The urban-residential site EDI had

the lowest average (±st.dev.) $PM_{10-2.5}/PM_{10}$ ratio (51±21%), and MAP in Greeley had the second

lowest ratio (53±20%). The traffic influenced sites in Denver had the highest average ratios;

though ALS and DMAS ratios (59±28% and 56±19%, respectively) were lower than at

downtown-CAMP (70±15%). The average $PM_{10-2.5}/PM_{10}$ ratio across sites tended to increase as

proximity to local $PM_{10-2.5}$ emission sources decreased. A similar gradient in $PM_{10-2.5}/PM_{10}$ ratios

was observed in the United Kingdom, with curbside and roadside monitors having the highest

ratios (0.71 and 0.57 on average, respectively) and urban background or rural sites having the

lowest ratios (0.54-0.51; Liu and Harrison, 2011).

The proportion of semi-volatile material making up the total particulate mass showed

little seasonal variability for both the fine and coarse size fractions (Figure 4.S9). Slight peaks

were observed in monthly medians for the $PM_{2.5}$-SV/$PM_{2.5}$ ratio in winter at ALS, during fall at

EDI, and at the beginning of summer at MAP. Variability of the ratio within each month was

much larger than seasonal changes. It was hypothesized that during colder periods, this ratio

may increase due to more semivolatile material partitioning to the particulate phase. Instead, it

appears the total semivolatile material in the fine mode varies roughly linearly with total $PM_{2.5}$ in

Colorado throughout the year, as demonstrated by Clements et al., (2013b). The $PM_{10-2.5}$-

SV/$PM_{10-2.5}$ ratio was even less seasonally variable and, as Figure 4.S9 shows, often was an

insignificant fraction of the total $PM_{10-2.5}$.

Differences between weekday and weekend mass concentrations can demonstrate how

varying levels in anthropogenic activity are related to ambient pollutant concentrations. Using

the nonparametric Kruskal-Wallis Test with daily averages (5% significance level), it was

determined that $PM_{10-2.5}$ concentrations on weekdays were significantly higher than

concentrations from weekends at all sites (all p-values < 0.05). $PM_{2.5}$ weekday-weekend

comparisons showed significant differences at ALS and CAMP (p-values of 0.02 for both tests).

$PM_{2.5}$ semi-volatile concentrations showed no significant differences between weekdays and

weekends. Diurnal patterns of $PM_{2.5}$-SV concentrations showed no weekday-weekend

dependencies (Figure 4.S10), suggesting the decrease in anthropogenic activities on weekends

does not affect semi-volatile concentrations. Instead, $PM_{2.5}$-SV concentrations tended to peak

around noon and overnight, regardless of day of week.

Median $PM_{2.5}$ and $PM_{10-2.5}$ mass concentrations for each hour of the day are compared

for weekdays and weekends alongside traffic count medians in Figure 4.5. $PM_{2.5}$ peaked in the

morning on weekdays, a trend that nearly disappeared on weekends. Bimodal diurnal profiles were observed on weekdays for $PM_{10-2.5}$ at CAMP, DMAS, and MAP, with peaks in the morning (6:00-8:00 AM) and late afternoon (6:00-8:00 PM). On weekdays, ALS and EDI $PM_{10-2.5}$ peaked only in the morning. Comparing $PM_{10-2.5}$ on weekdays to weekends, the morning peak disappears. This trend can be explained partially by the lack of a morning peak in traffic, or morning 'rush hour', on the weekends. Morning peaks in mass concentrations and traffic occurred simultaneously between 6:00 and 7:00 AM on weekdays, concomitantly with the peak in morning traffic. Afternoon traffic counts were not greatly reduced on weekends, and the afternoon $PM_{10-2.5}$ peak observed on weekdays persisted through the weekend at CAMP and DMAS, though the magnitude of the peak was reduced. Morning and afternoon air pollutant peaks may also have been enhanced by the diurnal dynamics of the boundary layer height.

Figure 4.5 Diurnal trends (time-of-day medians) of (a) $PM_{2.5}$ on weekdays, (b) $PM_{2.5}$ on weekends, (c) $PM_{10-2.5}$ on weekdays, (d) $PM_{10-2.5}$ on weekends, (e) weekday traffic volumes, and (f) weekend traffic volumes
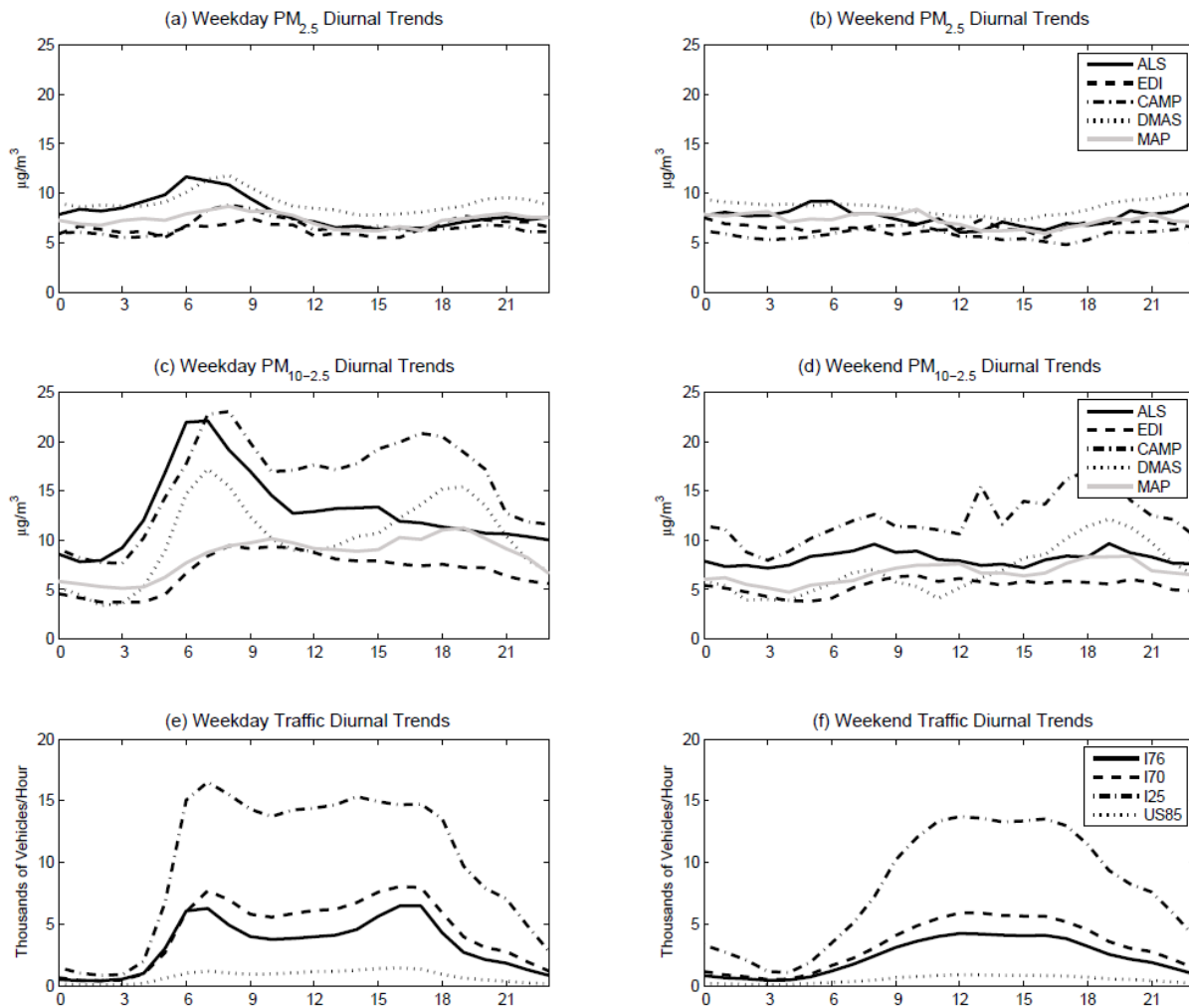
On the seasonal time scale, we observed major differences in morning peak magnitude for $PM_{10-2.5}$ measured at traffic-influenced sites. As shown in Figure 4.6, ALS, CAMP, and DMAS $PM_{10-2.5}$ median concentrations in the winter and spring reached 13-15 $\mu g/m^3$ during the morning hours. In summer and fall, peak $PM_{10-2.5}$ morning concentrations ranged from 15 to 20 $\mu g/m^3$. It is hypothesized that traffic-related emissions are largely turbulent resuspension of road dusts,and thse emissions increased during this period due to higher temperatures and lower soil moisture. Increases in the resuspension of road dusts during dry periods has been

115

demonstrated previously (Almeida et al., 2006). Charron et al. (2005) hypothesized that roadway conditions, including surficial moisture content, played a significant role in road dust resuspension rates. By observing compositional increases in $PM_{10-2.5}$ after rain events, Amato et al. (2013) suggested that traffic-related emissions depend heavily on the inhibition of resuspension due to particle moisture content. The diurnal pattern in $PM_{10-2.5}$ at EDI tended to not change seasonally. Interestingly, the afternoon peak observed in Greeley disappears during the spring, while throughout the rest of the year maximum hourly median concentrations of 10-14 $\mu g/m^3$ were measured between 6:00 and 9:00 PM at MAP.

Figure 4.6 Diurnal $PM_{10-2.5}$ trends (time-of-day medians) for (a) winter, (b) spring, (c) summer, and (d) fall
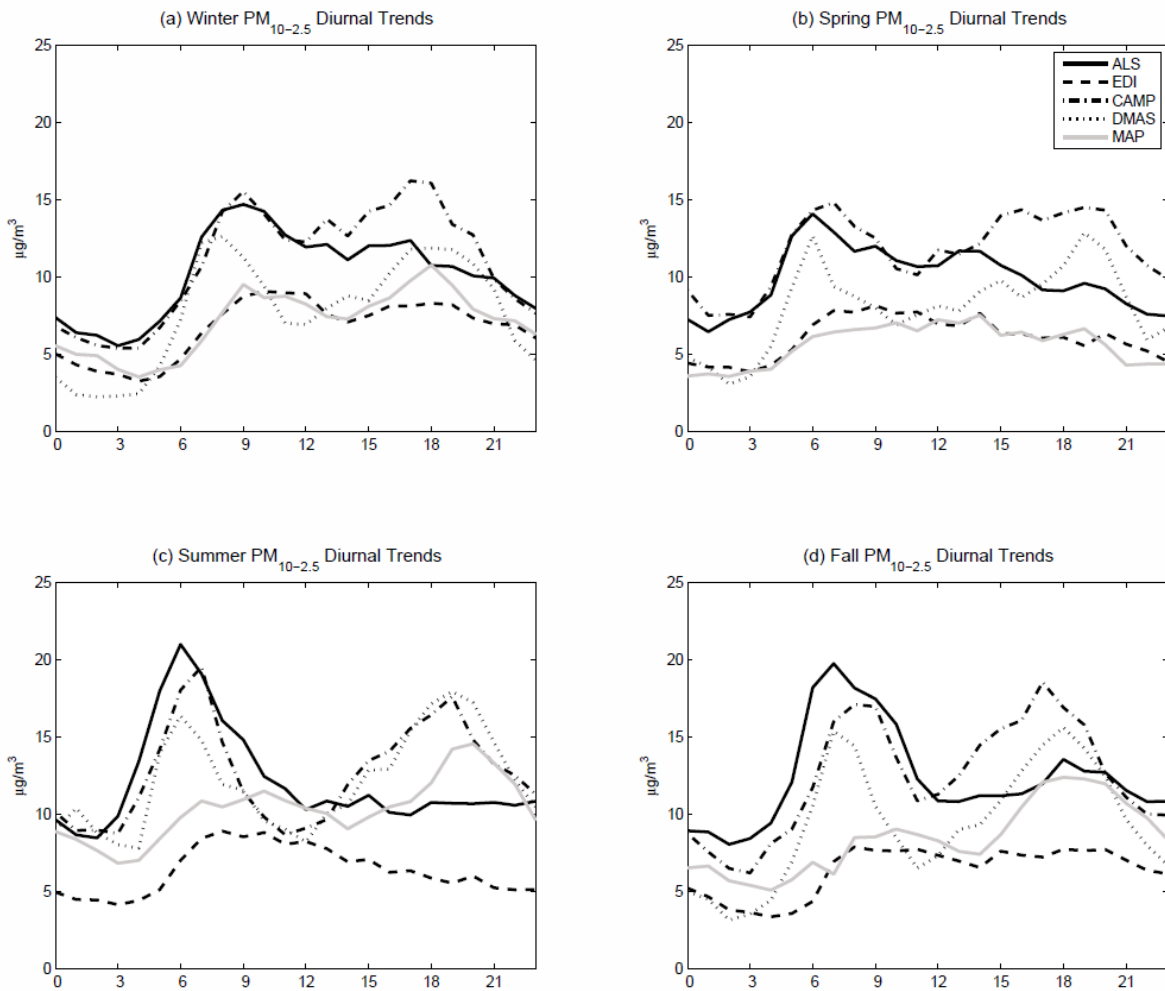
Diurnal trends in $PM_{2.5}$ varied somewhat by season (Figure 4.S11). During winter and fall, diurnal patterns in mass concentrations were distinct, with a morning peak followed by a decrease in concentrations until 3:00 to 4:00 PM, when concentrations increased again to nighttime levels. Nighttime increases in concentrations were not observed in the median mass concentrations during the summer and spring months. Spring concentrations were the least diurnally variable. The diurnal trends of $PM_{2.5}$-SV concentrations also varied seasonally, as shown in Figure 4.S12. $PM_{2.5}$ tended to peak in the early mornings, while $PM_{2.5}$-SV tended to peak in the middle of the day, close to noon (Figure 4.S10). The diurnal variability of $PM_{2.5}$-SV was accentuated during the winter, fall, and to a lesser degree during the summer. The highest midday median peak $PM_{2.5}$-SV values were measured in winter and fall when cold temperatures and daytime nitrate production could increase the total semivolatile material in the particulate phase. Increased concentrations of $PM_{2.5}$ nitrate in Denver during winter were measured by Dutton et al. (2010a), supporting this hypothesis. $PM_{2.5}$-SV concentrations at all three sites co-varied similarly in all seasons, suggesting there was little site dependence for the diurnal profiles of semivolatile mass concentrations in Colorado, even when comparing across urban and rural cities.

During the seasonal variability assessment, it was mentioned that daily averages of $PM_{2.5}$-SV tended to vary linearly with total $PM_{2.5}$. On the hourly time scale though, this trend did not hold. As Figures 4.S11 and 4.S12 show, the diurnal patterns for total and semivolatile $PM_{2.5}$ are distinctly different. Variability in the diurnal patterns of $PM_{2.5}$ and $PM_{2.5}$-SV is the likely cause for much of the scatter observed in the plots between daily averages of $PM_{2.5}$ and $PM_{2.5}$-SV. The linear trend observed for daily averages is a convenient simplification of the dynamics between nonvolatile and semivolatile components which occur on time scales less than 24-hours. These dynamics depend on availability of semivolatile species, which varies seasonally and diurnally with the formation of ammonium nitrate during cold periods and with the formation

of semivolatile organic species via oxidation of volatile organic compounds during the daytime (Eatough et al., 2003; Donahue et al., 2009).

4.3.5 Correlation Analysis

Correlations between particulate mass concentrations, meteorological variables, and gas-phase pollutants can reveal important trends describing pollutant sources and transport. Pearson's correlation coefficients were calculated for comparisons between particulate concentrations ($PM_{2.5}$, $PM_{10-2.5}$, and $PM_{2.5}$-SV) and three different sets of data: meteorological variables (RH, wind speed, soil moisture, soil temperature), gas phase species (O_3, NO, SO_2, and CO), and traffic counts. Relative humidity and wind speed from each monitoring site were used in meteorological comparisons, except at CAMP and DMAS which used ALS RH data and at EDI, which used CRG wind speed data. Gas-phase pollutant data and traffic counts from the nearest monitor to each site were used for correlation calculations. Table 4.S4 contains the combinations of particulate and meteorological/gas-phase/traffic data included in comparisons for each particulate matter monitoring site.

Table 4.S5 contains a summary of the correlation analysis. $PM_{2.5}$ was most correlated with gas-phase species, notably O_3 and NO. Ozone was negatively correlated with $PM_{2.5}$ due to having an inverse seasonal pattern, peaking in the summer instead of winter. As shown in Clements et al. (2013b) and Table 4.3 above, $PM_{2.5}$-SV concentrations varied linearly with total $PM_{2.5}$ concentrations, so it is not surprising that $PM_{2.5}$-SV was also well correlated with O_3, NO, and CO. Correlations with O_3 were similar for both $PM_{2.5}$ (-0.49 to -0.24) and $PM_{2.5}$-SV (-0.48 to -0.24), though NO and CO correlations for $PM_{2.5}$-SV were lower than for $PM_{2.5}$. This is likely due to the summertime peak in $PM_{2.5}$-SV not corresponding to increases in NO or CO. Interestingly, SO_2 was moderately correlated with $PM_{10-2.5}$ in Denver ($0.27 < \rho < 0.31$) and both ALS and EDI $PM_{10-2.5}$ data sets were moderately correlated with NO and CO ($0.25 < \rho < 0.35$).

Correlations with traffic counts were highest for $PM_{10-2.5}$ ($0.24 < \rho < 0.40$). Correlations were consistent though, and all sites were moderately correlated with traffic counts from the nearest major roadway. Traffic counts were highly spatially correlated ($0.84 < \rho < 0.94$). $PM_{10-2.5}$ was negatively correlated with relative humidity, a relationship that will be explored further with nonparametric regression. Wind speed was not correlated with $PM_{10-2.5}$ and was negatively correlated with $PM_{2.5}$ and $PM_{2.5}$-SV. Poor correlation between $PM_{10-2.5}$ and wind speed was due to the nonlinear nature of the relationship, as shown by Clements et al. (2012), which is also addressed using the full data set via nonparametric regression. The diluting effect of high wind speeds on well-mixed pollutants drives the negative association with $PM_{2.5}$ and $PM_{2.5}$-SV. MAP $PM_{10-2.5}$ was negatively associated with soil moisture, while soil temperature was positively correlated. Though a subset of results are presented in Table 4.S5, the full correlation table shows strong spatial correlations for O_3 ($0.87 < \rho < 0.90$), NO ($0.79 < \rho < 0.86$), SO_2 ($0.56 < \rho < 0.69$), CO ($0.61 < \rho < 0.67$), RH ($0.43 < \rho < 0.90$), and wind speed ($0.47 < \rho < 0.85$) as well as colinearity between all gas-phase pollutants, the weakest correlations being between SO_2 and other species. It should be noted that in Colorado, $PM_{10-2.5}$ daily averages had spatial correlations similar to those found for SO_2 and CO and only slightly lower than $PM_{2.5}$ and NO.

It was hypothesized that the relationships with meteorological variables were seasonally variable and that during specific times of the year, variables like wind speed may be driving changes in $PM_{10-2.5}$ concentrations. To investigate this hypothesis, moving correlation analysis with a one-month window was performed using hourly average $PM_{10-2.5}$ mass concentration data and traffic counts, relative humidity, wind speed, soil moisture (only for MAP), and soil temperature (only for MAP). Due to the brevity of the data sets, CAMP and MCA data were excluded from this analysis.

Seasonal relationships were observed for correlations between DMAS $PM_{10-2.5}$ and traffic counts, with correlations peaking in the winter and reaching a minimum in the summer of each year, as shown in Figure 4.7. Lower correlation values and a weaker seasonal pattern were

observed for correlations between ALS PM$_{10\text{-}2.5}$ and I-76 traffic counts in 2010 and 2011 (Figure 4.S12b). In 2009, spring and winter peaks in traffic correlations at ALS were observed. No significant seasonal trends were observed for moving correlations between EDI and MAP and traffic counts. The seasonal trends observed at DMAS and ALS for correlations between PM$_{10\text{-}2.5}$ and traffic demonstrate that site proximity to local sources, like interstate highways, plays a large role in driving PM$_{10\text{-}2.5}$ concentrations.

Figure 4.7 Smoothed (Δθ=4 hours) moving correlation time series between (a) ALS PM$_{10\text{-}2.5}$ and I-76 traffic counts, and (b) DMAS PM$_{10\text{-}2.5}$ and I-70 traffic counts
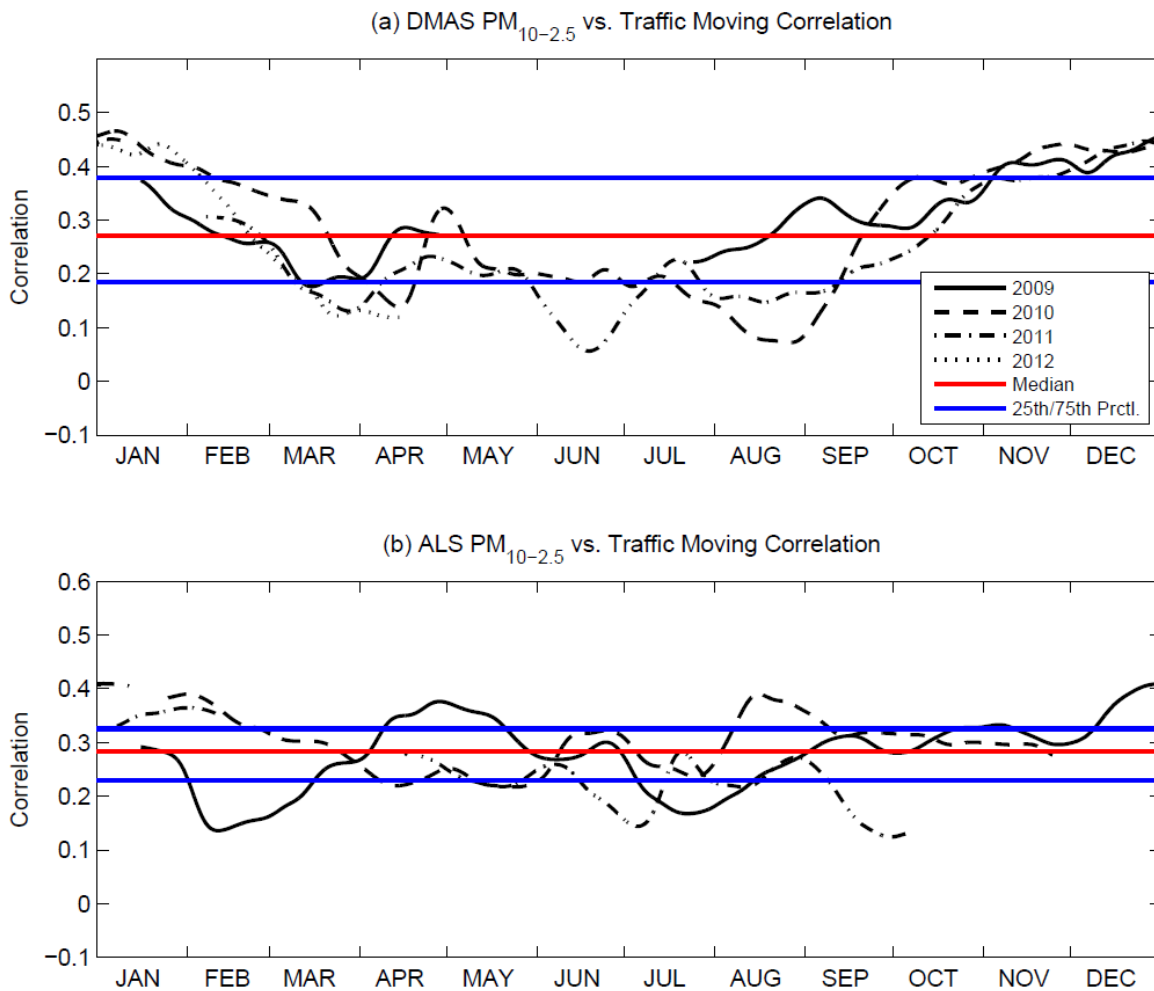
For the moving correlation analysis between wind speed and $PM_{10-2.5}$, two peaks were captured at all sites, one during February 2009 and the other during May of 2010 (Figure 4.S13). The increase in wind speed and relative humidity correlations in February 2009 corresponded to a peak in wind speeds and dip in relative humidity in both cities during that time. The May 2010 peak did not correspond with a consistent change in meteorological conditions. Wind speed correlations were generally positive during summer and fall, and were typically negative in winter, showing seasonality to the effects of resuspension and dilution on $PM_{10-2.5}$ concentrations.

Moving correlations with relative humidity were typically negative in late spring, suggesting low concentrations measured during April and May after the March peak in $PM_{10-2.5}$ concentrations may be due to suppression of resuspension by increased RH levels (Figure 4.S14). A similar trend was observed in Greeley for the moving correlation analysis between $PM_{10-2.5}$ and soil moisture. Concentrations tended to be negatively correlated with soil moisture during late spring and early summer when soil moisture was at its highest values (Figure 4.S15). During fall and winter, soil moisture tended to be positively correlated with $PM_{10-2.5}$, through peak correlation values were low (around 0.30). From this analysis we observe a more intricate relationship between moisture and $PM_{10-2.5}$ concentrations: at high soil moisture and RH levels $PM_{10-2.5}$ resuspension was inhibited and when soil moisture dropped to around 15% resuspension was enhanced. In between these ranges soil moisture was not a dominant factor driving $PM_{10-2.5}$ concentrations. Moving correlation analysis with soil temperature revealed no consistent patterns (Figure 4.S16).

4.3.6 Nonparametric Regression

Nonparametric regression (NPR) was utilized for observing the average relationships between $PM_{10-2.5}$ and $PM_{2.5}$ concentrations and meteorological parameters. NPR was performed between particulate concentrations and wind speed, wind direction, relative humidity, and soil

moisture using optimal smoothing parameters derived from cross validation and averaged over all sites for each particulate size range and meteorological variable. Soil moisture relationships were assessed for particulate data collected only in Greeley. The same pairs of particulate and meteorological monitoring sites used for the correlation analysis above were implemented in the NPR analysis. It is noted that wind speed sensors were located at 10.5 m at all sites except ALS, which had a 14.0 m tower. A wind profile power law correction was considered at ALS, but would only adjust wind speeds by 4% and was thus not implemented. Wind speed and direction data were excluded from the NPR if wind speeds were below 0.5 m/s, an approximate threshold for transitioning from 'calm' conditions.

Nonparametric regressions between both particulate size modes and relative humidity are shown in Figures 4.8a and 4.8c. $PM_{10-2.5}$ and $PM_{2.5}$ had opposing trends with relative humidity, with $PM_{10-2.5}$ decreasing and $PM_{2.5}$ increasing as RH increases. Above 50% RH, $PM_{10-2.5}$ concentrations tended to decrease rapidly, dropping to below 5 $\mu g/m^3$ for ALS, EDI, DMAS, and MAP when relative humidity levels were over 90%. Maximum $PM_{10-2.5}$ concentrations from the regressions occurred for RH below 50% at all sites. It is suspected that the large decrease in $PM_{10-2.5}$ mass concentrations observed above 50% RH was related to water sorption on surfaces, requiring increased energy for resuspension to occur. The resulting increase in $PM_{2.5}$ mass concentrations with increased relative humidity is likely due to hygroscopic growth and the partitioning of water-soluble ionic species to the particle phase above their deliquescence relative humidities.

Figure 4.8 Nonparametric regressions (dashed lines are 95% confidence intervals) between: (a) $PM_{10-2.5}$ and RH; (b) $PM_{10-2.5}$ and wind speed; (c) $PM_{2.5}$ and RH; and (d) $PM_{2.5}$ and wind speed
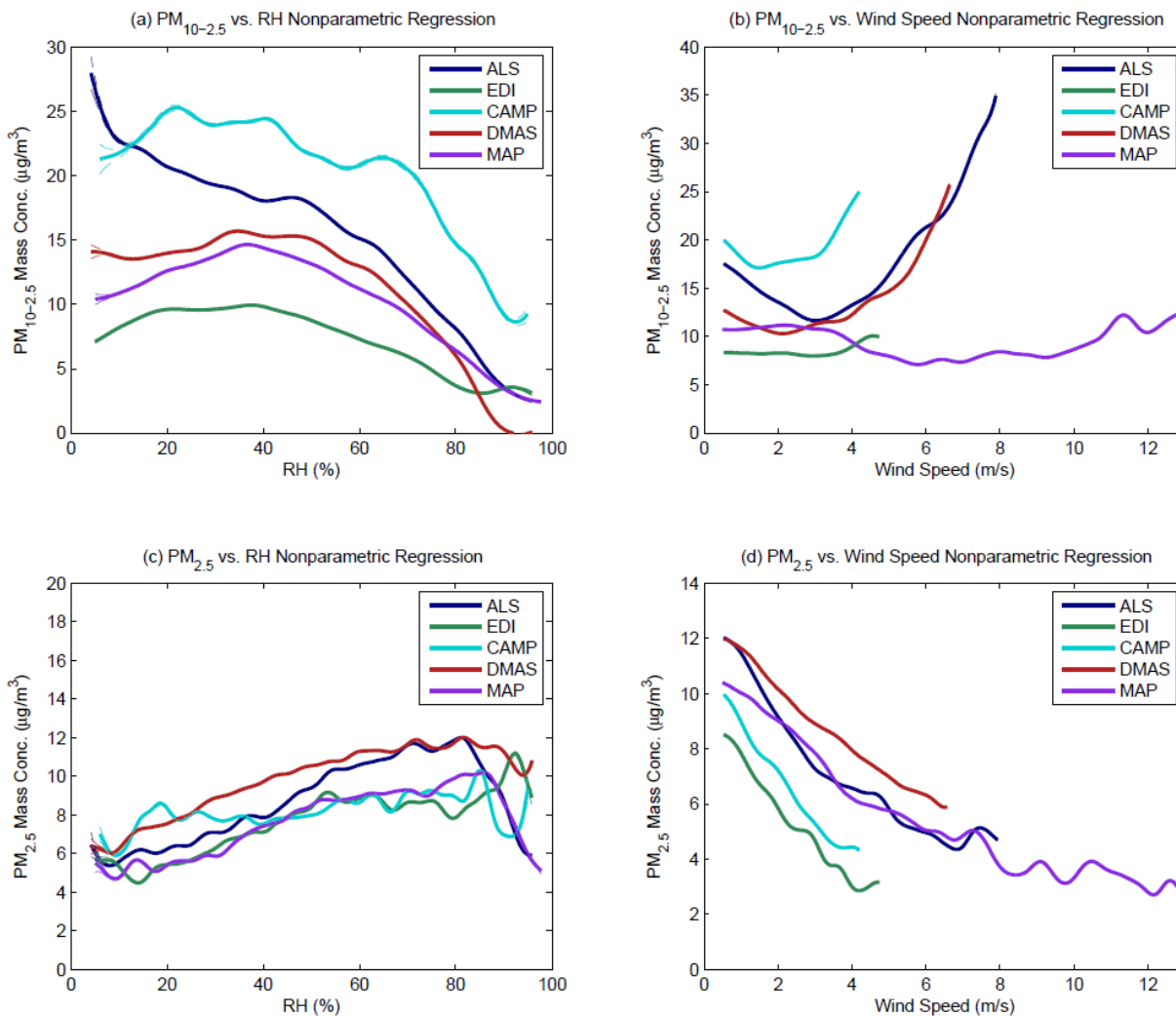
Wind speed also displayed inverse relationships with $PM_{2.5}$ and $PM_{10-2.5}$ as speeds increased, shown in Figures 4.8b and 4.8d. Wind speeds above the 99th percentile for each site are not displayed in Figures 4.8b and 4.8d due to limited data coverage and high uncertainties in those regions of the regressions. Wind speed $PM_{10-2.5}$ regressions at ALS, DMAS, and CAMP displayed a U-shaped profile, diluting in concentration up to 2-3 m/s, then showing a strong resuspension pattern above 3 m/s. EDI $PM_{10-2.5}$ does not appear to be sensitive to wind speed, though lower winds in general were experienced at EDI (less than 5 m/s). A similar range of

wind speeds were measured at CAMP, but due to the close proximity to traffic emissions a significant resuspension effect was observed. Wind speeds were greatest in Greeley, though only a slight resuspension effect was observed at wind speeds above 10 m/s. $PM_{2.5}$ in general decreased in concentration as wind speeds increased, again highlighting the dilution effect of well mixed pollutants at elevated wind speeds.

The seasonality in correlations between wind speed and $PM_{10-2.5}$ suggests the wind speed profile also shifts seasonally. This was assessed by plotting seasonal wind speed regressions for two sites in Denver for which correlation trends were the strongest, EDI and DMAS (Figure 4.S17). It was hypothesized that during fall and winter, when correlations were typically negative, dilution would have a greater impact on $PM_{10-2.5}$ concentrations than resuspension. At EDI this hypothesis proved true, and fall and winter NPRs showed $PM_{10-2.5}$ concentrations diluted for wind speeds up to about 3 m/s before weak resuspension is observed. No U-shape was observed at EDI during summer and spring. Of the seasonal DMAS regressions, dilution was observed in fall for wind speeds up to 3.5 m/s. At DMAS, resuspension was significant during all times of the year.

A seasonal dependence of $PM_{10-2.5}$ on wind speed was also observed by Hien et al. (2002) in Vietnam and by Moore et al. (2010) in Los Angeles, California. Studies in the United Kingdom and Europe have identified similar relationships between $PM_{10-2.5}$ and wind speed to those presented here, with sites located near sources showing more resuspension than background or residential sites and with most sites showing some kind of U-shape with dilution decreasing concentrations as wind speed increases until resuspension effects become significant at higher wind speeds (Harrison et al., 2001; Charron and Harrison, 2005; Liu and Harrison, 2011; Barmpadimos et al., 2012).

Due to the suspected influence of RH on resuspension, additional NPRs with wind speed were assessed using data sets from when RH was above and below 50%. This threshold was chosen because of the significant decrease in average concentrations observed above

50% RH. Resuspension at ALS was heavily inhibited at elevated RHs, as shown in Figure 4.9, while MAP showed no differences and little resuspension in both RH regimes.

Figure 4.9 Nonparametric regressions between $PM_{10-2.5}$ and wind speed at (a) ALS and (b) MAP, stratified by relative humidity (50%)
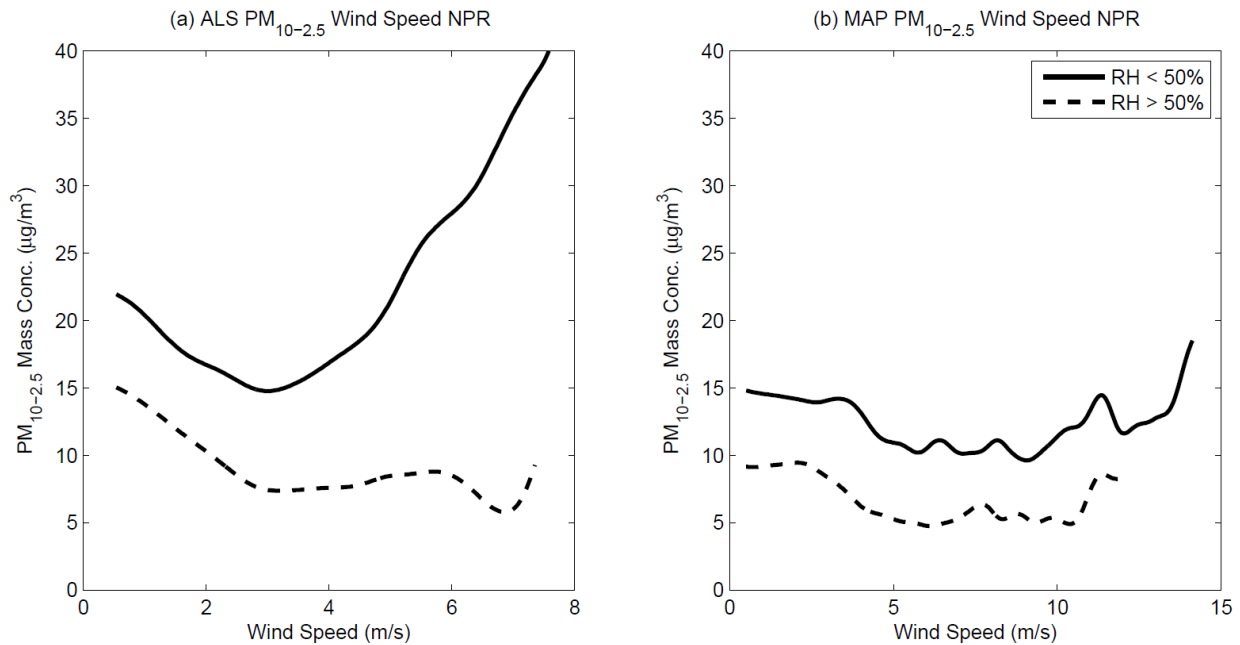
NPRs with soil moisture showed $PM_{10-2.5}$ concentrations decreased with increasing soil moisture (Figure 4.S18), with levels above 25% showing greatly decreased $PM_{10-2.5}$ concentrations. A peak was also observed at very low soil moisture levels (below 13%). These trends were also observed in the moving correlation analysis and are related to the complex dynamics of resuspension. Average $PM_{10-2.5}$ values tended to vary little with soil moisture values of 12 to 25%. No consistent trend was observed between $PM_{2.5}$ and soil moisture.

Wind direction nonparametric regressions were performed to verify the results of Clements et al. (2012) and to investigate CAMP and DMAS, as they were not included in the previous analysis. Wind direction NPRs for $PM_{10-2.5}$ and $PM_{2.5}$ are found in Figures 4.S19 and 4.S20. Nearly all wind direction peaks and trends identified previously by Clements et al. (2012),

which used about a single year of data, were also identified using the longer time series. MAP $PM_{10-2.5}$ was the exception and was more smoothed in this study, showing only a slight increase with winds from the east. $PM_{2.5}$ at ALS, EDI, and DMAS peaked in the general direction of downtown Denver, while CAMP had a strong peak with winds from the northeast, a trend also observed for $PM_{10-2.5}$ at this site. Greeley $PM_{2.5}$ showed a slight enhancement with winds from the south and northwest, the general directions of Denver and Fort Collins/I-25, respectively.

ALS $PM_{10-2.5}$ peaked with winds out of the west, the direction of the gravel pit and I-76. A secondary peak was identified with winds from the southwest. Potential sources in this direction include I-270, located 2.2 km southwest of ALS, and a large industrial region in northern Denver just past I-270 to the southwest. EDI $PM_{10-2.5}$ had a general increase in concentrations with winds coming from the northeast and southeast. Possible nearby sources include the intersection of I-70 and I-25 2 km to the northeast of EDI and I-25 to the southeast 2.5 km away from the site.

The NPR with CAMP $PM_{10-2.5}$ displayed multiple peaks with wind from the northeast, east, southwest, and northwest. CAMP is located in downtown Denver with intersections within 20 m of the monitoring site to the north, south, and west. A major one-way road (Broadway) runs north-to-south directly east of CAMP as well. Brake wear is a known component of $PM_{10-2.5}$ in Colorado (Clements et al., 2013a) and the close proximity of CAMP to multiple intersections suggests peaks in the wind direction NPR may be due to intersection-related emissions that include braking and accelerating. Braking and accelerating around corners, two common activities at intersections, were both shown to greatly enhance road dust and brake wear emissions on a test track in Korea (Kwak et al., 2013). Due to Broadway being a one-way street with traffic traveling north-to-south, the northeastern peak in both $PM_{10-2.5}$ and $PM_{2.5}$ concentrations was likely a result of the plume of primary emissions and road dust resuspension from traffic along Broadway.

The importance of local traffic on DMAS $PM_{10-2.5}$ concentrations is also highlighted in the wind direction NPR, with a peak with winds from the northeast, the direction of I-25 less than half a kilometer away. DMAS $PM_{10-2.5}$ also tended to be increased with winds from the southwest, west, and northwest. Due to the seasonality observed in the correlation between DMAS $PM_{10-2.5}$ and traffic, it was suspected that seasonal NPRs with wind direction would reveal that I-25 traffic is an important source in the winter, decreasing in importance in other seasons. As shown in Figure 4.S21, a strong influence from I-25 was observed in winter, with the traffic-related peak getting less significant in the spring and fall. In the summer, I-25 was indistinguishable from other sources of $PM_{10-2.5}$ at DMAS.

4.4 CONCLUSIONS

The CCRUSH study characterized $PM_{10-2.5}$ and $PM_{2.5}$ (and $PM_{2.5}$-SV) concentrations in urban and rural environments in Colorado. In this study we show that the temporal variability in $PM_{10-2.5}$ concentrations in Colorado was driven by shifts in meteorological conditions and the strength of nearby emission sources. Traffic influenced sites in Denver had the highest $PM_{10-2.5}$ concentrations, while the urban- and rural-residential sites had similar average concentrations. Peak monthly median $PM_{10-2.5}$ concentrations occurred in March and throughout the summer/fall. $PM_{10-2.5}$ was less spatially correlated and was more heterogeneous than $PM_{2.5}$ within Denver, though comparisons were similar for both size fractions when compared across cities. $PM_{10-2.5}$ spatial correlations had a distinct seasonal pattern, peaking in spring and decreasing throughout the summer and early fall. Morning peaks in $PM_{10-2.5}$ and $PM_{2.5}$ concentrations were shown to decrease significantly on the weekends because of a decrease in traffic counts, and therefore traffic-related emissions. Traffic-influenced sites (DMAS and ALS) showed some seasonality for correlations with traffic counts, typically peaking in the winter. Moisture levels, indicated by relative humidity and soil moisture, were shown to inhibit resuspension when elevated and enhance resuspension only during extremely dry periods. For $PM_{10-2.5}$ it was shown that local source strength and meteorological changes greatly impacted the temporal variability observed at each site. Resuspension of $PM_{10-2.5}$ was also shown to be inhibited by increased RH.

4.5 ACKNOWLEDGEMENTS

4.6 REFERENCES

Almeida, S.M., Pio, C.A., Freitas, M.C., Reis, M.A., Trancoso, M.A. 2006. Source apportionment of atmospheric urban aerosol based on weekdays/weekend variability: evaluation of road re-suspended dust contribution. Atmospheric Environment 40, 2058-2067.

Amato, F., Schaap, M., Denier van der Gon, H.A.C., Pandolfi, M., Alastuey, A., Keuken, M., Querol, X. 2013. Short-term variability of mineral dust, metals and carbon emission from road dust resuspension. Atmospheric Environment 74, 134-140.

Barmpadimos, I., Keller, J., Oderbolz, D., Hueglin, C., Prevot, A.S.H. 2012. One decade of parallel fine ($PM_{2.5}$) and coarse (PM_{10}-$PM_{2.5}$) particulate matter measurements in Europe: trends and variability. Atmospheric Chemistry and Physics 12, 3189-3203.

Barnhart, H.X., Haber, M., Song, J. 2002. Overall Concordance Correlation Coefficient for Evaluating Agreement Among Multiple Observers. Biometrics 58, 1020-1027.

Brunekreef, B., Forsberg, B, 2005. Epidemiological evidence of effects of coarse ambient particles on health, European Respiratory Journal 26, 309-318.

Charron, A., Harrison, R.M. 2005. Fine ($PM_{2.5}$) and Coarse ($PM_{2.5-10}$) Particulate Matter on A Heavily Trafficked London Highway: Sources and Processes. Environmental Science and Technology 39, 7768-7776.

Cheung, K., Daher, N., Kam, W., Shafer, M.M., Ning, Z., Schauer, J.J., Sioutas, C., 2011. Spatial and temporal variation of chemical composition and mass closure of ambient coarse particulate matter ($PM_{10-2.5}$) in the Los Angeles area, Atmospheric Environment 45, 2651-2662.

Cheung, K., Olson, M.R., Shelton, B., Schauer, J.J., Sioutas, C. 2012. Seasonal and spatial variations of individual organic compounds of coarse particulate matter in the Los Angeles Basin. Atmospheric Environment 59, 1-10.

Clements, N., Piedrahita, R., Ortega, J., Peel, J.L., Hannigan, M., Miller, S.L., Milford, J.B., 2012. Characterization and Nonparametric Regression of Rural and Urban Coarse Particulate Matter Mass Concentrations in Northeastern Colorado, Aerosol Science and Technology 46(1), 108-123.

Clements, N., Eav, J., Xie, M., Hannigan, M.P., Miller, S.L., Navidi, W., Peel, J.L., Schauer, J.J., Shafer, M., Milford, J.B., 2013. Concentrations and Source Insights for Trace Elements in Fine and Coarse Particulate Matter in Northeastern Colorado, Atmospheric Environment, *submitted*.

Clements, N., Milford, J.B., Miller, S.L., Navidi, W., Peel, J.L., Hannigan, M.P., 2013. Errors in Coarse Particulate Matter ($PM_{10-2.5}$) Mass Concentrations and Spatiotemporal Characteristics when Using Subtraction Estimation Methods, Journal of the Air and Waste Management Association, *accepted*.

Countess, R.J., Wolff, G.T., Cadle, S.H., 1980. The Denver winter aerosol: A comprehensive chemical characterization, Journal of the Air Pollution Control Association 30(11), 1194-1200.

Countess, R.J., Cadle, S.H., Groblicki, P.J., Wolff, G.T., 1981. Chemical analysis of size-segregated samples of Denver's ambient particulate, Journal of the Air Pollution Control Association 31(3), 247-252.

Donahue, N.M., Robinson, A.L., Pandis, S.N. 2009. Atmospheric organic particulate matter: From smoke to secondary organic aerosol. Atmospheric Environment 43, 94-106.

Dutton, S.J., Schauer, J.J., Vedal, S., Hannigan, M.P., 2009. $PM_{2.5}$ characterization for time series studies: Pointwise uncertainty estimation and bulk speciation methods applied in Denver, Atmospheric Environment 43, 1136-1146.

Dutton, S.J., Rajagopalan, B., Vedal, S., Hannigan, M.P. 2010. Temporal patterns in daily measurements of inorganic and organic speciated $PM_{2.5}$ in Denver. Atmospheric Environment 44, 987-998.

Dutton, S.J., Vedal, S., Piedrahita, R., Milford, J.B., Miller, S.L., Hannigan, M.P., 2010. Source apportionment using positive matrix factorization on daily measurements of inorganic and organic speciated $PM_{2.5}$, Atmospheric Environment 44, 2731-2741.

Eatough, D.J., Long, R.W., Modey, W.K., Eatough, N.L. 2003. Semi-volatile secondary organic aerosol in urban atmospheres: meeting a measurement challenge. Atmospheric Environment 37, 1277-1292.

Favez, O., Cachier, H., Sciare, J., Le Moullec, Y., 2007. Characterization and contribution to $PM_{2.5}$ of semi-volatile aerosols in Paris (France), Atmospheric Environment 41, 7969-7976.

Grover, B.D., Eatough, N.L., Eatough, D.J., Chow, J.C., Watson, J.G., Ambs, J.L., Meyer, M.B., Hopke, P.K., Al-Horr, R., Later, D.W., Wilson, W.E., 2006. Measurement of Both Nonvolatile and Semi-Volatile Fractions of Fine Particulate Matter in Fresno, CA, Aerosol Science and Technology 40, 811-826.

Haagenson, P.L. 1979. Meteorological and Climatological Factors Affecting Denver Air Quality. Atmospheric Environment 13, 79-85.

Harrison, R.M., Yin, J., Mark, D., Stedman, J., Appleby, R.S., Booker, J., Moorcroft, S. 2001. Studies of the coarse particles (2.5-10 µm) component in UK urban atmospheres. Atmospheric Environment 35, 3667-3679.

Harrison, R.M., Jones, A.M., Gietl, J., Yin, J., Green, D.C., 2012. Estimation of the Contributions of Brake Dust, Tire Wear, and Resuspension to Nonexhaust Traffic Particles Derived from Atmospheric Measurements, Environmental Science and Technology 46, 6523-6529.

Henry, R.C., Chang, Y.-S., Spiegelman, C.H., 2002. Locating nearby sources of air pollution by nonparametric regression of atmospheric concentration on wind direction, Atmospheric Environment 36, 2237-2244.

Hien, P.D., Bac, V.T., Tham, H.C., Nhan, D.D., Vinh, L.D. 2002. Influence of meteorological conditions on $PM_{2.5}$ and $PM_{2.5-10}$ concentrations during the monsoon season in Hanoi, Vietnam. Atmospheric Environment 36, 3473-3484.

Host, S., Larrieu, S., Pascal, L., Blanchard, M., Declercq, C., Fabre, P., Jusot, J.-F., Chardon, B., Le Terte, A., Wagner, V., Prouvost, H., Lefranc, A., 2008. Short-term associations between fine and coarse particles and hospital admissions for cardiorespiratory diseases in six French cities, Occupational Environmental Medicine 65, 544-551.

Huang, Q., McConnell, L.L., Razote, E., Schmidt, W.F., Vinyard, B.T., Torrents, A., Hapeman, C.J., Maghirang, R., Trabue, S.L., Prueger, J., Ro, K.S., Utilizing single particle Raman microscopy as a non-destructive method to identify sources of PM_{10} from cattle feedlot operations, Atmospheric Environment 66, 17-24.

Huffman, J.A., Sinha, B., Garland, R.M., Snee-Pollmann, A., Gunthe, S.S., Artaxo, P., Martin, S.T., Andreae, M.O., Poschl, U., 2012. Size distributions and temporal variations of biological aerosol particles in the Amazon rainforest characterized by microscopy and real-time UV-APS fluorescence techniques during AMAZE-08, Atmospheric Chemistry and Physics 12, 11997-12019.

Hwang, I., Hopke, P.K., Pinto, J.P., 2008. Source Apportionment and Spatial Distributions of Coarse Particles During the Regional Air Pollution Study, Environmental Science and Technology 42, 3524-3530.

Iinuma, Y., Kahnt, A., Mutzel, A., Boge, O., Herrmann, H. 2013. Ozone-Driven Secondary Organic Aerosol Production Chain. Environmental Science & Technology 47, 3639-3647.

Kavouras, I.G., Etyemezian, V., Xu, J., DuBois, D.W., Green, M., Pitchford, M., 2007. Assessment of the local windblown component of dust in the western United States, Journal of Geophysical Research 112, D08211.

Kim, D., Ramanathan, V., 2008. Solar radiation budget and radiative forcing due to aerosols and clouds. Journal of Geophysical Research 113, D02203.

Kumar, P., Hopke, P.K., Raja, S., Casuccio, G., Lersch, T.L., West, R.R., 2012. Characterization and heterogeneity of coarse particles across an urban area, Atmospheric Environment 46, 446-459.'

Kwak, J.H., Kim, H., Lee, J., Lee, S. 2013. Characterization of non-exhaust coarse and fine particles from on-road driving and laboratory measurements. Science of the Total Environment 458-460, 273-282.

Lagudu, U.R.K., Raja, S., Hopke, P.K., Chalupa, D.C., Utell, M.J., Casuccio, G., Lersch, T.L., West, R.R., 2011. Heterogeneity of coarse particles in an urban area, Environmental Science & Technology 45, 3288-3296.

Lewis, C.W., Baumgardner, R.E., Stevens, R.K., Russwurm, G.M., 1986. Receptor modeling study of Denver winter haze, Environmental Science and Technology 20, 1126-1136.

Li, R., Wiedinmyer, C., Baker, K.R., Hannigan, M.P. 2013. Characterization of coarse particulate matter in the western United States: a comparison between observation and modeling. Atmospheric Chemistry and Physics 13, 1311-1327.

Lin, L.I.-K., 1989. A Concordance Correlation Coefficient to Evaluate Reproducibility, Biometrics 45(1), 255-268.

Liu, Y.-J., Harrison, R.M. 2011. Properties of coarse particles in the atmosphere of the United Kingdom. Atmospheric Environment 45, 3267-3276.

Malig, B.J., Ostro, B.D., 2009. Coarse particles and mortality: evidence from a multi-city study in California, Occupational and Environmental Medicine 66(12), 832-839.

Malig, B.J., Green, S., Basu, R., Broadwin, R., 2013. Coarse particles and respiratory emergency department visits in California, American Journal of Epidemiology 178(1), 58-69.

Malm, W.C., Pitchford, M.L., McDade, C., Ashbaugh, L.L., 2007. Coarse particle speciation at selected locations in the rural continental United States, Atmospheric Environment 41, 2225-2239.

Meister, K., Johansson, C., Forsberg, B., 2012. Estimated short-term effects of coarse particles on daily mortality in Stockholm, Sweden, Environmental Health Perspectives 120, 431-436.

Moore, K.F., Verma, V., Minguillon, M.C., Sioutas, C. 2010. Inter- and Intra-Community Variability in Continuous Coarse Particulate Matter (PM10-2.5) Concentrations in the Los Angeles Area. Aerosol Science and Technology 44(7), 526-540.

Neff, W.D. 1997. The Denver Brown Cloud Studies from the Perspective of Model Assessment Needs and the Role of Meteorology. Journal of the Air and Waste Management Association 47(3), 269-285.

Pakbin, P., Hudda, N., Cheung, K.L., Moore, K.F., Sioutas, C. 2010. Spatial and Temporal Variability of Coarse (PM10-2.5) Particulate Matter Concentrations in the Los Angeles Area. Aerosol Science and Technology 44(7), 514-525.

Pakbin, P., Ning, Z., Shafer, M.M., Schauer, J.J., Constantinos, S., 2011. Seasonal and Spatial Coarse Particle Elemental Concentrations in the Los Angeles Area, Aerosol Science and Technology 45(8), 949-963.

Perez, L., Tobias, A., Querol, X., Pey, J., Alastuey, A., Diaz, J., Sunyer, J., 2012. Saharan dust, particulate matter and cause-specific mortality: A case-crossover study in Barcelona (Spain), Environment International 48, 150-155.

Pohlker, C., Wiedemann, K.T., Sinha, B., Shiraiwa, M., Gunthe, S.S., Smith, M., Su, H., Artaxo, P. Chen, Q., Cheng, Y., Elbert, W., Gilles, M.K., Kilcoyne, A.L.D., Moffet, R.C., Weigand, M., Martin, S.T., Poschl, U., Andreae, M.O. 2012. Biogenic Potassium Salt Particles as Seeds for Secondary Organic Aerosol in the Amazon. Science 337, 1075-1078.

Qiu, H., Yu, I.T.-S., Tian, L., Wang, X., Tse, L.A., Tam, W., Wang, T.W., 2012. Effects of coarse
    particulate matter on emergency hospital admissions for respiratory diseases: A time-
    series analysis in Hong Kong, Environmental Health Perspectives 120, 572-576.

Querol, X., Pey, J., Pandolfi, M., Alastuey, A., Cusack, M., Perez, N., Moreno, T., Viana, M.,
    Mihalopoulos, N., Kallos ,G., Kleanthous, S. 2009. African dust contributions to mean
    ambient PM_{10} mass-levels across the Mediterranean Basin. Atmospheric Environment
    43, 4266-4277.

Ray, A.J., Barsugli, J.J., Averyt, K.B., Wolter, K., Hoerling, M., Doesken, N., Udall, B., Webb,
    R.S. 2008. Climate Change in Colorado: A Synthesis to Support Water Resources
    Management and Adaptation - A report for the Colorado Water Conservation Board. CU-
    NOAA Western Water Assessment.

Sciare, J., Cachier, H., Sarda-Esteve, R., Yu, T., Wang, X., 2007. Semi-volatile aerosol in
    Beijing (R.P. China): Characterization and influence on various $PM_{2.5}$ measurements,
    Journal of Geophysical Research 112, D18202.

Seinfeld, J.H., Spyros, P.N., 2006. Atmospheric Chemistry and Physics - From Air Pollution to
    Climate Change, 2nd Edition, John Wily & Sons.

Stafoggia, M., Samoli, E., Alessandrini, E., Cadum, E., Ostro, B., Berti, G., Faustini, A.,
    Jacquemin, B., Linares, C., Pascal, M., Randi, G., Ranzi, A., Stivanello, E., Forastiere,
    F., the MED-PARTICLES Study Group, 2013. Short-term associations between fine and
    coarse particulate matter and hospitalizations in Southern Europe: Results from the
    MED-PARTICLES project, Environmental Health Perspectives Advance Publication.

Stevens, B., Feingold, G, 2009. Untangling aerosol effects on clouds and precipitation in a
    buffered system, Nature 461, 607-613.

Tecer, L.H., Alagha, O., Karaca, F., Tuncel, G., Eldes, N., 2008. Particulate matter ($PM_{2.5}$, $PM_{10-2.5}$, and PM_{10}) and children's hospital admissions for asthma and respiratory diseases: A

bidirectional case-crossover study, Journal of Toxicology and Environmental Health, Part A: Current Issues 71(8), 512-520.

Thermo Scientific, 2009. TEOM 1405-DF: Dichotomous Ambient Particulate Monitor with FDMS Option. 42-010815 Revision A.003.

Toth, J.J., Johnson, R.H. 1985. Summer Surface Flow Characteristics over Northeast Colorado. Monthly Weather Review 113, 1458-1469.

U.S. Bureau of the Census. 2012. *Annual Estimates of the Resident Population for Counties of Colorado: April 1, 2010 to July 1, 2011.* Prepared by the United States Census Bureau, Population Division. http://www.census.gov/popest/data/counties/totals/2011/tables/CO-EST2011-01-08.csv.

U.S. Department of Agriculture. 2007. *2007 Census Volume 1, Chapter 2: County Level Data, Table 1. County Summary Highlights: 2007.* Prepared by the United States Department of Agriculture. http://www.agcensus.usda.gov/Publications/2007/Full_Report/Volume_1,_Chapter_2_County_Level/Colorado/.

U.S. EPA. 2004. *US EPA Air Quality Criteria for Particulate Matter (Final Report, Oct, 2004).* U.S. Environmental Protection Agency, Washington, DC, EPA 600/P-99/002aF-bF.

Usher, C.R., Michel, A.E., Grassian, V.H. 2003. Reactions on Mineral Dust. Chemical Reviews 103, 4883-4939.

Wang, G., Kawamura, K., Xie, M., Hu, S., Cao, J., An, Z., Waston, J.G., Chow, J.C. 2009. Organic Molecular Compositions and Size Distributions of Chinese Summer and Autumn Aerosols from Nanjing: Characteristic Haze Event Caused by Wheat Straw Burning. Environmental Science and Technology 43, 6493-6499.

Wang, M., Ghan, S., Ovchinnikov, M., Liu, X., Easter, R., Kassianov, E., Qian, Y., Morrison, H., 2011. Aerosol indirect effects in a multi-scale aerosol-climate model PNNL-MMF, Atmospheric Chemistry and Physics 11, 5431-5455.

Wilson, J.G., Kingham, S., Pearce, J., Sturman, A.P., 2005. A review of intraurban variations in particulate air pollution: Implications for epidemiological research, Atmospheric Environment 39, 6444-6462.

Xie, M., Piedrahita, R., Dutton, S.J., Milford, J.B., Hemann, J.G., Peel., J.L., Miller, S.L., Kim, S.-Y., Vedal, S., Sheppard, L., Hannigan, M.P. 2013. Positive matrix factorization of a 32-month series of daily $PM_{2.5}$ speciated data with incorporation of temperature stratification. Atmospheric Environment 65, 11-20.

Yajima, Y., Nishino, H., 1999. Estimation of the autocorrelation function of a stationary time series with missing observations. Sankhya Ser. A 61, 189-207.

Zanobetti, A., Schwartz, J., 2009. The effect of fine and coarse particulate air pollution on mortality: A national analysis, Environmental Health Perspectives 117, 898-903.

Zaveri, R.A., Shaw, W.J., Cziczo, D.J., Schmid, B., Ferrare, R.A., Alexander, M.L., Alexandrov, M., Alvarez, R.J., Arnott, W.P., Atkinson, D.B., Baidar, S., Banta, R.M., Barnard, J.C., Beranek, J., Berg, L.K., Brechtel, F., Brewer, W.A., Cahill, J.F., Cairns, B., Cappa, C.D., Chand, D., China, S., Comstock, J.M., Dubey, M.K., Easter, R.C., Erickson, M.H., Fast, J.D., Floerchinger, C., Flowers, B.A., Fortner, E., Gaffney, J.S., Gilles, M.K., Gorkowski, K., Gustafson, W.I., Gyawali, M., Hair, J., Hardesty, R.M., Harworth, J.W., Herndon, S., Hiranuma, N., Hostetler, C., Hubbe, J.M., Jayne, J.T., Jeong, H., Jobson, B.T., Kassianov, E.I., Kleinman, L.I., Kluzek, C., Knighton, B., Kolesar, K.R., Kuang, C., Kubatova, A., Langford, A.O., Laskin, A., Laulainen, N., Marchbanks, R.D., Mazzoleni, C., Mei, F., Moffet, R.C., Nelson, D., Obland, M.D., Oetjen, H., Onasch, T.B., Ortega, I., Ottaviani, M., Pekour, M., Prather, K.A., Radney, J.G., Rogers, R.R., Sandberg, S.P., Sedlacek, A., Senff, C.J., Senum, G., Setyan, A., Shilling, J.E., Shrivastava, M., Song, C., Springston, S.R., Subramanian, R., Suski, K., Tomlinson, J., Volkamer, R., Wallace, H.W., Wang, J., Weickmann, A.M., Worsnop, D.R., Yu, X.-Y., Zelenyuk, A., Zhang, Q.

2012. Overview of the 2010 Carbonaceous Aerosols and Radiative Effects Study

(CARES). Atmospheric Chemistry and Physics 12, 7647-7687.

4.7 SUPPLEMENTAL INFORMATION

Table 4.S1 Meteorological and Gas-Phase Pollutant Monitoring Site Information

Monitoring Site		Meteorological Variables	Gaseous Pollutants
Denver	ALS	Temperature, RH, Wind Speed/Direction	-
	WBY	-	O_3, NO, SO_2, CO
	EDI	Temperature, RH	-
	CAMP	Temperature, Wind Speed/Direction	NO, SO_2, CO
	DMAS	Temperature, Wind Speed/Direction	O_3, NO, SO_2, CO
	CRG	Wind Speed/Direction	-
	STP	Precipitation, Snowfall, Snow Depth	-
Greeley	MAP	Temperature, RH	-
	MCA	Temperature, RH	-
	GRET	Temperature	O_3, CO
	GREA	Wind Speed/Direction, Precipitation, Snowfall, Snow Depth	-

Table 4.S2 Average (± standard deviation) traffic per hour of the two nearest major roadways to the CCRUSH and CDPHE monitoring sites

PM Monitoring Site	1st Nearest Major Roadway (distance in km, CDOT ID)	Average ± St. Dev. Traffic Counts per Hour of 1st Nearest Roadway	2nd Nearest Major Roadway (distance in km, CDOT ID)	Average ± St. Dev. Traffic Counts per Hour of 2nd Nearest Roadway
ALS	I-76 (0.5, 103387)	1524±887	I-270 (2.2, 00057)	1916±1109
EDI	I-70 (2.0, 000510)	2011±1194	I-25 (2.5, 000501)	4653±2606
CAMP	I-25 (1.8, 000501)	4653±2606	I-70 (3.3, 000510)	2011±1194
DMAS	I-25 (<0.5, 000501)	4653±2606	I-70 (8.5, 000510)	2011±1194
MAP	US-85 (2.7, 103712)	329±194	US-34 (3.1, 000245)	754±477

Table 4.S3 COD values for spatial comparisons with daily average $PM_{2.5}$ and $PM_{10-2.5}$ mass concentrations

COD		PM₂.₅					PM₁₀₋₂.₅					PM₂.₅-SV		
		ALS	EDI	CAMP	DMAS	MAP	ALS	EDI	CAMP	DMAS	MAP	ALS	EDI	MAP
PM₂.₅	ALS	0.00												
	EDI	0.22	0.00											
	CAMP	0.15	0.22	0.00										
	DMAS	0.17	0.27	0.18	0.00									
	MAP	0.23	0.29	0.27	0.27	0.00								
PM₁₀₋₂.₅	ALS	0.39	0.47	0.35	0.38	0.42	0.00							
	EDI	0.29	0.34	0.29	0.32	0.31	0.33	0.00						
	CAMP	0.50	0.56	0.49	0.43	0.48	0.33	0.47	0.00					
	DMAS	0.38	0.47	0.41	0.36	0.41	0.24	0.34	0.23	0.00				
	MAP	0.37	0.42	0.39	0.38	0.37	0.30	0.27	0.40	0.30	0.00			
PM₂.₅-SV	ALS	0.61	0.56	0.59	0.65	0.55	0.71	0.59	0.79	0.72	0.62	0.00		
	EDI	0.62	0.59	0.61	0.67	0.61	0.71	0.60	0.79	0.73	0.65	0.30	0.00	
	MAP	0.60	0.53	0.52	0.62	0.56	0.69	0.55	0.75	0.71	0.62	0.32	0.36	0.00

Table 4.S4 Input variables for meteorological and gas-phase correlation analysis with $PM_{2.5}$ and $PM_{10-2.5}$

PM Monitoring Site	ALS	EDI	CAMP	DMAS	MAP
O₃	WBY	DMAS	DMAS	DMAS	GRET
NO	WBY	DMAS	CAMP	DMAS	-
SO₂	WBY	DMAS	CAMP	DMAS	-
CO	WBY	DMAS	CAMP	DMAS	GRET
Traffic Count	I-76	I-70	I-25	I-25	US-85
RH	ALS	EDI	ALS	ALS	MAP
Wind Speed	ALS	CRG	CAMP	DMAS	GREA
Soil Moisture and Temperature	-	-	-	-	NUN

Table 4.S5 Correlation values between daily average particulate mass concentrations and gas-phase pollutants, meteorological conditions, and traffic counts

ρ	PM$_{2.5}$ (µg/m^3)					PM$_{10\text{-}2.5}$ (µg/m^3)					PM$_{2.5}$-SV (µg/m^3)		
	ALS	EDI	CAMP	DMAS	MAP	ALS	EDI	CAMP	DMAS	MAP	ALS	EDI	MAP
O$_3$ (ppm)	-0.49	-0.24	-0.28	-0.42	-0.49	-0.11	-0.03	0.13	0.04	-0.04	-0.48	-0.24	-0.31
NO (ppb)	0.61	0.34	0.56	0.38	NA	0.29	0.35	0.15	0.21	NA	0.46	0.31	NA
SO$_2$ (ppb)	0.17	0.11	0.25	0.40	NA	0.27	0.31	0.27	0.27	NA	0.01	0.01	NA
CO (ppm)	0.60	0.39	0.43	0.56	0.58	0.25	0.35	0.14	0.16	0.18	0.46	0.27	0.28
Traffic (vehicles/day)	-0.02	-0.06	0.07	0.03	-0.02	0.40	0.37	0.38	0.36	0.24	-0.10	-0.09	0.00
RH (%)	0.18	0.14	0.16	0.31	0.20	-0.56	-0.29	-0.26	-0.45	-0.45	0.41	0.13	0.22
Wind Speed (m/s)	-0.33	-0.27	-0.28	-0.28	-0.41	-0.01	-0.12	-0.17	-0.09	-0.15	-0.27	-0.24	-0.30
Soil Moisture (%)	NA	NA	NA	NA	-0.08	NA	NA	NA	NA	-0.27	NA	NA	0.04
Soil Temperature (°C)	NA	NA	NA	NA	-0.25	NA	NA	NA	NA	0.20	NA	NA	-0.09

Figure 4.S1 Regional map of the CCRUSH, CDPHE, and meteorological monitoring sites
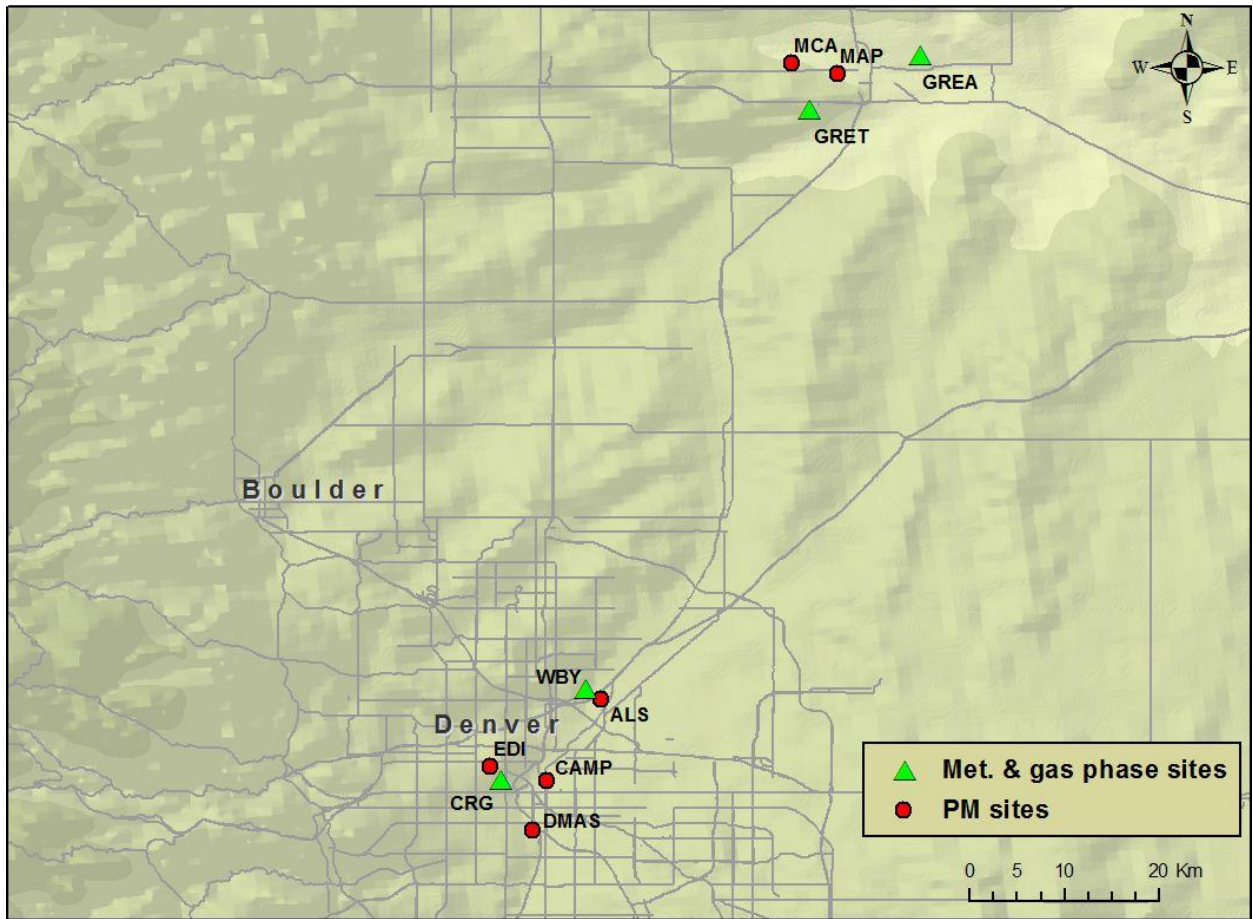
Figure 4.S2 Seasonal hodographs of ALS wind data with marker color representing time of day ranging from black (0:00), to gray (12:00), to white (23:00)
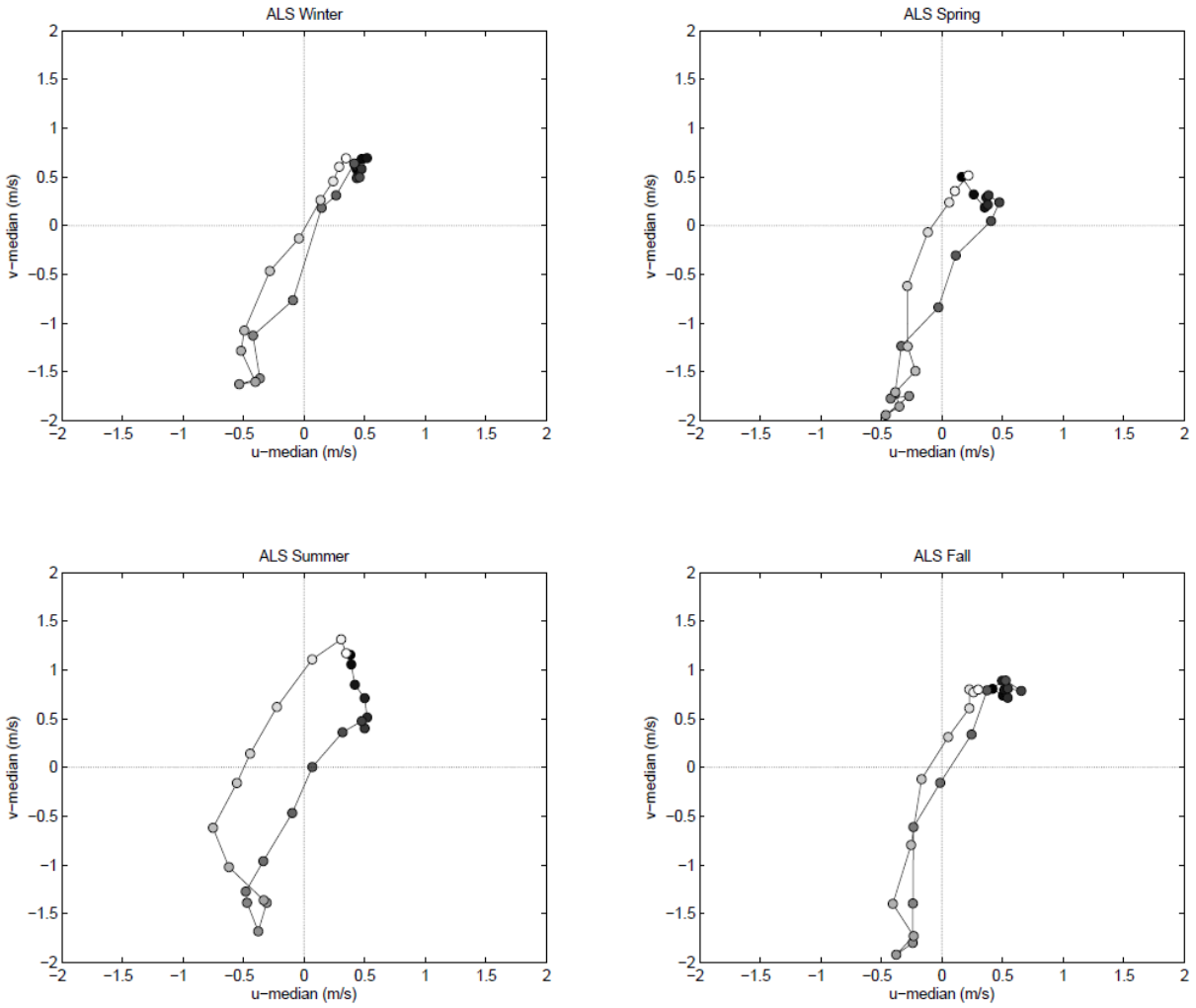
Figure 4.S3 Seasonal hodographs of MAP wind data with marker color representing time of day ranging from black (0:00), to gray (12:00), to white (23:00)
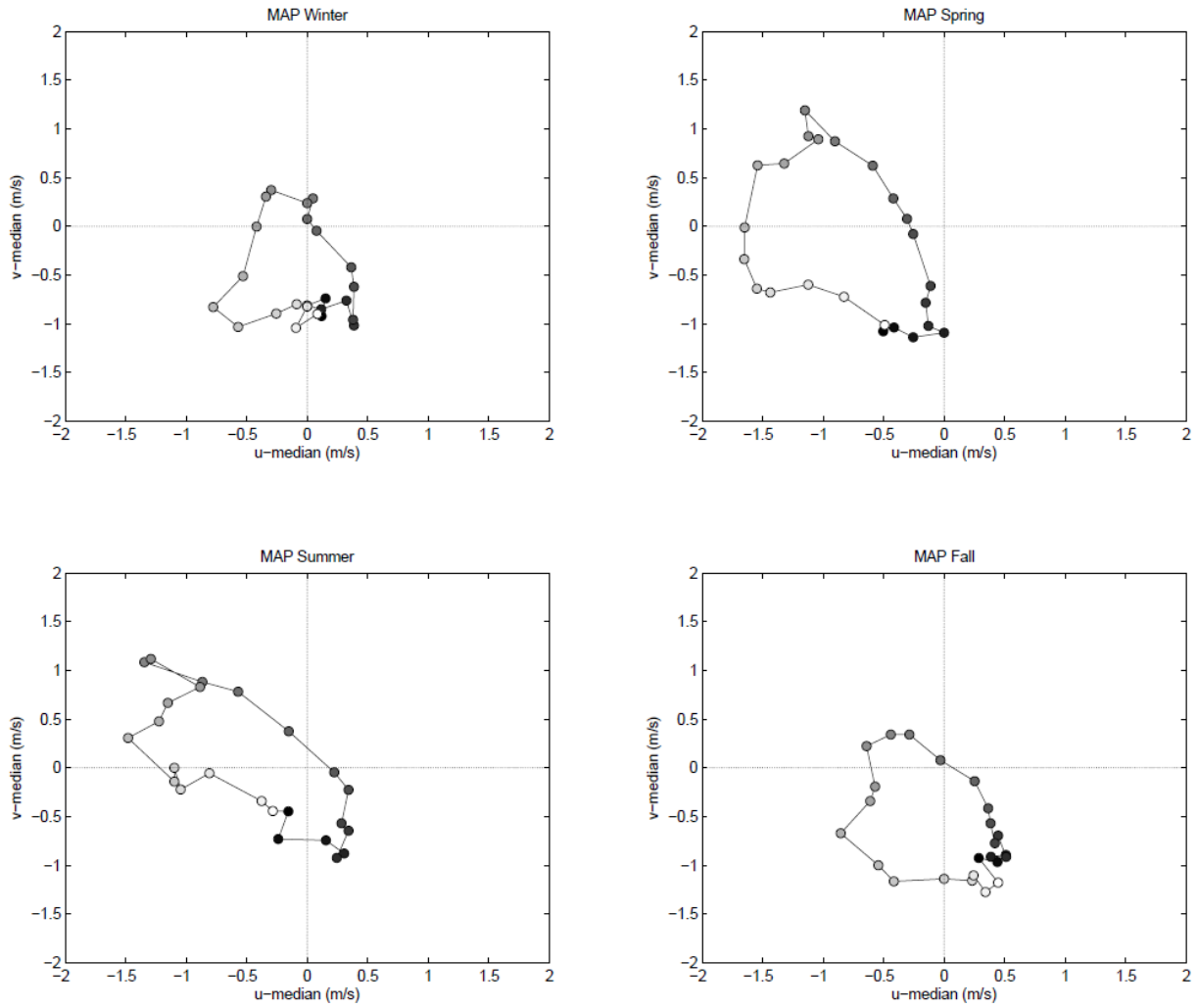
Figure 4.S4 Seasonal wind roses for ALS

ALS Winter Wind Rose (m/s)

ALS Spring Wind Rose (m/s)

ALS Summer Wind Rose (m/s)

ALS Fall Wind Rose (m/s)

146
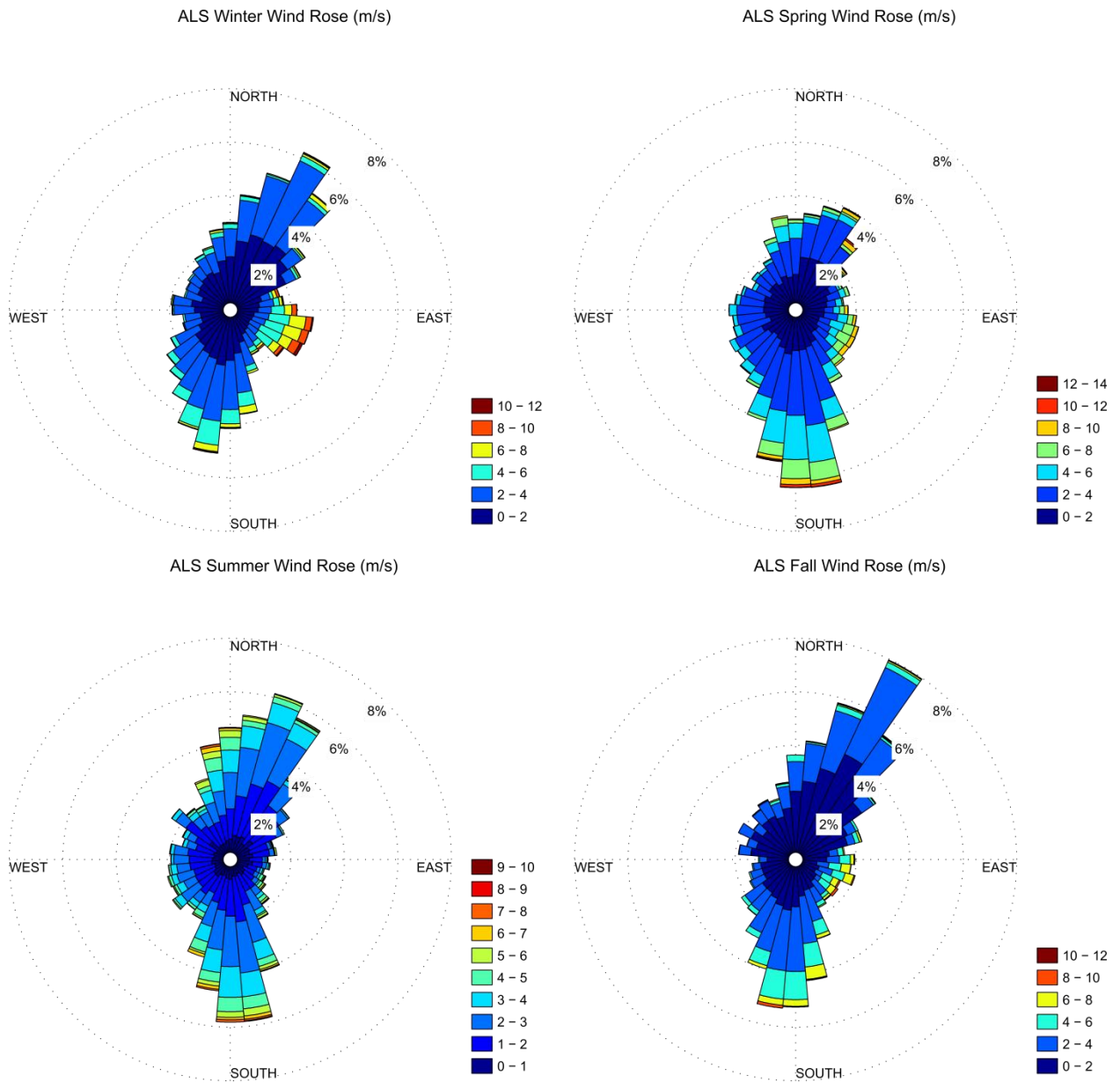
Figure 4.S5 Seasonal wind roses for MAP

MAP Winter Wind Rose (m/s)

MAP Spring Wind Rose (m/s)

MAP Summer Wind Rose (m/s)

MAP Fall Wind Rose (m/s)

147
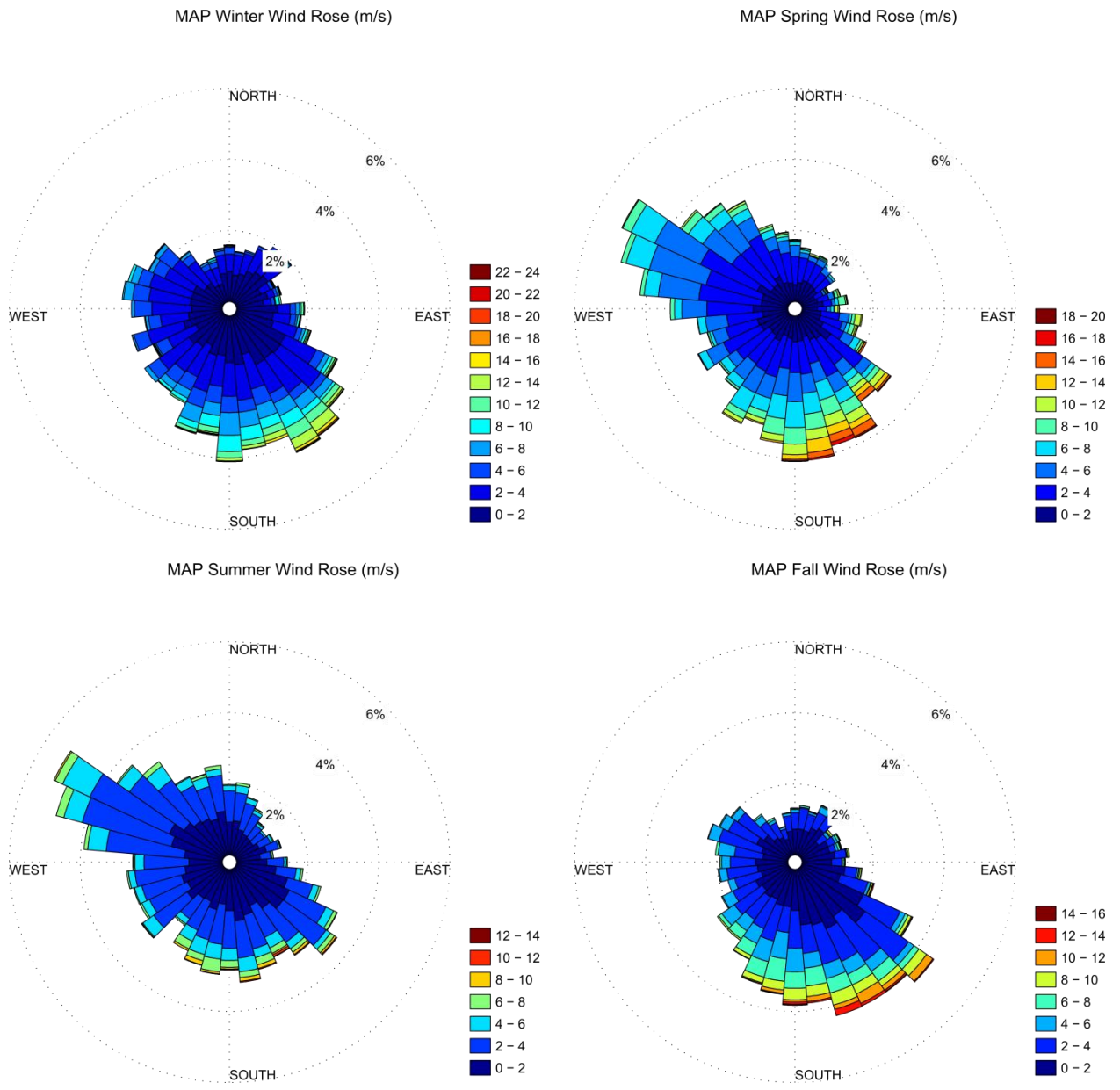
Figure 4.S6 Annual moving correlation plot for PM$_{10\text{-}2.5}$ (hourly averaged) spatial comparisons between MAP and (a) ALS, (b) CAMP, (c) EDI, and (d) DMAS (Gaussian kernel smoothed, Δθ=4 hours)
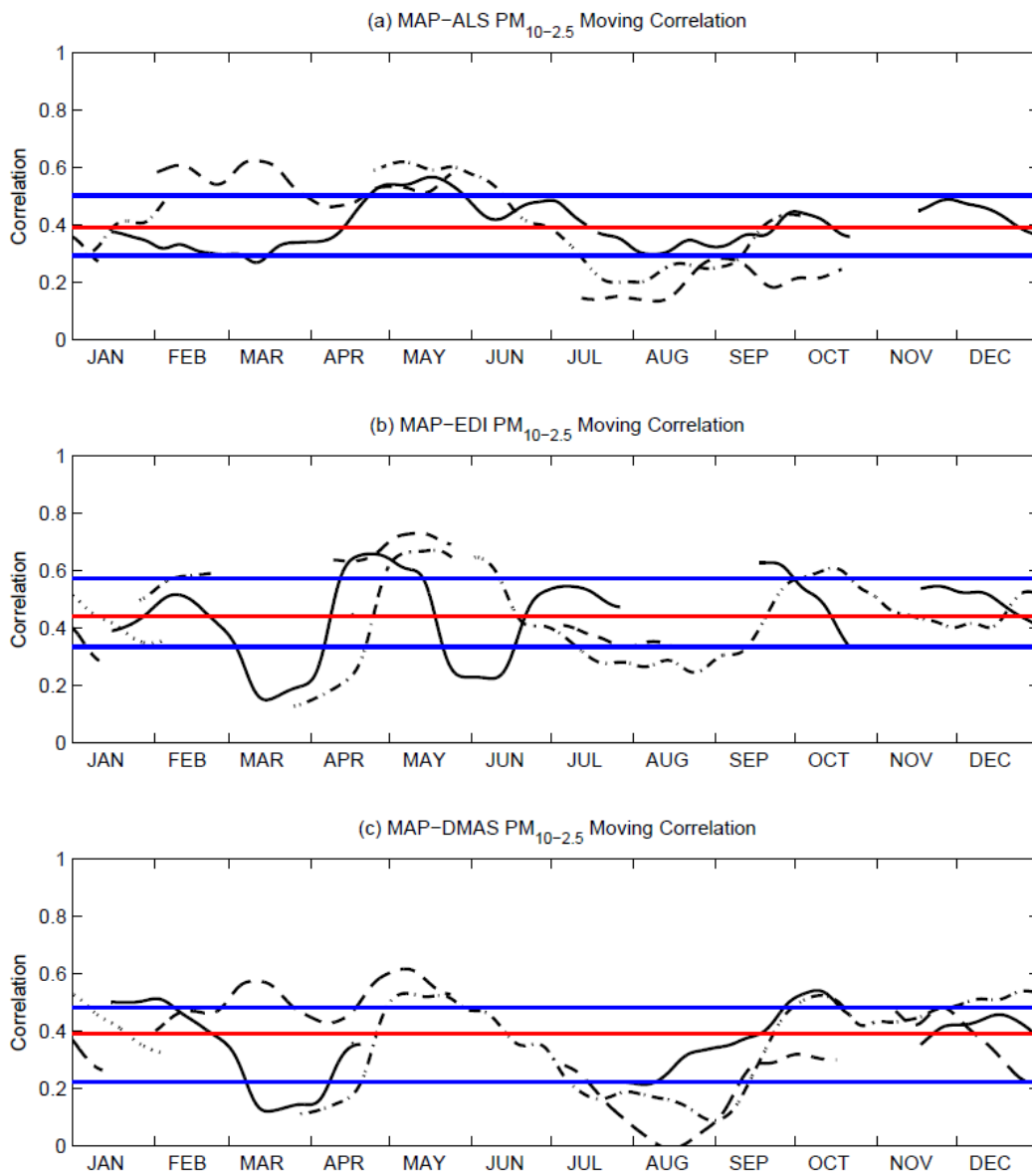
Figure 4.S7 Annual moving correlation plot for PM$_{2.5}$ (hourly averaged) spatial comparisons between (a) ALS and EDI, (b) ALS and DMAS, (c) ALS and MAP, (d) MAP and EDI, and (e) MAP and DMAS (Gaussian kernel smoothed, Δθ=4 hours)
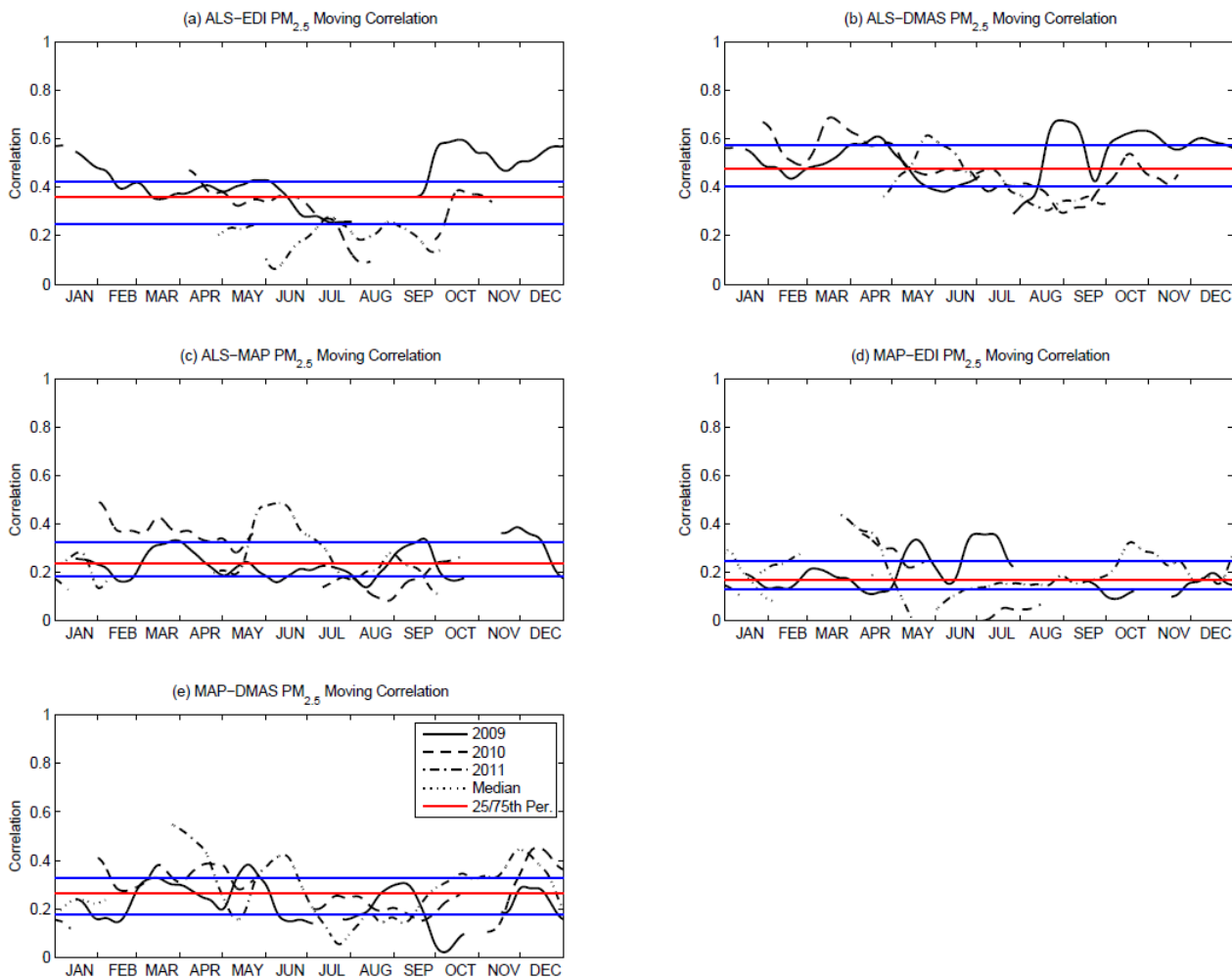
Figure 4.S8 Monthly boxplots of $PM_{10-2.5}/PM_{10}$ ratios (from daily averages) for (a) ALS, (b) EDI, (c) MAP, (d) CAMP, (e) DMAS, and (f) mean (±st.dev.) ratio for each site
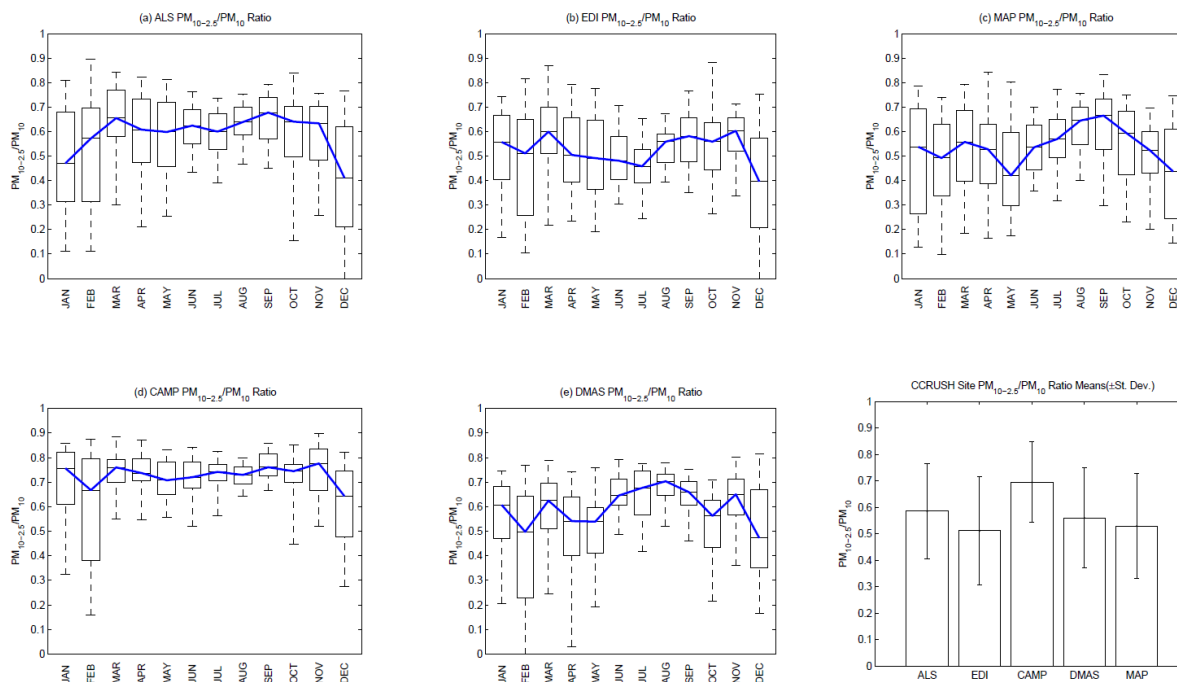
Figure 4.S9 Monthly boxplots of semivolatile mass concentration ratios (from daily averages) for (a) ALS $PM_{2.5}$, (b) EDI $PM_{2.5}$, (c) MAP $PM_{2.5}$, (d) ALS $PM_{10-2.5}$, (e) EDI $PM_{10-2.5}$, and (f) MAP $PM_{10-2.5}$
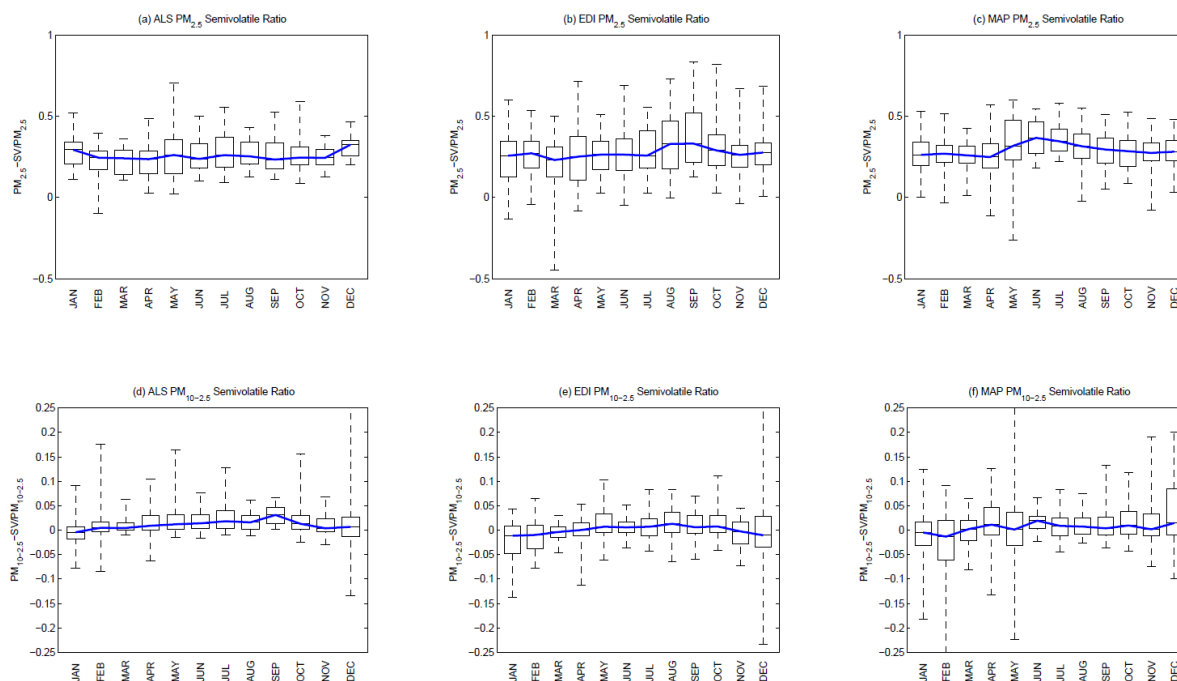
Figure 4.S10 Diurnal trends of PM$_{2.5}$-SV on (a) weekdays and (b) weekends

(a) Weekday PM$_{2.5}$-SV Diurnal Trends

(b) Weekend PM$_{2.5}$-SV Diurnal Trends
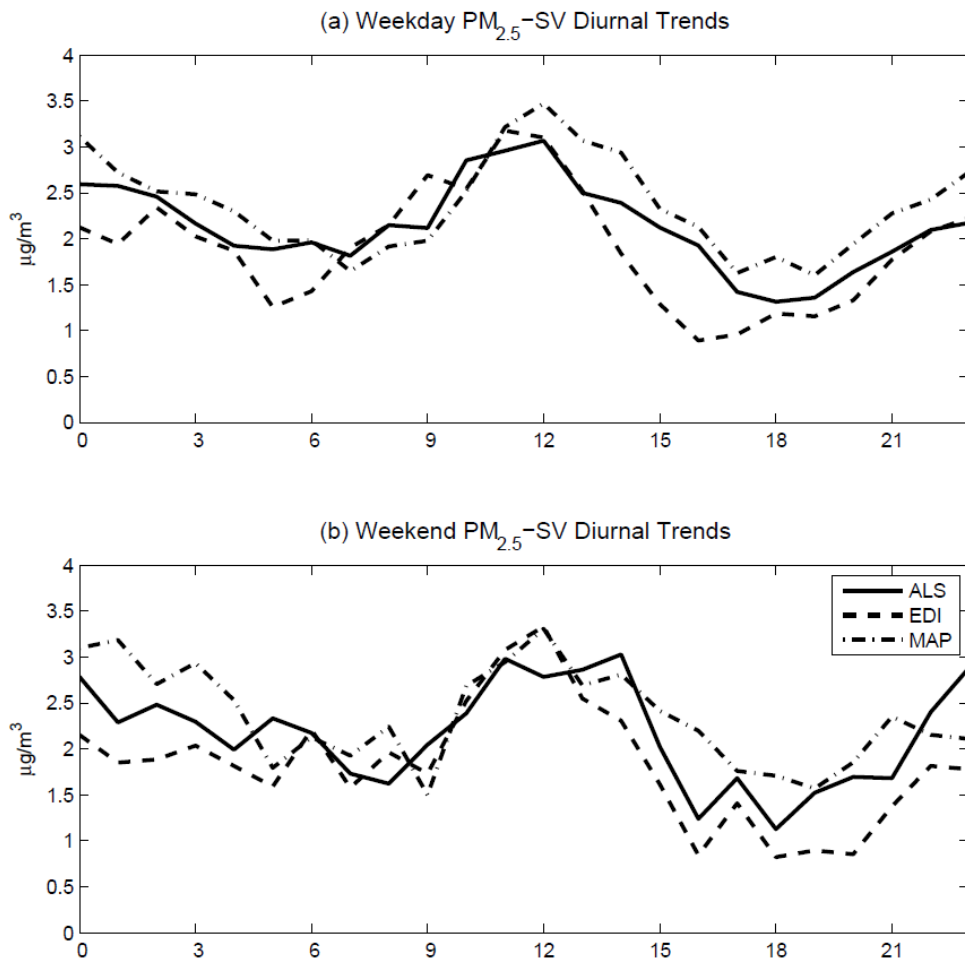
Figure 4.S11 Diurnal PM$_{2.5}$ trends (time-of-day medians) for (a) winter, (b) spring, (c) summer, and (d) fall

152
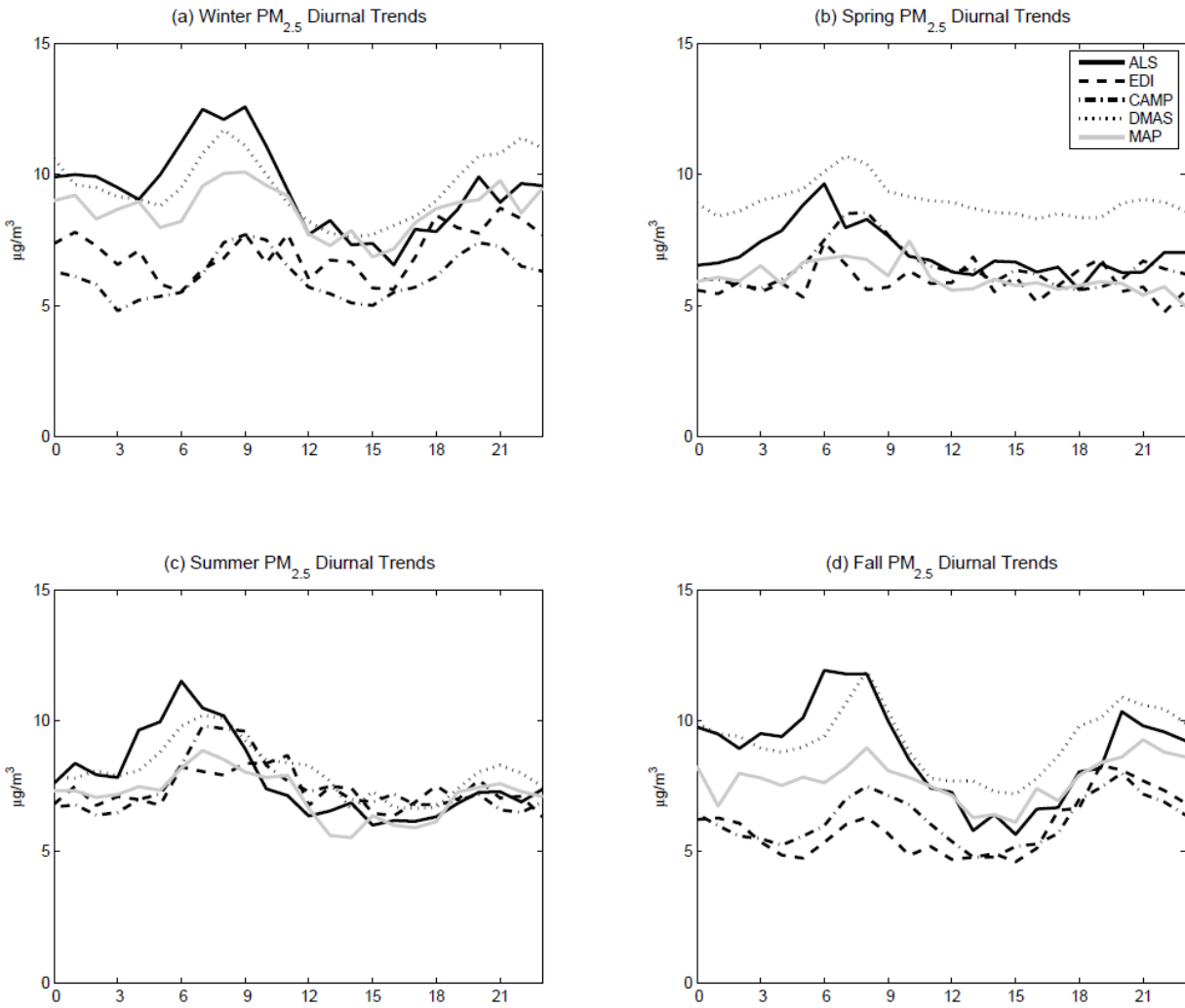
Figure 4.S12 Diurnal PM$_{2.5}$-SV trends (time-of-day medians) for (a) winter, (b) spring, (c) summer, and (d) fall
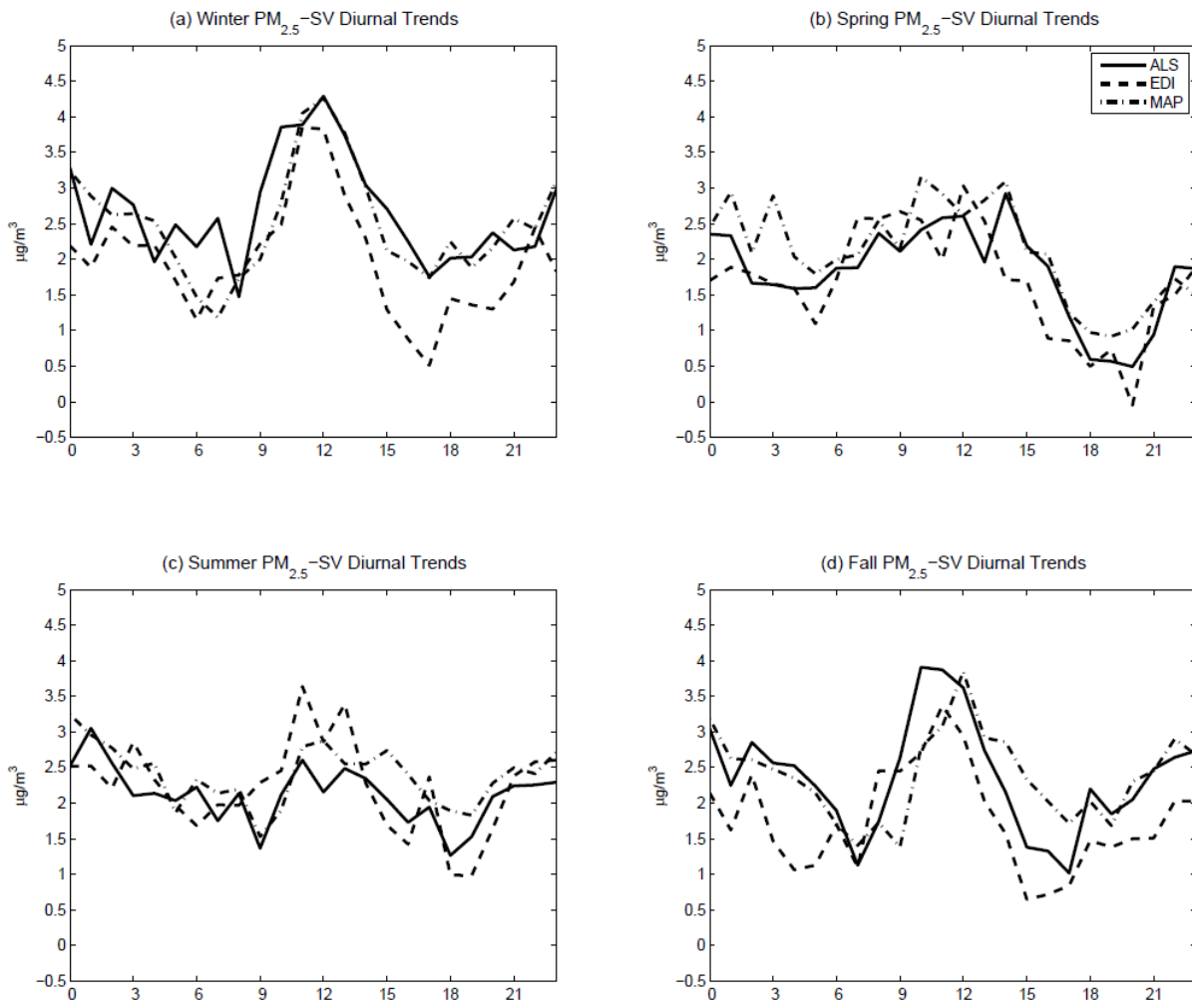
Figure 4.S13 Smoothed (Δθ=4 hours) moving correlation time series between wind speed and PM$_{10\text{-}2.5}$ from (a) ALS, (b) EDI, (c) DMAS, and (d) MAP
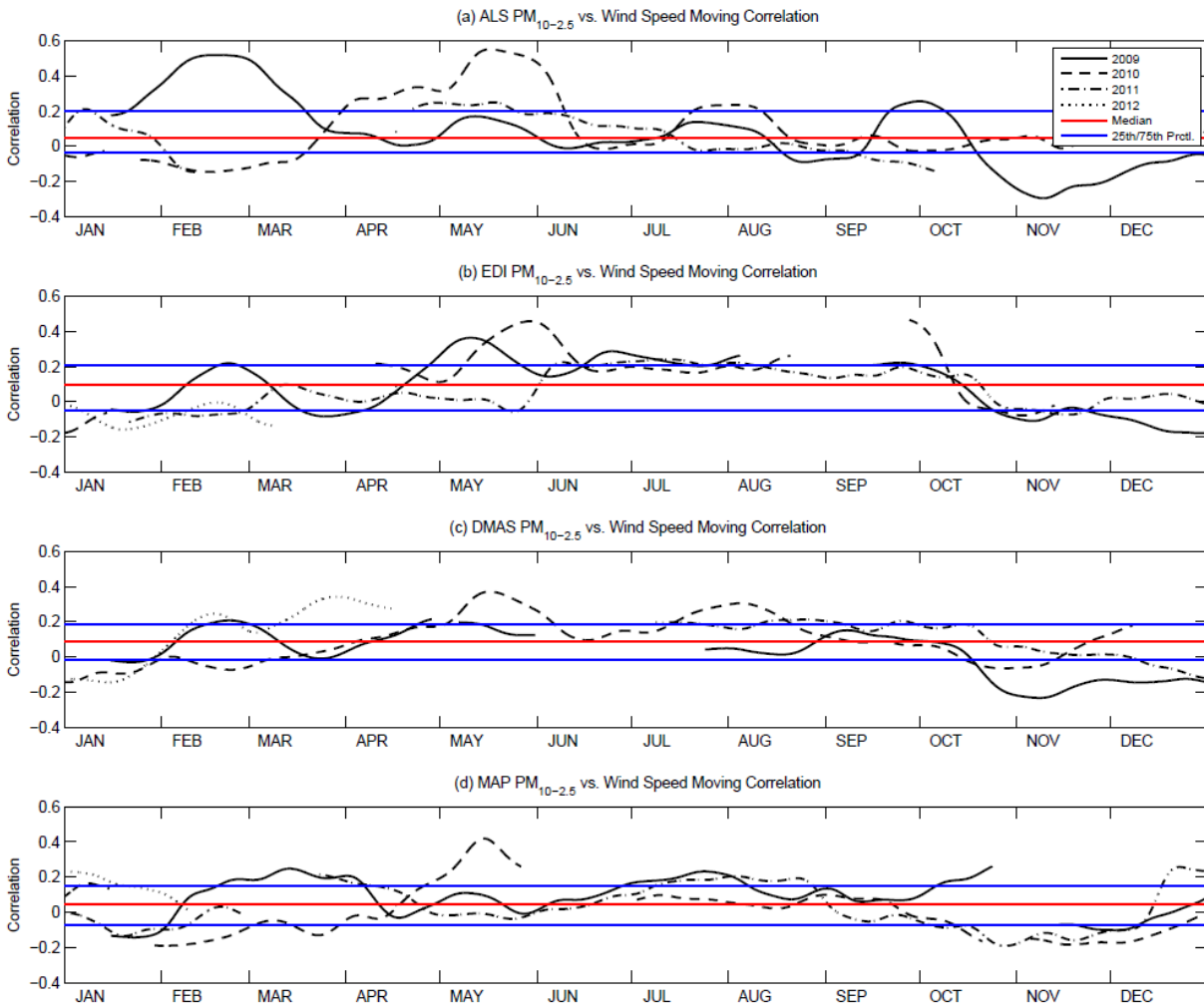
Figure 4.S14 Smoothed (Δθ=4 hours) moving correlation time series between relative humidity and $PM_{10-2.5}$ from (a) ALS, (b) EDI, (c) DMAS, and (d) MAP

155
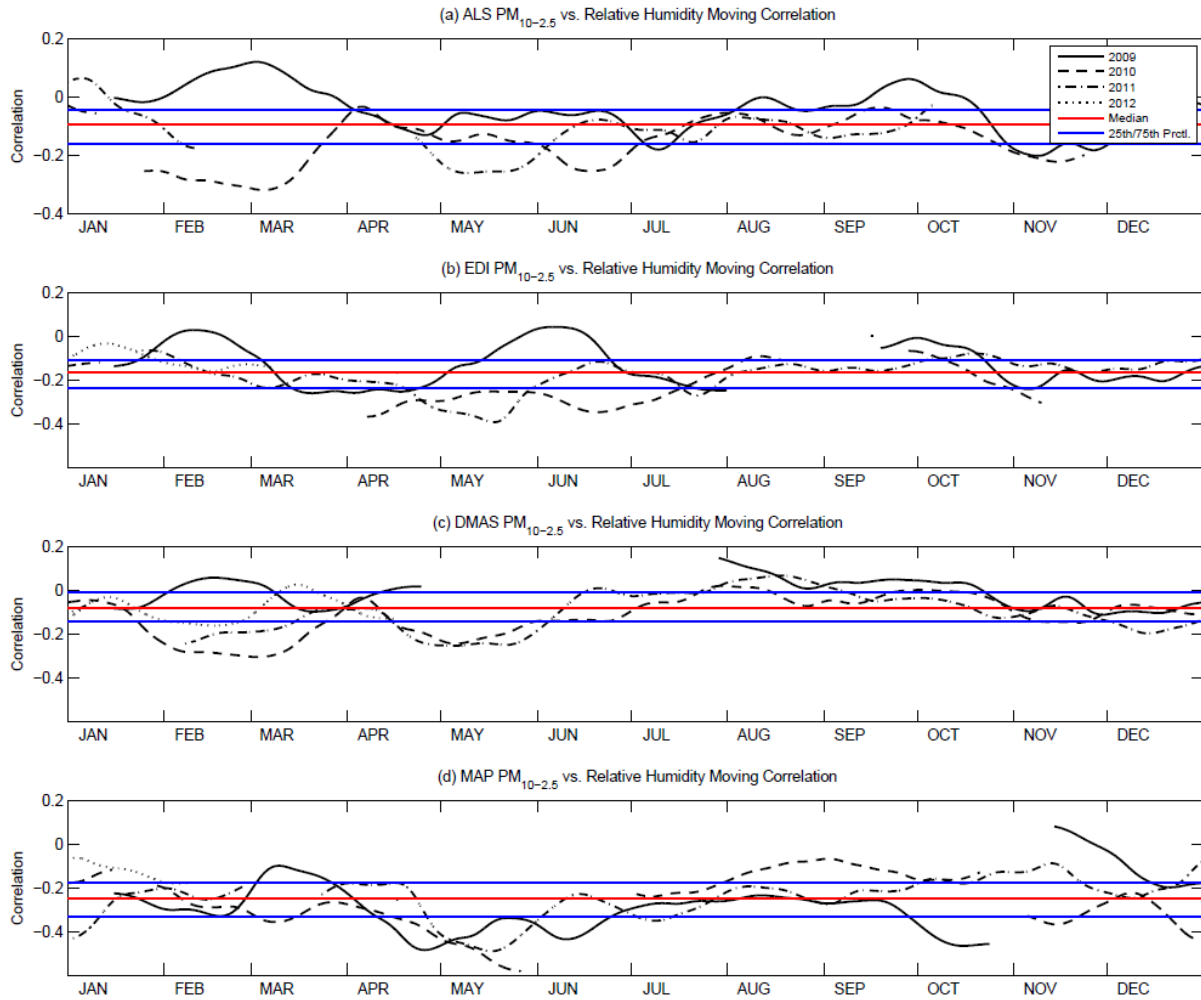
Figure 4.S15 Smoothed (Δθ=4 hours) time series of (a) Nunn soil moisture and (b) moving correlation between MAP PM$_{10-2.5}$ and soil moisture
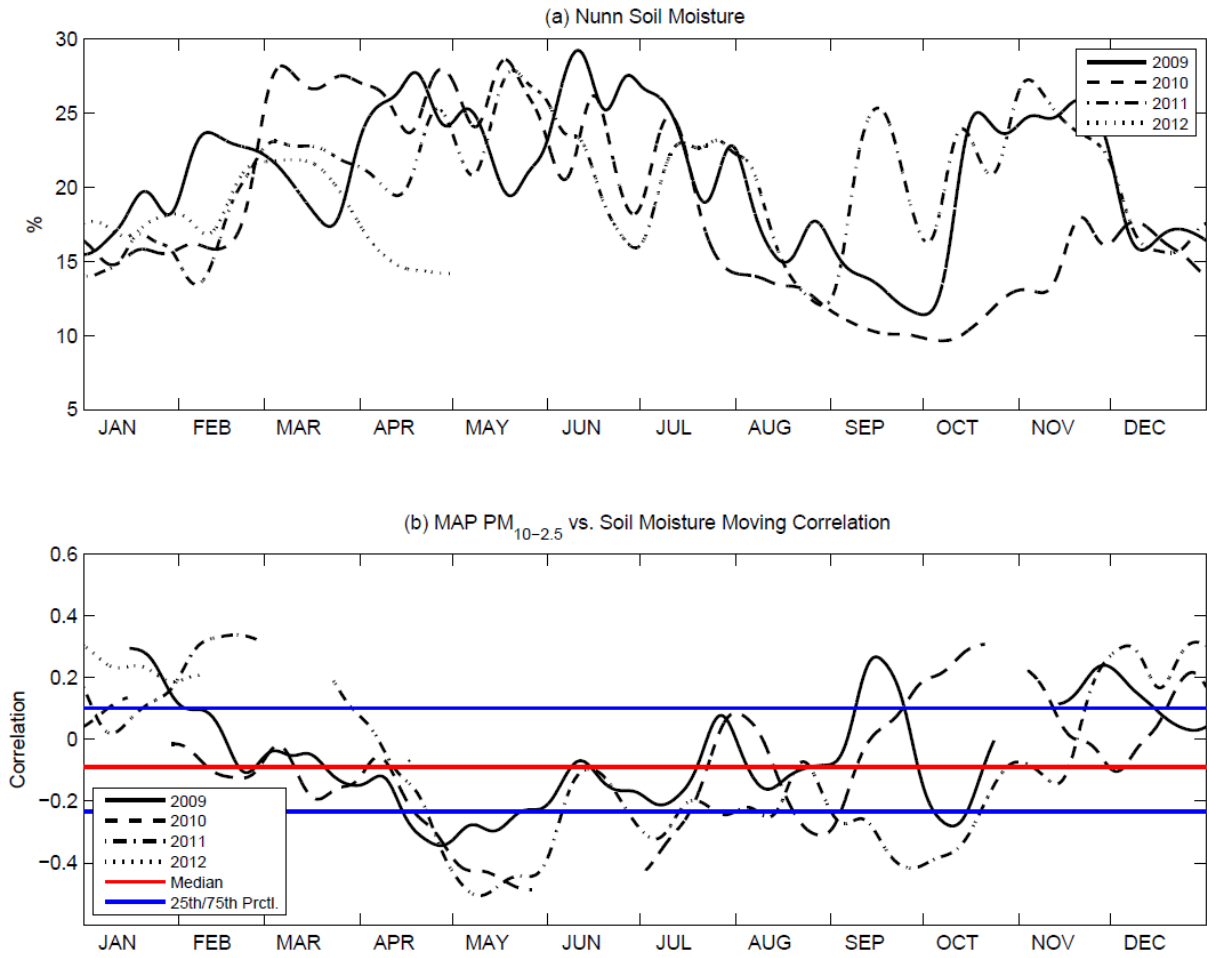
Figure 4.S16 Smoothed (Δθ=4 hours) time series of (a) Nunn soil temperature and (b) moving correlation between MAP $PM_{10\text{-}2.5}$ and soil temperature
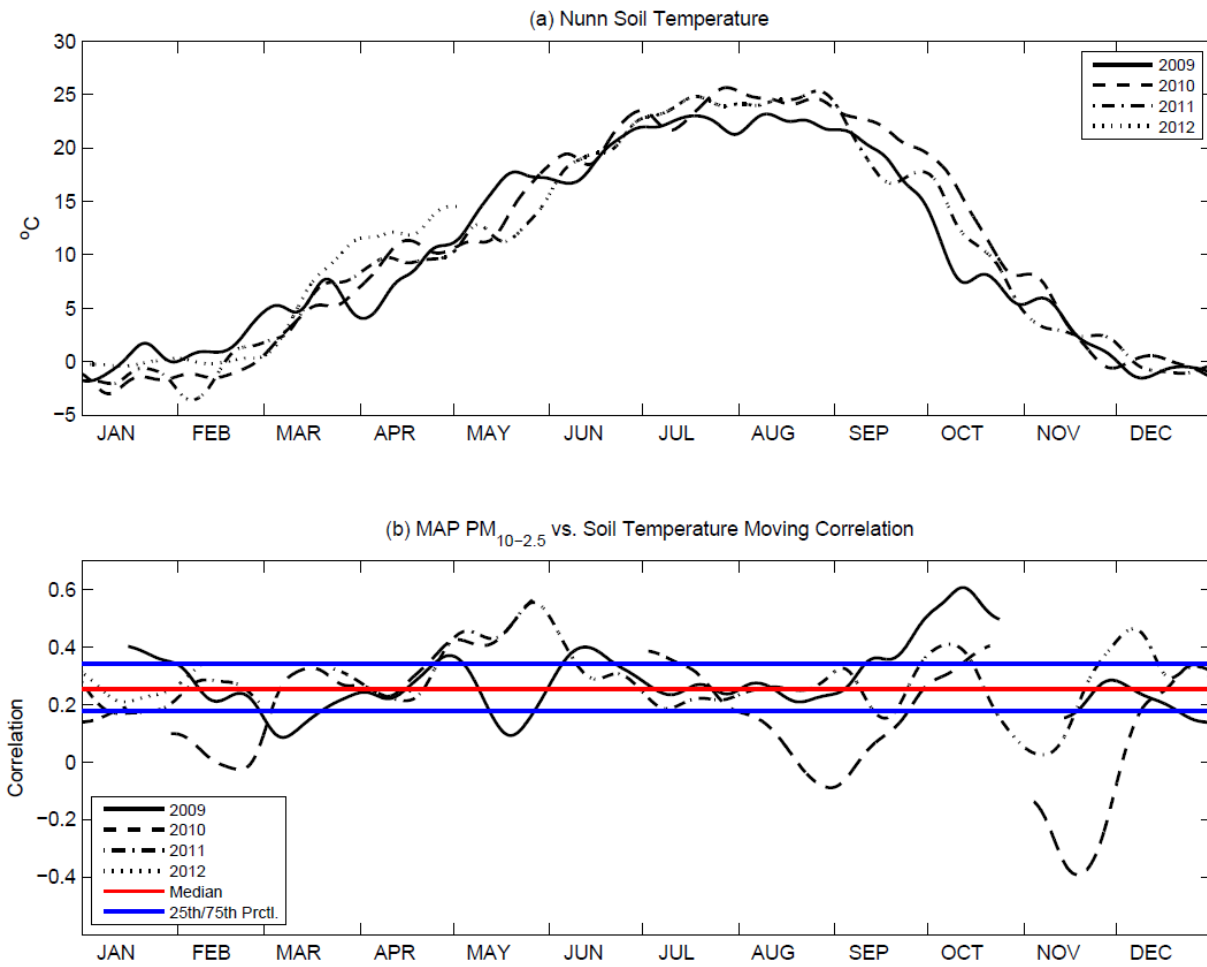
Figure 4.S17 Seasonal nonparametric regressions (thin lines are 95% confidence intervals) between wind speed and (a) DMAS $PM_{10-2.5}$ and (b) EDI $PM_{10-2.5}$
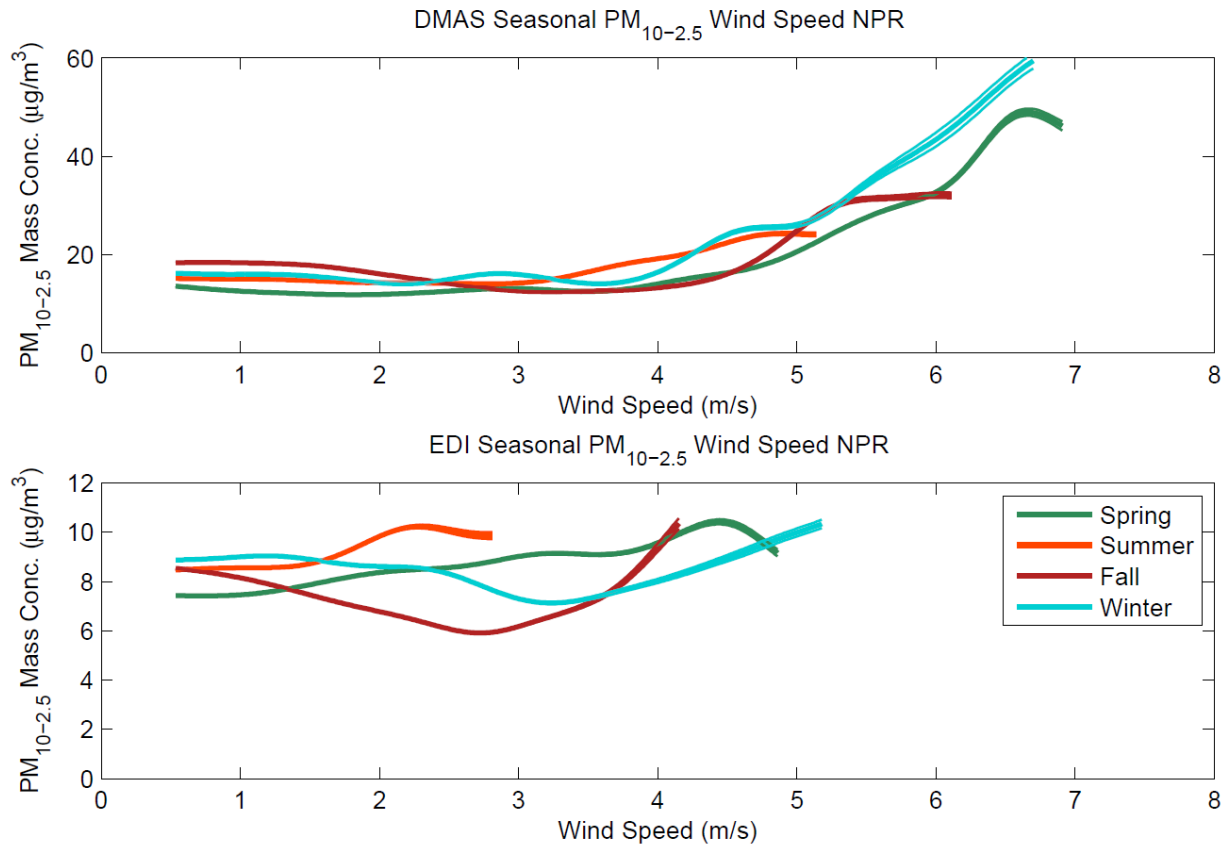
Figure 4.S18 Nonparametric regressions (dashed lines are 95% confidence intervals) between soil moisture and MAP (a) PM$_{10\text{-}2.5}$ and (b) PM$_{2.5}$

(a) MAP PM$_{10-2.5}$ vs. Soil Moisture NPR

(b) MAP PM$_{2.5}$ vs. Soil Moisture NPR
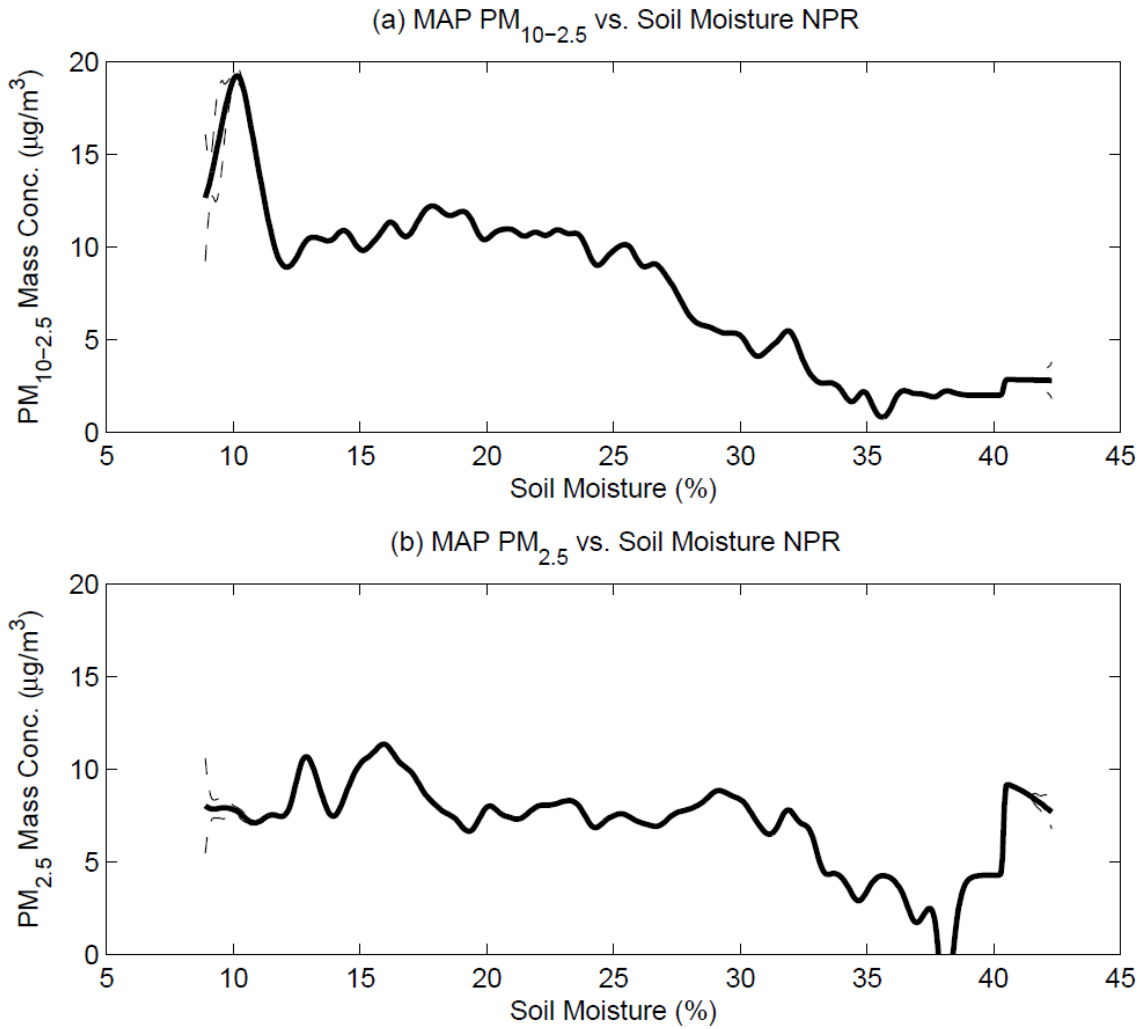
Figure 4.S19 Nonparametric regressions (dashed lines are 95% confidence intervals) between PM$_{10-2.5}$ and wind direction for (a) ALS, (b) EDI, (c) CAMP, (d) DMAS, and (e) MAP

(a) ALS PM$_{10-2.5}$ vs. Wind Direction NPR
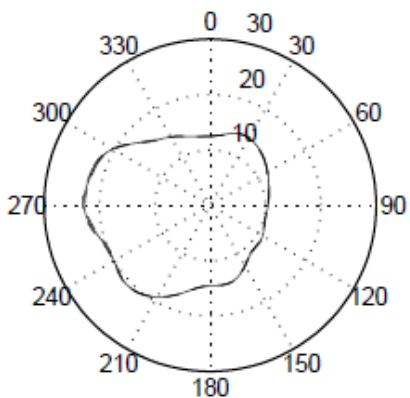
(b) EDI PM$_{10-2.5}$ vs. Wind Direction NPR
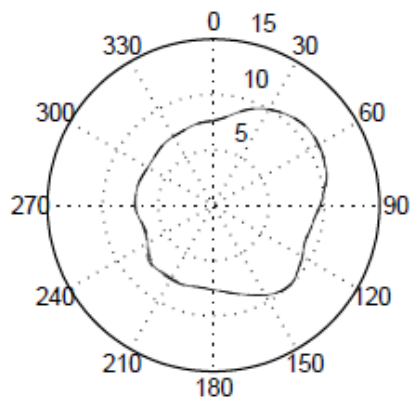
(c) CAMP PM$_{10-2.5}$ vs. Wind Direction NPR
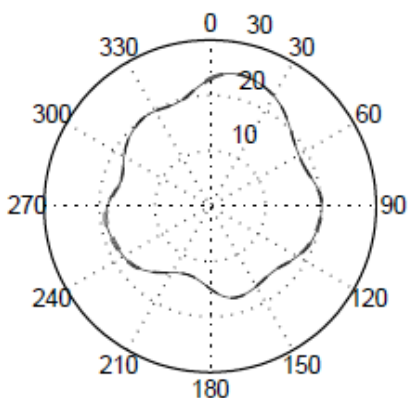
(d) DMAS PM$_{10-2.5}$ vs. Wind Direction NPR
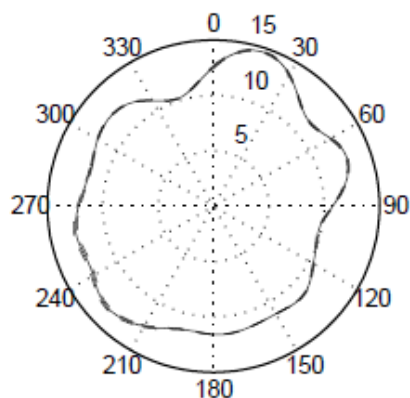
(e) MAP PM$_{10-2.5}$ vs. Wind Direction NPR

160
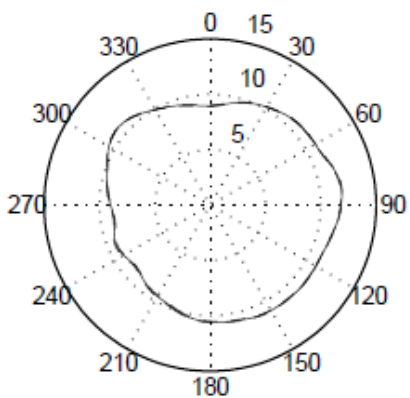
Figure 4.S20 Nonparametric regressions (dashed lines are 95% confidence intervals) between PM$_{2.5}$ and wind direction for (a) ALS, (b) EDI, (c) CAMP, (d) DMAS, and (e) MAP

(a) ALS PM$_{2.5}$ vs. Wind Direction NPR
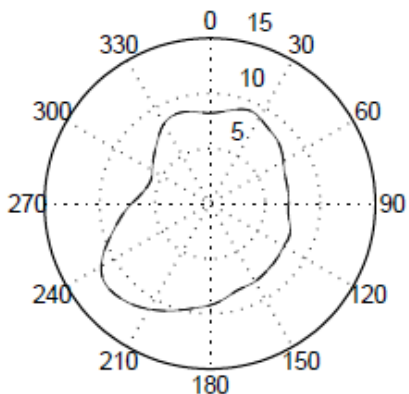
(b) EDI PM$_{2.5}$ vs. Wind Direction NPR
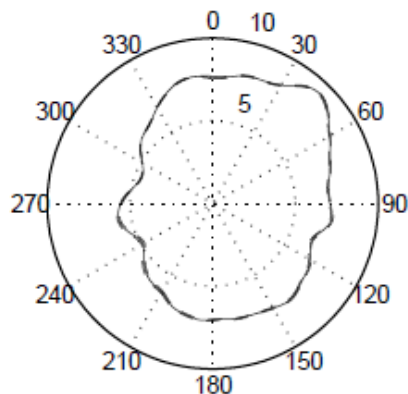
(c) CAMP PM$_{2.5}$ vs. Wind Direction NPR
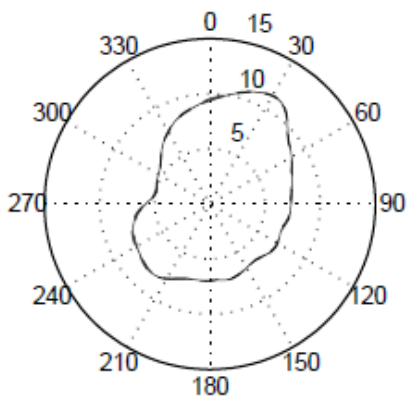
(d) DMAS PM$_{2.5}$ vs. Wind Direction NPR
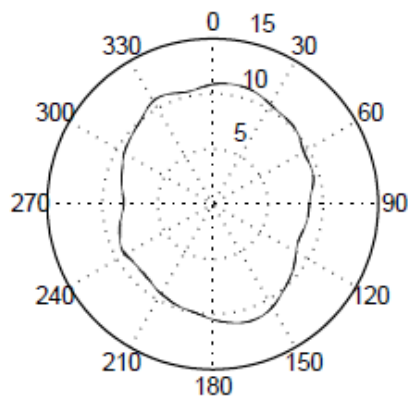
(e) MAP PM$_{2.5}$ vs. Wind Direction NPR
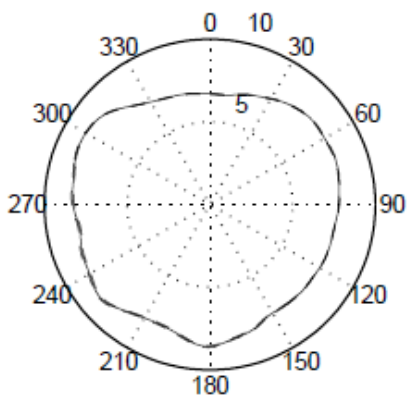
Figure 4.S21 Nonparametric regressions (dashed lines are 95% confidence intervals) between DMAS $PM_{10-2.5}$ and wind direction during (a) spring, (b) summer, (c) fall, and (d) winter

(a) Spring DMAS $PM_{10-2.5}$ vs. Wind Direction NPR
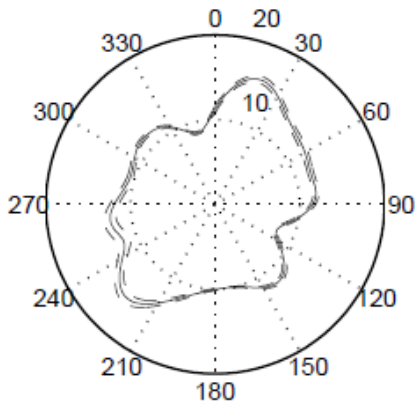
(b) Summer DMAS $PM_{10-2.5}$ vs. Wind Direction NPR
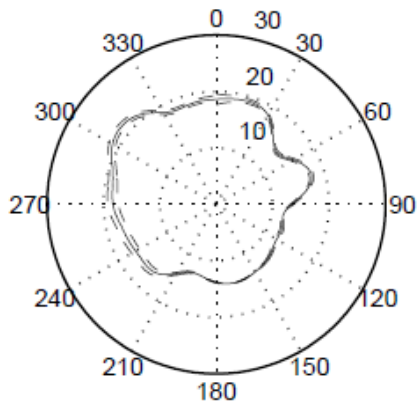
(c) Fall DMAS $PM_{10-2.5}$ vs. Wind Direction NPR
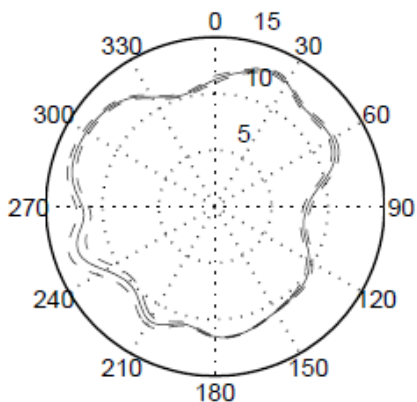
(d) Winter DMAS $PM_{10-2.5}$ vs. Wind Directon NPR
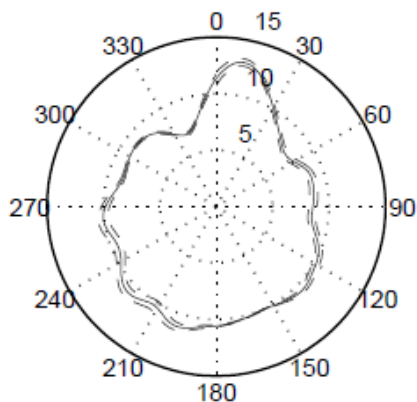
CHAPTER 5

CONCENTRATIONS AND SOURCE INSIGHTS FOR TRACE ELEMENTS IN FINE AND COARSE PARTICULATE MATTER IN NORTHEASTERN COLORADO

Nicholas Clements[a], Jenny Eav[b], Mingjie Xie[a], Michael P. Hannigan[a], Shelly L. Miller[a], William Navidi[c], Jennifer L. Peel[d], James J. Schauer[e], Martin M. Shafer[e], Jana B. Milford[a]

[a]Department of Mechanical Engineering, College of Engineering and Applied Science, University of Colorado at Boulder, Boulder, CO, 80309-0427

[b]Environmental Health Sciences, School of Public Health, University of California, Berkeley, Berkeley, CA, 94720

[c]Department of Applied Mathematics and Statistics, Colorado School of Mines, Golden, CO, 80401

[d]Department of Environmental and Radiological Health Sciences, Colorado State University, Fort Collins, CO, 80523

[e]Environmental Chemistry and Technology Program, University of Wisconsin-Madison, Madison, WI, 53706

5.0 ABSTRACT

The Colorado Coarse Rural-Urban Sources and Health (CCRUSH) study is a multi-year study focused on characterizing the mass, composition and sources of coarse particulate matter ($PM_{10-2.5}$) in Denver and Greeley, CO and evaluating how differences in PM concentrations and composition across locations might influence associations observed with health outcomes. Between the two cities, Denver is expected to have greater influence of industry and motor vehicles as a source of $PM_{10-2.5}$. Greeley is a smaller city with greater expected influence of agricultural activity. As part of the CCRUSH study, we collected integrated 24-hour samples of PM from four sites in Denver and Greeley at six day intervals from February 2010 to March 2011. Dichotomous samplers with Teflon filters were used to obtain samples for gravimetric and elemental analysis. Magnetic Sector Inductively Coupled Plasma-Mass Spectroscopy (SF-ICP-MS) was used to analyze digests of monthly composited filter samples for 49 elements. Thirty-nine elements were retained for statistical analysis after excluding those with low signal-to-noise ratios. The elements Sb, Cd, Zn, Mo, As, B, Cu, Pb, and W had crustal enrichment factors greater than 10 in both the $PM_{2.5}$ and $PM_{10-2.5}$ size ranges in both Denver and Greeley. Using positive matrix factorization (PMF) with bootstrap uncertainty estimation, we identified five factors influencing the element concentrations: a crustal factor contributing to both $PM_{2.5}$ and $PM_{10-2.5}$; a sodium-dominated $PM_{10-2.5}$ factor likely associated with road salt; a vehicle abrasion factor contributing in both size ranges; a regional sulfur factor contributing mainly to $PM_{2.5}$ and likely associated with coal combustion; and a local catalyst factor identified with high Ce and La enrichment in $PM_{2.5}$ at one of the sites in Denver.

5.1 INTRODUCTION

Particulate matter (PM) in both the fine (less than 2.5 microns aerodynamic diameter, $PM_{2.5}$) and coarse (2.5 to 10 microns, $PM_{10-2.5}$) size ranges is associated with harmful effects on human health (EPA, 2009). Over the past two decades, PM characterization and health impact studies have focused primarily on the fine fraction. As a result, understanding of the spatial and temporal variability, composition, and health effects of coarse PM is comparatively limited. This paper adds to the body of information on the chemical composition of $PM_{10-2.5}$ with detailed trace element data from four monitoring sites in Denver and Greeley, CO. The sites in Denver are expected to reflect urban influences including high traffic volumes, while those in Greeley are expected to represent a smaller community with greater influence from nearby agricultural activity. As part of the Colorado Coarse Rural-Urban Sources and Health (CCRUSH) study (Clements et al., 2012), the trace element data complement approximately three years of continuous hourly $PM_{10-2.5}$ and $PM_{2.5}$ mass concentration measurements from the same sampling sites, which will be analyzed for associations with data on birth outcomes and cardiovascular and respiratory hospital visits.

Published data indicate that compared to $PM_{2.5}$, $PM_{10-2.5}$ contains greater fractions of crustal elements such as aluminum, iron, and calcium, and also contributes ions, certain transition metals, organic, and biological material (e.g., Milford and Davidson, 1985; 1987; Boreson, et al., 2004; Hueglin et al., 2005; Malm et al., 2007). $PM_{10-2.5}$ is commonly derived from abrasive mechanical processes and resuspension, including construction and agricultural activities, tire and brake wear, road surface wear, vegetative debris, soil erosion, and sea spray (Patterson and Gillette, 1977; Duce et al, 1976; Thorpe and Harrison, 2008). In contrast, $PM_{2.5}$ is more likely to be produced from combustion, high-temperature industrial processes, and secondary atmospheric formation (Seinfeld and Pandis, 2006). Given the nature of sources of

$PM_{10-2.5}$, trace element profiles are especially useful to assist in source identification for this size range.

Information on $PM_{10-2.5}$ composition is also required to improve our understanding of what $PM_{10-2.5}$ characteristics are associated with health impacts, and how those associations might differ across time and location. Brunekreef and Forsberg (2005) reviewed nearly 60 studies that evaluated health effects of short-term exposure to $PM_{10-2.5}$ and concluded that for some endpoints, including chronic obstructive pulmonary disease, asthma, and respiratory admissions, $PM_{10-2.5}$ could have as strong as or a stronger effect than $PM_{2.5}$. Short-term increases in $PM_{10-2.5}$ have been positively associated with mortality in several studies (e.g., Castillejos et al., 2000; Mar et al., 2000; Ostro et al., 2000; Villeneuve et al., 2003; Zanobetti and Schwartz, 2009). Although some studies have speculated about which constituents of $PM_{10-2.5}$ might be linked to health effects (e.g., Shafer et al., 2010), the relationship between $PM_{10-2.5}$ composition and health responses is not well understood.

A limited number of recent studies have provided data on $PM_{10-2.5}$ elemental composition and used the data to draw inferences about potential sources. Sources or factors widely identified as contributing to the coarse size fraction include crustal material or mineral dust, and vehicle and road abrasion (Hueglin et al., 2005 (Switzerland); Karanasiou et al., 2009 (Athens, Greece); Moreno et al., 2011 (Barcelona, Spain); Moreno et al., 2013 (Madrid, Spain); Amato et al., 2011 (Barcelona, Spain); Pakbin et al., 2011 (Los Angeles, CA); Kumar et al., 2012 (Syracuse, NY)). Sea salt has also been identified as a contributing factor in coastal areas (Karanasiou et al., 2009; Amato et al., 2011; Pakbin et al., 2011) and road salt has been identified in areas with snowy winters (Kumar et al., 2012). Contributions from industrial sources have been identified in some larger cities (Moreno et al., 2011; Amato et al., 2011; Pakbin et al., 2011). Using adaptive clustering of element abundances determined with scanning electron microscopy, Kumar et al. (2012) inferred a minor contribution from biological matter based on the presence of P and C.

166

In the largest $PM_{10-2.5}$ characterization effort to date, Cheung et al. (2011) examined the chemical composition of $PM_{10-2.5}$ at 10 sampling sites in the Los Angeles Basin, from 24-hour samples collected once per week from April 2008 to March 2009. The study found that overall, crustal material and other trace elements (including non-sea salt Na, Cu, Zn, and Ba) accounted for almost half of reconstructed $PM_{10-2.5}$ mass. Inorganic ions and organic matter typically contributed about 20%. Contributions of crustal material and trace elements were higher at the inland sites (Riverside and Lancaster) than at most of the urban Los Angeles sites, except in winter. Cheung et al. (2011) found relatively high crustal enrichment factors (CEF) for trace elements associated with traffic: Sb, Sn, Mo, S, Cu, Pb, Zn, and Ba (in order of their CEFs), compared to Taylor and McLennan's (1985) profile for the upper continental crust. Enrichment factors were generally highest at the urban Los Angeles sites, and lowest at the rural desert site in Lancaster.

The CCRUSH study is focused on comparing the health effects of $PM_{10-2.5}$ and understanding $PM_{10-2.5}$ composition and sources in Denver and Greeley, CO. A previous publication from the study characterized the spatial and temporal patterns of $PM_{2.5}$ and $PM_{10-2.5}$ mass concentrations collected during the first six to 12 months of continuous sampling at the CCRUSH monitoring sites (Clements et al., 2012). The work highlighted the influence of wind speed on $PM_{10-2.5}$ concentrations, located source regions, and showed that $PM_{10-2.5}$ is highly temporally variable compared to $PM_{2.5}$. This paper presents the complementary elemental analysis of $PM_{2.5}$ and $PM_{10-2.5}$ from 24-hour filter samples collected at the CCRUSH sites every sixth day from February 2010 to March 2011. CEFs were calculated to assess the influence of crustal and non-crustal sources on the trace element concentrations. Factor analysis of the trace element data was conducted using PMF with bootstrap uncertainty analysis to further delineate potential sources. Future work will utilize results from these analyses to inform results from a three-year time-series study examining acute health effects in response to short-term exposure to $PM_{10-2.5}$.

5.2 METHODS

5.2.1 Site Descriptions

Sampling was conducted at two elementary schools in Denver: Edison (EDI) and Alsup (ALS). The two sites in Greeley, which is located about 80 km northeast of Denver, were Maplewood Elementary (MAP) and McAuliffe Elementary (MCA). ALS is located about 11 km northeast of downtown Denver, on the north end of an industrial suburb and east of the intersection of CO Highway 36 and Interstates 25, 270 and 76. EDI is an urban-residential site located in a neighborhood 5 km west-northwest of downtown Denver near the intersection of Interstates 25 and 70. Both sites in Greeley are in residential neighborhoods, with MCA located in the suburban fringe of town and MCA located 5 km east of MCA, near the town center. Clements et al. (2012) provide further details about the sampling locations.

5.2.2 Sample Collection

Ambient $PM_{10-2.5}$ and $PM_{2.5}$ samples were collected every sixth day from February 2010 to March 2011 from the rooftop of all four sites. All samples were collected using medium-flow dichotomous filter samplers assembled in-house according to the schematic in Figure 5.S1 of the supplementary information. Samples were collected from midnight to midnight on the sampling day.

Each filter sampler was equipped with a 50 liter per minute (lpm) PM_{10} inlet (Misra et al., 2003) and a virtual impactor (VI) with a 2.5 μm cutpoint (Misra et al., 2001). The VI separates the incoming PM_{10} sample stream into $PM_{10-2.5}$ and $PM_{2.5}$ streams with outlet flows of 48 lpm (major flow) for $PM_{2.5}$ and 2 lpm (minor flow) for $PM_{10-2.5}$. The two sample streams are then split equally and the particles deposited on Teflon (47 mm, 2μm pore size, Pall Gelman Teflon) and quartz filters (47 mm, Pall Gelman Tissuequartz). Four critical orifices controlled sampler flows and flow totalizers measured sampled air volumes. Quartz filters were used for carbon analyses

(not reported here). Teflon filters were weighed before and after sampling in a custom-built weigh box with temperature kept in the range from 23.9 to 27.2°C and relative humidity from 25-50%. Filters were allowed to equilibrate in the weigh box for at least 24 hours prior to weighing (Dutton et al., 2009).

Filters were combined into monthly composites for each site before elemental analysis. Filters from the two Greeley sites, MAP and MCA were further pooled, with the resulting composites identified hereinafter as GRE. $PM_{10-2.5}$ mass concentration correlations between the two Greeley sites were very high (R=0.97; Clements et al., 2012), supporting our use of composited filters. For quality control, filters flagged as having human or instrumental error were excluded. The study produced a total of 70 monthly composite samples and an additional 12 field blank monthly composites. Due to missing samples, monthly composites for ALS and EDI included from two to five every sixth day samples. Those for GRE included from four to eight samples.

5.2.3 Elemental Analysis and Uncertainty Estimation

Monthly composites were analyzed for 49 elements by Magnetic Sector Inductively Coupled Plasma-Mass Spectroscopy (SF-ICPMS) at the Wisconsin State Laboratory of Hygiene following the digestion and instrumental analysis methods described by von Schneidemesser et al. (2010). The SF-ICPMS mass data were corrected for field blanks by subtracting the median mass value of all field blanks for each element. Due to the use of a VI in the dichotomous sampler, a small fraction of $PM_{2.5}$ (approximately 0.04) is inherently included in the $PM_{10-2.5}$ outlet flow of the VI (Misra et al., 2001). This fraction of $PM_{2.5}$ is equal to the ratio of the VI minor outlet ($PM_{10-2.5}$) volumetric flow rate to the VI major outlet flow for each of the samples. The median of the ratios from each batch of filter samples was used to calculate the amount of $PM_{2.5}$ to subtract from the corresponding $PM_{10-2.5}$ monthly composite. Negative values were replaced with zeros.

Propagation of errors was used to estimate the overall uncertainty in the PM elemental concentration values, accounting for uncertainties in laboratory analysis of composite filters, field blank corrections, and flow volume. The laboratory analytical uncertainties included (also sum-of-squares propagated) components from (1 – ICPMS precision) the standard deviation of triplicate analyses of each sample with the SF-ICP-MS; (2 – method blank subtraction) the standard deviation of five laboratory method blanks for each analysis batch; and (3 – digestion recovery) the long-term standard deviation of digestion recovery uncertainties. Uncertainty in field blank corrections was taken as the standard deviation of the blank values for each element. Uncertainty in flow volume was estimated as 1% of total volume, for each filter. The elements Sc, Ni, Y, Rh, Pd, Ag, Sn, Pt, and Lu were omitted from further analysis because their median ratio of concentration to estimated uncertainty (signal to noise) was less than three for both $PM_{2.5}$ and $PM_{10\text{-}2.5}$ samples. Holmium was omitted because the ratio was less than two for the $PM_{2.5}$ size fraction. Among the excluded elements, Ni and Sn were expected to be present at detectable levels, but Ni had relatively high analytical uncertainty and Sn relatively large uncertainty in its field blank correction. Our analysis focused on the 39 remaining elements.

5.2.4 Enrichment Factors

Crustal enrichment factors (Zoller et al., 1974) were calculated to provide a general assessment of crustal influence on the elemental composition of $PM_{2.5}$ and $PM_{10\text{-}2.5}$. CEFs compare elemental concentrations found in PM with corresponding element concentrations found in crustal material, as:

$$CEF = \left. \frac{C_{i,PM}/C_{Al,PM}}{} \middle/ C_{i,crust}/C_{Al,crust} \right. \tag{1}$$

where C is the concentration in PM or crustal material, the subscript i denotes the element being considered, and Al is used as the reference element. The average upper continental crust composition reported by Taylor and McLennan (1985) has been widely used to calculate CEF

values (e.g., Cheung et al., 2011) and is used here to facilitate comparison with other studies. Values of CEF near unity suggest crustal weathering as the predominant source of the element. CEF values greater than 10 are usually taken to indicate that the elemental concentrations in PM are enriched relative to a crustal source. Values of CEF should be interpreted as only rough indicators of crustal contributions as the comparison is limited by spatial variations in crustal composition and the physical fractionation of these materials during aerosol suspension and transport (Reimann and De Caritat, 2000).

5.2.5 Factor Analysis

We used two-way Positive Matrix Factorization (PMF2) (Paatero, 1998a; 1998b) in the robust mode to perform factor analysis. PMF2 is a multivariate receptor model solved by minimizing the sum of the squared, scaled residuals (Q) in concentrations estimated as the sum of the products of factor profiles and contributions, under a positivity constraint. PMF was applied to a data set with 70 samples for 27 elements. Twelve of the elements considered in other parts of the study (B, Ti, Rb, Sr, Nb, Cs, Tl, Nd, Eu, Dy, Yb, and Th and Sr) were omitted from the PMF modeling due to having relatively low concentrations, high correlation with other elements that were retained, and/or limited value for source identification. We examined PMF results for four and five-factor solutions. This choice was guided by a principal components analysis of the same data set that identified four components with eigenvalues greater than one that explained about 90% of the variance. The behavior of Q as a function of the rotational parameter FPEAK has been used to provide insight into the rotational stability of modeling results, with a lower Q value corresponding to a more stable PMF solution. FPEAK was set to zero for all PMF runs reported here.

The method of Hemann et al. (2009) was applied to the data set to assess uncertainty of PMF solutions. Briefly, 1000 replicate data sets were generated from the original data set by resampling blocks of samples (with block size chosen algorithmically) with replacement using a

stationary block bootstrap technique (Politis et al., 2004) and then each block of samples was

independently analyzed with PMF2. Multilayer feed forward neural networks were trained to

sort and align the factors from each PMF bootstrap solution to the factors found in the base

case, by matching factor profiles. A PMF bootstrap solution was retained for use in subsequent

analysis only when each factor could be uniquely matched to a base case factor. The number

of factors used in the final model was determined using two criteria: the interpretability of

resultant PMF factor profiles and the success rate in factor matching for the bootstrap runs.

5.3 RESULTS AND DISCUSSION

5.3.1 Overview of Element Concentrations

Table 5.1 presents a statistical summary of the monthly composite concentrations for selected elements in the $PM_{2.5}$ and $PM_{10-2.5}$ size ranges at ALS, EDI, and GRE. Statistics were calculated based on the composited samples, which reduced the standard deviations compared to what would be seen if individual 24-hour filters had been analyzed. In addition to the mean and standard deviation, the table also shows the uncertainty in the element concentration values as the median coefficient of variation (COV; standard deviation (σ) divided by the mean) calculated through propagation of errors for each individual concentration value. For the elements listed in Table 5.1, the median 1σ uncertainties in concentrations range from 6 to 24 percent.

Table 5.1 Mean and standard deviation of composite concentrations of selected elements, reconstructed mass associated with the elements, and total mass in fine ($PM_{2.5}$) and coarse ($PM_{10-2.5}$) size fractions (ng m^{-3})

Element	ALS $PM_{2.5}$	EDI $PM_{2.5}$	GRE $PM_{2.5}$	ALS $PM_{10-2.5}$	EDI $PM_{10-2.5}$	GRE $PM_{10-2.5}$	Median COV
	n = 14	n = 10	n = 11	n = 14	n = 10	n = 11	-
Na	28.7±15.4	23.1±10.6	16.2±9.75	87.7±85.5	53.8±40.0	48.0±43.0	0.11
Al	41.5±28.5	28.7±14.9	22.6±12.4	95.5±54.7	57.3±23.3	66.2±44.6	0.10
P	4.78±3.00	2.57±1.11	2.40±1.40	5.60±3.02	3.74±2.03	9.09±8.97	0.08
S	179±65.0	216±77.6	129±78.1	33.2±15.3	28.3±11.7	30.5±27.3	0.09
K	40.5±27.0	33.7±12.2	28.5±20.0	80.0±44.9	47.7±23.0	68.5±61.1	0.13
Ca	48.2±33.7	25.4±13.2	19.6±10.8	101±53.9	51.4±23.1	53.1±37.9	0.13
Fe	89.1±59.8	55.9±20.9	33.5±22.1	130±70.6	85.4±41.0	68.6±52.6	0.15
Cu	2.36±1.73	2.70±1.59	1.03±0.733	1.65±1.13	1.75±1.11	0.861±0.671	0.17
Zn	12.7±11.3	3.89±2.15	2.19±1.59	3.54±2.37	2.24±1.31	1.36±0.942	0.18
As	0.204±0.146	0.188±0.098	0.097±0.054	0.039±0.016	0.036±0.013	0.034±0.028	0.24
Sb	0.467±0.406	0.379±0.184	0.190±0.224	0.228±0.175	0.266±0.197	0.110±0.112	0.06
Pb	1.06±0.642	1.01±0.480	0.562±0.357	0.447±0.294	0.331±0.183	0.207±0.151	0.13
La	0.241±0.139	0.083±0.055	0.025±0.010	0.121±0.059	0.054±0.024	0.047±0.032	0.06
Ce	0.326±0.191	0.130±0.065	0.056±0.026	0.227±0.111	0.115±0.054	0.107±0.073	0.06
Total Elem.	472±210	411±132	267±142	580±292	359±122	372±259	-
Recon. Mass	1490±598	1400±478	912±460	1730±870	1080±362	1160±771	-
Total Mass	6480±2060	5700±1640	5760±1760	7900±4250	4410±890	6380±3150	-

Total element concentrations shown in Table 5.1 are the sum of concentrations for 39 elements, as discussed in the methods section. The table also shows the total mass concentrations and standard deviations for the filter samples determined by gravimetric analysis. Finally, an estimate of reconstructed mass associated with the elements is presented, calculated by assuming the dominant crustal materials are present as the oxides MgO, Al_2O_3, K_2O, CaO, Fe_2O_3, and TiO_2 (Chow et al., 1994), sodium is present as NaCl, and sulfur as $(NH_4)_2SO_4$. Silicon was not measured, but is estimated to be present in a ratio of 3.4:1 with Al and treated as SiO_2 for mass reconstruction purposes (Hueglin et al. 2005; Countess et al., 1980).

For comparison with the total mass concentrations reported in Table 5.1, EPA (2009) reported a national mean $PM_{2.5}$ concentration for the period from 2005 – 2007 of 12 µg m^{-3}, based on nearly 350,000 observations, and a national mean $PM_{10-2.5}$ concentration of 13 µg m^{-3}, based on just over 12,000 observations. Thus the filter samples from ALS, EDI and GRE reflect $PM_{2.5}$ concentrations that are about half of the 2005 - 2007 national average. Filter sample $PM_{10-2.5}$ concentrations at the three sites range from one-third of the national average at GRE to three-fifths at ALS.

As shown in Table 5.1, total element concentrations in the $PM_{2.5}$ size fraction were highest at ALS, followed by EDI and then GRE. The total $PM_{2.5}$ element concentrations at ALS were almost 80% higher than those at GRE; concentrations at EDI were over 50% higher than those at GRE. In the $PM_{10-2.5}$ size fraction, total element concentrations were highest at ALS, followed by GRE and EDI. The total $PM_{10-2.5}$ element concentrations at ALS were almost 60% higher than those at GRE, while concentrations at EDI were 3% lower than those at GRE. Averaged by season and across sites, total element concentrations were highest in fall for both $PM_{2.5}$ and $PM_{10-2.5}$. Seasonal averages and standard deviations for total element concentrations in the $PM_{2.5}$ size range were 384±128 ng m^{-3} in winter; 329±113 ng m^{-3} in spring; 286±147 ng m^{-3} in summer and 538±251 ng m^{-3} in fall. For total element concentrations in the $PM_{10-2.5}$ size

174

range, the averages and standard deviations were: 392±257 ng m^{-3} in winter; 315±123 ng m^{-3} in spring; 442±138 ng m^{-3} in summer and 639±336 ng m^{-3} in fall.

For PM$_{2.5}$, the average total element concentrations range from 4.6% at GRE to 7.3% at ALS of the average total PM$_{2.5}$ mass concentrations measured gravimetrically for the Teflon filter samplers. For PM$_{10\text{-}2.5}$, the average total element concentrations are from 5.8% at GRE to 8.1% at EDI of the average total mass concentrations. The element fractions of PM$_{10\text{-}2.5}$ mass measured in this study are lower than those that Pakbin et al. (2011) recently found for sampling sites in the Los Angeles basin. The trace element concentrations reported in their study sum to 15 to 20% of the annual average PM$_{10\text{-}2.5}$ mass concentrations.

Reconstructed mass concentrations in Table 5.1 are from 3.2 to 3.4 times greater than total element concentrations for PM$_{2.5}$, and about 3.0 to 3.1 times greater for PM$_{10\text{-}2.5}$. The reconstructed mass associated with the reported elements thus comprises from 16 – 24% of total PM$_{2.5}$ mass concentrations and 18 – 24% of PM$_{10\text{-}2.5}$ mass concentrations at the Denver and Greeley monitoring sites.

Trends across sites and sizes in concentrations of individual elements shown in Table 5.1 generally follow the trends for the total element concentrations, with the highest concentrations of individual elements at ALS for both size ranges, and the lowest concentrations at GRE for the PM$_{2.5}$ size range and at EDI for the PM$_{10\text{-}2.5}$ size range. However, the highest concentrations of S and Cu in the fine size range are seen at EDI, not ALS. The highest concentrations of P in the coarse size range are seen at GRE.

Elemental concentrations (and total mass concentrations) reported here for the PM$_{10\text{-}2.5}$ size range are generally lower than those reported for the Los Angeles Basin for April 2008 – March 2009 (Cheung et al., 2011). As representative examples, the highest concentrations reported in Table 5.1 above for Al, Ca, Fe, Zn, and Cu are respectively 40, 40, 55, 30 and 80% lower than the lowest concentrations reported by Cheung et al. (2011). Elemental concentrations reported here display an even sharper contrast with those published for Denver

in previous decades. Lewis et al. (1986) reported trace element concentrations in the $PM_{2.5}$ and

$PM_{15 -2.5}$ (2.5 to 15 μm) size ranges based on measurements made in a vacant parking lot 10 km

northeast of Denver's city center during twenty days in January 1982. They used a 16.7 L min^{-1}

dichotomous sampler with Teflon filters on a 12-hour schedule, collecting samples from 0600 –

1800 and 1800 – 0600 MST. Samples were analyzed using X-ray fluorescence. Elemental

concentrations in $PM_{2.5}$ reported by Lewis et al. (1986) are one to five times higher than those

we measured for wintertime samples collected at ALS for P, S, K, Ca, Fe, Cu and Zn; 14 times

higher than those reported here for Al, and 280 times higher for Pb. Elemental concentrations

of $PM_{15-2.5}$ exceed those found in this study for $PM_{10-2.5}$ by factors of four to ten for S, K, Ca, Fe,

Cu and Zn; a factor of 38 for Al; and a factor of 236 for Pb. For Ca, Fe, and Al, some of the

difference may be accounted for by larger size range of the dichotomous sampler used by Lewis

et al. (up to 15 μm). This is not likely to be a significant factor for the other elements listed, as

their airborne mass size distributions exhibit little mass in particles larger than 10 μm in

aerodynamic diameter (Milford and Davidson, 1985).

5.3.2 Elemental Mass Composition by Size and Location

Figures 5.1(a) and (b) show median values of the fraction of total element mass

contributed by each of the trace elements for which concentrations were quantified in this study.

For $PM_{2.5}$, S is the most abundant element, comprising 44 to 53% of elemental mass,

depending on the site. Fe, Ca, K, Al, and Na follow with elemental mass fractions of 5 – 16%.

About 95% of the total $PM_{2.5}$ element concentration is accounted for by the first eight elements

shown in Figure 5.2(a). For $PM_{10-2.5}$, Fe, Ca, Al, and K are the most abundant elements, each

contributing from 13 to 22% of elemental mass, depending on the site. Na and S are next in

abundance, with $PM_{10-2.5}$ elemental fractions of 6 to 10%. About 90% of the total $PM_{10-2.5}$

element concentration is accounted for by the first eight elements in Figure 5.2(b).

Along with PM mass concentrations, differences in composition across sites are important to identify for future health studies, as they may help explain differences across the sites in observed health effects. For both the $PM_{2.5}$ and $PM_{10-2.5}$ size ranges, Figure 5.1 shows that the median elemental mass fractions are generally consistent across sites. Although application of the Kruskal-Wallis test indicates differences across sites are statistically significant for elemental mass fractions of 15 of 39 elements in the $PM_{2.5}$ size range and 16 of 39 elements in the $PM_{10-2.5}$ size range, most of the differences are less than a factor of two in magnitude. In the $PM_{2.5}$ size range, the exceptions are that the proportions of elemental mass contributed by Zn, La, Ce and Tl are at least twice as high at ALS as at one or both of the other sites; and that the proportion contributed by Mo is less than half as high at GRE as at the other two sites. In the $PM_{10-2.5}$ size range, the median proportion of elemental mass contributed by Mo at Greeley is less than half that at the two other sites; and the proportions contributed by Sb and W are more than twice as high at Edison as at Greeley.

Figure 5.1 Median mass fractions of elements across sampling sites for (a) fine and (b) coarse size fractions. Asterisks indicate elements for which mass fractions differ significantly across sites

177
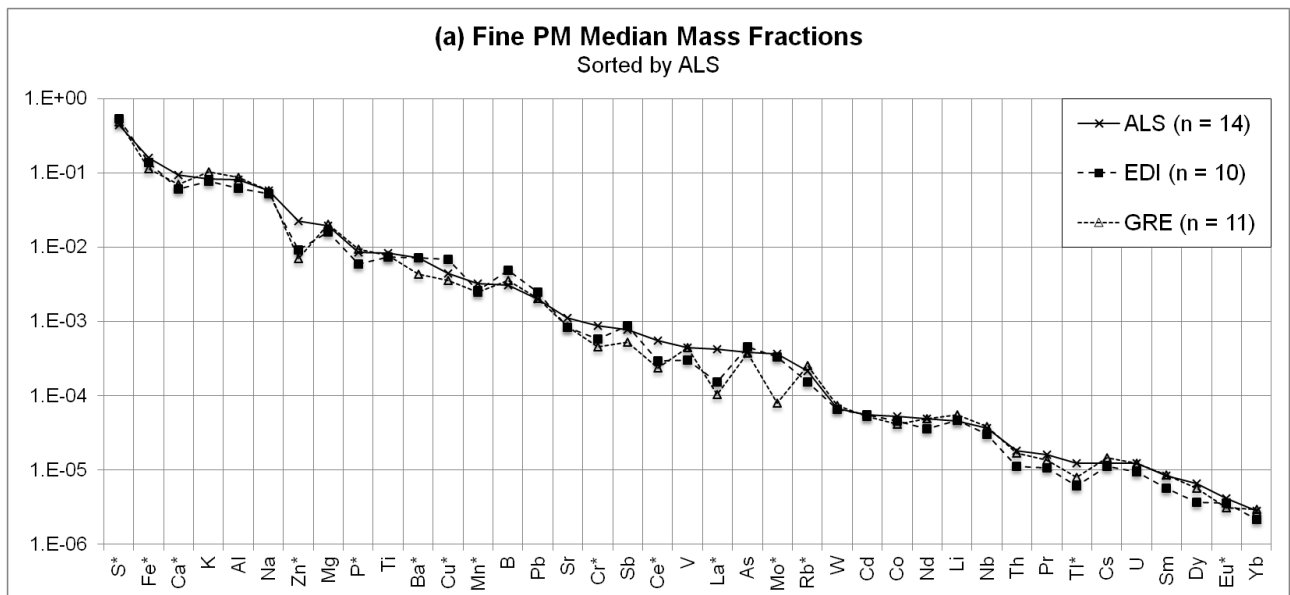
Figure 5.1 (*continued*) Median mass fractions of elements across sampling sites for (a) fine and (b) coarse size fractions. Asterisks indicate elements for which mass fractions differ significantly across sites
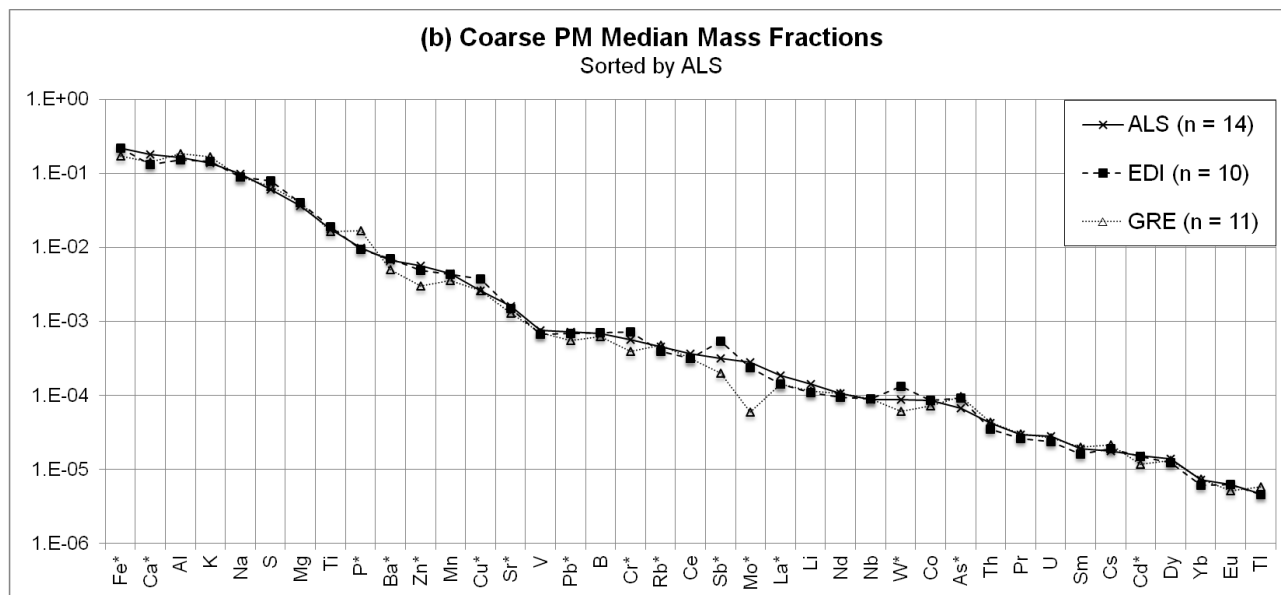
5.3.3 Distribution of Elements Between PM$_{2.5}$ and PM$_{10-2.5}$

To illustrate how the size distribution of elements differs across locations, Figure 5.2 shows median ratios of concentrations in the PM$_{2.5}$ and PM$_{10-2.5}$ size classes. At all three locations, S, As, B, Cd, Zn, Pb, Tl, Sb, Cu, and Mo are primarily found in the PM$_{2.5}$ size fraction. La is primarily found in the PM$_{2.5}$ size fraction at ALS and EDI but is mostly in the PM$_{10-2.5}$ size range in the samples from GRE. Similarly, Ce is primarily found in PM$_{2.5}$ at ALS, about evenly distributed at EDI and mostly found in the PM$_{10-2.5}$ size fraction at GRE. For the remaining compounds the median ratio of PM$_{2.5}$ to PM$_{10-2.5}$ concentrations is less than one. The size preferences shown in Figure 5.2 are generally consistent with size distributions reported in the literature (Milford and Davidson, 1985; Hays et al., 2011). However, size distributions for Cr, Cs, Mn, U, V and W appear to be shifted more toward the PM$_{10-2.5}$ size range than expected based on mass median diameters reported in older studies (Milford and Davidson, 1985). This

may be due to a shift in sources over time or across locations from emissions associated with

high temperature industrial sources to emissions from abrasive processes.

Figure 5.2 Median ratios of element concentrations in $PM_{2.5}$ and $PM_{10-2.5}$ size ranges by sampling site
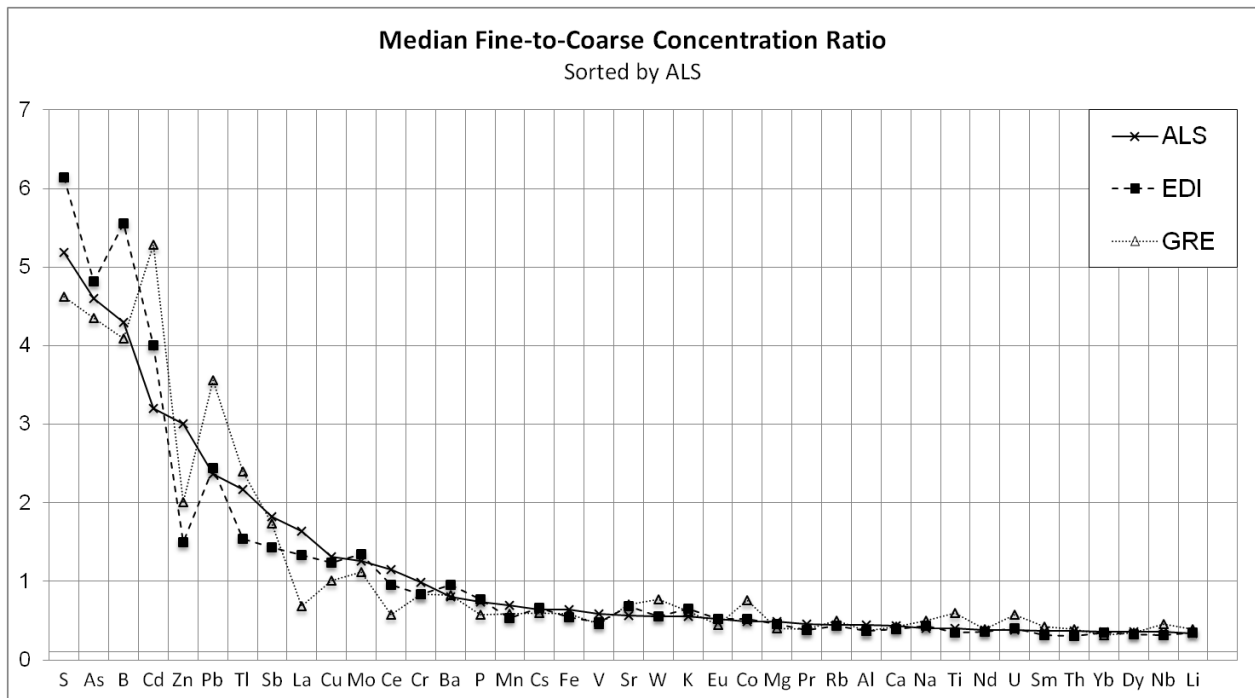
5.3.4 Crustal Enrichment Factors

Figure 5.3 shows crustal enrichment factors calculated for element concentrations in

$PM_{2.5}$ and $PM_{10-2.5}$, using Al as the reference compound and the upper continental crust

reference values from Taylor and McLennan (1985). The elements Sb, Cd, Zn, Mo, As, B, Cu,

Pb and W have CEF values above 10 for all three sites and in both the $PM_{2.5}$ and $PM_{10-2.5}$ size

ranges, suggesting enrichment from non-crustal sources. As expected, CEF values are

generally higher for $PM_{2.5}$ than $PM_{10-2.5}$, particularly for the more highly enriched elements. In

the $PM_{10-2.5}$ size range, CEF values for the more highly enriched elements are higher at ALS

and EDI than at GRE, which is consistent with the hypothesis that non-crustal influences would

be greater in Denver than Greeley.

Figure 5.3 Crustal enrichment factors for $PM_{2.5}$ and $PM_{10-2.5}$ element concentrations based on Taylor and McLennan's (1985) elemental profile for the upper continental crust
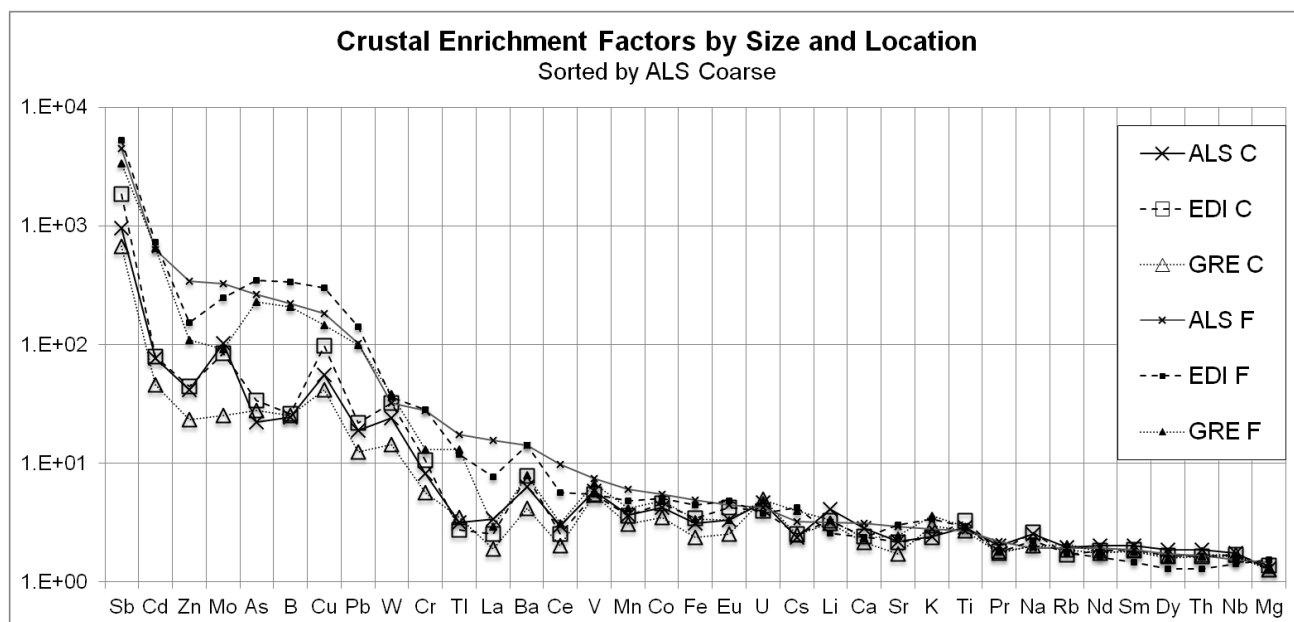
In the $PM_{2.5}$ fraction, La and Ce stand out as relatively highly enriched at EDI and

especially at ALS. To investigate this finding further, Table 5.S1 in the supplementary

information shows ratios of La to other lanthanide elements quantified in this study in

comparison to corresponding ratios for three potential sources: fluidized catalytic converters

used in petroleum refineries (Kulkarni et al., 2006); automobile catalytic converters (Kulkarni et

al., 2006); and the upper continental crust (Taylor and McLennan, 1985). The finding that both

La and Ce are enriched at ALS and EDI suggests automobile catalysts as a potential source

(Moreno et al., 2008). However, two refineries located within 4 km of ALS might contribute to

the greater degree of La enrichment at that location.

For four sites in the Los Angeles Basin, Cheung et al. (2011) reported CEFs for 22 elements in $PM_{10-2.5}$, also using Taylor and McLennan's (1985) upper continental crust profile. They reported CEF values above 10 for Sb, Sn, Mo, S, Cu, Pb, Zn, and Ba, and did not report CEF values for Cd, As, B, or W. As in our study, they found Sb to be the most highly enriched element, with CEF values above 1000 at three of their four sites. Antimony is used in multiple vehicle components including brake linings; other studies have similarly reported high CEF values for this metal at traffic-influenced sites (Iijima et al., 2009; Belzile et al., 2011). Cheung et al.'s CEF values for Mo, Cu, and Zn were close to those reported for $PM_{10-2.5}$ in this study, while their CEF values for Pb and Ba were respectively about three and four times higher than those found here.

As noted above, Lewis et al. (1986) reported trace element concentrations in the $PM_{2.5}$ and $PM_{15-2.5}$ size ranges from northeast Denver site for January 1982. For comparison with our results, we calculated CEFs for the elements reported in their study, again using the Taylor and McLennan reference profile. The average element concentrations that Lewis et al. (1986) report yield CEF values below 10 for K, Ca, Ti, Mn, Fe, Rb, and Sr in both for $PM_{2.5}$ and $PM_{15-2.5}$ size ranges, consistent with our findings. Lewis et al.'s concentrations also yield CEF values in line with those found here for several more enriched elements, including Ba, Cr, and Zn. On the other hand, sharp differences are apparent for Cu, Cd, and Pb. The average $PM_{15-2.5}$ concentrations reported by Lewis et al. for Cu, Pb, and Cd yield CEF values of 9 for Cu, 140 for Pb, and 3200 for Cd. Their average $PM_{2.5}$ concentrations yield CEFs of 77 for Cu, 3300 for Pb and 12,500 for Cd. Our CEF values for Cu are thus about two to four times higher than those calculated for Lewis et al.'s data. In contrast, Lewis et al.'s concentrations yield CEF values for Pb and Cd that are 10 to 40 times higher than those found in our study. Sharp reductions in Pb enrichment have been observed in other cities and are generally attributed to the phase out of leaded gasoline (Cheung et al., 2012; Gianini et al., 2012). The reduction in Cd enrichment may

be due to improved emissions controls for coal combustion and metal processing, as well as reduced use of Cd in pigments and plating materials (Klepper et al., 1995; Pacyna et al., 2009).

5.3.5 Factor Analysis Results

Positive matrix factorization was applied to a dataset with concentrations of 27 elements in both the $PM_{2.5}$ and $PM_{10-2.5}$ size ranges. A solution with five factors was selected as providing interpretable factor profiles and yielding a success rate of about 60% in factor matching for the bootstrap runs, which was the best rate achieved with this dataset. The inability to achieve a higher matching rate is likely due to the relatively small number of observations (70) used in the PMF model. Figure 5.4 presents normalized factor profiles, showing the fraction of the individual element concentrations accounted for by each factor. Non-normalized profiles showing elemental mass fractions are presented in the supplementary information (Figure 5.S2). Error bars in Figure 5.4 represent ± one standard deviation in the profile estimates from the bootstrap sampling runs, for the subset of samples with factors that matched those estimated from the original data set.

As shown in Figure 5.4, Factor 1 accounts for most of the Na and significant Li and W. Factor 2 accounts for most of the crustal elements, including half or more of the Fe, Al, Ca, and Mg and the rare earth elements including Pr and Sm. Factor 3 accounts for more than 80% of the S in the data set. Factor 3 also accounts for more than half of the observed As, Cd, and Pb. Factor 4 accounts for significant fractions of the metals that are characteristic of vehicle abrasion processes such as brake and tire wear, including Cu, Sb, Zn, Mo, and Ba (Lough et al. 2005; Thorpe and Harrison, 2008). Finally, Factor 5 accounts for a high proportion of the La and about half of the Ce, two rare earth elements that are found in zeolite catalyst materials (Kulkarni et al., 2006; Moreno et al., 2008). The factors identified using PMF closely follow the correlation structure of the data set, which is shown in Table 5.S2 in the supplementary information. For example, Pearson correlation coefficients with Na (Factor 1) are greater than

0.7 only for Li and W. Elements with correlations above 0.7 for Al (Factor 2), S (Factor 3), Sb (Factor 4), and La (Factor 5) are similarly associated with the corresponding factors.

As expected, the more abundant elements dominate the factor profiles when they are presented in terms of element mass fractions (Figure 5.S2 of the supplementary information). Factor 1 is comprised primarily of Na (53%) and Fe (16%). The elemental mass in Factor 2 is dominated by Al (23%), K (18%), Ca (21%) and Fe (24%). S comprises 80% of the elemental mass in factor 3. While Factor 4 is identified by metals that are markers of brake and tire wear, its elemental mass is dominated by Fe (52%), Ca (13%) and K (12%). Similarly, while Factor 5 is uniquely identified by La and Ce, its elemental mass is comprised mainly of Fe (20%), Al (18%), Ca (17%) and S (16%).

Figure 5.4 Normalized PMF factor profiles for 27 elements based on concentrations in $PM_{2.5}$ and $PM_{10-2.5}$ in Denver and Greeley, CO
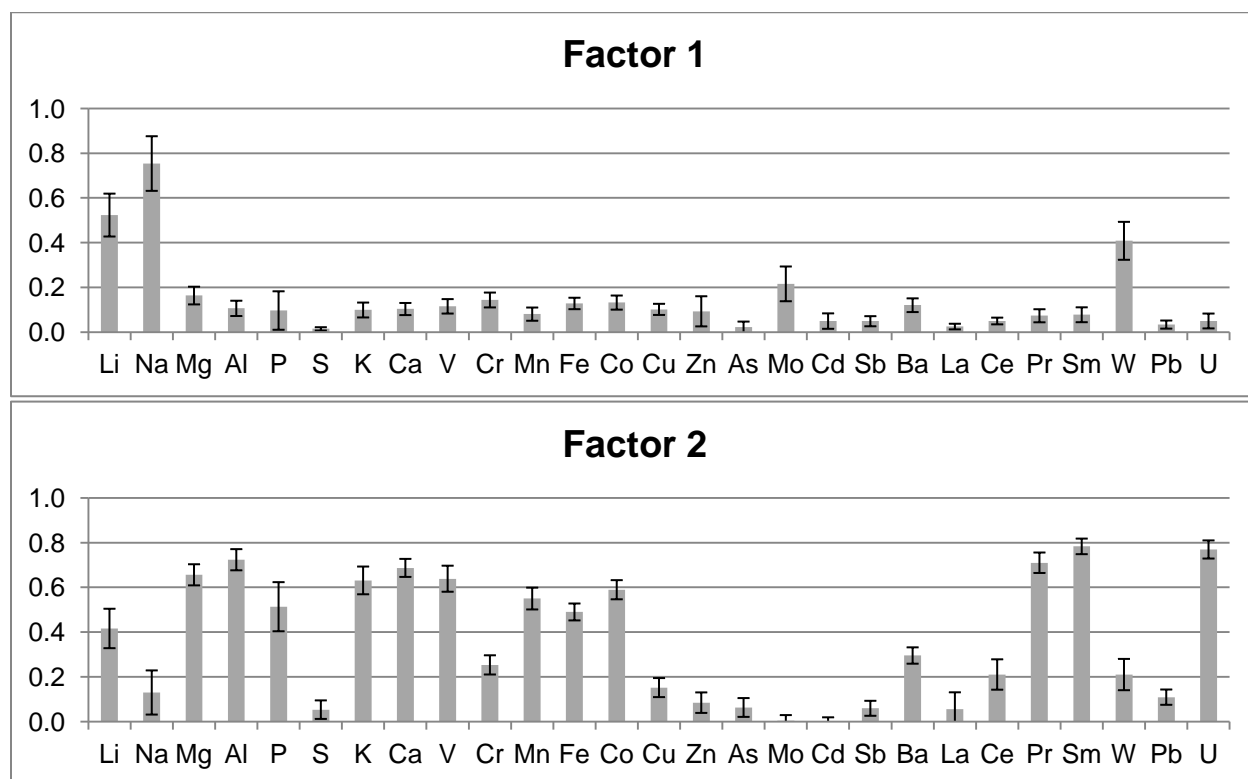
Figure 5.4 (*continued*) Normalized PMF factor profiles for 27 elements based on concentrations in $PM_{2.5}$ and $PM_{10-2.5}$ in Denver and Greeley, CO
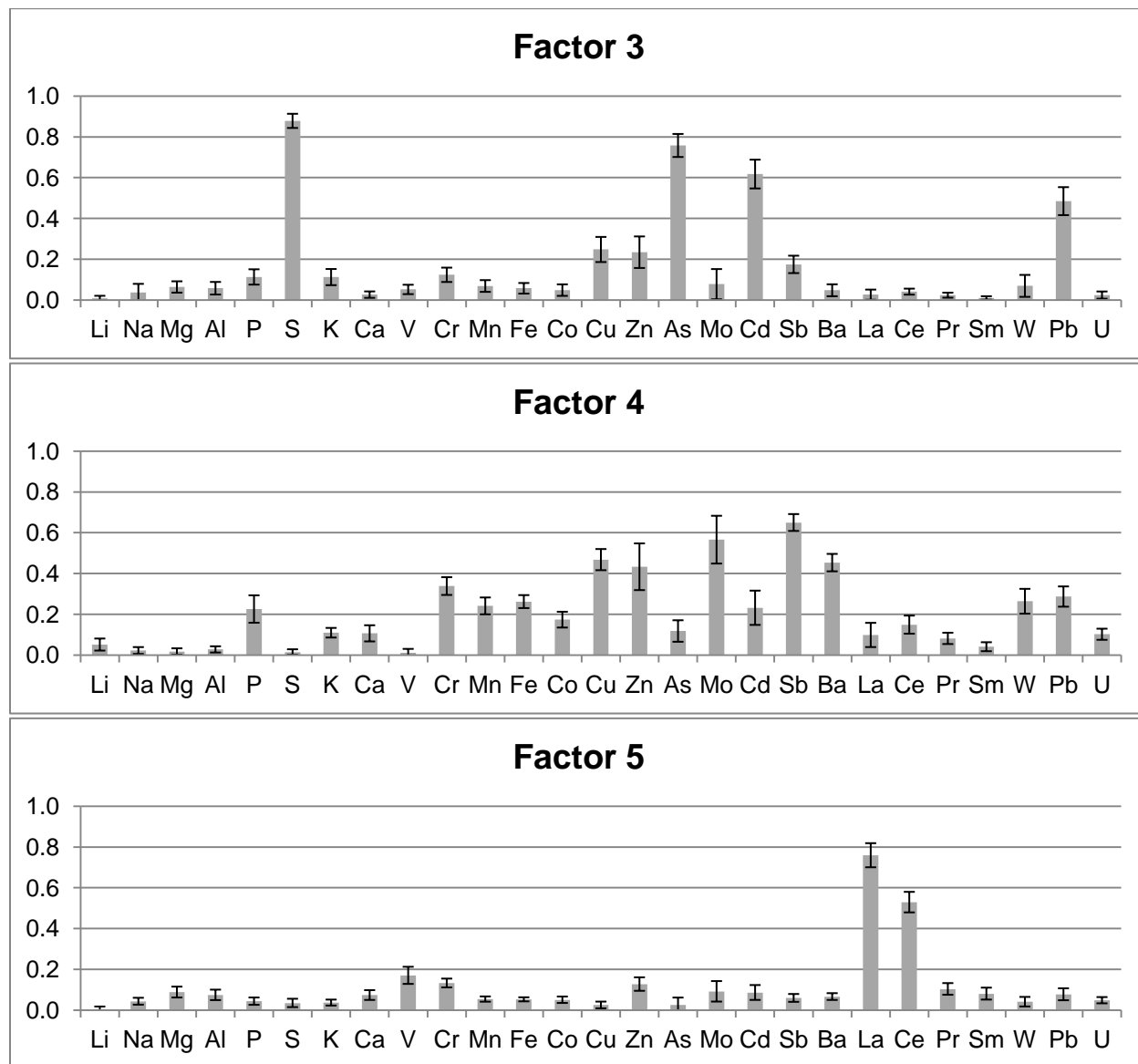
Table 5.2 summarizes the contributions of each of the five factors to the summed concentrations of the 27 elements in the $PM_{2.5}$ and $PM_{10-2.5}$ modes at each of the three sampling locations. Table 5.2 also shows the median coefficients of variation for estimated contributions to individual composite samples, as estimated using bootstrap resampling and computed only

for the subset of bootstrap samples with factors that matched those estimated from the original data set.

Factors 1 and 2 contribute most to the element concentrations in the $PM_{10-2.5}$ fraction. Factor 1, which is distinguished as explaining a large fraction of the Na, contributes from 19% of $PM_{10-2.5}$ element concentrations at GRE to 26% at EDI. Factor 1 contributes 7 - 8% of $PM_{2.5}$ element concentrations at the three sites. $PM_{10-2.5}$ contributions for factor 1 show pronounced seasonality and are highest in winter at all three sites. (Seasonal contributions for all of the factors are shown in Figures 5.S3 and 5.S4 in the supplementary information.) The prominence of Na and seasonality of this factor suggest that it might be identified with road salt. Comparison of filter sampling dates with timing of snowfall events reported for the Denver Stapleton and Greeley UNC monitoring sites in the Global Historical Climatology Network (NCDC, 2012) supports this inference. For composite samples with one or more filters collected on days with snow that day or on one or more of the four preceding days, Factor 1 contributions to $PM_{10-2.5}$ at ALS (n = 6), EDI (n = 6) and GRE (n = 3) had averages and standard deviations of 251± 205, 107±72, and 102±42 ng m^{-3}, respectively. In contrast, for composite samples with no filters collected during or soon after snowfall events, the Factor 1 contributions at ALS (n = 8), EDI (n = 4) and GRE (n = 8) were 60±40, 33±12, and 30±21 ng m^{-3}. Kumar et al. (2012) similarly identified as road salt a cluster of elements including Na and Cl, which was only present in their winter samples from Syracuse, NY.

Table 5.2 Average and standard deviation of factor contributions to summed concentrations of 27 elements, by size and site, along with estimates of statistical sampling uncertainty

	Factor 1	Factor 2	Factor 3	Factor 4	Factor 5
	Absolute Element Contributions (ng/m^3)				
ALS PM$_{2.5}$	29.6±28.7	87.5±111	196±89.5	79.3±81.3	51.5±37.0
EDI PM$_{2.5}$	26.0±17.8	50.3±52.7	245±112	49.8±29.8	15.0±12.2
GRE PM$_{2.5}$	20.0±14.9	69.8±57.4	152±97.2	15.8±12.8	3.65±1.88
ALS PM$_{10-2.5}$	136±162	331±197	19.3±11.5	39.7±42.5	25.7±16.5
EDI PM$_{10-2.5}$	77.0±66.1	182±102	21.1±10.3	49.1±44.0	8.66±4.28
GRE PM$_{10-2.5}$	49.0±42.6	245±207	23.1±23.2	12.2±18.5	7.14±4.61
	Median Bootstrap Coefficient of Variation				
ALS PM$_{2.5}$	0.34	0.18	0.09	0.17	0.25
EDI PM$_{2.5}$	0.26	0.16	0.06	0.17	0.33
GRE PM$_{2.5}$	0.21	0.07	0.05	0.2	0.53
ALS PM$_{10-2.5}$	0.25	0.07	0.19	0.23	0.43
EDI PM$_{10-2.5}$	0.3	0.09	0.11	0.15	0.49
GRE PM$_{10-2.5}$	0.71	0.1	0.13	0.31	0.6

Containing most of the crustal elements, Factor 2 appears to be resuspended crustal material and road dust. This factor contributes from 52% of total PM$_{10-2.5}$ element concentrations at EDI to 70% at GRE. Factor 2 makes the second largest contribution to PM$_{2.5}$ element concentrations, from 13% at EDI to 28% at GRE. As shown in the supplementary information, PM$_{10-2.5}$ contributions from Factor 2 are highest in fall, followed by summer, spring, and winter. The seasonality may be explained in part by meteorological conditions, which are summarized in Figures 5.S5a and 5.S5b in the supplementary information. As shown, precipitation, relative humidity and soil moisture were all relatively low in fall and summer compared to spring and winter.

Factor 3, which is distinguished by S, contributes the largest fraction of PM$_{2.5}$ element concentrations at all three sites, ranging from 46% at ALS to 62% at EDI. Factor 3 contributes

most to PM$_{2.5}$ element concentrations in fall followed by winter, spring, and summer (Figure 5.S3). The factor appears to be regional in nature, as contributions show relatively strong correspondence across the sampling sites. The PM$_{2.5}$ size fraction, presence of S, and regional distribution of Factor 3 suggests that it could be identified with secondary sulfate formation, likely tied to SO$_2$ emissions from coal combustion. There are three coal-fired power plants within 100 km of the ALS and EDI sites, with the closest located 4 km from ALS and 9 km from EDI. Four coal-fired power plants are within 100 km of the GRE sites, with the closest about 60 km away.

While the S in Factor 3 is likely derived from coal combustion, the appearance of As, Cd and Pb along with S may be due to their primary occurrence in the PM$_{2.5}$ size fraction (Figure 5.2) as opposed to their having a common source. This combination of elements may thus be an artifact of applying PMF to a pooled set of PM$_{2.5}$ and PM$_{10-2.5}$ data with a limited number of samples. When correlation coefficients are calculated just for samples in the PM$_{2.5}$ size fraction, concentrations of As, Cd and Pb are all more highly correlated with several other elements than they are with S. Furthermore, reported PM$_{2.5}$ emissions from controlled coal-fired power plants in Denver show non-detectable levels of As and Cd, and mass fractions below 0.1% for lead (EPA, 2004).

Factor 4, which contains elements commonly associated with brake and tire wear, contributes 15% of PM$_{2.5}$ element concentrations at ALS and 13% at EDI, but only 6% at GRE. The factor contributes 13% of PM$_{10-2.5}$ element concentrations at EDI, 6% at ALS and 3% at GRE. Contributions from Factor 4 are highest in fall. Other recent studies of PM$_{10-2.5}$ in urban areas have found PMF factors or principal components marked by a similar set of elements, which they have variously identified as "traffic", "road dust" or "vehicle abrasion" (Moreno et al, 2011; 2012; Pabkin et al., 2011). The finding that Factor 4 has greater influence in Denver than in Greeley is consistent with its identification with motor vehicles, considering the traffic density in the two cities. During the study period, the most heavily traveled roadways within 5 km of the

monitoring sites in Greeley had average traffic counts of 350 to 750 vehicles per hour. In contrast, the Denver monitoring sites were both within 5 km of interstate highways with traffic counts of up to 4650 vehicles per hour (CDOT, 2013).

Finally, Factor 5, with elevated levels of La and Ce, contributes 15% of $PM_{2.5}$ element concentrations at ALS, with especially high contributions in summer. It has lower contributions for $PM_{10-2.5}$ element concentrations at ALS and for both size fractions at the other sites. As discussed above in the section on enrichment factors, this factor may be associated with emissions from automotive catalysts or fluidized catalysts used in refining, or both.

5.4 CONCLUSIONS

The CCRUSH study was designed to compare concentrations and characteristics of $PM_{2.5}$ and $PM_{10-2.5}$ across locations in northeastern Colorado, including sites anticipated to have industrial, traffic, and agricultural influences. The results presented here indicate element concentrations in $PM_{2.5}$ are 50 to 80% higher in Denver than in Greeley, while concentrations in $PM_{10-2.5}$ are 60% higher at the more industrial ALS location in Denver than at either the residential EDI site in Denver or in Greeley. The median elemental composition of $PM_{10-2.5}$ is generally consistent across sites, with differences in elemental mass fractions of less than a factor of two for most elements. Exceptions include Mo, which displays relatively low mass fractions in Greeley, and Sb and W, which display relatively high mass fractions at EDI. The split between $PM_{2.5}$ and $PM_{10-2.5}$ for most elements is also generally consistent across sites, with the exception of La and Ce. These two rare earth elements are relatively enriched in the $PM_{2.5}$ size range at ALS.

We found the elements Sb, Cd, Zn, Mo, As, B, Cu, Pb, and W to have crustal enrichment factors greater than 10 in both the $PM_{2.5}$ and $PM_{10-2.5}$ size ranges at all of our sites, suggesting large influences from non-crustal sources. CEFs at our northeastern CO sites are similar to those reported recently for the Los Angeles Basin (Cheung et al., 2011). Compared to CEFs calculated from PM concentrations reported for January 1992 (Lewis et al., 1996) for northeast Denver, values found in this study for Cd and Pb are lower by more than an order of magnitude. On the other hand, the CEF for Cu found in this study is higher than the value calculated from the concentrations Lewis et al. (1996) reported.

Application of PMF to a subset of the data including 27 elements and 70 observations distinguished five factors contributing to trace element concentrations in $PM_{2.5}$ or $PM_{10-2.5}$ at the three northeastern CO sites. A crustal factor contributed 52 – 70% of the $PM_{10-2.5}$ trace element concentrations, with the highest contribution at GRE followed by ALS and then EDI. A factor that

appears to be due to road salt contributed 19 – 26% of $PM_{10\text{-}2.5}$ element concentrations, with the highest fractional contribution at EDI, followed by ALS and then GRE. A factor likely due to vehicle abrasion was estimated to contribute from 3% of $PM_{10\text{-}2.5}$ element concentrations at GRE to 13% at EDI. This same factor contributed from 6 – 15% of $PM_{2.5}$ trace element concentrations. The largest contributor to $PM_{2.5}$ trace element concentrations across the three sites was a factor containing most of the S, which is likely associated with coal combustion. Finally, the ALS site was unique in having a 15% contribution to $PM_{2.5}$ element concentrations from a factor distinguished by La and Ce, which appears to be associated with automotive catalysts or catalyst use at petroleum refineries. Overall, the results support the hypothesis that crustal sources are relatively influential in Greeley, with industrial and vehicular sources contributing more to $PM_{10\text{-}2.5}$ in Denver. In future work we will examine whether these contrasts can help explain differences between the two cities in health effects of short-term exposure to $PM_{10\text{-}2.5}$.

5.5 ACKNOWLEDGEMENTS

5.6 REFERENCES

Amato, F., Viana, M., Richard, A., Furger, M., Prevot, A.S.H., Nava, S., Lucarelli, F., Bukowiecki, N., Alastuey, A., Reche, C., Moreno, T., Pandolfi, M., Pey, J., Querol, X., 2011. Size and time-resolved roadside enrichment of atmospheric particulate pollutants. Atmospheric Chemistry and Physics 11, 2917-2931.

Belzile, N., Chen, Y.-W., Filella, M., 2011. Human exposure to antimony: I. Sources and intake, Critical Reviews in Environmental Science and Technology 41(14), 1309-1373.

Boreson, J., Dillner, A.M., Peccia, J., 2004. Correlating bioaerosol load with PM2.5 and PM10cf concentrations: A comparison between natural desert and urban-fringe aerosols. Atmospheric Environment 38, 6029-2041.

Brunekreef, B., Forsberg, B., 2005. Epidemiological evidence of effects of coarse airborne particles on health. European Respiratory Journal 26, 309–318.

Castillejos, M., Borja-Aburto, V.H., Dockery, D., Gold, D.R., Loomis, D., 2000. Airborne coarse particles and mortality. Inhalation Toxicology 12, 61-72.

CDOT, 2013. Online Transportation Information System, Traffic Data Explorer. Colorado Department of Transportation. Available at http://dtdapps.coloradodot.info/Otis/TrafficData, last accessed March 29, 2013.

Cheung, K., Daher, N., Kam, W., Shafer, M.M., Ning, Z., Schauer, J.J., Sioutas, C., 2011. Spatial and temporal variation of chemical composition and mass closure of ambient coarse particulate matter ($PM_{10-2.5}$) in the Los Angeles area. Atmospheric Environment 45, 2651–2662.

Cheung, K., Shafer, M.M., Schauer, J.J., Sioutas, C., 2012. Historical trends in the mass and chemical species concentrations of coarse particulate matter in the Los Angeles Basin and relation to sources and air quality regulations. Journal of the Air & Waste Management Association 62, 541-556.

Chow, J.C., Watson, J.G., Fujita, E.M., Zhiqiang, L., Lawson, D.R., Ashbaugh, L.L., 1994. Temporal and spatial variations of $PM_{2.5}$ and PM_{10} aerosol in the Southern California Air Quality Study. Atmospheric Environment 28, 2061-2080.

Clements, N., Piedrahita, R., Ortega, J., Peel, J.L., Miller, S.L., Milford, J.B., Hannigan, M., 2012. Characterization and nonparametric regression of rural and urban coarse particulate matter mass concentrations in northeastern Colorado. Aerosol Science and Technology 46, 108–123.

Countess, R.J., Wolff, G.T., Cadle, S.H., 1980. The Denver winter aerosol: a comprehensive chemical characterization. Journal of the Air Pollution Control Association 30, 1194-1200.

Duce, R.A., Hoffman, G.L., Ray, B.J., Fletcher, I.S., Wallace, G.T., Fasching, J.L., Piotrowicz, S.R., Walsh, P.R., Hoffman, E.J., Miller, J.M., Heffter, J.L., 1976. Trace metals in the marine atmosphere: sources and fluxes, in H.L. Windom and R.A. Duce eds., Marine Pollutant Transfer, D.C. Heath, Lexington, MA, pp. 77-119.

Dutton, S.J., Schauer, J.J., Vedal, S., Hannigan, M.P., 2009. $PM_{2.5}$ characterization for time series studies: Pointwise uncertainty estimation and bulk speciation methods applied in Denver. Atmospheric Environment 43, 1136-1146.

EPA, 2004. Speciate Data Browser, Coal Combustion Profiles 3191 and 3192, U.S. Environmental Protection Agency, available at http://cfpub.epa.gov/si/speciate.

EPA, 2009. Integrated Science Assessment for Particulate Matter. EPA/600/R-08/139F. U.S. Environmental Protection Agency, Washington, DC.

Gianini, M., Gehrig, R., Fischer, A., Ulrich, A., Wichser, A., Hueglin, C., 2012. Chemical composition of PM10 in Switzerland: An analysis for 2008/2009 and changes since 1998/1999. Atmospheric Environment 54, 97-106.

Hays, M.D., Cho, S-H, Baldauf, R., Schauer, J.J., Shafer, M., 2011. Particle size distributions of metal and non-metal elements in an urban near-highway environment. Atmospheric Environment 45, 925-934.

Hemann, J.G., Brinkman, G.L., Dutton, S.J., Hannigan, M.P., Milford, J.B., Miller, S.L., 2009. Assessing positive matrix factorization model fit: a new method to estimate uncertainty and bias in factor contributions at the measurement time scale. Atmospheric Chemistry and Physics 9(2), 497-513.

Hueglin, C., Gehrig, R., Baltensperger, U., Gysel, M., Monn, C., Vonmont, H., 2005. Chemical characterization of PM2.5, PM10 and coarse particles at urban, near-city and rural sites in Switzerland. Atmospheric Environment 39, 637-651.

Iijima, A., Sato, K., Fujitani, Y., Fujimori, E., Saito, Y., Tanabe, K., Ohara, T., Kozawa, K., Furuta, N., 2009. Clarification of the predominant emission sources of antimony in airborne particulate matter and estimation of their effects on the atmosphere of Japan. Environmental Chemistry 6, 122–132.

Karanasiou, A.A., Siskos, P.A., Elefheriadis, K., 2009. Assessment of source apportionment by Positive Matrix Factorization analysis on fine and coarse urban aerosol size fractions. Atmospheric Environment 43, 3385-3395.

Klepper, G., Michaelis, P., Mahlau, G., 1995. Industrial Metabolism: A Case Study of the Economics of Cadmium Control, Kieler Studien 268.

Kulkarni, P., Chellam, S., Fraser, M., 2006. Lanthanum and lanthanides in atmospheric fine particles and their apportionment to refinery and petrochemical operations in Houston, TX. Atmospheric Environment 40, 508–520.

Kumar, P., Hopke, P.K., Raja, S., Casuccio, G., Lersch, T.L., West, R., 2012. Characterization and heterogeneity of coarse particles across an urban area. Atmospheric Environment 46, 449-459.

Lewis, C.W., Baumgardner, R.E., Stevens, R.K., 1986. Receptor modeling study of Denver winter haze. Environmental Science and Technology 20, 1126-1136.

Lough, G.C., Schauer, J., Park, J.-S., Shafer, M.M., Deminter, J.T., Weinstein, J.P., 2005. Emissions of metals associated with motor vehicle roadways. Environmental Science and Technology 39, 826–836.

Malm, W. C., Pitchford,, M., McDade, C., Ashbaugh, L., 2007. Coarse particle speciation at selected locations in the rural continental United States. Atmospheric Environment 41, 2225–2239.

Mar, T.F., Norris, G.A., Koenig, J.Q., Larson, T.V., 2000. Associations between air pollution and mortality in Phoenix, 1995-1997. Environmental Health Perspectives 108, 347-353.

Milford, J.B., Davidson, C.I., 1985. The sizes of particulate trace elements in the atmosphere – a review. Journal of the Air Pollution Control Association 35, 1249-1260.

Milford, J.B., Davidson, C.I., 1987. The sizes of particulate sulfate and nitrate in the atmosphere – a review. Journal of the Air Pollution Control Association 37, 125-134.

Misra, C., Geller, M.D., Shah, P., Sioutas, C., Solomon, P.A., 2001. Development and evaluation of a continuous coarse (PM 10 –PM 2.5) particle monitor. Journal of the Air & Waste Management Association 51, 1309–1317.

Misra, C., Geller, M.D., Sioutas, C., Solomon, P.A., 2003. Development and evaluation of a PM 10 impactor-inlet for a continuous coarse particle monitor. Aerosol Science and Technology 37, 271–281.

Moreno, T., Querol, X., Alastuey, A., Pey, J., Cruz Minguillon, M., Perez, N., Bernabe, R., Blanco, S., Cardenas, B., Gibbons, W., 2008. Lanthanoid geochemistry of urban atmospheric particulate matter. Environmental Science and Technology 42, 6502-6507.

Moreno, T., Querol, X., Alastuey, A., Reche, C., Cusack, M., Amato, F., Padolfi, M., Pey, J., Richard, A., Prevot, A.S.H., Furger, M., Gibbons, W., 2011. Variations in time and space

of trace metal aerosol concentrations in urban areas and their surroundings. Atmospheric Chemistry and Physics 11, 9415-9430.

Moreno, T., Karanasiou, A., Amato, F., Lucarelli, F., Nava, S., Calzolai, G., Chiari, M., Coz, E., ARinano, B., Lumbreras, J., Borge, R., Boldo, E., Linares, C., Alastuey, A., Querol, X., Gibbons, W., 2013. Daily and hourly sourcing of metallic and mineral dust in urban air contaminated by traffic and coal-burning emissions. Atmospheric Environment 68, 33-44.

NCDC, 2012. Global Historical Climatology Network – Daily, National Climatic Data Center, http://www.ncdc.noaa.gov/oa/climate/ghcn-daily, accessed Oct. 4, 2012.

Ostro, B.D., Broadwin, R., Lipsett, M.J., 2000. Coarse and fine particles and daily mortality in the Coachella Valley, California: A follow-up study. Journal of Exposure Analysis and Environmental Epidemiology 10, 412-419.

Paatero, P., 1998a. User's Guide for Positive Matrix Factorization Program PMF2 and PMF3, Part 1: Tutorial. University of Helsinki, Helsinki, Finland.

Paatero, P., 1998b. User's Guide for Positive Matrix Factorization Program PMF2 and PMF3, Part 2: Reference. University of Helsinki, Helsinki, Finland.

Pacyna, J.M., Pacyna, E.G., Wenche, A., 2009. Changes of emissions and atmospheric deposition of mercury, lead, and cadmium. Atmospheric Environment 43, 117-127.

Pakbin, P., Ning, Z., Shafer, M.M., Schauer, J., Sioutas, C., 2011. Seasonal and spatial coarse particle elemental concentrations in the Los Angeles area. Aerosol Science and Technology 45, 949–963.

Patterson, E., Gillette, D., 1977. Commonalities in measured size distributions for aerosols having a soil-derived component. Journal of Geophysical Research 82, 2074.

Politis, D. N., Romano, J.P, 1994. The stationary bootstrap. Journal of the American Statistics Association 89 (428), 1303-1313.

Reimann, C., De Caritat, P., 2000. Intrinsic flaws of element enrichment factors (EFs) in environmental geochemistry. Environmental Science and Technology 34, 5084–5091.

Seinfeld, J.H., Pandis, S.N. 1996. Atmospheric Chemistry and Physics. John Wiley & Sons, New York.

Shafer, M.M., Perkins, D.A., Antkiewicz, D.S., Stone, E.A., Quraishi, T.A., Schauer, J.J. 2010. Reactive oxygen species activity and chemical speciation of size-fractionated atmospheric particulate matter from Lahore, Pakistan: an important role for transition metals. Journal of Environmental Monitoring 12, 704-715.

Taylor, S.R., McLennan, S.M., 1985. The Continental Crust: Its Composition and Evolution. Blackwell, Oxford England.

Thorpe, A., Harrison, R.M., 2008. Sources and properties of non-exhaust particulate matter from road traffic: a review. Science of the Total Environment 400, 270-282.

Villeneuve, P.J., Burnett, R.T., Shi, Y., Krewski, D., Goldberg, M.S., Hertzman, C., Chen, Y., Brook, J., 2003. A time-series study of air pollution, socioeconomic status, and mortality in Vancouver, Canada. Journal of Exposure Analysis and Environmental Epidemiology 13, 427-435.

Von Schneidemesser, E., Stone, A., Quraishi, t., Shafer, M.M., Schauer, J.J., 2010. Toxic metals in the atmosphere in Lahore, Pakistan. Science of the Total Environment 408, 1640-1648.

Zanobetti, A., Schwartz, J., 2009. The effect of fine and coarse particulate air pollution on mortality: a national analysis. Environmental Health Perspectives 117, 898-903.

Zoller, W.H., Gladney, E.S., Duce, R.A., 1974. Atmospheric concentrations and sources of trace metals at the South Pole, Science 183, 198.

5.7 SUPPLEMENTAL INFORMATION

Table 5.S1 Average ratios of concentrations of lanthanum to those of other lanthanide series elements by size and location, along with ratios characteristic of fluid catalytic converters (FCC) at petroleum refineries (Kulkarni et al., 2006); automobile catalytic converters (Kulkarni et al., 2006); and upper continental crust (UCC; Taylor and McLennan, 1985)

Site/Source	La/Ce	La/Pr	La/Nd	La/Sm
ALS PM$_{2.5}$	0.75	35	12	74
EDI PM$_{2.5}$	0.62	20	6.3	42
GRE PM$_{2.5}$	0.46	7.8	2.1	13
ALS PM$_{10-2.5}$	0.54	7.5	2.1	12
EDI PM$_{10-2.5}$	0.48	6.1	1.6	9.3
GRE PM$_{10-2.5}$	0.44	4.8	1.3	7.2
UCC	0.47	4.2	1.2	6.7
FCC catalyst	4.3	9.7	6.4	55
Auto catalyst	0.7	9.4	2.9	200

Table 5.S2 Pearson correlation coefficients for pairs of trace elements (n = 70)

	Li	Na	Mg	Al	P	S	K	Ca
Li	1	0.848	0.762	0.719	0.537	-0.208	0.743	0.715
Na	0.848	1	0.488	0.421	0.241	-0.267	0.408	0.418
Mg	0.762	0.488	1	0.971	0.678	-0.274	0.884	0.913
Al	0.719	0.421	0.971	1	0.685	-0.274	0.908	0.92
P	0.537	0.241	0.678	0.685	1	-0.064	0.844	0.644
S	-0.208	-0.267	-0.274	-0.274	-0.064	1	-0.138	-0.206
K	0.743	0.408	0.884	0.908	0.844	-0.138	1	0.873
Ca	0.715	0.418	0.913	0.92	0.644	-0.206	0.873	1
Ti	0.755	0.462	0.907	0.917	0.713	-0.25	0.952	0.914
V	0.706	0.423	0.878	0.891	0.664	-0.31	0.885	0.894
Cr	0.333	0.214	0.306	0.325	0.26	0.325	0.349	0.406
Mn	0.722	0.405	0.835	0.849	0.694	-0.009	0.901	0.918
Fe	0.765	0.492	0.845	0.846	0.632	-0.046	0.867	0.91
Co	0.778	0.482	0.858	0.855	0.664	-0.131	0.905	0.907
Cu	0.302	0.184	0.295	0.27	0.263	0.51	0.367	0.414
Zn	0.117	0.036	0.053	0.032	0.177	0.438	0.091	0.178
As	-0.127	-0.168	-0.194	-0.194	0.063	0.79	-0.079	-0.108
Sr	0.763	0.443	0.898	0.897	0.647	-0.108	0.902	0.955
Mo	0.366	0.308	0.244	0.224	0.235	0.348	0.258	0.425
Cd	-0.014	-0.087	-0.073	-0.072	0.07	0.753	0.006	0.045
Sb	0.196	0.086	0.164	0.175	0.236	0.499	0.284	0.321
Cs	0.771	0.452	0.936	0.93	0.696	-0.063	0.918	0.889
Ba	0.616	0.405	0.619	0.621	0.471	0.177	0.672	0.763
La	0.14	0.034	0.232	0.239	0.157	0.237	0.178	0.287
Ce	0.348	0.172	0.454	0.471	0.332	0.16	0.418	0.514
Pr	0.707	0.4	0.951	0.986	0.667	-0.239	0.9	0.944
Nd	0.721	0.416	0.957	0.99	0.665	-0.271	0.907	0.945
Sm	0.715	0.411	0.958	0.99	0.674	-0.291	0.903	0.935
W	0.805	0.774	0.573	0.52	0.248	-0.098	0.545	0.604
Pb	0.104	-0.014	0.056	0.047	0.147	0.719	0.136	0.164
U	0.709	0.371	0.896	0.936	0.79	-0.218	0.981	0.905

Table 5.S2 (*continued*) Pearson correlation coefficients for pairs of trace elements (n = 70)

	Ti	V	Cr	Mn	Fe	Co	Cu	Zn
Li	0.755	0.706	0.333	0.722	0.765	0.778	0.302	0.117
Na	0.462	0.423	0.214	0.405	0.492	0.482	0.184	0.036
Mg	0.907	0.878	0.306	0.835	0.845	0.858	0.295	0.053
Al	0.917	0.891	0.325	0.849	0.846	0.855	0.27	0.032
P	0.713	0.664	0.26	0.694	0.632	0.664	0.263	0.177
S	-0.25	-0.31	0.325	-0.009	-0.046	-0.131	0.51	0.438
K	0.952	0.885	0.349	0.901	0.867	0.905	0.367	0.091
Ca	0.914	0.894	0.406	0.918	0.91	0.907	0.414	0.178
Ti	1	0.916	0.345	0.916	0.912	0.956	0.378	0.075
V	0.916	1	0.335	0.861	0.85	0.881	0.25	0.086
Cr	0.345	0.335	1	0.578	0.571	0.533	0.571	0.739
Mn	0.916	0.861	0.578	1	0.981	0.955	0.593	0.381
Fe	0.912	0.85	0.571	0.981	1	0.957	0.626	0.387
Co	0.956	0.881	0.533	0.955	0.957	1	0.49	0.28
Cu	0.378	0.25	0.571	0.593	0.626	0.49	1	0.582
Zn	0.075	0.086	0.739	0.381	0.387	0.28	0.582	1
As	-0.175	-0.212	0.556	0.121	0.095	-0.016	0.567	0.696
Sr	0.925	0.867	0.464	0.935	0.932	0.937	0.481	0.241
Mo	0.293	0.281	0.779	0.562	0.593	0.484	0.689	0.828
Cd	-0.064	-0.092	0.615	0.269	0.256	0.116	0.668	0.773
Sb	0.277	0.212	0.723	0.564	0.575	0.445	0.842	0.765
Cs	0.92	0.84	0.362	0.884	0.871	0.887	0.41	0.095
Ba	0.698	0.627	0.637	0.881	0.904	0.799	0.814	0.546
La	0.16	0.362	0.513	0.368	0.369	0.273	0.364	0.589
Ce	0.404	0.566	0.594	0.591	0.595	0.506	0.464	0.589
Pr	0.911	0.896	0.37	0.887	0.883	0.873	0.332	0.113
Nd	0.923	0.897	0.337	0.878	0.876	0.877	0.307	0.07
Sm	0.914	0.891	0.322	0.864	0.86	0.864	0.281	0.049
W	0.65	0.582	0.434	0.677	0.758	0.729	0.519	0.252
Pb	0.087	0.03	0.54	0.382	0.394	0.225	0.806	0.703
U	0.962	0.914	0.324	0.901	0.865	0.905	0.299	0.054

Table 5.S2 (*continued*) Pearson correlation coefficients for pairs of trace elements (n = 70)

	As	Sr	Mo	Cd	Sb	Cs	Ba	La
Li	-0.127	0.763	0.366	-0.014	0.196	0.771	0.616	0.14
Na	-0.168	0.443	0.308	-0.087	0.086	0.452	0.405	0.034
Mg	-0.194	0.898	0.244	-0.073	0.164	0.936	0.619	0.232
Al	-0.194	0.897	0.224	-0.072	0.175	0.93	0.621	0.239
P	0.063	0.647	0.235	0.07	0.236	0.696	0.471	0.157
S	0.79	-0.108	0.348	0.753	0.499	-0.063	0.177	0.237
K	-0.079	0.902	0.258	0.006	0.284	0.918	0.672	0.178
Ca	-0.108	0.955	0.425	0.045	0.321	0.889	0.763	0.287
Ti	-0.175	0.925	0.293	-0.064	0.277	0.92	0.698	0.16
V	-0.212	0.867	0.281	-0.092	0.212	0.84	0.627	0.362
Cr	0.556	0.464	0.779	0.615	0.723	0.362	0.637	0.513
Mn	0.121	0.935	0.562	0.269	0.564	0.884	0.881	0.368
Fe	0.095	0.932	0.593	0.256	0.575	0.871	0.904	0.369
Co	-0.016	0.937	0.484	0.116	0.445	0.887	0.799	0.273
Cu	0.567	0.481	0.689	0.668	0.842	0.41	0.814	0.364
Zn	0.696	0.241	0.828	0.773	0.765	0.095	0.546	0.589
As	1	-0.029	0.619	0.835	0.671	-0.062	0.318	0.349
Sr	-0.029	1	0.448	0.083	0.38	0.909	0.804	0.307
Mo	0.619	0.448	1	0.71	0.795	0.273	0.743	0.496
Cd	0.835	0.083	0.71	1	0.821	0.056	0.489	0.42
Sb	0.671	0.38	0.795	0.821	1	0.256	0.782	0.458
Cs	-0.062	0.909	0.273	0.056	0.256	1	0.664	0.211
Ba	0.318	0.804	0.743	0.489	0.782	0.664	1	0.443
La	0.349	0.307	0.496	0.42	0.458	0.211	0.443	1
Ce	0.295	0.54	0.566	0.403	0.528	0.44	0.623	0.956
Pr	-0.148	0.927	0.298	-0.009	0.253	0.916	0.691	0.323
Nd	-0.185	0.925	0.267	-0.049	0.217	0.921	0.67	0.262
Sm	-0.209	0.912	0.237	-0.071	0.195	0.919	0.646	0.249
W	0.008	0.655	0.52	0.152	0.469	0.589	0.733	0.177
Pb	0.741	0.217	0.676	0.847	0.784	0.203	0.594	0.447
U	-0.159	0.909	0.221	-0.06	0.232	0.916	0.645	0.193

Table 5.S2 (*continued*) Pearson correlation coefficients for pairs of trace elements (n = 70)

	Ce	Pr	Nd	Sm	W	Pb	U
Li	0.348	0.707	0.721	0.715	0.805	0.104	0.709
Na	0.172	0.4	0.416	0.411	0.774	-0.014	0.371
Mg	0.454	0.951	0.957	0.958	0.573	0.056	0.896
Al	0.471	0.986	0.99	0.99	0.52	0.047	0.936
P	0.332	0.667	0.665	0.674	0.248	0.147	0.79
S	0.16	-0.239	-0.271	-0.291	-0.098	0.719	-0.218
K	0.418	0.9	0.907	0.903	0.545	0.136	0.981
Ca	0.514	0.944	0.945	0.935	0.604	0.164	0.905
Ti	0.404	0.911	0.923	0.914	0.65	0.087	0.962
V	0.566	0.896	0.897	0.891	0.582	0.03	0.914
Cr	0.594	0.37	0.337	0.322	0.434	0.54	0.324
Mn	0.591	0.887	0.878	0.864	0.677	0.382	0.901
Fe	0.595	0.883	0.876	0.86	0.758	0.394	0.865
Co	0.506	0.873	0.877	0.864	0.729	0.225	0.905
Cu	0.464	0.332	0.307	0.281	0.519	0.806	0.299
Zn	0.589	0.113	0.07	0.049	0.252	0.703	0.054
As	0.295	-0.148	-0.185	-0.209	0.008	0.741	-0.159
Sr	0.54	0.927	0.925	0.912	0.655	0.217	0.909
Mo	0.566	0.298	0.267	0.237	0.52	0.676	0.221
Cd	0.403	-0.009	-0.049	-0.071	0.152	0.847	-0.06
Sb	0.528	0.253	0.217	0.195	0.469	0.784	0.232
Cs	0.44	0.916	0.921	0.919	0.589	0.203	0.916
Ba	0.623	0.691	0.67	0.646	0.733	0.594	0.645
La	0.956	0.323	0.262	0.249	0.177	0.447	0.193
Ce	1	0.55	0.496	0.482	0.36	0.461	0.431
Pr	0.55	1	0.997	0.994	0.538	0.11	0.936
Nd	0.496	0.997	1	0.997	0.545	0.072	0.942
Sm	0.482	0.994	0.997	1	0.526	0.046	0.939
W	0.36	0.538	0.545	0.526	1	0.262	0.512
Pb	0.461	0.11	0.072	0.046	0.262	1	0.075
U	0.431	0.936	0.942	0.939	0.512	0.075	1

Figure 5.S1 Filter sampler design and flow schematic

203
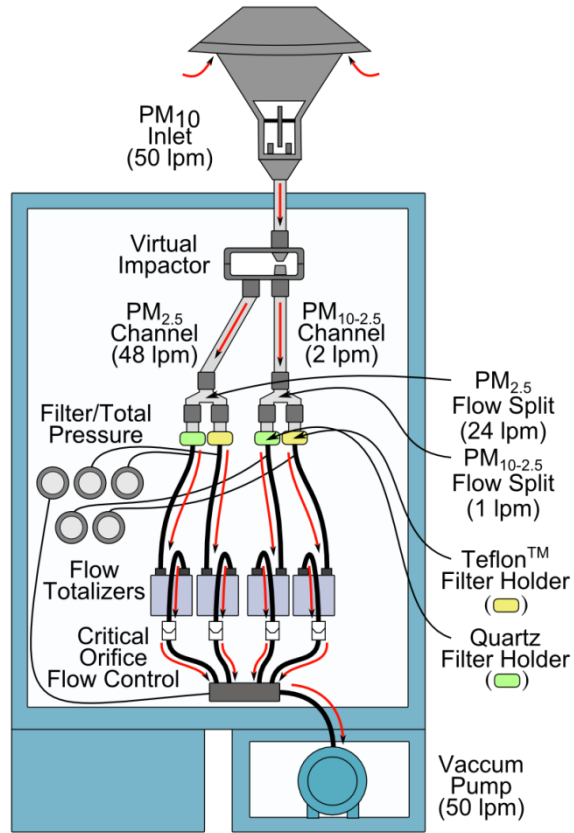
Figure 5.S2 Mass fraction factor profiles for 27 elements based on concentrations in $PM_{2.5}$ and $PM_{10\text{-}2.5}$ in Denver and Greeley, CO
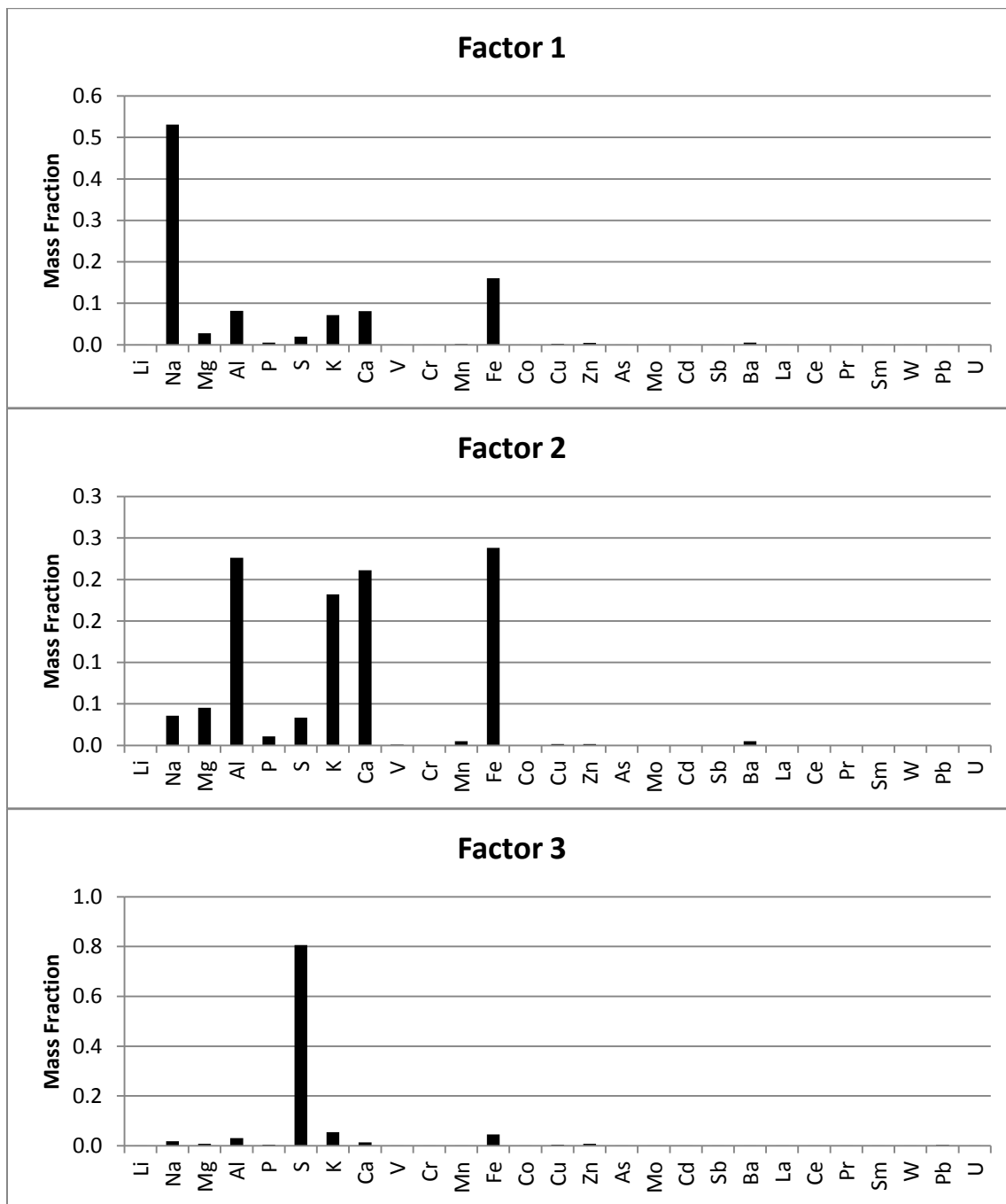
Figure 5.S2 (*continued*) Mass fraction factor profiles for 27 elements based on concentrations in PM$_{2.5}$ and PM$_{10\text{-}2.5}$ in Denver and Greeley, CO
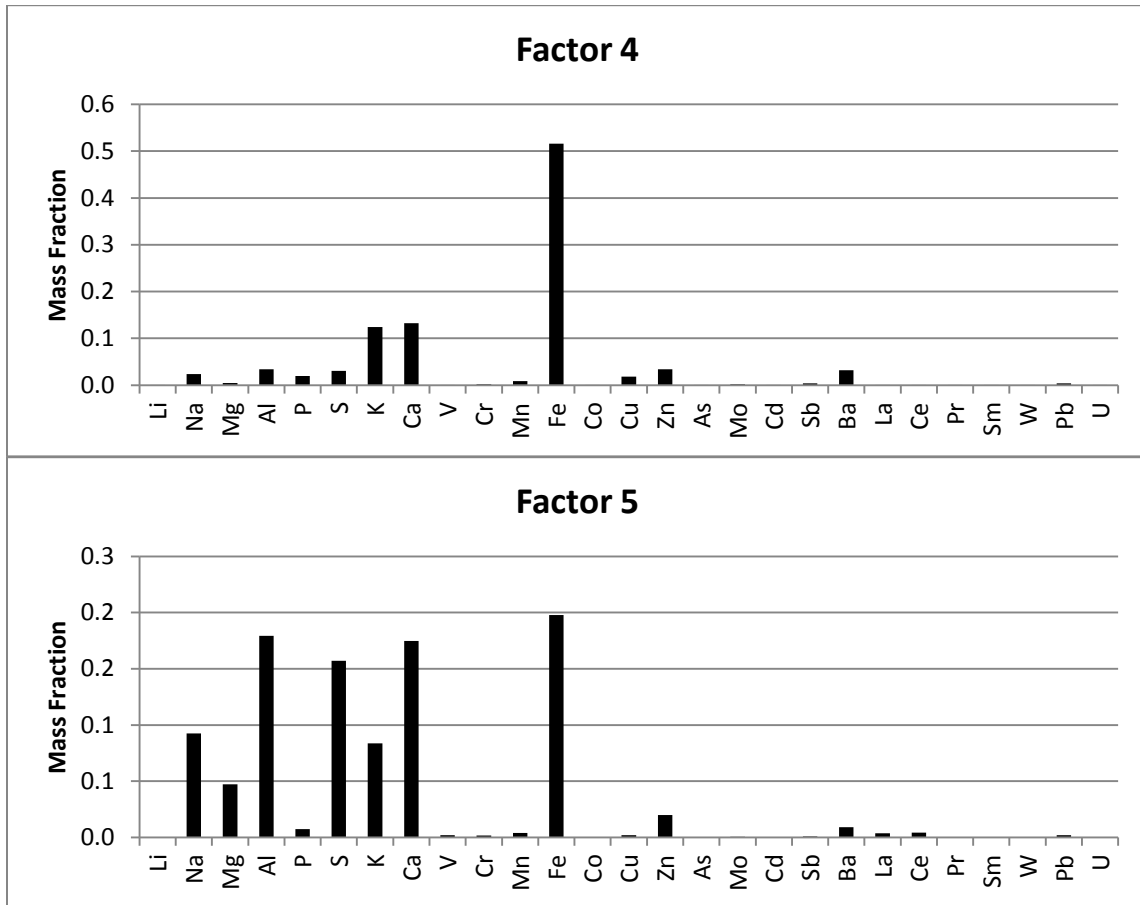
Figure 5.S3 Contributions of five factors to total mass concentrations of 27 elements in $PM_{2.5}$ by site and composite sample month, as estimated with PMF
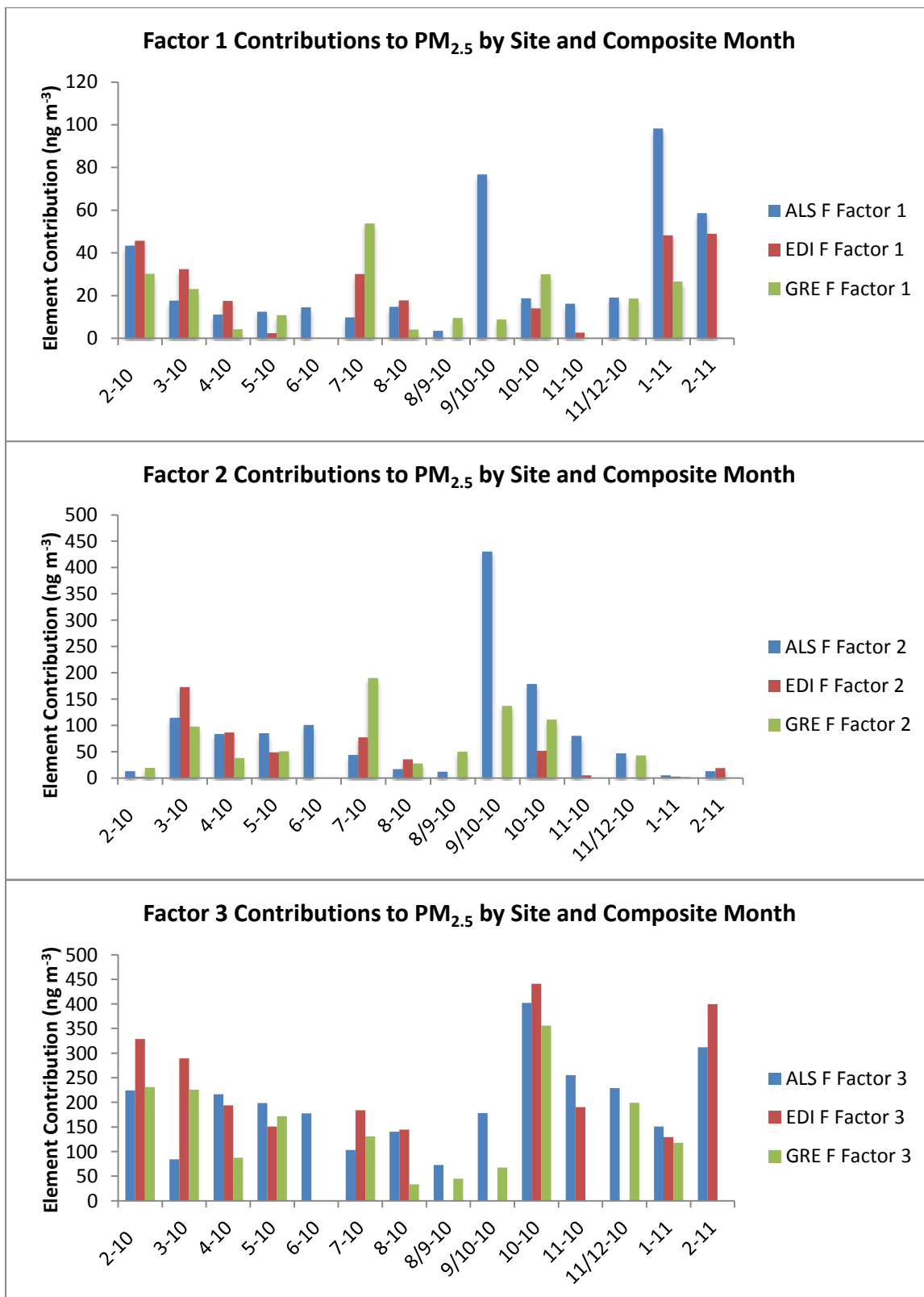
Figure 5.S3 (*continued*) Contributions of five factors to total mass concentrations of 27 elements in PM$_{2.5}$ by site and composite sample month, as estimated with PMF
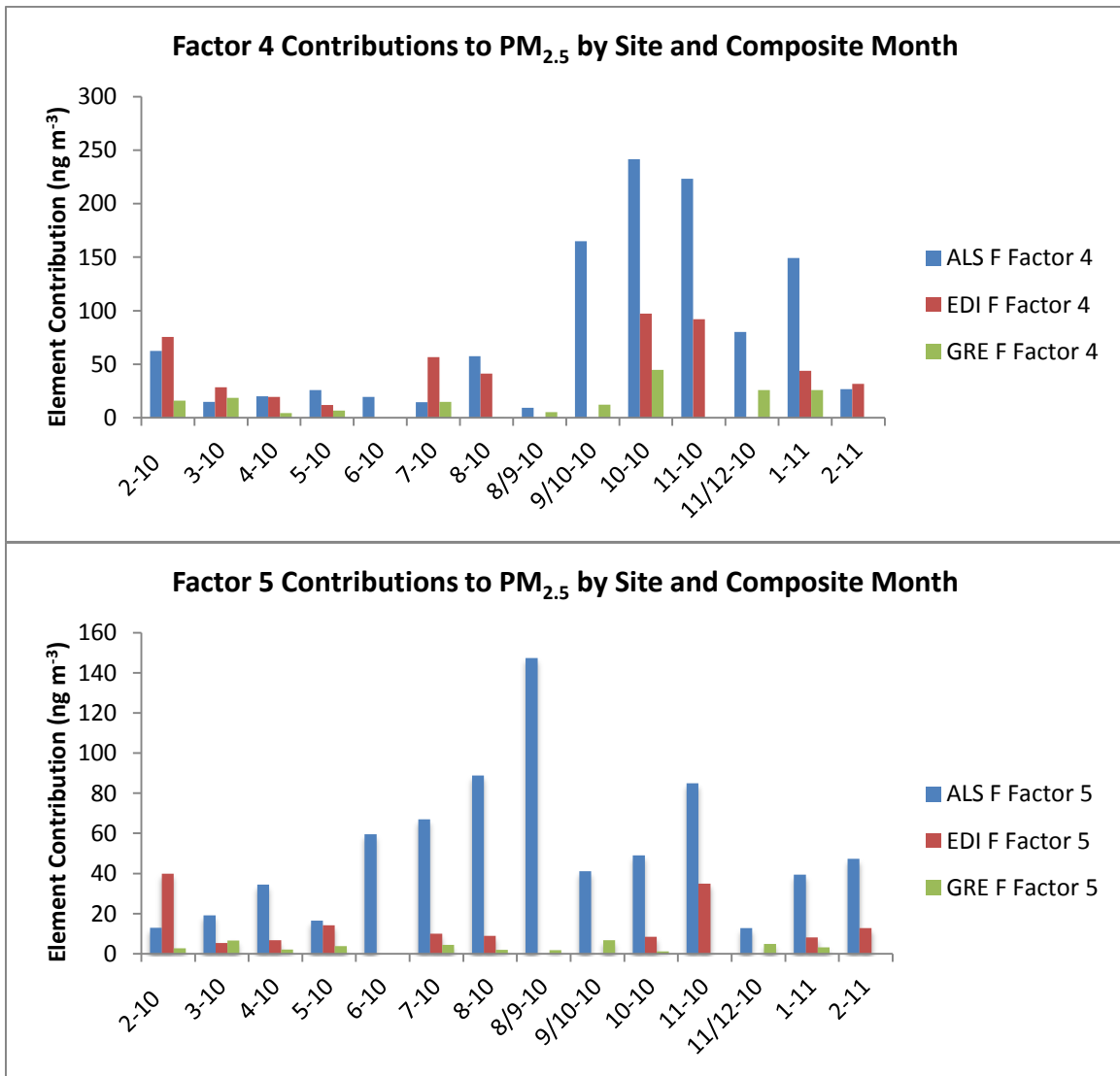
Figure 5.S4 Contributions of five factors to total mass concentrations of 27 elements in $PM_{10-2.5}$ by site and composite sample month, as estimated with PMF
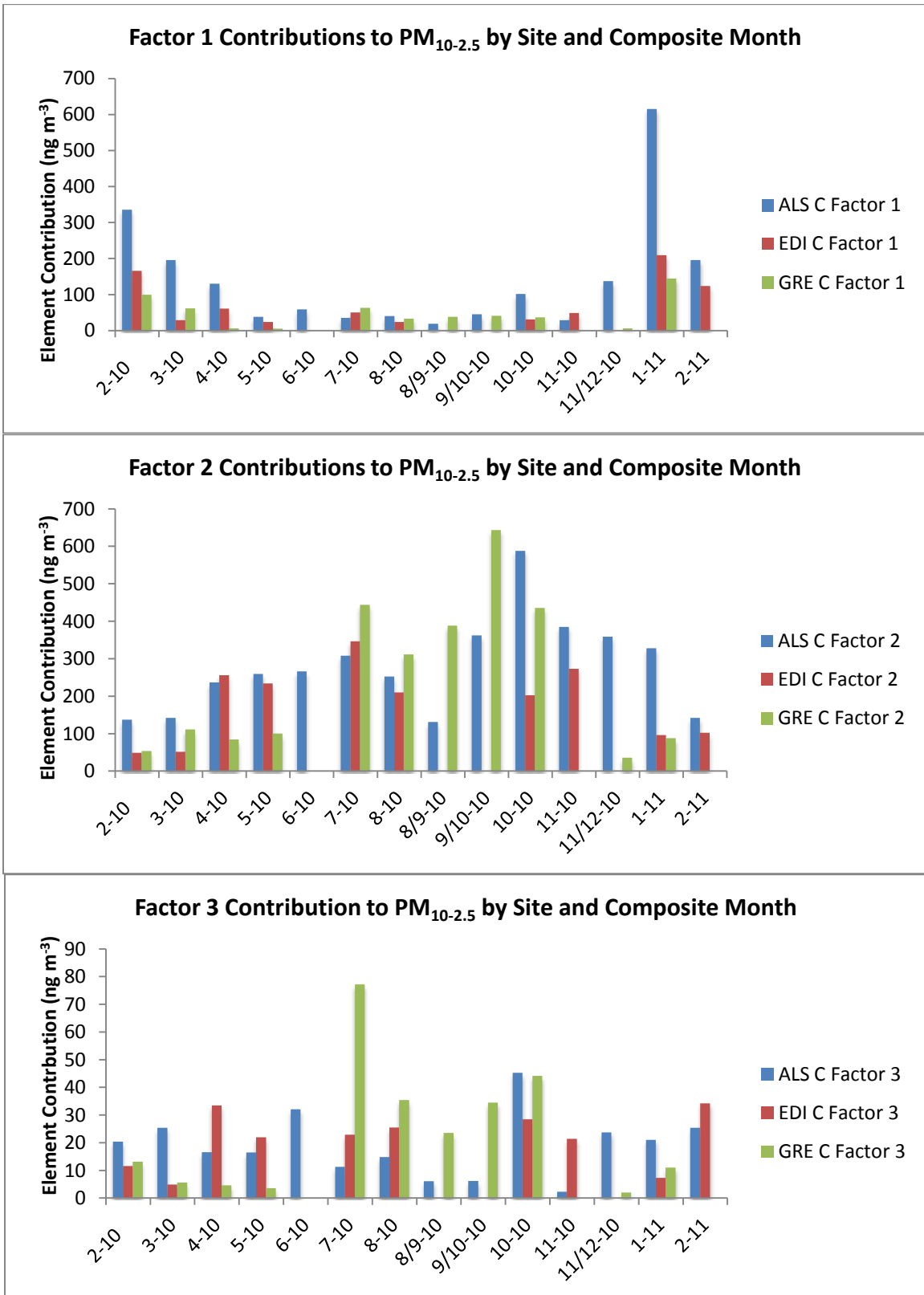
Figure 5.S4 (*continued*) Contributions of five factors to total mass concentrations of 27 elements in PM$_{10-2.5}$ by site and composite sample month, as estimated with PMF
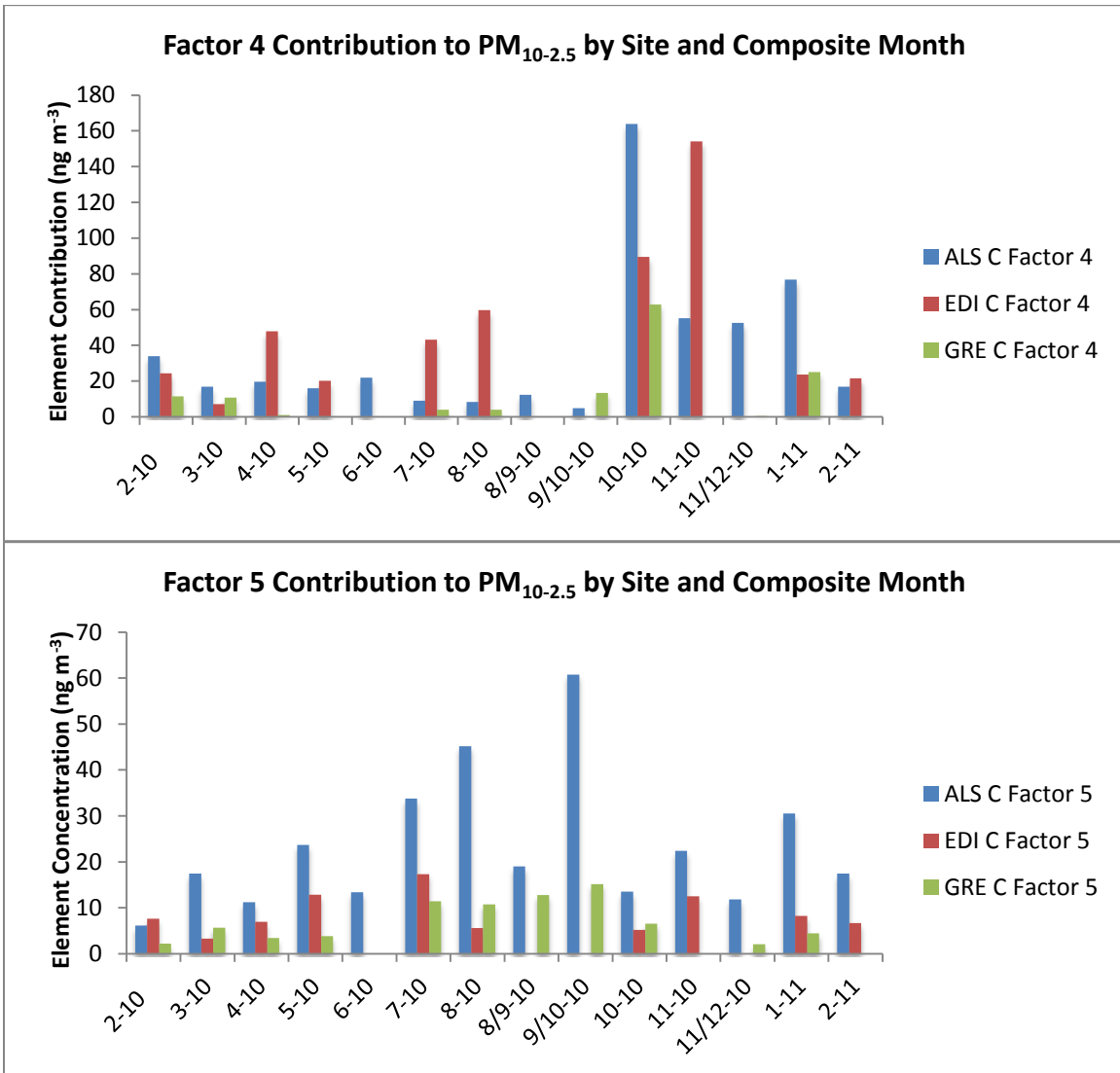
Figure 5.S5 Monthly median meteorological conditions for (a) Denver and (b) Greeley during the sampling campaign
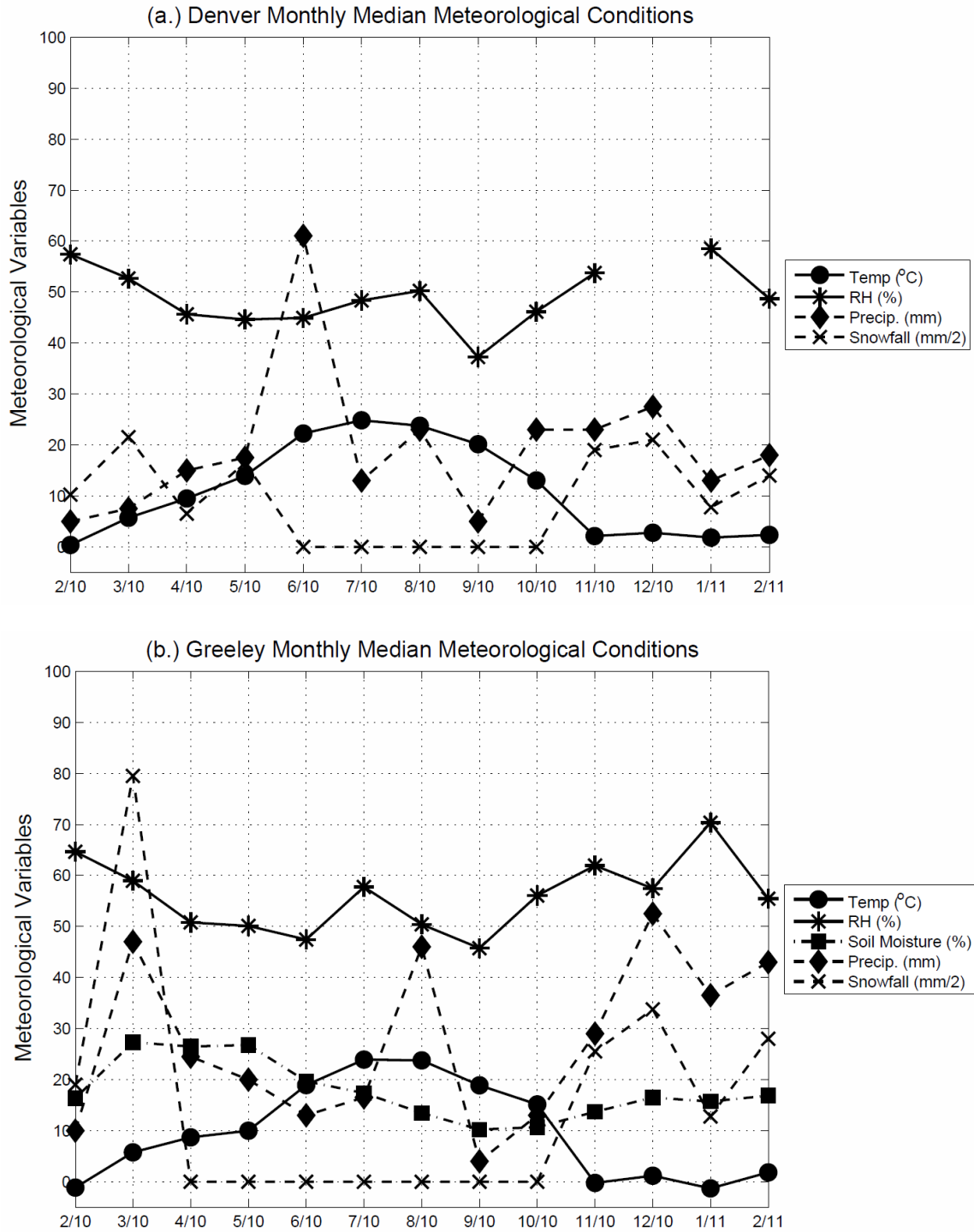
Note: Temperature and relative humidity were measured by the TEOM monitors at each CCRUSH site. Additional meteorological data were obtained from the Colorado Department of Public Health and Environment (CDPHE) for their monitoring sites in Denver and Greeley. The CDPHE data set includes ambient temperature (COMM, WBY, CAMP, DMAS, and CRG in Denver and GRET in Greeley) and relative humidity (DMAS). Precipitation and snowfall data were downloaded from the National Oceanic and Atmospheric Administration's National Climatic Data Center (http://www.ncdc.noaa.gov/) for the Denver International Airport and Greeley UNC sites. Soil moisture data were obtained for the Nunn #1 site operated by the United States Department of Agriculture National Resources Conservation Service (http://www.wcc.nrcs.usda.gov/nwcc/site?sitenum=2017&state=co). Monthly median values were derived from daily averages of the meteorological variables. Temperature and relative humidity were averaged across all sites in each city prior to calculating monthly medians.

CHAPTER 6

THE ORGANIC COMPONENT OF COARSE AND FINE PARTICULATE MATTER IN URBAN AND RURAL COLORADO: BULK CHARACTERISTICS, UV-VIS ABSORBANCE, FLUORESCENCE, AND ENDOTOXIN CONTENT

Nicholas Clements[a], Tiffany Duhl[a], Kaelin M. Cawley[b], Allison Moore[a], Kelly Albano[b], Kelli Fischer[a], Bounkheana Chhun[b], Jennifer Sobieray[b], Fernando L. Rosario-Ortiz[b], Jana B. Milford[a], Shelly L. Miller[a], Jennifer L. Peel[c], Michael P. Hannigan[a]

[a]Department of Mechanical Engineering, College of Engineering and Applied Science, University of Colorado at Boulder, Boulder, CO, 80309-0427

[b]Department of Civil, Environmental, and Architectural Engineering, University of Colorado at Boulder, Boulder, CO, 80309-0427

[c]Department of Environmental and Radiological Health Sciences, Colorado State University, Fort Collins, CO, 80523

6.0 ABSTRACT

While much is known about the health risks and climate effects of fine ($PM_{2.5}$) and coarse ($PM_{10-2.5}$) particulate matter, the organic matter found in both fractions is still under investigation. In this study, the organic matter from $PM_{10-2.5}$ and $PM_{2.5}$ filter samples collected every sixth day for over a year was characterized using bulk characterization methods including: total organic and elemental carbon, organic carbon peak fractions, water-soluble carbon and nitrogen, UV-vis absorbance, fluorescence, and endotoxin content. Filters were collected at four sites, two located in urban Denver and two in relatively rural Greeley, Colorado as part of the Colorado Coarse Rural-Urban Sources and Health (CCRUSH) study. Of the total particulate mass, organic matter contributed 35% of the $PM_{10-2.5}$ and 58% of the $PM_{2.5}$ total mass. $PM_{10-2.5}$ organic matter was 32% water soluble. In contrast, $PM_{2.5}$ was 75% water soluble. Organic carbon that volatilized at low temperatures during bulk carbon analysis dominated fine aerosols, while higher temperature peak fractions contributed substantially to $PM_{10-2.5}$. High correlation was found for the lowest organic peak fraction (PK_{340}) across size fractions and space and indicates a similar source or atmospheric process is contributing to low molecular weight organic compounds in both size fractions. Specific ultraviolet absorbance at 254 nm ($SUVA_{254}$) values, indicative of aromaticity, were elevated in both size fractions at a traffic-influenced site relative to rural and residential-urban sites. $SUVA_{254}$ values in Greeley were similar to those for agricultural soils and fell between values measured at the two sites in Denver. Fulvic and humic-like fluorescence peaks dominated $PM_{2.5}$ samples but were not measured in the coarse mode. Instead, $PM_{10-2.5}$ fluorescence peaked in the tryptophan and tyrosine-like regions. $SUVA_{254}$ and Humification index values peaked in winter for $PM_{2.5}$, a trend attributed to residential woodsmoke emissions. Endotoxin concentrations were significantly higher in Greeley and in $PM_{10-2.5}$, a trend that is likely due to cattle feedlot and agricultural emissions in the region.

6.1 INTRODUCTION

Elevated concentrations of ambient particulate matter, or aerosols, in the troposphere are a known public health threat (US EPA, 2004). Climatologically, aerosols are involved in cloud formation and light scattering and absorption, important factors in the solar radiation budget of the Earth (Forster et al., 2007). Ambient particulate matter is typically categorized by aerodynamic diameter, which is indicative of sources and composition. Ambient particulate mass distributions typically have two distinct peaks, one located below 2.5 µm (fine particulate matter, $PM_{2.5}$), and another between 2.5 and 10 µm (coarse particulate matter, $PM_{10-2.5}$).

Fine particles are typically generated through fuel combustion, biomass burning, and industrial processes as well as through biogenic- and anthropogenic-influenced secondary oxidation pathways in the atmosphere and through nucleation (Dutton et al., 2009a; Fast et al., 2009; Seinfeld and Pandis, 2006). From 4.5 years of sampling $PM_{2.5}$ at a single urban site, The Denver Aerosol Sources and Health (DASH) study showed that on average $PM_{2.5}$ was composed of 12% nitrate, 14% sulfate, 7% elemental carbon, and 39% organic carbon. Using a OM:OC conversion ratio of 1.8, $PM_{2.5}$ measured during the DASH study was 70% organic matter (Dutton et al., 2009b). $PM_{2.5}$ source factors in Denver determined via positive matrix factorization with one-year of daily concentrations of organic molecular markers revealed a wintertime woodsmoke factor, a motor oil combustion factor, a motor vehicle exhaust factor, a biogenic emissions factor, an n-alkane factor (mixed sources), and an inorganic ion factor (nitrate, sulfate, ammonium; Dutton et al., 2010b; Xie et al., 2013).

In contrast, coarse particles are typically generated through abrasive mechanical processes and/or resuspension. $PM_{10-2.5}$ composition tends to be heterogeneous within urban environments because of the influence of local sources and the short atmospheric lifetime of coarse particles (Hwang et al., 2008; Cheung et al., 2011; Lagudu et al., 2011; Moreno et al., 2011; Kumar et al., 2012; Clements et al., 2013a). Composition of $PM_{10-2.5}$ also tends to be

214

highly variable across ecological regions due to shifts in source importance by geographic location (Malm et al., 2007). Mineral dust is a ubiquitous component of $PM_{10-2.5}$, though separating the influence of turbulent road dust emissions, construction activities, agricultural activities, and geogenic dust resuspension is often difficult (e.g. Hwang et al., 2008; Pakbin et al., 2011; Clements et al., 2013a). Other major components of $PM_{10-2.5}$ include sea salt near coasts, road salt in snowy regions, inorganic ions (mostly nitrate and sulfate), brake and tire wear-related elements (e.g. Ba, Zn, Cu, Sb, Cr), and organic matter (Malm et al., 2007; Cheung et al., 2011; Clements et al., 2013a). Reconstructed elemental mass, where dominant mineral oxides are taken into account, explained 16-24% of the total $PM_{10-2.5}$ mass measured in Colorado (Clements et al., 2013a). The organic fraction of $PM_{10-2.5}$ has not been well characterized, though it is believed to be largely a mixture of biological particles (fungi, bacteria, pollen spores, and plant detritus), soil organic matter, and to a lesser extent anthropogenic organic species related to vehicular emissions in urban areas (Puxbaum and Tenze-Kunit, 2003; Cheung et al., 2012; Bowers et al., 2013).

In 2006 the EPA rejected a proposal to regulate $PM_{10-2.5}$ in the United States. Lack of knowledge about the health impact and toxicology of coarse particles in rural areas was cited as one reason for the decision (US EPA, 2006). In the following years, the agency funded multiple studies with the goal of improving the scientific understanding of this pollutant. These studies ranged widely in scope and included spatial field campaigns (e.g. Cheung et al., 2011; Clements et al., 2013b), toxicology studies (e.g. Brook et al., 2013), and an epidemiological campaign. The Colorado Coarse Rural-Urban Sources and Health (CCRUSH) study is one such study funded by the US EPA with the goal of characterizing the composition, sources, and health impacts of $PM_{10-2.5}$ in urban and rural environments in Colorado. Two field campaigns were conducted during the CCRUSH study. For three years (2009-2012), continuous $PM_{10-2.5}$ and $PM_{2.5}$ mass concentration data were collected with TEOM 1405-DFs. This data set will be a key component in an epidemiological study of acute health effects and birth related-issues.

During the second year of continuous monitoring (2010-2011), collocated dichotomous filter samplers were operated every sixth day. Teflon and quartz filter samples were used in multiple compositional analyses, many of which are presented here. Elemental concentrations from monthly composites of Teflon filters were the focus of a recent paper assessing $PM_{10-2.5}$ and $PM_{2.5}$ sources (Clements et al., 2013a). Continuous mass concentration data revealed a strong inter-dependence between $PM_{10-2.5}$ mass concentrations, traffic, and meteorological conditions (relative humidity, soil moisture, wind speed/direction) which is related to the ability of material to be resuspended, either through turbulent traffic dispersion or from increased wind speeds/low soil moisture (Clements et al., 2013b).

Characterization of atmospheric organic matter via single-molecule analysis and quantification (e.g. GC/MS, LC/MS, and AMS) is unable to characterize a significant portion of the organic mass due to its high molecular weight and complexity. This fraction is referred to as HUmic LIke Substances, or HULIS, because of its resemblance to humic substances found in soil and aquatic systems. HULIS, commonly characterized as a mixture of high molecular weight polyacids, constitutes a substantial fraction of the water soluble organic carbon (WSOC) found in atmospheric aerosols, ranging from as low as 15-32% in the Amazon to 60-72% at a high-alpine site in Switzerland and at a rural site in China (Krivacsy et al., 2001; Mayol-Bracero et al., 2002; Lin et al., 2010). Due to the difficulty associated with characterizing this type of organic matter, a wide range of analytical methods have been used to investigate its properties (e.g. UV-vis absorbance, fluorescence, NMR spectroscopy, FTIR spectroscopy). Sources of fine particulate HULIS in the atmosphere are seasonal, with secondary organic aerosols (SOA) contributing throughout the year, peaking in summer, and biomass burning (e.g. residential wood burning) contributing during fall and winter (Duarte et al., 2005; Duarte et al., 2007; Feczko et al., 2007; Duarte et al., 2008; Baduel et al., 2010; Lin et al., 2012; Zhang et al., 2012). HULIS is typically isolated from bulk WSOC using various solid phase extraction methods (Baduel et al., 2009). Non-HULIS WSOC includes carboxylic acids (e.g. oxalic acid),

216

saccharides (from bioaerosols), and a range of low molecular weight acidic and/or polar organic compounds that may have similar sources to HULIS, namely secondary atmospheric oxidation of precursor species and biomass burning (Graham et al., 2002; Huang et al., 2006; Sullivan and Weber, 2006; Jia et al., 2010; Hegde and Kawamura, 2012).

In this study, we use bulk characterization methods to study the total and water-soluble organic fractions of $PM_{2.5}$ and $PM_{10-2.5}$. It was hypothesized that qualities of $PM_{2.5}$ water soluble organic matter would have distinct seasonal patterns due to shifts in source importance (wood smoke in winter, SOA formation in summer). It was also hypothesized that $PM_{10-2.5}$ would resemble the water soluble fraction of natural organic matter found in soils and aeolian dust and that $PM_{10-2.5}$ WSOC would be more terrestrial than atmospheric "HULIS" as traditionally defined. Due to the high-level of agricultural activity around Greeley and the identification of cow-gut (fecal) bacteria on the same filter set (Bowers et al., 2013), it was also hypothesized that $PM_{10-2.5}$ organic matter in Greeley could have identifiable differences from samples collected in urban Denver.

6.2 METHODS

6.2.1 Monitoring Sites

One goal of the CCRUSH study was to compare the composition of $PM_{10-2.5}$ and $PM_{2.5}$ in urban and rural environments. To accomplish this, filter sampling was conducted in Denver and Greeley, Colorado. Denver is Colorado's largest city; the Denver metropolitan region contains half the state's population (US Census Bureau, 2012). Greeley is located 75 km northeast of Denver in Weld county, an agricultural region of Colorado that grows large quantities of corn, sunflowers, and winter wheat, and in 2007 the county contained almost a million (987,892) acres of cropland (US Department of Agriculture, 2007). Two large cattle feedlots with a combined capacity of 167,000 head of cattle are located near Greeley (JBS Five Rivers Cattle Feeding, 2013). Both study cities are part of the Front Range of Colorado, a series of cities and towns running north-south along the I-25 corridor located at the far western edge of the Great Plains in the shadow of the Rocky Mountains. The Front Range region is semi-arid and experiences four distinct seasons characterized by volatile and windy springs, hot summers with frequent afternoon thunderstorms, cold and quick falls, and snowy winters. Dominant local air flow patterns are that of a mountain valley, flowing along the drainage of the South Platte River northwards (down-slope) at night and southwards (up-slope) during the day (Haagenson, 1979; Clements et al., 2013b).

Dichotomous filter samplers were sited on four elementary school rooftops, two in Denver and two in Greeley, Colorado. Alsup Elementary School (ALS) is located in a residential area in the industrial suburb of Commerce City, northeast of downtown Denver. Within close proximity to ALS are both a gravel pit and I-76; local sources that contribute significantly to the mass concentrations and temporal variability measured at this site (Clements et al., 2013a; Clements et al., 2013b). Edison Elementary School (EDI) is located east of downtown Denver in a residential neighborhood. Edison is located far enough from local sources that they do not

appear to significantly affect total mass concentration variability at this site, though two interstates, I-70 and I-25, are located 2.0 and 2.5 km away, respectively, and vehicular emissions were a significant elemental source at residential EDI (Clements et al., 2013a). In Greeley, Maplewood (MAP) and McAuliffe (MCA) Elementary Schools were both located in residential neighborhoods. MAP is nearer to the town center of Greeley, and MCA is northwest of MAP in the town's suburban fringe. Table 6.1 contains site and sampler descriptions, including average filter sampler flow rates.

Table 6.1 CCRUSH monitoring site and sampler descriptions

Monitoring Site	ALS	EDI	MAP	MCA
City	Denver	Denver	Greeley	Greeley
Coordinates	39.83N 104.94W	39.76N 105.04W	40.42N 104.71W	40.43N 104.77W
Site Description	Industrial-Residential	Urban-Residential	Rural-Residential	Rural-Residential
Inlet Height (m)	6	9	9	10
Median PM$_{2.5}$ Flow Rate (lpm)	42.99	43.40	42.56	41.72
Median PM$_{10-2.5}$ Flow Rate (lpm)	2.01	2.05	1.93	2.03

6.2.2 Filter Collection

Dichotomous filter samplers were built in-house and were based on a simple design from previous campaigns (e.g. the DASH PM$_{2.5}$ sampler, Dutton et al., 2009b). Samplers were designed to be operated at 50 lpm and utilized a modified PM$_{10}$ inlet and virtual impactor (VI; 2.5 µm cutpoint, 48 lpm major flow, 2 lpm minor flow) system (Misra et al., 2001; Misra et al., 2003). Following separation in the virtual impactor, PM$_{10-2.5}$ and PM$_{2.5}$ sample volumes were split equally and deposited onto 47 mm Teflon (Pall Gelman Teflo Membrane Filter, 2 µm thickness) and quartz (Pall Gelman Tissuequartz Filter) filters. Pressure gages monitored changes in filter

pressure drop during sample collection. Flow rates were controlled passively using manifolds of critical orifices and monitored using flow totalizers. Mechanical timers were used to set sampling times, which ran from midnight to midnight on the sample day. Figure 6.1 is a schematic of the filter samplers used in this study. Filters were transported to and from sites in chilled coolers and stored in freezers (<0°C) until use in compositional analyses. $PM_{2.5}$ channel flow rates deviated slightly from the intended filter sampler design flow of 48 lpm, with site medians ranging from 41.7 to 43.4 lpm. $PM_{10-2.5}$ channel flow rates did not vary significantly from the 2 lpm design flow.

Figure 6.1 CCRUSH dichotomous filter sampler schematic
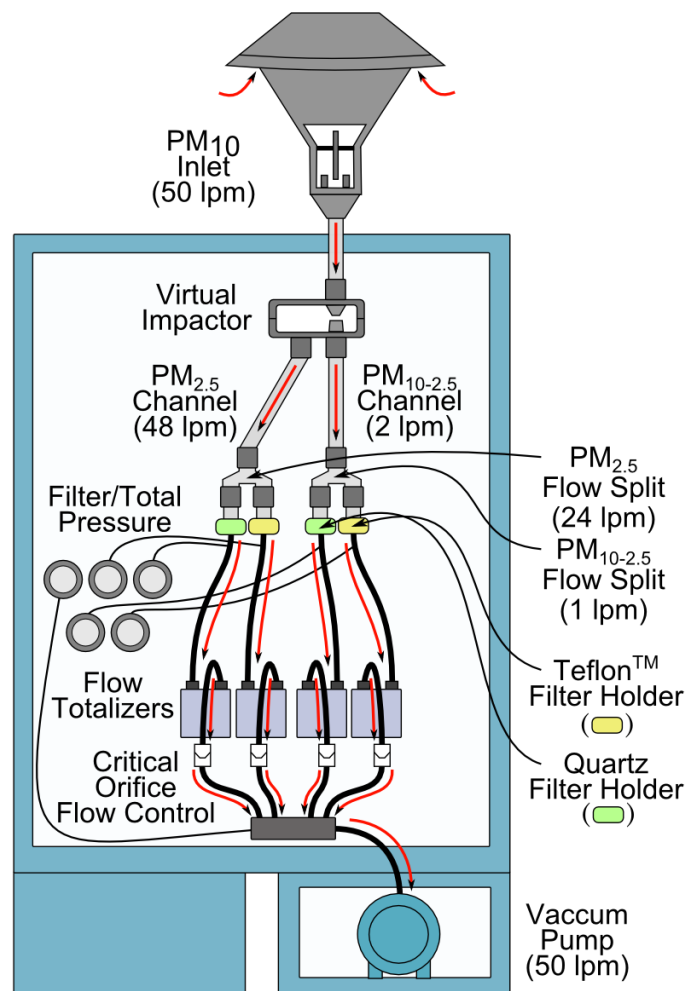
Filter samples were collected every sixth day from 2/19/2010 to 3/10/2011 at all sites. Sites were visited within 48 hours after sampling to collect the filters, and field blanks of each filter media type were carried to monitoring sites during filter deployment and collection. Some gaps in the data exist and are mainly the result of not having access to sites during holidays and school breaks, though human errors did result in two extended periods of missing data. From 8/18/2010 to 10/5/2010 (9 sample days), EDI samples were excluded due to a sampler inlet malfunction, and from 7/1/2010 to 7/19/2010 (5 sample days) MAP had a pinched $PM_{10-2.5}$ sample tube which affected flow rates, leading to these samples also being excluded from further analyses.

For the endotoxin measurements, water soluble carbon analyses, and elemental concentrations, monthly composite filter sets were analyzed. Unfortunately, due to availability of sample media, consistent sets of filters were not included in composites for each analysis, so direct comparison between the results was not always possible. Table 6.S1 in the supplemental information is a list of all filter sampling days and the associated analyses performed on each collected filter.

6.2.3 Compositional Analyses

6.2.3.1 Mass Concentrations

Teflon filters were analyzed gravimetrically for particulate mass concentrations. Before and after sampling, Teflon filters were weighed in a temperature and relative humidity controlled weigh box using a microbalance (LabServe model BP210D, Sartorius Corporation) following the methods of Dutton et al. (2009b). Weigh box control filters were used to monitor scale drift. Due to the virtual impactor, a small proportion of $PM_{2.5}$ deposits in the $PM_{10-2.5}$ channel. Masses were corrected by subtracting from the $PM_{10-2.5}$ mass the associated $PM_{2.5}$ mass multiplied by the ratio of minor to inlet flows of the virtual impactor (Clements et al., 2012). The median mass of

all field blank filters was subtracted from the sample filters to correct for contamination. The minimum detection limit (MDL) of the gravimetric analysis in this study, based on 2 times the standard deviation of the filter blank masses, was 2.9 µg/m^3. Below detection limit (BDL) samples were given values 50% the minimum detection limit. Mass concentration uncertainties were estimated for each sample based on propagation of error of the uncertainties in mass measurements, sampling time, and sampled volume (Dutton et al., 2009b).

6.2.3.2 Bulk Organic Carbon and Elemental Carbon Concentrations

All quartz filters were analyzed for bulk elemental carbon (EC) and organic carbon (OC) concentrations using the thermal-optical method (Laboratory OCEC Analyzer, Sunset Laboratories). Prior to field use, all quartz filters were baked at 500°C for at least 12 hours. Filter samples collected from 2/19/2010 to 11/16/2010 were analyzed at the Wisconsin State Laboratory of Hygiene (WSLH) and samples collected from 12/4/2010 to 3/10/2011 were analyzed at the University of Colorado at Boulder (CU) on a different OCEC Analyzer. A filter punch (1.5 cm^2) was taken from each quartz filter and analyzed on one of the two instruments following protocols described by the manufacturer. In order for results from the two instruments to be comparable, extensive testing was performed on the CU instrument in order to match the temperature ramping protocol used by the WSLH instrument. Details of the parameter file inputs from each instrument are included in Table 6.S2. Figure 6.S1 shows the differences in temperature profiles for the two instruments. The WSLH instrument is an older design and does not require power and time constants in the parameter file to run, which results in poor temperature ramping performance (over shooting and variable temperatures during peaks). Because of this, multiple lines of input parameters were required for each peak to recreate the temperature profile of the WSLH instrument. As the CU instrument oven was not able to heat as quickly as the WSLH instrument, the two highest temperature steps took longer to reach peak temperatures on the CU instrument. To maintain consistency, the time at each peak

temperature was kept consistent between the two methods. Future work will include analyzing a set of filters on each instrument to directly assess comparability. Bulk EC and OC concentrations were corrected using field blank medians and corrected for deposition of $PM_{2.5}$ into the $PM_{10-2.5}$ channel because of the virtual impactor.

6.2.3.3 Organic Carbon Peak Fractions

During bulk organic carbon analysis, four increasing discrete temperature plateaus (Table 6.S2) were reached prior to the instrument switching to an oxygenated atmosphere for elemental carbon quantification. It was hypothesized that differences in bulk characteristics of the organic matter in each particulate size fraction could be identified by comparing the contributions of each peak fraction to the total organic carbon. Organic carbon concentrations from the four temperature plateaus (PK_{340}, PK_{500}, PK_{615}, and PK_{900}), where subscripts represent peak temperature in Celsius, and pyrolized carbon (PC) concentrations were extracted from the bulk organic carbon data sets and corrected through median field blank subtraction and for the influence of the virtual impactor. MDLs, calculated as 2 times the standard deviation of the field blank concentrations, were 0.05 ugC/m^3 for OC, 0.03 ugC/m^3 for PK_{340}, 0.02 ugC/m^3 for PK_{500}, 0.01 ugC/m^3 for PK_{615}, 0.01 ugC/m^3 for PK_{900}, and insignificant for EC and PC (< 0.001 ugC/m^3). BDL values were replaced with 50% the MDL value. Uncertainties for EC, OC, and all peak fractions were estimated via propagation of error of the uncertainties from the thermal-optical quantification method, sampling time, and sampled volume.

6.2.3.4 Aqueous Extractions

To characterize the water soluble fraction of particulate matter, aqueous extracts of composited sets of quartz filters were analyzed for total water soluble organic carbon (WSOC), total dissolved nitrogen (TDN), UV and visible light absorbance, and fluorescence. Roughly twelve composites for each size fraction and monitoring site were analyzed. To perform the

extractions, composited filter pieces were placed in an amber glass jar with 15-20 mL of MilliQ water and sonicated in an ice bath for an hour at neutral pH. Composited filter pieces were half of the original quartz filter, minus the 1.5 cm^2 punch for bulk carbon analysis, for a total area of 2.85 cm^2/filter piece. Following sonication, aqueous solutions were filtered through a baked 25-mm borosilicate glass fiber filter to remove insoluble components (GF/F, 0.7 μm nominal pore size, Whatman Ltd.). An additional 15-20 mL of MilliQ water was then added to the amber jar and filter samples were sonicated in an ice bath again for an hour. Slurries from the second extraction were filtered and added to the original solution, resulting in 30-40 mL of extract solution.

6.2.3.5 Analysis of the Water Soluble Fraction

Aqueous extracts were first analyzed on a UV-vis spectrometer (Cary 100Bio, Agilent Technologies) which measures absorbance of light with wavelengths ranging from 200 to 800 nm (1 nm increments), which includes the UV and visible ranges, through a 1 cm pathlength cuvette. Absorbance values were zeroed internally for a lab blank (MilliQ water), though a field blank correction was not performed on the sample absorbance spectra. Median field blank spectra are included in figures for reference

Directly following UV-vis analysis, extracts were analyzed for fluorescence on a Horiba FluoroMax 4. Excitation-emission matrices (EEMs) were collected for excitation wavelengths of 240-450 nm (10 nm increments) and emission wavelengths of 300-560 nm (2 nm increments). Slit widths of 5 nm were used for both excitation and emission modes. Corrections applied to EEMs include Raman normalization, inner filter correction, lab blank subtraction, and cuvette corrections. Like the UV-vis data, EEMs were not field blank corrected, though EEMs for all field blanks had low peak intensities (<0.35) and similar peak regions.

After extracts were analyzed for UV-vis absorbance and fluorescence, extract vials were sent to the Kiowa Environmental Chemistry Laboratory in Boulder, Colorado to be analyzed for

water soluble organic carbon and total dissolved nitrogen (TDN) on a Shimadzu TOC-V CSN Total Organic Carbon Analyzer. This instrument determines concentrations of WSOC and TDN by acidifying the sample (pH < 2.0) and injecting it into a total carbon combustion tube, where carbonaceous components are decomposed to CO_2 and nitrogen-containing compounds are decomposed into NO. CO_2 is then quantified with a non-dispersive infrared gas analyzer (NDIR) and oxides of nitrogen are quantified with a chemiluminescence gas analyzer. TDN includes ionic (NO_3^- and NH_4^+) and organic forms of water soluble nitrogen. Instrument detection limits provided by Kiowa for 2013 were 0.031 mgC/L for WSOC and 0.008 mgN/L for TDN quantification (*personal communication*). MDLs based on 2 times the standard deviation of filter blank concentrations were 0.81 mgC/m^3 (0.30 mgC/L) and 0.20 mgN/m^3 (0.14 mgN/L) and BDL samples were replaced with 50% the MDL. Note that instrument detection limits were at least an order of magnitude smaller than the minimum detection limits based on field blanks.

6.2.3.6 Endotoxin Concentrations

Endotoxin is a lipopolysaccharide found in the cell wall of Gram-negative bacteria and may be related to air pollution health effects, especially in the indoor environment (Wang et al., 2005; Degobbi et al., 2011). Endotoxin concentrations were assessed using the Kinetic-QCL Limulus Amebocyte Lysate (LAL) Assay (Lonza Group Ltd.). Monthly composite sets of 3-5 pieces of 1/8th sections of quartz filters were extracted in 2 mL/filter piece pyrogen-free 0.05% Tween solution via sonication in an ice bath for an hour. Following sonication, samples were vortexed and 700 µL of the extract was placed in a 2 mL centrifuge tube. Samples were centrifuged at 2200 rpm for 10 minutes. Supernatant was then pippetted in to separate vials prior to transferring 100 µL of each sample into a 96-well plate. Filter sample and field blank extracts were analyzed in duplicate. Once plated, samples were incubated in a microplate reader (ELX808 Ultra Microplate Reader, BioTek Instruments, Inc.) at 37°C for at least 15 minutes. Following incubation, 100 µL of reconstituted LAL Reagent was added to each well,

timing the placement of reagent into wells within 5-10 seconds for reaction time corrections. The

formation of p-nitroaniline through the activation of a proenzyme catalyzed by the presence of

endotoxin is detected via absorption at 405 nm and monitored until the reaction runs to

completion. Calibration curves were generated for each sample batch (4 batches total) from a

serial dilution of a standard solution with endotoxin unit (EU) concentrations of 0.005, 0.05, 0.5,

5, and 50 EU/mL. All endotoxin calibration curves had coefficient of determination (R^2) values

greater than 0.98. Blanks of pyrogen-free water, Tween solution, and field blank filter samples

were also included in each analysis batch. The MDL for the endotoxin analysis, based on 2

times the standard deviation of filter blank concentrations, was 0.194 EU/m^3. BDL samples were

replaced with 50% of the MDL. Concentrations were corrected using the average virtual

impactor correction over the set of filters in each composite.

6.2.3.7 Data Analysis

Absorbance values were normalized by the concentrations of organic carbon in extract

solutions, resulting in specific UV-vis absorbance (SUVA). Increases in the SUVA at 254 nm

(SUVA$_{254}$) are correlated with increases in aromaticity for aquatic and airborne natural organic

matter as determined by carbon-13 nuclear magnetic resonance (Weishaar et al., 2003; Duarte

et al., 2005). SUVA$_{254}$ values were calculated for all composite samples and were compared to

SUVA at 280 nm to check for signal interference. Trends in SUVA values were the same at 254

and 280 nm, suggesting interference was not an issue for these samples. For SUVA$_{254}$

calculations, the median field blank absorbance at 254 nm and median field blank extract

concentration (mgC/L) were subtracted from sample absorbance and WSOC concentrations.

The fluorescence index (FI = I(Ex$_{370}$,Em$_{450}$)/I(Ex$_{370}$,Em$_{500}$)), derived from fluorescence

intensities of sample EEMs, typically ranges from 1.4 to 1.9 for aquatic organic matter, with low

values indicating terrestrial origin and high values suggesting microbial processing (Chen et al.,

2003). The FI investigates EEM peak shape, and the 360-380 nm peak location is important for

226

properly assessing the FI. The location of this peak did not vary significantly sample to sample, averaging (±st.dev.) 365±2 nm and ranging from 376 to 362, therefore it was assumed that peak location was not significantly affecting FI results. In aerosols, an increased FI may not necessarily indicate microbial processing, but instead materials that resemble microbially processed organic matter in structure (i.e. HULIS).

The Humification Index (HIX), also derived from sample EEMs, was calculated as the ratio of the sum of emission intensities from 435 to 480 nm over the sum of emission intensities from 300 to 345 nm and from 435-480 nm, using an excitation wavelength of 254 nm (Ohno, 2002). HIX values defined in this way increase from 0 to 1 with increased degree of humification. "Humification" in the atmosphere may indicate atmospheric oxidation or biomass burning processes, particularly for $PM_{2.5}$, as opposed to microbially-mediated humification in soil and aquatic environments. Negative HIX values, resulting from low fluorescence intensities and EEM corrections, were replaced with missing values as these indices were not able to be determined. Only $PM_{10-2.5}$ samples had this issue. Using the EEMs of $PM_{10-2.5}$ and $PM_{2.5}$, the applicability of these indices for interpreting qualitative characteristics of airborne organic matter will be assessed.

6.3 RESULTS AND DISCUSSION

6.3.1 Bulk EC/OC and Organic Peak Fractions

The summary statistics for the mass and bulk carbon concentrations are presented in Table 6.2. For calculating the percent mass explained by organic carbon, mean values were converted from organic carbon to organic matter concentrations with a conversion factor of 1.8 (Cheung et al., 2011). $PM_{2.5}$ was over half organic matter, ranging from 52 to 65%. Organic matter contributed to 34 to 43% of the coarse particulate mass. Using the same conversion factor, the DASH study found $PM_{2.5}$ was 70% organic matter, which is similar to the value measured at the residential site, EDI (Dutton et al., 2009b). The DASH study utilized a residential monitor located south of downtown Denver. Elevated concentrations of $PM_{10-2.5}$ and $PM_{2.5}$ mass, organic carbon and elemental carbon were measured at ALS, relative to the other three sites. This was observed in other analyses from the CCRUSH study (e.g. Clements et al., 2012; Clements et al., 2013a; Clements et al., 2013b) and is largely a result of local source emissions (traffic/gravel pit operations) near ALS. Average $PM_{10-2.5}$ mass and bulk carbon concentrations measured in Greeley (MAP, MCA) typically fell between traffic-influenced ALS and residential EDI. $PM_{2.5}$ OC and EC concentrations were elevated in Denver compared to Greeley. Lower EC concentrations in Greeley compared to Denver are indicative of decreased regional traffic emissions. Local traffic counts on major highways in Greeley were an order of magnitude lower than those in Denver during the CCRUSH study (Clements et al., 2013b). $PM_{2.5}$ EC concentrations were an order of magnitude larger than $PM_{10-2.5}$ EC concentrations.

Table 6.2 Summary statistics of the mass and bulk carbon concentrations

Size Fraction	Site	Mass	OC		EC		PK$_{340}$		PK$_{500}$		PK$_{615}$		PK$_{900}$		Pyrol	
		Mean (St.Dev.)	Mean (St.Dev.)	Mean % Mass[a]	Mean (St.Dev.)	Mean % Mass	Mean (St.Dev.)	Mean % OC	Mean (St.Dev.)	Mean % OC	Mean (St.Dev.)	Mean % OC	Mean (St.Dev.)	Mean % OC	Mean (St.Dev.)	Mean % OC
		(µg/m3)	(µg/m3)	%	(µg/m3)	%	(µg/m3)	%	(µg/m3)	%	(µg/m3)	%	(µg/m3)	%	(µg/m3)	%
PM$_{10-2.5}$	ALS	8.35 (6.02)	2.00 (0.93)	43	0.06 (0.09)	1	0.37 (0.23)	19	0.65 (0.33)	0.32	0.35 (0.18)	17	0.53 (0.28)	27	0.11 (0.11)	5
	EDI	5.09 (3.61)	1.19 (0.54)	42	0.04 (0.07)	1	0.28 (0.20)	24	0.38 (0.17)	0.32	0.19 (0.09)	16	0.29 (0.17)	25	0.05 (0.06)	4
	MAP	6.76 (4.77)	1.26 (0.77)	34	0.02 (0.02)	0	0.24 (0.17)	19	0.47 (0.30)	0.37	0.22 (0.17)	18	0.29 (0.20)	23	0.05 (0.05)	4
	MCA	5.78 (4.09)	1.16 (0.60)	36	0.02 (0.02)	0	0.24 (0.16)	20	0.40 (0.21)	0.35	0.21 (0.14)	18	0.27 (0.16)	23	0.04 (0.05)	4
PM$_{2.5}$	ALS	7.07 (4.88)	2.30 (1.03)	59	0.46 (0.32)	7	0.80 (0.39)	35	0.53 (0.24)	0.23	0.27 (0.13)	12	0.47 (0.26)	20	0.24 (0.27)	10
	EDI	5.68 (2.94)	2.04 (0.65)	65	0.27 (0.19)	5	0.69 (0.29)	34	0.48 (0.17)	0.24	0.25 (0.10)	12	0.40 (0.18)	19	0.22 (0.18)	11
	MAP	5.93 (3.51)	1.72 (0.91)	52	0.16 (0.15)	3	0.58 (0.30)	34	0.45 (0.24)	0.26	0.21 (0.13)	12	0.31 (0.22)	18	0.16 (0.14)	9
	MCA	5.26 (2.95)	1.70 (0.65)	58	0.16 (0.12)	3	0.56 (0.22)	33	0.47 (0.19)	0.27	0.22 (0.11)	13	0.32 (0.16)	19	0.14 (0.10)	8

[a] Conversion factor of 1.8 used to convert organic carbon to organic matter

Across monitoring sites, contributions of OC and EC to total mass and organic peak fraction contributions to OC were remarkably similar. PM$_{10-2.5}$ tended to be contributed to mainly by PK$_{500}$ and PK$_{900}$, the second and fourth temperature peaks, respectively, whereas PM$_{2.5}$ was contributed to mainly by PK$_{340}$ and PK$_{500}$, the first and second peaks. Lower temperature peak fractions contributed substantially more OC to PM$_{2.5}$ compared to PM$_{10-2.5}$, as organic compounds with low molecular weights and/or higher volatilities contribute significantly to the mass of fine particles (e.g. Zaveri et al., 2012). PM$_{2.5}$ in this region was 27% semivolatile (at 30°C) and semivolatile concentrations peaked during summertime when low molecular weight secondary organic aerosol particles form through photooxidation pathways (Clements et al., 2013b). PM$_{10-2.5}$ had higher contributions from higher temperature peak fractions, likely because the coarse fraction contains biological particles and soil organic matter, the constituents of which tend to have higher molecular weights and are much less volatile than the organic matter found in PM$_{2.5}$ (e.g. Stone et al., 2011).

The coefficient of variability (COV), calculated as the ratio of the time series standard deviation to the mean, is indicative of temporal variability. Table 6.S3 contains COVs calculated for $PM_{10-2.5}$ and $PM_{2.5}$ mass concentrations and bulk organic carbon concentrations. For both particulate size fractions, EC was more temporally variable than OC, likely because EC is highly seasonal, peaking in the winter. Of the OC peak fractions, pyrolized carbon (PC) was the most temporally variable for both size fractions. For all bulk carbon fractions, $PM_{10-2.5}$ was more temporally variable than $PM_{2.5}$. ALS and Greeley $PM_{10-2.5}$ and $PM_{2.5}$ OC concentrations tended to peak during the fall, where as no clear seasonal peak was observed at EDI. Limited winter sampling reduces the significance of this result, as $PM_{2.5}$ OC concentrations peaked during the winter in the DASH study and utilized multiple years of daily sampling (Dutton et al., 2010a). PK_{340} concentrations increased notably in the winter for both size fractions.

Contributions from organic peak fractions exhibited interesting seasonalities, as shown in Figure 6.2. Moving from spring to winter, PK_{340} and PK_{500} showed the same temporal trends in both size fractions, with PK_{340} increasing in contributions and PK_{500} decreasing in contributions. PK_{900} contributions did not vary much seasonally, while contributions from PK_{615} peaked slightly in summer for both $PM_{10-2.5}$ and $PM_{2.5}$. $PM_{2.5}$ pyrolized carbon contributions increased significantly during fall, a trend that was enhanced in Denver (17%) compared to Greeley (12%). Contributions of PC to the coarse mode were low. Elemental carbon peaked in winter samples of $PM_{2.5}$, which was also observed in the DASH study (Dutton et al., 2010a).

Figure 6.2 Seasonal median contributions of organic peak fractions to (a) $PM_{10-2.5}$ and (b) $PM_{2.5}$
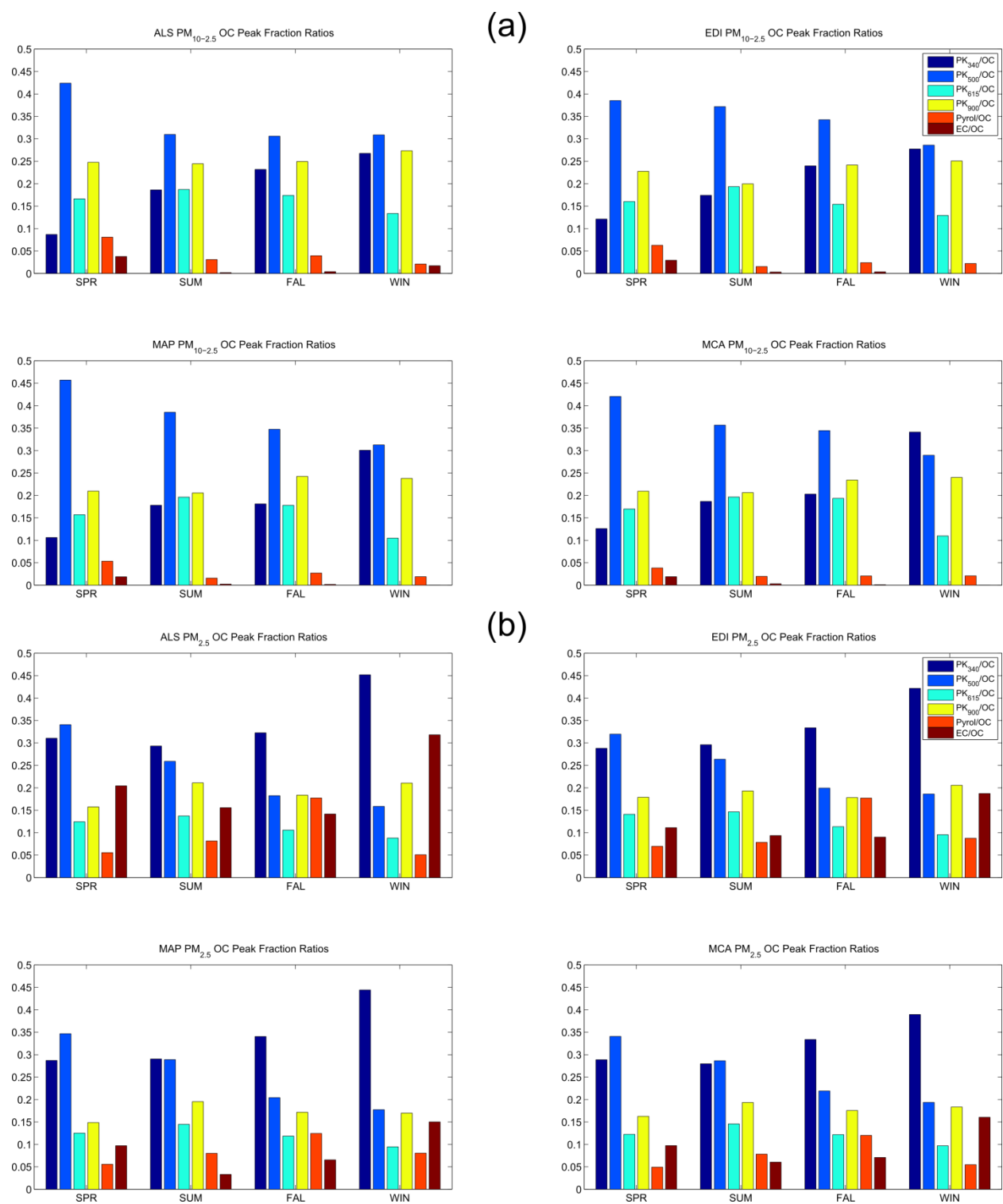
Correlation relationships can help identify trends in sources and transport. Correlations between size fractions, sites, and between bulk carbon fractions were calculated for all time series combinations. Due to the high dimensionality of the data set, only a select set of correlations are presented in Table 6.3, focusing on comparisons for ALS $PM_{10-2.5}$. Shading in Table 6.3 ranges from red to green as correlations increase. Correlations with MCA $PM_{2.5}$ are excluded in Table 6.3, but follow similar trends to those observed with MAP $PM_{2.5}$. $PM_{10-2.5}$ mass concentrations were less correlated within Denver ($\rho=0.58$) than within Greeley ($\rho=0.70$). A higher correlation was expected in Greeley because monitoring sites were separated by less distance in Greeley (3 km) than Denver (7 km). ALS $PM_{10-2.5}$ mass was more correlated with MAP and MCA $PM_{10-2.5}$ concentrations ($\rho=0.70$ and 0.74, respectively) than for comparisons between EDI and the Greeley sites ($\rho=0.48$ and 0.49, respectively), suggesting temporal patterns observed at ALS are more similar to trends observed in Greeley than those observed at EDI. $PM_{2.5}$ mass concentrations were more correlated than $PM_{10-2.5}$ in both Denver ($\rho=0.75$) and Greeley ($\rho=0.84$). The spatial correlation trends measured with the filter samples were consistent with spatial comparisons from the continuous mass concentration data set (Clements et al., 2013b).

In Denver, $PM_{2.5}$ OC ($\rho=0.80$) was more correlated than $PM_{10-2.5}$ OC ($\rho=0.67$), though in Greeley correlations for both size fractions were the same ($\rho=0.78$). For spatial comparisons between cities for both size fractions, total OC tended to be moderately correlated ($0.38<\rho<0.69$). Correlations between OC and mass were generally high and ranged from 0.57 (MAP) to 0.79 (ALS and EDI) for $PM_{10-2.5}$ and from 0.64 (EDI) to 0.81 (ALS) for $PM_{2.5}$.

Table 6.3 Correlations for comparisons between ALS $PM_{10-2.5}$ bulk carbon concentrations and EDI/MAP $PM_{10-2.5}$ and $PM_{2.5}$ bulk carbon concentrations

ρ		ALS $PM_{10-2.5}$							
		Mass	EC	OC	PK$_{340}$	PK$_{500}$	PK$_{615}$	PK$_{900}$	Pyrol
ALS $PM_{10-2.5}$	Mass	1.00							
	EC	0.07	1.00						
	OC	0.79	0.23	1.00					
	PK$_{340}$	0.65	-0.22	0.63	1.00				
	PK$_{500}$	0.72	0.29	0.89	0.39	1.00			
	PK$_{615}$	0.75	0.30	0.92	0.44	0.76	1.00		
	PK$_{900}$	0.70	0.33	0.95	0.52	0.81	0.89	1.00	
	Pyrol	0.37	0.28	0.59	0.00	0.45	0.69	0.60	1.00
EDI $PM_{10-2.5}$	Mass	0.58	0.46	0.67	0.36	0.62	0.61	0.69	0.33
	EC	0.01	0.63	0.14	-0.20	0.14	0.23	0.14	0.44
	OC	0.48	0.25	0.67	0.58	0.47	0.53	0.71	0.38
	PK$_{340}$	0.26	-0.06	0.27	0.72	0.00	0.08	0.27	0.02
	PK$_{500}$	0.48	0.27	0.67	0.35	0.74	0.48	0.65	0.25
	PK$_{615}$	0.46	0.41	0.65	0.24	0.43	0.72	0.72	0.60
	PK$_{900}$	0.51	0.32	0.71	0.51	0.51	0.58	0.79	0.38
	Pyrol	0.15	0.16	0.29	-0.06	0.11	0.38	0.36	0.65
MAP $PM_{10-2.5}$	Mass	0.70	0.05	0.66	0.51	0.50	0.68	0.65	0.42
	EC	-0.11	0.50	0.03	-0.41	0.15	0.13	0.11	0.24
	OC	0.65	-0.19	0.62	0.47	0.46	0.64	0.55	0.45
	PK$_{340}$	0.55	-0.27	0.47	0.84	0.17	0.37	0.40	0.03
	PK$_{500}$	0.54	-0.18	0.51	0.25	0.50	0.53	0.43	0.39
	PK$_{615}$	0.58	-0.14	0.59	0.36	0.43	0.67	0.54	0.49
	PK$_{900}$	0.66	-0.12	0.63	0.40	0.45	0.67	0.59	0.55
	Pyrol	0.32	0.01	0.35	-0.01	0.23	0.43	0.39	0.73
MCA $PM_{10-2.5}$	Mass	0.74	-0.01	0.72	0.48	0.60	0.76	0.65	0.48
	EC	-0.08	0.71	0.18	-0.38	0.14	0.36	0.34	0.48
	OC	0.58	-0.04	0.69	0.54	0.42	0.71	0.68	0.46
	PK$_{340}$	0.46	-0.30	0.37	0.87	0.11	0.21	0.28	-0.16
	PK$_{500}$	0.54	-0.05	0.66	0.39	0.55	0.68	0.60	0.41
	PK$_{615}$	0.53	0.04	0.66	0.35	0.40	0.78	0.68	0.59
	PK$_{900}$	0.54	0.12	0.68	0.40	0.38	0.75	0.74	0.60
	Pyrol	0.06	0.19	0.26	-0.12	0.04	0.39	0.39	0.66
ALS $PM_{2.5}$	Mass	0.64	0.07	0.51	0.48	0.40	0.49	0.48	0.25
	EC	0.58	0.41	0.57	0.32	0.55	0.50	0.59	0.20
	OC	0.62	-0.02	0.66	0.63	0.51	0.61	0.56	0.32
	PK$_{340}$	0.49	-0.15	0.50	0.77	0.29	0.34	0.45	0.01
	PK$_{500}$	0.53	0.22	0.56	0.23	0.64	0.58	0.42	0.33
	PK$_{615}$	0.54	0.12	0.65	0.42	0.47	0.75	0.59	0.52
	PK$_{900}$	0.49	0.04	0.55	0.60	0.40	0.48	0.49	0.17
	Pyrol	0.51	-0.13	0.48	0.31	0.38	0.51	0.38	0.51
EDI $PM_{2.5}$	Mass	0.21	0.17	0.17	0.14	0.16	0.12	0.19	0.04
	EC	0.49	0.50	0.40	0.23	0.36	0.35	0.46	0.08
	OC	0.38	0.10	0.43	0.46	0.24	0.41	0.41	0.28
	PK$_{340}$	0.28	-0.13	0.27	0.72	0.03	0.10	0.28	-0.15
	PK$_{500}$	0.25	0.33	0.27	-0.16	0.41	0.33	0.19	0.31
	PK$_{615}$	0.29	0.33	0.44	0.10	0.21	0.64	0.48	0.61
	PK$_{900}$	0.27	0.11	0.34	0.43	0.13	0.31	0.34	0.20
	Pyrol	0.30	-0.06	0.30	0.19	0.19	0.34	0.24	0.40
MAP $PM_{2.5}$	Mass	0.51	0.22	0.45	0.34	0.42	0.39	0.42	0.20
	EC	0.37	0.23	0.45	0.24	0.48	0.30	0.46	0.25
	OC	0.59	-0.06	0.62	0.56	0.47	0.55	0.58	0.26
	PK$_{340}$	0.47	-0.13	0.46	0.68	0.24	0.34	0.45	0.04
	PK$_{500}$	0.55	-0.01	0.56	0.29	0.61	0.53	0.50	0.24
	PK$_{615}$	0.59	-0.06	0.62	0.46	0.45	0.65	0.60	0.35
	PK$_{900}$	0.57	-0.06	0.59	0.56	0.42	0.53	0.57	0.26
	Pyrol	0.54	0.05	0.58	0.37	0.45	0.55	0.55	0.50

Compositional correlations followed similar trends at each site, and are summarized for ALS $PM_{10-2.5}$ in Table 6.3. $PM_{10-2.5}$ OC was better correlated with PK_{500}, PK_{615}, and PK_{900} ($\rho > 0.79$) than with PK_{340} and PC ($\rho < 0.69$). Correlations among $PM_{10-2.5}$ peak fractions were also higher for PK_{500}, PK_{615}, and PK_{900} than PK_{340}. A similar trend was observed for $PM_{2.5}$, the dominant peak fractions PK_{340}, PK_{500}, and PK_{900} were more correlated with each other and total OC than PK_{615} and PC. Correlations between $PM_{2.5}$ EC and organic carbon peak fractions were highest at ALS, highlighting the presence of nearby traffic emissions. $PM_{10-2.5}$ EC was generally poorly correlated with other carbon fractions. PC was generally more correlated with PK_{615} and PK_{900} than lower temperature peak fractions, a trend observed for both particulate size fractions.

Interestingly, for comparisons between cities, $PM_{10-2.5}$ PK_{340} stood out as highly correlated ($0.74 < \rho < 0.87$) and PK_{615} and PK_{900} were low to moderately correlated ($0.32 < \rho < 0.78$). $PM_{10-2.5}$ PK_{340} concentrations were also well correlated with $PM_{2.5}$ PK_{340} concentrations in Denver ($0.55 < \rho < 0.77$) and in Greeley ($0.48 < \rho < 0.68$). These results suggest separate sources for $PM_{10-2.5}$ PK_{340} and higher temperature peak fractions in Colorado. Because PK_{340} was homogenous spatially and across size fractions, it was suspected that low molecular weight compounds commonly observed in the fine fraction are also present in coarse mode particulates. Using peak fractions alone, we were unable to identify compounds driving spatial correlation of PK_{340}. Multiple previous studies have identified low molecular weight organic species in $PM_{10-2.5}$. Carboxylic acids and fatty acids were observed in the coarse mode in China during both haze (biomass burning impacted) and non-haze days (Wang et al., 2009; Wang et al., 2011), and Cheung et al. (2012) identified vehicular emission-related organic compounds (PAHs, hopanes, and steranes) in the coarse mode in Los Angeles. PAHs were also measured in considerable concentrations in $PM_{10-2.5}$ in Brazil (Bourotte et al., 2005). Analysis of the water-soluble fraction may shed light on this trend, though characterization of the insoluble fraction may also be required as only 32% of coarse organic matter was water-soluble.

For $PM_{2.5}$, correlations between OC and peak fraction concentrations were generally high ($\rho > 0.70$). Correlations between $PM_{2.5}$ peak fractions were typically higher in Greeley ($0.30 < \rho < 0.90$) than Denver ($-0.12 < \rho < 0.85$). Correlations between $PM_{10-2.5}$ and $PM_{2.5}$ mass concentrations varied widely, ranging from 0.74 and 0.64 at MAP and ALS to 0.33 and 0.34 at EDI and MCA, respectively, and followed no consistent trend. For comparison, low correlations were observed between size fraction mass concentrations using three years of daily monitoring data (Clements et al., 2013b).

6.3.2 Water Soluble Organic Carbon and Total Dissolved Nitrogen

All twelve filter composites listed in the WSOC analysis column of Table 6.S1 were analyzed for WSOC concentrations, TDN concentrations, UV-vis absorbance, and fluorescence. Table 6.4 summarizes the results from these analyses, including mean and standard deviations of $SUVA_{254}$, the fluorescence index (FI), and the humification index (HIX). Averaged across the four monitoring sites, $PM_{2.5}$ and $PM_{10-2.5}$ organic matter was 75% and 32% water soluble, respectively. The highest concentrations of WSOC and the highest contributions of WSOC to total organic carbon were measured at EDI for both fractions, while ALS organic matter was the least water soluble.

Table 6.4 Statistical summary of the WSOC analysis

Size Fraction	Site	Number of Samples	Mean (St.Dev.) WSOC	WSOC/OC	Mean (St.Dev.) TDN	Mean (St.Dev.) $SUVA_{254}$	Mean (St.Dev.) FI	Mean (St.Dev.) HIX	Number of HIX values
		-	($\mu gC/m^3$)	%	($\mu gN/m^3$)	(mgC/L-m)	-	-	-
$PM_{10-2.5}$	ALS	12	0.50 (0.49)	24	0.13 (0.17)	3.9 (2.9)	1.33 (0.06)	0.23 (0.15)	9
	EDI	10	0.46 (0.33)	45	0.11 (0.15)	1.1 (0.7)	1.34 (0.07)	0.20 (0.18)	6
	MAP	11	0.32 (0.24)	28	0.13 (0.16)	2.5 (3.5)	1.32 (0.06)	0.15 (0.05)	5
	MCA	12	0.37 (0.36)	32	0.11 (0.07)	2.5 (2.1)	1.31 (0.07)	0.11 (0.05)	5
$PM_{2.5}$	ALS	12	1.53 (0.59)	66	0.66 (0.59)	3.1 (1.1)	1.42 (0.06)	0.38 (0.11)	12
	EDI	10	1.70 (0.65)	85	0.71 (0.67)	2.2 (1.0)	1.46 (0.07)	0.45 (0.11)	10
	MAP	11	1.29 (0.62)	78	0.69 (0.59)	2.2 (0.8)	1.44 (0.04)	0.38 (0.11)	11
	MCA	12	1.15 (0.42)	70	0.58 (0.35)	2.1 (0.8)	1.42 (0.03)	0.35 (0.12)	12

Time series of WSOC and TDN concentrations are presented in Figure 6.3. Within the coarse fraction, WSOC was not correlated spatially and showed no obvious temporal patterns, though it was fairly well correlated between size fractions at ALS (ρ=0.64) and MAP (ρ=0.69) and moderately correlated for other spatial comparisons across size fractions (Table 6.S4). EDI WSOC was the exception and showed poor correlation for nearly all comparisons. $PM_{2.5}$ WSOC was well correlated within Greeley (ρ=0.74) and between Greeley sites and ALS. WSOC concentrations at ALS in both size fractions increased starting in June and peaked in the second half of October, though no samples were available to analyze from November or December to understand the full extent of this peak. $PM_{2.5}$ and $PM_{10-2.5}$ WSOC concentrations in Greeley also peaked in late October concurrently with ALS. WSOC concentrations were highly variable for both fractions in the spring and early summer. Low correlations with EDI can be partially attributed to missing 2 composite samples, especially for comparisons with the MAP time series which is also missing 1 sample. EDI also exhibited a strong peak in May in both size fractions which did not occur at the other sites. Decreased $PM_{10-2.5}$ WSOC concentrations in winter corresponded to simultaneous reductions in total mass and organic carbon concentrations (Clements et al., 2013b). OC and WSOC were highly correlated in the $PM_{2.5}$ size fraction ($0.80 < \rho < 0.89$) and moderately correlated for the coarse fraction ($0.52 < \rho < 0.68$), except at EDI which was poorly correlated for both size fractions ($\rho < 0.17$). The moderate to high correlation between size fractions for WSOC was surprising and may be related to a common source, but further chemical speciation of this fraction would be required to understand what may be contributing to this relationship.

Figure 6.3 $PM_{10-2.5}$ and $PM_{2.5}$ time series of WSOC and TDN concentrations
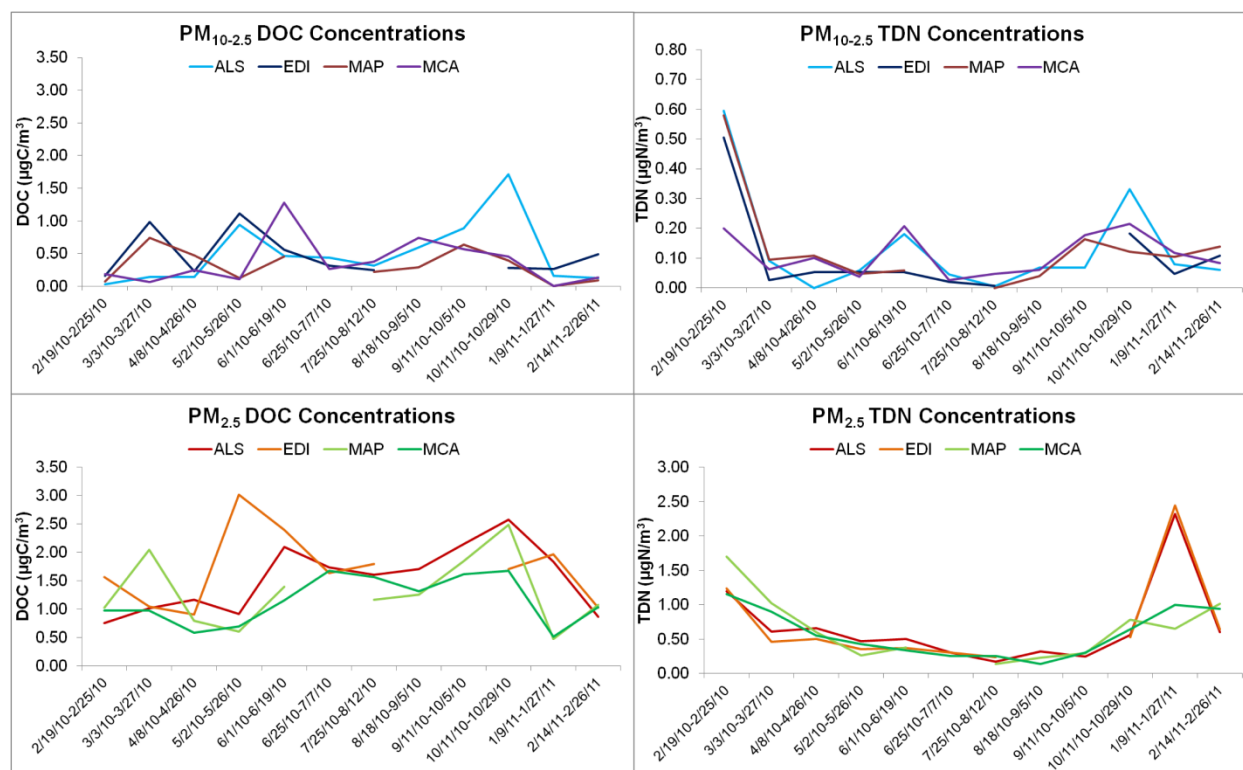
PM$_{2.5}$ contained 5.5 times more dissolvable nitrogen than PM$_{10-2.5}$. Roughly equivalent

concentrations of TDN were measured across all sites for each size fraction. As shown in Figure

6.3 above, dissolvable nitrogen peaked in the winter in both size fractions. PM$_{2.5}$ TDN followed

the same annual trend as nitrate measured in the DASH study (Dutton et al., 2010a). Using the

TOC analyzer for nitrogen quantification, we are unable to separate the influence of ionic nitrate

and ammonium from dissolvable organic nitrogen. Nitrate and ammonium are the dominant

forms of nitrogen found in PM$_{2.5}$ in many urban areas (e.g. Jimenez et al., 2009), and nitrate

contributed significantly to the secondary ionic content of PM$_{10-2.5}$ in urban areas such as Los

Angeles, United States (Cheung et al., 2011), Rio de Janeiro, Brazil (Mariani and Mello, 2007),

and western India (Kumar and Sarin, 2010). Coarse mode nitrate is commonly found in excess

relative to concentrations of ammonium (and the formation of ammonium nitrate), and instead

partitions to the coarse mode via heterogeneous reactions on the surfaces of mineral particles

(Usher et al., 2003). TDN in the coarse mode followed the temporal pattern of the road salt factor determined using PMF on element concentrations in Clements et al. (2013b). The presence of road salts (Mg and Ca) in the winter may increase the amount of heterogeneously reacted nitrate in the coarse mode, as these mineral salts have a higher heterogeneous uptake coefficients than silicon, aluminum, and iron containing minerals (Usher et al., 2003). Spatially, $PM_{10-2.5}$ TDN was well correlated in Colorado (Table 6.S4), with comparisons between ALS, EDI, and MAP ranging from 0.85 to 0.97. Comparisons with MCA were lower ($0.51<\rho<0.69$). Within both cities, $PM_{2.5}$ TDN was highly correlated ($\rho>0.89$), though spatial correlations between cities were reduced.

With ionic nitrogen measurements, the organic nitrogen component could be quantified through subtraction from TDN concentrations (e.g. Zhang et al., 2002). Organic nitrogen may contribute considerable mass to $PM_{2.5}$ TDN concentrations; 18% of fine aerosol in Davis, California was organic nitrogen, which includes such compounds as amino acids, organic nitrates, nitro-aromatics, and humic substances (Zhang et al., 2002). Characterization of the organic nitrogen in fine and coarse aerosols would compliment UV-vis spectroscopy and fluorescence analysis as similar sources have been identified using the three techniques, namely soil dust and biomass burning (Duarte et al., 2005; Jickells et al., 2013). Organic nitrogen characterization may also aide in differentiating rural and urban coarse organic matter, as agriculture-related organic nitrogen compounds could be identified (Jickells et al., 2013).

6.3.3 UV-Vis Spectroscopy

Specific UV-vis absorbance (SUVA), or the UV and visible light absorbance per milligram water-soluble carbon, was calculated for all measured wavelengths (200-800 nm). ALS and MCA $PM_{10-2.5}$ and $PM_{2.5}$ SUVA values for wavelengths ranging from 240 to 400 nm are shown in Figure 6.4 (EDI and MAP are found in Figure 6.S2). SUVA values for both size fractions were comparable at wavelengths below 240 nm, meaning carbon found in both size

fractions was similarly light-absorbing on a per mass basis. WSOC was found in higher

concentrations in $PM_{2.5}$, which lead to fine aerosols absorbing 1.9 times more light at 254 nm.

Below 240 nm, inorganic components, particularly nitrogen containing compounds (i.e. nitrate)

appeared to affect absorbance values as absorbance (and SUVA) values below 240 nm

followed the same temporal pattern as TDN (not shown). $PM_{10-2.5}$ SUVA tended to vary more

sample to sample than for $PM_{2.5}$ and exhibited the lowest and highest SUVA values measured.

Figure 6.4 SUVA values for each composite (C1-C12) for (a) ALS $PM_{10-2.5}$, (b) ALS $PM_{2.5}$, (c) MCA $PM_{10-2.5}$, and (d) MCA $PM_{2.5}$
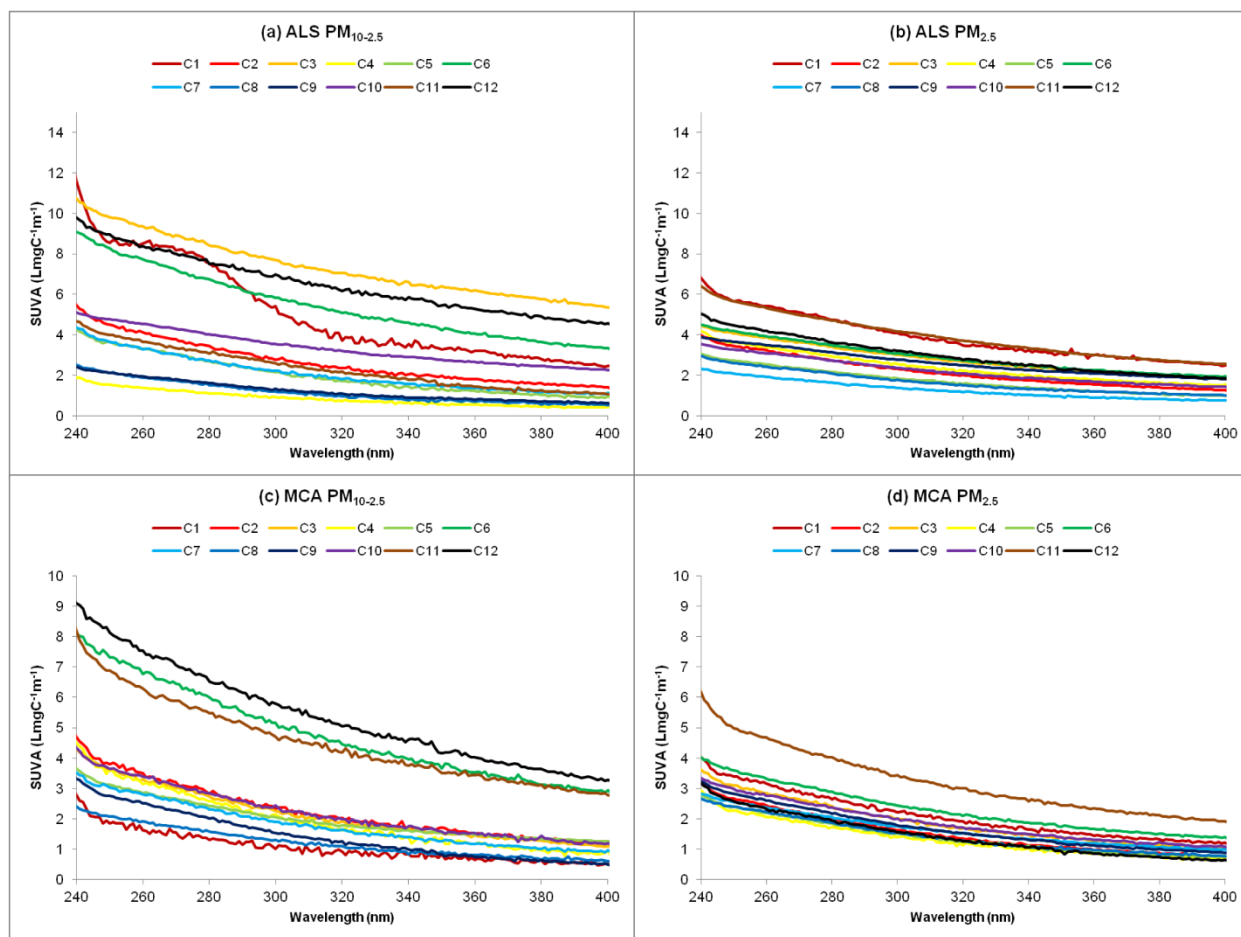
As noted above, $SUVA_{254}$ values are indicative of the aromaticity of organic matter.

Average $SUVA_{254}$ values were similar for both size fractions, suggesting the organic matter of

both size fractions were similarly aromatic. $PM_{10\text{-}2.5}$ $SUVA_{254}$ values were higher than the associated $PM_{2.5}$ $SUVA_{254}$ values at ALS, MAP, and MCA, though differences were not statistically significant. EDI $PM_{10\text{-}2.5}$ $SUVA_{254}$ was statistically significantly lower than ALS $PM_{10\text{-}2.5}$ $SUVA_{254}$ (t-test, $p<0.008$). This signifies that the nature of soil organic matter was different at EDI. EDI is surrounded by neighborhoods with tall deciduous trees, the litter of which may be contributing to the higher percent water soluble carbon and the more aliphatic nature of the organic matter measured at this site. Plant litter is highly soluble and less aromatic than microbially decomposed soil organic matter (Berg, 2000). The highest $SUVA_{254}$ values on average for both size fractions were measured at traffic-influenced ALS. Vehicular emissions of PAHs are likely to contribute to the increase of $PM_{2.5}$ $SUVA_{254}$ at ALS, and may have contributed to the aromaticity of $PM_{10\text{-}2.5}$, as coarse-bound PAHs have been measured in low concentrations at traffic-influenced sites in previous studies (Bourotte et al., 2005; Cheung et al. 2012). ALS $PM_{10\text{-}2.5}$ has been shown to be highly influenced by resuspended particles (Clements et al., 2013b), and soil organic matter can also contribute to high $SUVA_{254}$ values. Average Greeley $PM_{10\text{-}2.5}$ $SUVA_{254}$ values were between those measured at the two sites in Denver and likely reflect $SUVA_{254}$ values typical for resuspended soil organic matter.

For comparison with aquatic natural organic matter, highly aromatic humic acids have $SUVA_{254}$ values around 5 $LmgC^{-1}m^{-1}$, and aromatic-dominant fulvic acids have $SUVA_{254}$ values around 3 $LmgC^{-1}m^{-1}$ (Weishaar et al., 2003). The average $SUVA_{254}$ for EDI $PM_{10\text{-}2.5}$ was 1.1 $LmgC^{-1}m^{-1}$, which is comparable to fulvic acids with the highest aliphatic content reported by Weishaar et al. (2003). ALS $PM_{10\text{-}2.5}$ and $PM_{2.5}$ $SUVA_{254}$ values were comparable to many aromatic-fulvic acids, while rural particulate matter, with $SUVA_{254}$ values from 2.1 to 2.5, was typically less aromatic than aquatic fulvic acids. $SUVA_{254}$ in agricultural soils exhibited the same $SUVA_{254}$ values as those measured in Greeley (2.1-2.5, Marschner et al., 2003), while in a similar study $SUVA_{254}$ values from Utah grassland soil were typically lower, around 1.4 (Van Miegroet et al., 2003).

Baduel et al. (2010) found that PM_{10} HULIS exhibited highly seasonal $SUVA_{250}$, ranging from 2 $LmgC^{-1}m^{-1}$ in summer to above 5 $LmgC^{-1}m^{-1}$ in winter. Correlations between the HULIS fraction and wood burning tracers in winter and oxalic acid in summer lead investigators to suggest seasonal shifts were due to shifting sources, with summertime SOA-influenced HULIS being much less aromatic than wintertime woodsmoke aerosol. In Colorado, $PM_{2.5}$ $SUVA_{254}$ also peaked during the winter (Figure 6.S2), suggesting woodsmoke emissions were affecting both Front Range communities. A summertime increase in $SUVA_{254}$ in both size fractions was measured in composite 6 (6/25-10-7/7/10) at ALS, EDI, and MCA (no data available from MAP composite 6). $PM_{10-2.5}$ $SUVA_{254}$ followed no obvious patterns temporally and peaked at each site during different parts of the year. The highly temporal variable nature of dust emissions likely drives the high temporal variability of $PM_{10-2.5}$ $SUVA_{254}$ values.

6.3.4 Fluorescence Spectroscopy

Presented here is a summary of the indices derived from EEMs for all samples and a qualitative interpretation of EEM spectra. A detailed analysis of the fluorescence spectra, which will include parallel factor (PARAFAC) modeling, is ongoing and will not be the focus of this section. Figures 6.5a, 6.5b, and 6.5d below contain EEMs indicative of typical spectra observed during the CCRUSH campaign for each particulate type. $PM_{10-2.5}$ tended to have peak intensities in the Tryptophan-like (T; I(Ex=275,Em=310)) and Tyrosine-like (B; I(Ex=275,Em=340)) regions (Figure 6.5a), while $PM_{2.5}$ had higher contributions from fulvic-like (A; I(Ex=260,Em=380-460)) and humic-like (C; I(Ex=350,Em=420-480)) regions, as traditionally defined (Coble, 1996). $PM_{2.5}$ contributions from the humic-like region, which can also be indicative of SOA production (Lee et al., 2013), tended to increase during the summer months (Figure 6.5b). During the winter, the C peak was not prevalent and the fulvic peak tended to exhibit a shoulder around 350 nm (Figure 6.5d). Figure 6.5c is an interesting $PM_{10-2.5}$ sample as it exhibits the largest deviation from "typical" $PM_{10-2.5}$ fluorescence. The intensity peak at I(Ex=300,Em=400) in Figure 6.5c was

categorized by Santin et al. (2009) as microbial humic-like, and this is the only sample to peak strongly in this region.

PARAFAC modeling is similar to principle component analysis, and will simplify the large EEM dataset into "source" EEM components that explain much of the variance in sample EEMs. The temporal and spatial variability in these source components will be very useful in further understanding the fluorescent portion of aerosol WSOC.

Figure 6.5 Example EEMs of (a) MAP C10 (10/11/2010-10/29/2010) $PM_{10-2.5}$, (b) MAP C5 (6/1/2010-6/19/2010) $PM_{2.5}$, (c) EDI C12 (2/14/2011-2/26/2011) $PM_{10-2.5}$, and (d) ALS C11 (1/9/2011-1/27/2011) $PM_{2.5}$
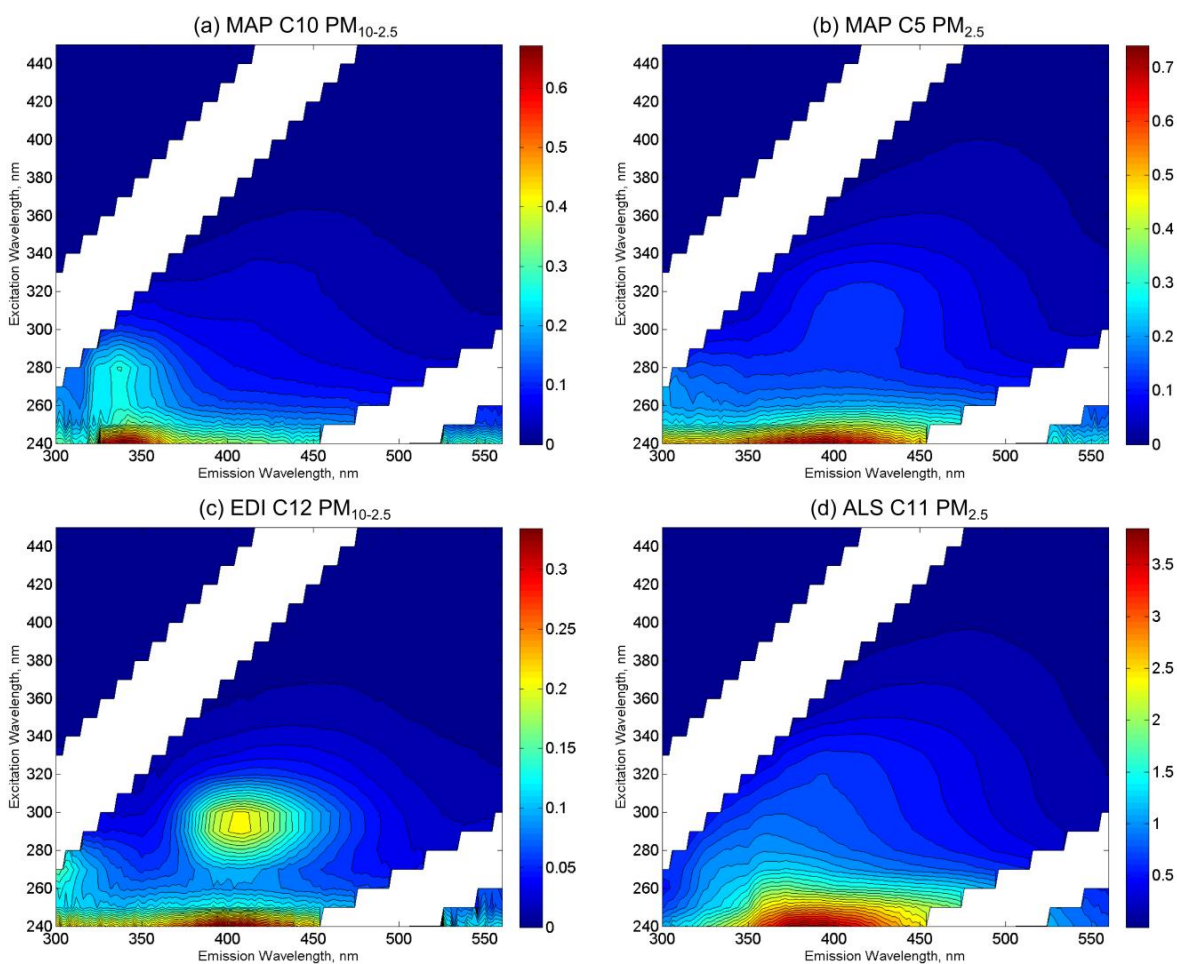
Average $PM_{2.5}$ fluorescence and humification indices (FI, HIX) were higher than the associated $PM_{10-2.5}$ value at all sites, showing that $PM_{10-2.5}$ tended to be more terrestrial, or soil derived, and less humified than $PM_{2.5}$. As Figure 6.6 shows, the fluorescence index did not vary much temporally, and $PM_{10-2.5}$ FIs were consistently lower than the fine fraction. Interestingly, the FI peaked in composite 11 (1/9/11-1/27/11) in both size fractions in Denver, while no peak occurred in Greeley. Low HIX values in the coarse mode were driven by high contributions from the T and B peak regions coupled with low contributions from the A region, whereas the A region was dominant in $PM_{2.5}$ samples. Due to detection limit issues, HIX values were not able to be calculated for three to seven $PM_{10-2.5}$ samples at each site, limiting the interpretability of the index for large particles in this study. $PM_{2.5}$ HIX values were highly seasonal and did not suffer from detection limit issues, peaking around 0.5 in winter and dipping down to around 0.2 in summer, as shown in Figure 6.6. Similar seasonalities were observed for both $SUVA_{254}$ and HIX in the fine mode, meaning as aromaticity increased, likely along with woodsmoke HULIS emissions, fine aerosols appeared more "humified". Winter is also when the organic peak fraction PK_{340} peaked in concentration and mass contribution for both particulate size fractions, and further investigations should be performed to understand the impact of woodsmoke burning on both $PM_{2.5}$ and $PM_{10-2.5}$ organic concentrations.

Figure 6.6 (a) $PM_{10-2.5}$ and $PM_{2.5}$ fluorescence indices time series, and (b) $PM_{2.5}$ humification index time series (C=$PM_{10-2.5}$, F = $PM_{2.5}$)
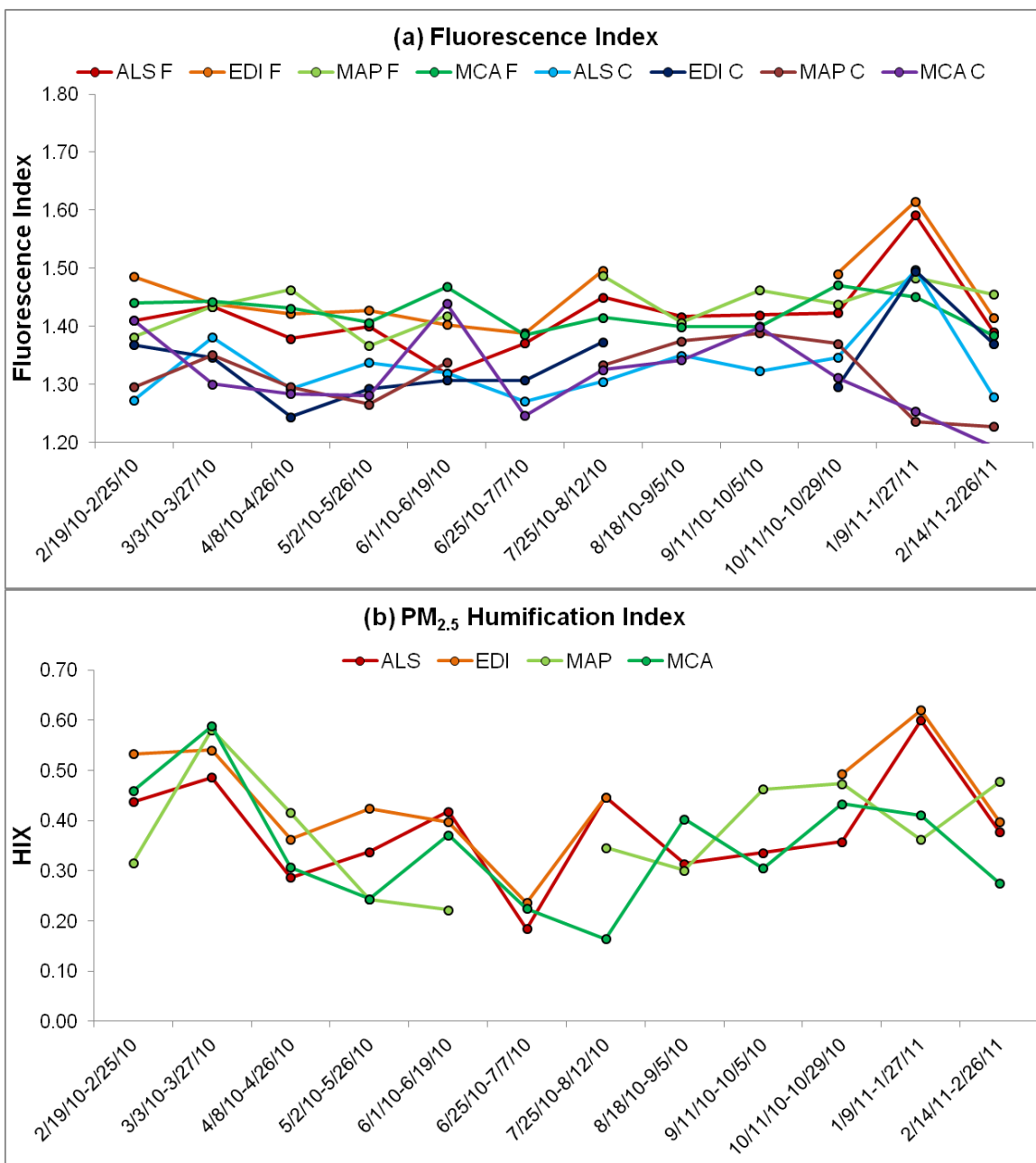
6.3.5 Endotoxin Concentrations

Twelve composite filter sets (Table 6.S1) were analyzed for endotoxin content for each

particulate size fraction and monitoring site. Substantially higher endotoxin concentrations were

observed in Greeley compared to Denver and in the coarse fraction compared to the fine

fraction. Average (±st. dev.) $PM_{10-2.5}$ and $PM_{2.5}$ endotoxin concentrations in Greeley were

2.45 ± 2.73 EU/m^3 and 0.80 ± 1.71 EU/m^3, respectively. $PM_{2.5}$ endotoxin concentrations were often

below detection limit except during summer/fall when endotoxin concentrations tended to

increase in general. For example, all $PM_{2.5}$ endotoxin data at EDI was below detection limit and

only composites C4, C7, and C8 at ALS were above the MDL. $PM_{10-2.5}$ endotoxin concentrations

in Denver averaged (±st.dev.) 0.60 ± 0.51 EU/m^3. Figure 6.7 shows the distinct seasonal trend

observed in $PM_{10-2.5}$ endotoxin concentrations, peaking in the C7 sample in Greeley (9/5/2010-

9/17/2010). Smaller springtime peaks in endotoxin concentrations were also observed in

Greeley, though in different samples at each site. $PM_{2.5}$ endotoxin concentrations also peaked in

sample C7 in Greeley. Denver $PM_{10-2.5}$ endotoxin concentrations were similar to those

measured in PM_{10} from the urban Los Angeles, California area, and Greeley endotoxin

concentrations were comparable in concentrations and followed the same seasonal pattern as

rural sites from the same study in California (Mueller-Anneling et al., 2004). In two previous

studies, elevated concentrations of endotoxin in the coarse mode relative to the fine were

measured in the Pearl River Delta, China (Cheng et al., 2012) and in two small towns, Hettstedt

and Zerbst, in Germany (Heinrich et al., 2003).

The September peak in endotoxin concentrations occurred simultaneously with a peak in

$PM_{10-2.5}$ mass concentrations and corresponds to when cow fecal bacteria contribute

substantially to the bacterial diversity measured on the same filter set (Clements et al., 2013b;

Bowers et al., 2013). In two recent studies near dairy operations in southern Idaho, endotoxin

concentrations were elevated in total suspended particulates (TSP, <100 µm) downwind of the

dairy operation (Dungan and Leytem, 2009; Dungan et al., 2010). Manure particles were the

dominant PM_{10} particle type emitted from a cattle feedlot in Kansas, identified via Raman

microscopy (Huang et al., 2012). Regional agricultural activity and manure emissions from two

local feedlots are likely contributors to elevated endotoxin levels in Greeley that are not present

in Denver.

Figure 6.7 Time series of endotoxin concentrations measured at the four monitoring sites for (a) $PM_{10-2.5}$ and (b) $PM_{2.5}$
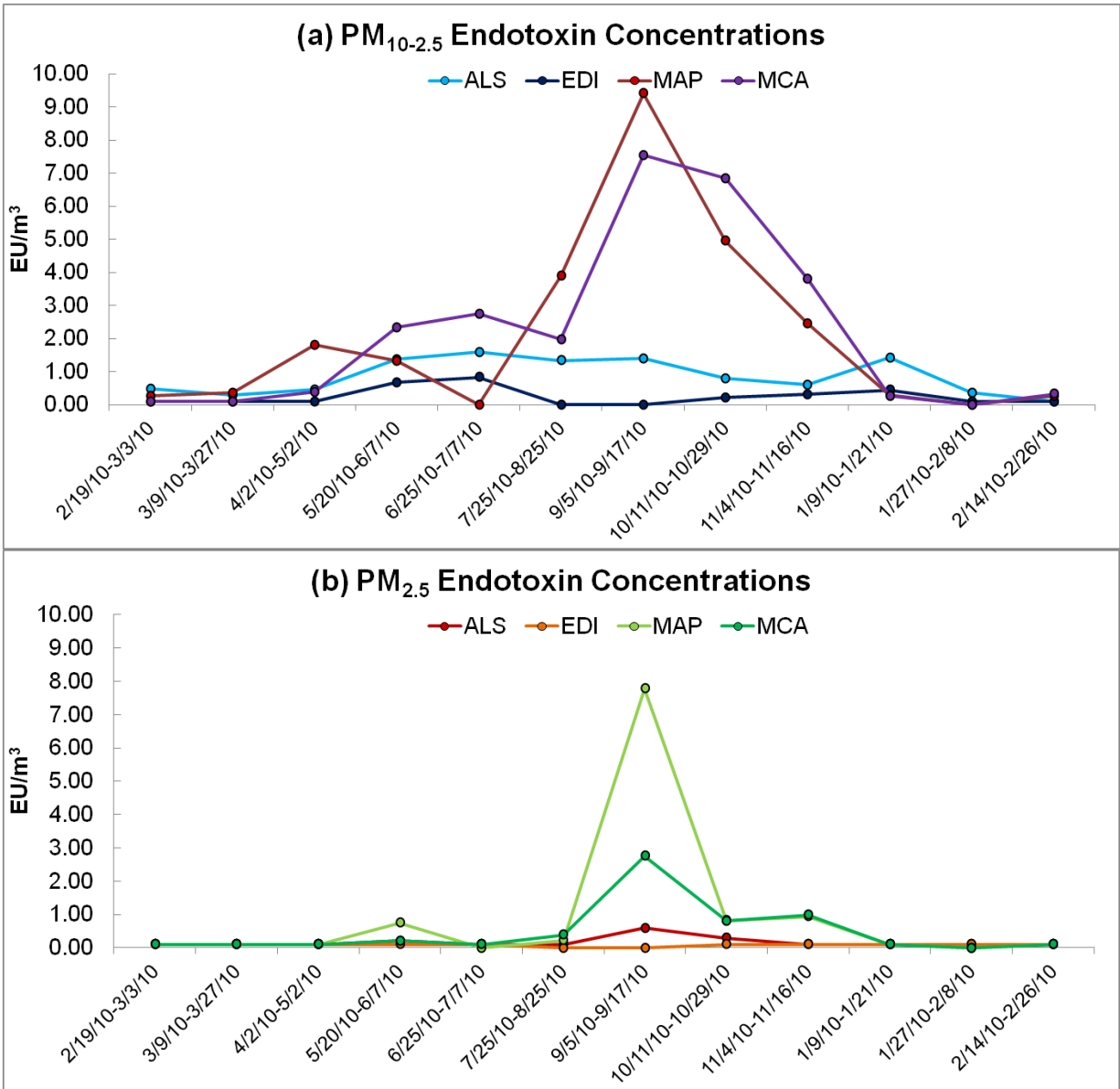
6.4 CONCLUSIONS

In this study, we utilized multiple bulk characterization methods to understand differences in organic matter composition and chemical characteristics between $PM_{10-2.5}$ and $PM_{2.5}$ in urban and rural environments. Organic matter constituted an estimated 39% and 58% of the $PM_{10-2.5}$ and $PM_{2.5}$ mass on average, assuming an OM:OC ratio of 1.8 for both size classes. $PM_{10-2.5}$ and $PM_{2.5}$ organic carbon was 32% and 75% water-soluble, respectively. $PM_{2.5}$ was mainly contributed to by organic carbon that volatilized at low temperatures (<500°C), while contributions from high temperature organic peak fractions were dominant in the coarse fraction. High spatial correlations were observed for the $PM_{10-2.5}$ low volatilization temperature organic carbon (PK_{340}) time series and PK_{340} concentrations were correlated across size fractions, likely due to a common source and/or partitioning effects. The highest $SUVA_{254}$ values were measured at a traffic-influenced site, suggesting vehicular emissions increase the aromaticity of both $PM_{10-2.5}$ and $PM_{2.5}$ organic matter. $PM_{10-2.5}$ $SUVA_{254}$ values in Greeley were similar to values measured in agricultural soils and fell between values measured at the two monitoring sites in Denver. The residential site in Denver exhibited the lowest $PM_{10-2.5}$ $SUVA_{254}$ values but the highest percent water soluble carbon, suggesting highly soluble and aliphatic plant litter is contributing to the water soluble fraction at this site. $PM_{2.5}$ fluorescence peaked in the fulvic and humic-like regions, while $PM_{10-2.5}$ peaked in the tryptophan and tyrosine-like regions, suggesting biological particles are the most important fluorescent component of $PM_{10-2.5}$. The lack of a humic or fulvic-like peak in coarse samples is somewhat at odds with the high $SUVA_{254}$ values measured in this fraction as it is likely that much of the $PM_{10-2.5}$ aromaticity was from eroded soil organic matter. Organo-mineral complexing of humic substances can quench the fluorescence in the humic and fulvic-like regions, and may explain the lack of fluorescence in these regions for $PM_{10-2.5}$ samples (Ohno et al., 2008) In the $PM_{2.5}$ fraction, HIX and $SUVA_{254}$ values peaked in the winter, a trend likely influenced by residential woodsmoke emissions. Endotoxin

concentrations were significantly elevated in Greeley, particularly in the coarse fraction, a trend

attributed to nearby cattle feedlot and agricultural emissions.

6.5 ACKNOWLEDGEMENTS

6.6 REFERENCES

Baduel, C., Voisin, D., Jaffrezo, J.L. 2009. Comparison of analytical methods for Humic Like Substance (HULIS) measurements in atmospheric particles. Atmospheric Chemistry and Physics 9, 5949-5962.

Baduel, C., Voisin, D., Jaffrezo, J.-L. 2010. Seasonal variations of concentrations and optical properties of water soluble HULIS collected in urban environments. Atmospheric Chemistry and Physics 10, 4085-4095.

Bourotte, C., Forti, M.-C., Taniguchi, S., Bicego, M.C., Lotufo, P.A. 2005. A wintertime study of PAHs in fine and coarse aerosols in Sao Paulo city, Brazil. Atmospheric Environment 39, 3799-3811.

Bowers, R.M., Clements, N., Emerson, J.B., Wiedinmyer, C., Hannigan, M.P., Fierer, N. 2013. Seasonal Variability in Bacterial and Fungal Diversity of the Near-Surface Atmosphere. Environmental Science and Technology, Article ASAP.

Brook, R.D., Bard, R.L., Kaplan, M.J., Yalavarthi, S., Morishita, M., Dvonch, J.T., Wang, L., Yang, H.-Y., Spino, C., Mukherjee, B., Oral, E.A., Sun, Q., Brook, J.R., Harkema, J., Rajagopalan, S. 2013. The effect of acute exposure to coarse particulate matter air pollution in a rural location on circulating endothelial progenitor cells: results from a randomized controlled study. Inhalation Toxicology 25(10), 587-592.

Chen, J., LeBoeuf, E.J., Dai, S., Gu, B. 2003. Fluorescence spectroscopic studies of natural organic matter fractions. Chemosphere 50, 639-647.

Cheng, J.Y.W., Hui, E.L.C., Lau, A.P.S. Bioactive and total endotoxins in atmospheric aerosols in the Pearl River Delta region, China. Atmospheric Environment 47, 3-11.

Cheung, K., Daher, N., Kam, W., Shafer, M.M., Ning, Z., Schauer, J.J., Sioutas, C. 2011. Spatial and temporal variation of chemical composition and mass closure of ambient coarse

particulate matter (PM$_{10-2.5}$) in the Los Angeles area. Atmospheric Environment 45, 2651-2662.

Cheung K., Olson, M.R., Shelton, B., Schauer, J.J., Sioutas, C. 2012. Seasonal and spatial variations of individual organic compounds of coarse particulate matter in the Los Angeles Basin. Atmospheric Environment 59, 1-10.

Clements, N., Piedrahita, R., Ortega, J., Peel, J.L., Hannigan, M.P., Miller, S.L., Milford, J.B. 2012. Characterization and Nonparametric Regression of Rural and Urban Coarse Particulate Matter Mass Concentrations in Northeastern Colorado. Aerosol Science and Technology 46(1), 108-123.

Clements, N., Eav, J., Xie, M., Hannigan, M.P., Miller, S.L., Navidi, W., Peel, J.L., Schauer, J.J., Shafer, M.M., Milford, J.B. 2013. Concentrations and Source Insights for Trace Elements in Fine and Coarse Particulate Matter in Northeastern Colorado. Atmospheric Environment. *In review.*

Clements, N., Milford, J.B., Miller, S.L., Peel, J.L., Hannigan, M.P. 2013. Spatiotemporal and Meteorological Trends of Total and Semivolatile PM$_{10-2.5}$ and PM$_{2.5}$ Mass Concentratons in Northeastern Colorado. *In prep.*

Coble, P.G. 1996. Characterization of marine and terrestrial DOM in seawater using excitation-emission matrix spectroscopy. Marine Chemistry 51, 325-346.

Degobbi, C., Hilario, P., Saldiva, N., Rogers, C. 2011. Endotoxin as modifier of particulate matter toxicity: a review of the literature. Aerobiologia 27, 97-105.

Duarte, R.M.B.O., Pio, C.A., Duarte, A.C. 2005. Spectroscopic study of the water-soluble organic matter isolated from atmospheric aerosols collected under different atmospheric conditions. Analytica Chimica Acta 530, 7-14.

Duarte, R.M.B.O., Santos, E.B.H., Pio, C.A., Duarte, A.C. 2007. Comparison of structural features of water-soluble organic matter from atmospheric aerosols with those of aquatic humic substances. Atmospheric Environment 41, 8100-8113.

Duarte, R.M.B.O., Silva, A.M.S., Duarte, A.C. 2008. Two-Dimensional NMR studies of Water-Soluble Organic Matter in Atmospheric Aerosols. Environmental Science and Technology 42, 8224-8230.

Dungan, R.S., Leytem, A.B. 2009. Airborne Endotoxin Concentrations at a Large Open-Lot Dairy in Southern Idaho. Journal of Environmental Quality 38, 1919-1923.

Dungan, R.S., Leytem, A.B., Bjorneberg, D.B. 2010. Year-long assessment of airborne endotoxin at a concentrated dairy operation. Aerobiologia 26, 141-148.

Dutton, S.J., Williams, D.E., Garcia, J.K., Vedal, S., Hannigan, M.P. 2009. $PM_{2.5}$ characterization for time series studies: Organic molecular marker speciation methods and observations from daily measurements in Denver. Atmospheric Environment 43, 2018-2030.

Dutton, S.J., Schauer, J.J., Vedal, S., Hannigan, M.P. 2009. $PM_{2.5}$ characterization for time series studies: Pointwise uncertainty estimation and bulk speciation methods applied in Denver. Atmospheric Environment 43, 1136-1146.

Dutton, S.J., Rajagopalan, B., Vedal, S., Hannigan, M.P. 2010. Temporal patterns in daily measurements of inorganic and organic speciated $PM_{2.5}$ in Denver. Atmospheric Environment 44, 987-998.

Dutton, S.J., Vedal, S., Piedrahita, R., Milford, J.B., Miller, S.L., Hannigan, M.P. 2010. Source apportionment using positive matrix factorization on daily measurements of inorganic and organic speciated $PM_{2.5}$. Atmospheric Environment 44, 2731-2741.

Fast, J., Aiken, A.C., Allan, J., Alexander, L., Campos, T., Canagaratna, M.R., Chapman, E., DeCarlo, P.F., de Foy, B., Gaffney, J., de Gouw, J., Doran, J.C., Emmons, L., Hodzic, A., Herndon, S.C., Huey, G., Jayne, J.T., Jimenez, J.L., Kleinman, L., Kuster, W., Marley, N., Russell, L., Ochoa, C., Onasch, T.B., Pekour, M., Song, C., Ulbrich, I.M., Warneke, C., Welsh-Bon, D., Wiedinmyer, C., Worsnop, D.R., Yu, X.-Y., Zaveri, R. 2009. Evaluating simulated primary anthropogenic and biomass burning organic

aerosols during MILAGRO: implications for assessing treatments of secondary organic aerosols. Atmospheric Chemistry and Physics 9, 6191-6215.

Feczko, T., Puxbaum, H., Kasper-Giebl, A., Handler, M., Limbeck, A., Gelencser, A., Pio, C., Preunkert, S., Legrand, M. 2007. Determination of water and alkaline extractable atmospheric humic-like substances with the TU Vienna HULIS analyzer in samples from six background sites in Europe. Journal of Geophysical Research 112, D23S10.

Forster, P., Ramaswamy V., Artaxo P., Berntsen T., Betts R., Fahey D.W., Haywood J., Lean J., Lowe D.C., Myhre G., Nganga J., Prinn R., Raga G., Schulz M., Van Dorland R. 2007. Changes in Atmospheric Constituents and in Radiative Forcing. In: Climate Change 2007: The Physical Science Basis. Contribution of Working Group I to the Fourth Assessment Report of the Intergovernmental Panel on Climate Change [Solomon, S., D. Qin, M. Manning, Z. Chen, M. Marquis, K.B. Averyt, M.Tignor and H.L. Miller (eds.)]. Cambridge University Press, Cambridge, United Kingdom and New York, NY, USA.

Graham, B., Mayol-Bracero, O.L., Guyon, P., Roberts, G.C., Decesari, S., Facchini, M.C., Artaxo, P., Maenhaut, W., Koll, P., Andreae M.O. 2002. Water-soluble organic compounds in biomass burning aerosols over Amazonia: 1. Characterization by NMR and GC-MS. Journal of Geophysical Research 107, D20 8047.

Haagenson, P.L. 1979. Meteorological and Climatological Factors Affecting Denver Air Quality. Atmospheric Environment 13, 79-85.

Hegde, P., Kawamura, K. 2012. Seasonal variations of water-soluble organic carbon, dicarboxylic acids, ketocarboxylic acids, and α-dicarbonyls in Central Himalayan aerosols. Atmospheric Chemistry and Physics 12, 6645-6665.

Heinrich, J., Pitz, M., Bischof, W., Krug, N., Borm, P.J.A. 2003. Endotoxin in fine ($PM_{2.5}$) and coarse ($PM_{2.5-10}$) particles mass of ambient aerosols. A temporo-spatial analysis. Atmospheric Environment 37, 3659-3667.

Huang, X.-F., Yu, J.Z., He, L.-Y., Yuan, Z. 2006. Water-soluble organic carbon and oxalate in aerosols at a coastal urban site in China: Size distribution characteristics, sources, and formation mechanisms. Journal of Geophysical Research 111, D22212.

Huang, Q., McConnell, L.L., Razote, E., Schmidt, W.F., Vinyard, B.T., Torrents, A., Hapeman, C.J., Maghirang, R., Trabue, S.L., Prueger, J., Ro, K.S. 2013. Utilizing single particle Raman microscopy as a non-destructive method to identify sources of PM_{10} from cattle feedlot operations. Atmospheric Environment 66, 17-24.

Hwang, I., Hopke, P.K., Pinto, J.P. 2008. Source Apportionment and Spatial Distributions of Coarse Particles During the Regional Air Pollution Study. Environmental Science and Technology 42, 3524-3530.

JBS Five Rivers Cattle Feeding. 2013. www.fiveriverscattle.com. Accessed 10/22/2013.

Jia, Y., Bhat, S., Fraser, M.P. 2010. Characterization of saccharides and other organic compounds in fine particles and the use of saccharides to track primary biologically derived carbon sources. Atmospheric Environment 44, 724-732.

Jickells, T., Baker, A.R., Cape, J.N., Nemitz, E. 2013. The cycling of organic nitrogen through the atmosphere. Philosophical Transactions of the Royal Society B 368, 20130115.

Jimenez, J.L., Canagaratna, M.R., Donahue, N.M., Prevot, A.S.H., Zhang, Q., Kroll, J.H., DeCarlo, P.F., Allan, J.D., Coe, H., Ng, N.L., Airken, A.C., Docherty, K.S., Ulbrich, I.M., Grieshop, A.P., Robinson, A.L., Duplissy, J., Smith, J.D., Wilson, K.R., Lanz, V.A., Hueglin, C., Sun, Y.L., Tian, J., Laaksonen, A., Raatikainen, T., Rautiainen, J., Vaattovaara, P., Ehn, M., Kulmala, M., Tomlinson, J.M., Collins, D.R., Cubison, M.J., Dunlea, E.J., Huffman, J.A., Onasch, T.B., Alfarra, M.R., Williams, P.I., Bower, K., Kondo, Y., Schneider, J., Drewnick, F., Borrmann, S., Weimer, S., Demerjian, K., Salcedo, D., Cottrell, L., Griffin, R., Takami, A., Miyoshi, T., Hatakeyama, S., Shimono, A., Sun, J.Y., Zhang, Y.M., Dzepina, K., Kimmel, J.R., Sueper, D., Jayne, J.T., Herndon, S.C., Trimborn, A.M., Williams, L.R., Wood, E.C., Middlebrook, A.M., Kolb, C.E.,

Baltensperger, U., Worsnop, D.R. 2009. Evolution of Organic Aerosols in the Atmosphere. Science 326, 1525-1529.

Krivacsy, Z., Gelencser, A., Kiss, G., Meszaros, E., Molnar, A., Hoffer, A., Meszaros, T., Sarvari, Z., Temesi, D., Varga, B., Baltensperger, U., Nyeki, S., Weingartner, E. 2001. Study on the Chemical Character of Water Soluble Organic Compounds in Fine Atmospheric Aerosol at the Jungfraujoch. Journal of Atmospheric Chemistry 39, 235-259.

Kumar, A., Sarin, M.M. 2010. Atmospheric water-soluble constituents in fine and coarse mode aerosols from high-altitude site in western India: Long-range transport and seasonal variability. Atmospheric Environment 44, 1245-1254.

Kumar, P., Hopke, P.K., Raja, S., Casuccio, G., Lersch, T.L., West, R.R. 2012. Characterization and heterogeneity of coarse particles across as urban area. Atmospheric Environment 46, 449-459.

Lagudu, U.R.K., Raja, S., Hopke, P.K., Chalupa, D.C., Utell, M.J., Casuccio, G., Lersch, T.L., West, R.R. 2011. Heterogeneity of Coarse Particles in an Urban Area. Environmental Science and Technology 45, 3288-3296.

Lee, H.J., Laskin, A., Laskin, J., Nizkorodov, S.A. 2013. Excitation-Emission Spectra and Fluorescence Quantum Yields for Fresh and Ages Biogenic Secondary Organic Aerosols. Environmental Science and Technology 47, 5763-5770.

Lin, P., Huang, X.-F., He, L.-Y., Zu, J.Z. 2010. Abundance and size distribution of HULIS in ambient aerosols at a rural site in South China. Journal of Aerosol Science 41, 74-87.

Lin, P., Rincon, A.G., Kalberer, M., Yu, J.Z. 2012. Elemental Composition of HULIS in the Pearl River Delta Region, China: Results Inferred from Positive and Negative Electrospray High Resolution Mass Spectrometric Data. Environmental Science and Technology 46, 7454-7462.

Malm, W.C., Pitchford, M.L., McDade, C., Ashbaugh, L.L. 2007. Coarse particle speciation at selected locations in the rural continental United States. Atmospheric Environment 41, 2225-2239.

Mariani, R.L., de Mello, W.Z. 2007. $PM_{2.5-10}$, $PM_{2.5}$, and associated water-soluble inorganic species at a coastal urban site in the metropolitan region of Rio de Janeiro. Atmospheric Environment 41, 2887-2892.

Marschner, P., Kandeler, E., Marschner, B. 2003. Structure and function of the soil microbial community in a long-term fertilizer experiment. Soil Biology and Biochemistry 35, 453-461.

Mayol-Bracero, O.L., Guyon, P., Graham, B., Roberts, G., Andreae, M.O., Decesari, S., Facchini, M.C., Fuzzi, S., Artaxo, P. 2002. Water-soluble organic compounds in biomass burning aerosols over Amazonia: 2. Apportionment of the chemical composition and importance of the polyacidic fraction. Journal of Geophysical Research 107, D20 8091.

Misra, C., Geller, M.D., Shah, P., Sioutas, C., Solomon, P.A. 2001. Development and Evaluation of a Continuous Coarse (PM_{10}-$PM_{2.5}$) Particle Monitor. Journal of the Air and Waste Management Association 51(9), 1309-1317.

Misra, C., Geller, M.D., Sioutas, C., Solomon, P.A. 2003. Development and Evaluation of a PM_{10} Impactor-Inlet for a Continuous Coarse Particle Monitor. Aerosol Science and Technology 37, 271-281.

Moreno T., Querol, X., Alastuey, A., Reche, C., Cusack, M., Amato, F., Pandolfi, F., Pey, J., Richard, A., Prevot, A.S.H., Furger, M., Gibbons, W. 2011. Variations in time and space of trace metal aerosol concentrations in urban areas and their surroundings. Atmospheric Chemistry and Physics 11, 9415-9430.

Mueller-Anneling, L., Avol, E., Peters, J.M., Thorne, P.S. 2004. Ambient Endotoxin
Concentrations in PM_{10} from Southern California. Environmental Health Perspectives
112, 583-588.

Ohno, T. 2002. Fluorescence Inner-Filtering Correction for Determining the Humification Index
of Dissolved Organic Matter. Environmental Science and Technology 36, 742-746.

Ohno, T., Amirbahman, A., Bro, R. 2008. Parallel Factor Analysis of Excitation-Emission Matrix
Fluorescence Spectra of Water Soluble Soil Organic Matter as Basis for the
Determination of Conditional Metal Binding Parameters. Environmental Science and
Technology 42, 186-192.

Pakbin, P., Ning, Z., Shafer, M.M., Schauer, J.J., Sioutas, C. 2011. Seasonal and Spatial
Coarse Particle Elemental Concentrations in the Los Angeles Area. Aerosol Science and
Technology 45(8), 949-963.

Puxbaum, H., Tenze-Kunit, M. 2003. Size distribution and seasonal variation of atmospheric
cellulose. Atmospheric Environment 37, 3693-3699.

Santin, C., Yamashita, Y., Otero, X.L., Alvarez, M.A., Jaffe, R. 2009. Characterizing humic
substances from estuarine soils and sediments by excitation-emission matrix
spectroscopy and parallel factor analysis. Biogeochemistry 96, 131-147.

Seinfeld, J.H., Spyros, P.N., 2006. Atmospheric Chemistry and Physics - From Air Pollution to
Climate Change, 2nd Edition, John Wily & Sons.

Stone, E.A., Yoon, S.-C., Schauer, J.J. 2011. Chemical Characterization of Fine and Coarse
Particles in Gosan, Korea during Springtime Dust Events. Aerosol and Air Quality
Research 11, 31-43.

Sullivan, A.P., Weber, R.J. 2006. Chemical characterization of ambient organic aerosol soluble
in water: 2. Isolation of acid, neutral, and basic fractions by modified size-exclusion
chromatography. Journal of Geophysical Research 111, D05315.

Weishaar, J.L., Aiken, G.R., Bergamaschi, B.A., Fram, M.S., Fujii, R., Mopper, K. 2003. Evaluation of Specific Ultraviolet Absorbance as an Indicator of the Chemical Composition and Reactivity of Dissolved Organic Carbon. Environmental Science and Technology 37, 4702-4708.

US Bureau of the Census. 2012. *Annual Estimates of the Resident Population for Counties of Colorado: April 1, 2010 to July 1, 2011*. Prepared by the United States Census Bureau, Population Division. http://www.census.gov/popest/data/counties/totals/2011/tables/CO-EST2011-01-08.csv.

US Department of Agriculture. 2007. Census of Agriculture: 2007 Census Volume 1, Chapter 2: County Level Data for Colorado.

US EPA. 2004. US EPA Air Quality Criteria for Particulate Matter (Final Report, Oct, 2004). US Environmental Protection Agency, Washington, DC, EPA 600/P-99/002aF-bF.

US EPA. 2006. 40 CFR Part 50: National Ambient Air Quality Standards for Particulate Matter, Vol. 71 No. 200.

Usher, C.R., Michel, A.E., Grassian, V.H. 2003. Reactions on Mineral Dust. Chemical Reviews 103, 4883-4939.

Van Miegroet, H., Boettinger, J.L., Baker, M.A., Nielsen, J., Evens, D., Stum, A. 2005. Soil carbon distribution and quality in a montane rangeland-forest mosaic in northern Utah. Forest Ecology and Management 220, 284-299.

Wang, X.-R., Zhang, H.-X., Sun, B.-X., Dai, H.-L., Hang, J.-Q., Eisen, E.A., Wegman, D.H., Olenchock, S.A., Christiani, D.C. 2005. A 20-year follow-up study on chronic respiratory effects of exposure to cotton dust. European Respiratory Journal 26(5), 881-886.

Wang, G., Kawamura, K., Xie, M., Hu, S., Cao, J., An, Z., Waston, J.G., Chow, J.C. 2009. Organic Molecular Compositions and Size Distributions of Chinese Summer and Autumn Aerosols from Nanjing: Characteristic Haze Event Caused by Wheat Straw Burning. Environmental Science and Technology 43, 6493-6499.

Wang, G., Chen, C., Li, J., Zhou, B., Xie, M., Hu, S., Kawamura, K., Chen, Y. 2011. Molecular composition and size distribution of sugars, sugar-alcohols and carboxylic acids in airborne particles during a severe urban haze event caused by wheat straw burning. Atmospheric Environment 45, 2473-2479.

Xie, M., Piedrahita, R., Dutton, S.J., Milford, J.B., Hemann, J.G., Peel, J., Miller, S.L., Kim, S.-Y., Vedal, S., Sheppard, L., Hannigan, M.P. 2013. Positive matrix factorization of a 32-month series of daily $PM_{2.5}$ speciation data with incorporation of temperature stratification. Atmospheric Environment 65, 11-20.

Zhang, Q., Anastasio, C., Jimenez-Cruz, M. 2002. Water-soluble organic nitrogen in atmospheric fine particles ($PM_{2.5}$) from northern California. Journal of Geophysical Research 107, D11.

Zhang, X., Liu, Z., Hecobian, A., Zheng, M., Frank, N.H., Edgerton, E.S., Weber, R.J. 2012. Spatial and seasonal variations of fine particle water-soluble organic carbon (WSOC) over the southeastern United States: implications for secondary organic aerosol formation. Atmospheric Chemistry and Physics 12, 6593-6607.

Zaveri, R.A., Shaw, W.J., Cziczo, D.J., Schmid, B., Ferrare, R.A., Alexander, M.L., Alexandrov, M., Alvarez, R.J., Arnott, W.P., Atkinson, D.B., Baidar, S., Banta, R.M., Barnard, J.C., Beranek, J., Berg, L.K., Brechtel, F., Brewer, W.A., Cahill, J.F., Cairns, B., Cappa, C.D., Chand, D., China, S., Comstock, J.M., Dubey, M.K., Easter, R.C., Erickson, M.H., Fast, J.D., Floerchinger, C., Flowers, B.A., Fortner, E., Gaffney, J.S., Gilles, M.K., Gorkowski, K., Gustafson, W.I., Gyawali, M., Hair, J., Hardesty, R.M., Harworth, J.W., Herndon, S., Hiranuma, N., Hostetler, C., Hubbe, J.M., Jayne, J.T., Jeong, H., Jobson, B.T., Kassianov, E.I., Kleinman, L.I., Kluzek, C., Knighton, B., Kolesar, K.R., Kuang, C., Kubatova, A., Langford, A.O., Laskin, A., Laulainen, N., Marchbanks, R.D., Mazzoleni, C., Mei, F., Moffet, R.C., Nelson, D., Obland, M.D., Oetjen, H., Onasch, T.B., Ortega, I., Ottaviani, M., Pekour, M., Prather, K.A., Radney, J.G., Rogers, R.R., Sandberg, S.P.,

Sedlacek, A., Senff, C.J., Senum, G., Setyan, A., Shilling, J.E., Shrivastava, M., Song, C., Springston, S.R., Subramanian, R., Suski, K., Tomlinson, J., Volkamer, R., Wallace, H.W., Wang, J., Weickmann, A.M., Worsnop, D.R., Yu, X.-Y., Zelenyuk, A., Zhang, Q. 2012. Overview of the 2010 Carbonaceous Aerosols and Radiative Effects Study (CARES). Atmospheric Chemistry and Physics 12, 7647-7687.

Table 6.S1 List of collected filters/composite sets of filters and analyses conducted

Sampling Date	Mass ALS	Mass EDI	Mass MAP	Mass MCA	Elements ALS	Elements EDI	Elements MAP	Elements MCA	EC/OC ALS	EC/OC EDI	EC/OC MAP	EC/OC MCA	WSOC ALS	WSOC EDI	WSOC MAP	WSOC MCA	Endotoxin ALS	Endotoxin EDI	Endotoxin MAP	Endotoxin MCA
2/19/2010					C1	C1	C1	C1					C1	C1	C1	C1	C1	C1	C1	C1
2/25/2010																				
3/3/2010							C2	C2					C2	C2	C2	C2				
3/9/2010					C2	C2											C2	C2	C2	C2
3/15/2010																				
3/21/2010					C2	C2	C2	C2					C2	C2	C2	C2	C2	C2	C2	C2
3/27/2010																				
4/2/2010																				
4/8/2010					C3	C3	C3	C3					C3	C3	C3	C3	C3	C3	C3	C3
4/14/2010																				
4/20/2010																				
4/26/2010																				
5/2/2010													C4	C4	C4	C4				
5/8/2010							C4	C4												
5/14/2010																				
5/20/2010													C4	C4	C4	C4	C4	C4	C4	C4
5/26/2010																				
6/1/2010													C5	C5	C5	C5	C4	C4	C4	C4
6/7/2010						C5														
6/13/2010																				
6/19/2010													C5	C5	C5	C5				
6/25/2010																				
7/1/2010													C6	C6		C6	C5	C5		C5
7/7/2010					C6	C6		C6												
7/13/2010																				
7/19/2010																				
7/25/2010																	C6	C6	C6	C6
7/31/2010					C7	C7	C7	C7					C7	C7	C7	C7				
8/6/2010																				
8/12/2010																				
8/18/2010					C8		C8	C8					C8		C8	C8	C6	C6	C6	C6
8/24/2010																				
8/30/2010																				
9/5/2010													C8		C8	C8				
9/11/2010					C9		C9	C9					C9		C9	C9	C7		C7	C7
9/17/2010																				
9/23/2010																				
9/29/2010					C9		C9	C9					C9		C9	C9				
10/5/2010																				
10/11/2010					C10	C10	C10	C10					C10	C10	C10	C10	C8	C8	C8	C8
10/17/2010																				
10/23/2010																				
10/29/2010							C10	C10					C10	C10	C10	C10	C8	C8	C8	C8
11/4/2010					C11	C11	C11	C11									C9	C9	C9	C9
11/10/2010																				
11/16/2010																				
11/22/2010							C12													
11/28/2010																				
12/4/2010																				
12/10/2010																				
12/16/2010																				
12/22/2010																				
12/28/2010																				
1/3/2011																				
1/9/2011					C13	C13	C13	C13					C11	C11	C11	C11	C10	C10	C10	C10
1/15/2011																				
1/21/2011																				
1/27/2011																				
2/2/2011					C14	C14											C11	C11		
2/8/2011																				
2/14/2011							C14	C14					C12	C12	C12	C12	C12	C12	C12	C12
2/20/2011					C14	C14														
2/26/2011																				
3/4/2011																				
3/10/2011																				

Table 6.S2 Laboratory OCEC analyzer temperature profile descriptions for the WSLH and CU instruments

Instrument Mode	WSHL Time (s)	WSHL Temperature (°C)	CU Time (s)	CU Temperature (°C)	Power Constant	Time Constant	Blower Speed (bits)
Helium	10	1	10	1	0.001	100	0
Helium	60	340	30	340	0.95	5	0
			10	340	0.93	15	0
			20	340	0.001	180	0
Helium	60	500	10	500	0.80	130	3
			20	500	0.95	20	0
			30	500	0.2	150	4
Helium	60	615	30	615	0.98	15	0
			15	615	0.95	20	4
			15	615	0.50	150	6
Helium	90	900	95	900	0.99	5	6
			10	900	0.99	90	0
			25	900	0.90	9150	0
Helium	45	0	45	1	0.001	100	16
Oxygen	45	575	45	575	0.70	50	0
Oxygen	45	650	45	650	0.50	30	0
Oxygen	45	725	45	725	0.40	25	0
Oxygen	45	800	45	800	0.40	25	0
Oxygen	100	910	100	910	0.40	20	0
CalibrationOx	30	1	30	1	0.001	100	16
CalibrationOx	80	0	80	0	0.001	100	16

Table 6.S3 Mass and bulk carbon coefficients of variability (COV)

Size Fraction	Site	COV							
		Mass	OC	EC	PK_{340}	PK_{500}	PK_{615}	PK_{900}	Pyrol
PM$_{10-2.5}$	ALS	0.72	0.47	1.58	0.63	0.51	0.51	0.53	1.02
	EDI	0.71	0.46	1.90	0.73	0.45	0.51	0.58	1.20
	MAP	0.71	0.61	1.47	0.71	0.64	0.78	0.70	1.03
	MCA	0.71	0.52	1.46	0.67	0.52	0.67	0.60	1.24
PM$_{2.5}$	ALS	0.69	0.45	0.70	0.49	0.44	0.48	0.55	1.13
	EDI	0.52	0.32	0.69	0.41	0.35	0.41	0.44	0.80
	MAP	0.59	0.53	0.89	0.53	0.53	0.59	0.70	0.85
	MCA	0.56	0.38	0.72	0.40	0.41	0.50	0.51	0.72

Table 6.S4 Spatial and particulate size fraction correlations for WSOC and TDN

ρ - WSOC		PM$_{10-2.5}$			PM$_{2.5}$			
		EDI	MAP	MCA	ALS	EDI	MAP	MCA
PM$_{10-2.5}$	ALS	0.14	0.19	0.27	0.65	0.42	0.56	0.50
	EDI		0.32	-0.08	-0.33	0.38	0.07	-0.26
	MAP			0.33	0.29	-0.34	0.69	0.34
	MCA				0.57	0.32	0.30	0.41
PM$_{2.5}$	ALS					0.24	0.52	0.59
	EDI						-0.26	-0.03
	MAP							0.74

ρ - TDN		PM$_{10-2.5}$			PM$_{2.5}$			
		EDI	MAP	MCA	ALS	EDI	MAP	MCA
PM$_{10-2.5}$	ALS	0.94	0.85	0.69	0.27	0.23	0.74	0.52
	EDI		0.97	0.61	0.25	0.27	0.81	0.60
	MAP			0.51	0.33	0.34	0.83	0.63
	MCA				0.23	0.26	0.35	0.28
PM$_{2.5}$	ALS					0.99	0.41	0.70
	EDI						0.32	0.67
	MAP							0.89

Figure 6.S1 Laboratory OCEC instrument temperature profiles for the WSLH and CU instruments
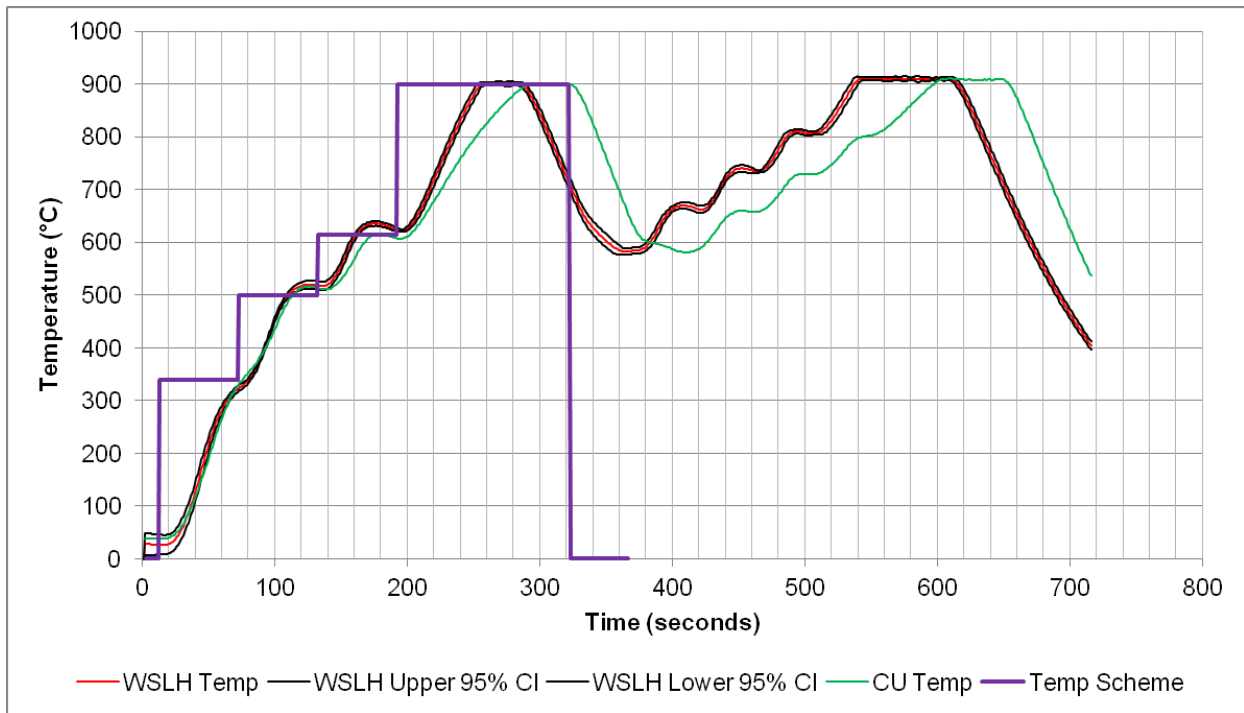
Figure 6.S2 SUVA values for each composite for (a) EDI $PM_{10-2.5}$, (b) EDI $PM_{2.5}$, (c) MAP $PM_{10-2.5}$, and (d) MAP $PM_{2.5}$
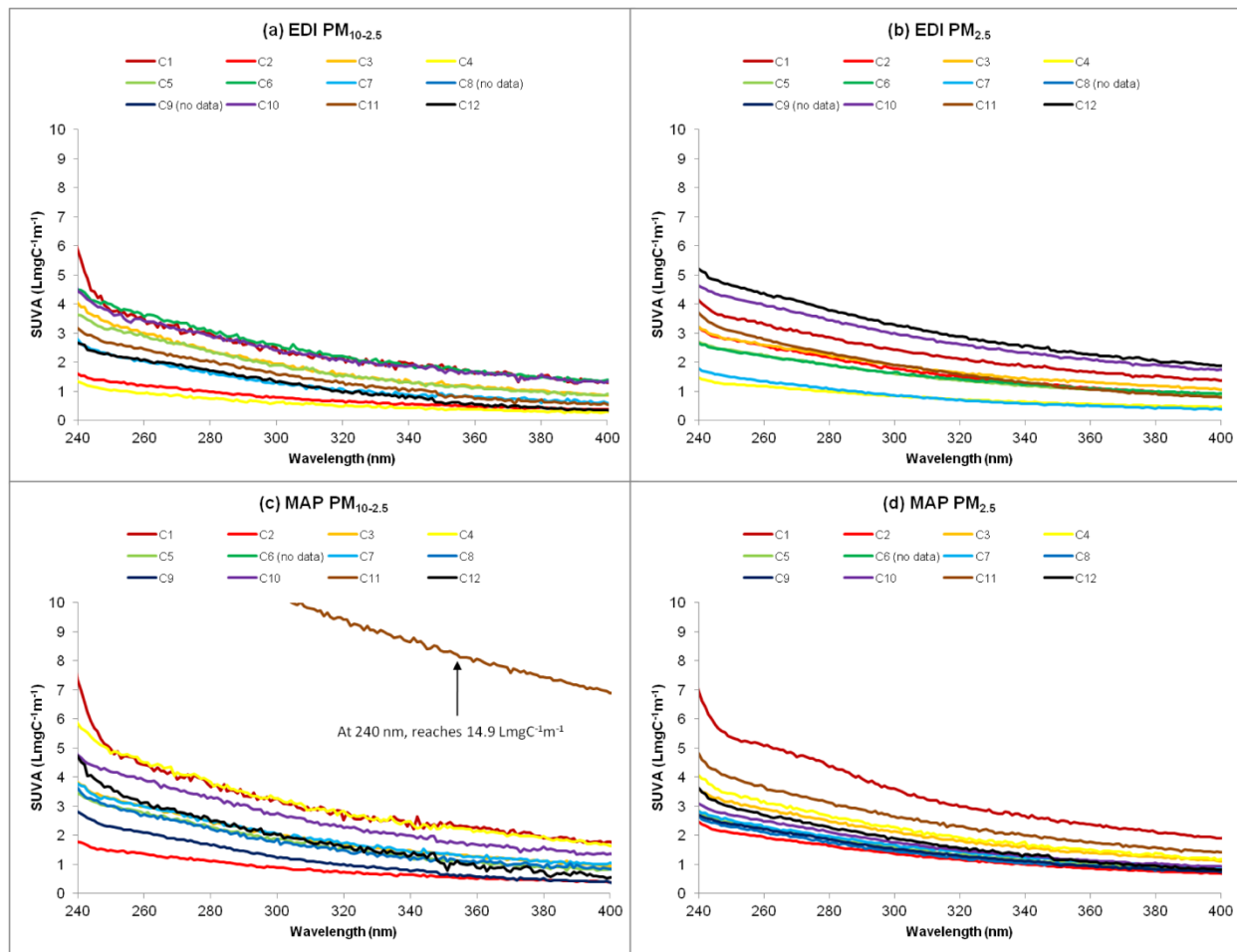
Figure 6.S3 Time series of (a) $PM_{10-2.5}$ and (b) $PM_{2.5}$ $SUVA_{254}$ values

266
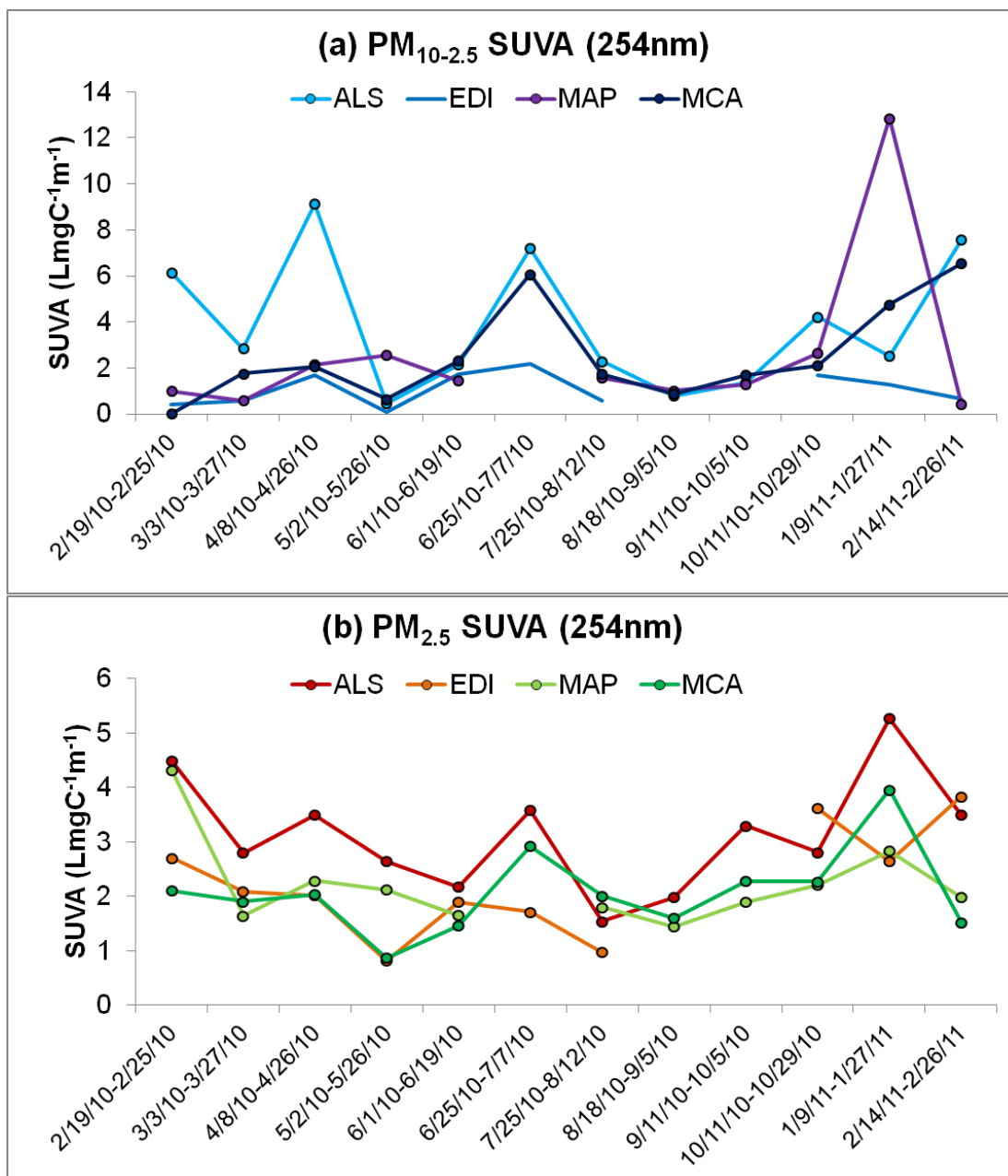
CHAPTER 7

SUMMARY AND CONCLUSIONS

7.1 SUMMARY OF THE CCRUSH STUDY FIELD CAMPAIGN

The goal of the CCRUSH study was to characterize the sources and health impact of urban and rural $PM_{10-2.5}$ in Colorado. The field campaign portion of the CCRUSH study included two sets of data: (1) three years of continuous mass concentrations from four sites in Denver and two sites in Greeley, and (2) compositional characterization of filter samples collected at two sites in Denver and two sites in Greeley over the course of a year. This dissertation presents the results of these research efforts in full.

In Chapters 2 and 4, continuous mass concentration time series were examined to observe relationships spatially, temporally, and with meteorological and source indicators. In Chapter 2, time series a year in length showed significant differences in $PM_{10-2.5}$ concentrations on weekdays and weekends and at night compared to during the day. These trends were generally attributed to human activity. Nonparametric regression was used for observing nonlinear relationships between $PM_{10-2.5}$ concentrations and wind conditions. $PM_{10-2.5}$ and $PM_{2.5}$ concentrations peaked with wind from the urban core in Denver. Nonparametric relationships between $PM_{10-2.5}$ and wind speed were site dependent and only sites with nearby source emissions showed a resuspension effect where concentrations increased with increased wind speeds. Chapter 4 expanded on the analysis from Chapter 2, using a longer time series and two additional $PM_{10-2.5}$ monitoring sites, from which data were provided by the Colorado Department of Public Health and Environment (CDPHE). In addition to confirming results in Chapter 2, the analysis in Chapter 4 revealed complex relationships between meteorological parameters and the temporal variability of $PM_{10-2.5}$ mass concentrations.

267

Chapter 3 presented an assessment of errors that arise from calculating $PM_{10-2.5}$ concentrations through subtraction of collocated $PM_{2.5}$ from PM_{10} measurements. TEOM instruments should be corrected for the loss of semivolatile mass from heated filter surfaces, though not all instruments in use by regulatory agencies in the United States have this capability. $PM_{10-2.5}$ concentrations were highly biased when semivolatile concentrations were not taken into account by one of the two collocated instruments, and summary statistics describing the spatial and temporal variability of the pollutant were impacted by the variability added to the time series when semivolatile matter was not quantified. A correction scheme involving estimation of the semivolatile fraction and calculation of the nonvolatile $PM_{10-2.5}$ fraction was implemented and shown to perform adequately. The errors addressed in this chapter could also impact results of health studies based on time series of erroneous $PM_{10-2.5}$ data, and it was recommended that epidemiological studies address these errors if data from TEOM instruments are included in the analysis. After correcting CDPHE data, all continuous mass concentration time series were supplied to the epidemiologists involved in the CCRUSH study. Results from the epidemiological campaign of the CCRUSH study are pending.

Chapters 5 and 6 detail the results of the year-long filter sampling campaign that occurred during the second year of continuous monitoring. The elemental composition of $PM_{10-2.5}$ and $PM_{2.5}$ was assessed in Chapter 5. Concentration enrichment factors showed vehicle-wear particles were enriched in both size fractions. Source identification via positive matrix factorization revealed five inorganic sources: road salt (predominately in winter), crustal material, regional sulfur, vehicle-wear, and a catalyst source that may be impacted by oil refinery and vehicular emissions. In Chapter 6 it was shown that the largest fraction of $PM_{2.5}$ organic matter was associated with by carbonaceous species volatilize at temperatures below 500°C, while $PM_{10-2.5}$ was dominated by high temperature peak fractions. Low temperature organic peak fractions in both $PM_{2.5}$ and $PM_{10-2.5}$ were highly spatially correlated and peaked in the winter, which may suggest temperature-related gas-particle partitioning impacts both size

fractions. The water-soluble organic fraction of $PM_{10-2.5}$ was more aromatic than that from $PM_{2.5}$ and tended to be more terrestrial. Fulvic and humic-like fluorescence peaks were prevalent in $PM_{2.5}$ samples and were not dominant in $PM_{10-2.5}$ samples. Instead, $PM_{10-2.5}$ water soluble carbon fluorescence was dominated by tryptophan and tyrosine-like regions, signifying impact from biological proteinaceous material is more important than humic substances in the coarse fraction. Fulvic and humic-like fluorescence in the $PM_{2.5}$ fraction was attributed to humic like substances (HULIS) and wintertime peaks in $PM_{2.5}$ aromaticity was attributed to emissions of woodsmoke related HULIS.

The CCRUSH study is one of the most detailed analyses of coarse mode aerosol to date, and coupled characterization of a time series of mass concentrations with high time resolution to a detailed compositional assessment. The results of the CCRUSH study will be important for informing future regulatory actions by the EPA regarding $PM_{10-2.5}$. Though much work has recently gone into characterize $PM_{10-2.5}$ around the world, the pollutant is still poorly understood and more research needs to be done to determine more exact source contributions; to separate road-generated, construction-generated, and geogenic dusts; to understand chemical changes $PM_{10-2.5}$ can undergo in the atmosphere; and to comprehensively understand the organic matter composition.

7.2 FUTURE RESEARCH DIRECTIONS

Looking forward, future $PM_{10-2.5}$ investigations should focus on: (1) understanding the dynamics of wind erosion-related emission processes, (2) separating the impact of crustal sources like road-wear particles, construction-related particles, and geogenic dust resuspension, and (3) explaining the sources of the organic fraction of coarse particles. Recent studies in Europe and the United States have revealed intricate relationships between ecological region, meteorological conditions, and ambient $PM_{10-2.5}$ mass concentrations (Clements et al., 2012; Barmpadimos et al., 2012; Li et al., 2013a; Li et al., 2013b), but long time series evaluating the impact of these parameters on source emissions are lacking. Amato et al. (2013) observed recovery of elemental composition following precipitation and observed different recovery times for road dusts, vehicle-wear, and geogenic dusts. Bioaerosol emissions are also highly dynamic with changing meteorological parameters like RH and rain (Elbert et al., 2007; Huffman et al, 2013), but emission rates are also poorly understood. No such studies are available for impact of snow, though snow has been implicated in leading to road salt emissions and increased road surface wear from studded tires (Antilla and Salmi, 2006; Kumar et al., 2012; Clements et al., 2013). Studies like Amato et al. (2013) should strive to reach parameterizations for emissions of $PM_{10-2.5}$ from sources for inclusion in models, which currently poorly predict $PM_{10-2.5}$ concentrations (Li et al., 2013a). Such parameterizations must include dependencies on ecological and meteorological parameters like soil moisture, precipitation, and the availability of resuspendable materials (organic and inorganic). Potentially important sources in need of detailed analysis include but are not limited to: road wear, vehicular-wear, construction activities, agricultural activities including farming and animal husbandry, geogenic dust and soil erosion emissions, industrial emissions, mining emissions, and marine emissions. It is likely that evaluation of the dynamics and composition of emissions from a wide range of

sources in multiple ecological and climatological regions will be required to fully capture the temporal variability of the pollutant worldwide.

Scientists attempting to understand the inorganic fraction should consider including evaluation of water-soluble elemental species and isotopic properties, as studies using these parameters have been able to distinguish geogenic from traffic and industrial dusts (e.g. Guegen et al., 2013; Clements et al., 2013). Carbonates in the coarse mode should also be investigated, as these components were measured in substantial concentrations in western India (Kumar and Sarin, 2010). Relating mineralogical properties to local soil or road wear emissions and comparing ternary diagrams of various sets of trace elements have also been useful in characterizing the inorganic fraction (Moreno et al., 2003; Moreno et al., 2007; Moreno et al., 2013; Varrica et al., 2013; Williamson et al., 2013).

Knowledge of the $PM_{10-2.5}$ organic fraction is currently limited and advanced speciation techniques will be required to fully characterize this complex mixture of soil organic carbon, adsorbed gas-phase species, and full or fragmented pieces of microbiological cells. Techniques like GC/MS that quantify concentrations of single organic compounds typically do not characterize the majority of $PM_{10-2.5}$ organic mass (e.g. Cheung et al., 2012) but are useful in understanding gas-particle partitioning of low molecular weight organic species to dust surfaces (Falkovich et al., 2004). Bulk characterization methods utilized in soil and aquatic natural organic matter studies will likely be very useful in understanding soil erosion processes that lead to geogenic resuspension of dust and can be coupled with mineralogical assessments to improve source identification. It is likely that full characterization of the $PM_{10-2.5}$ organic fraction will require multiple analytical steps quantifying the mass of of bioaerosols, high molecular weight soil organic matter, and low molecular weight compounds such as PAHs, hopanes, carboxylic acids, and saccharides.

7.3 REFERENCES

Amato, F., Schaap, M., Denier van der Gon, H.A.C., Pandolfi, M., Alastuey, A., Keuken, M., Querol, X. 2013. Short-term variability of mineral dust, metals, and carbon emissions from road dust resuspension. Atmospheric Environment 74, 134-140.

Antilla, P., Salmi, T. 2006. Characterizing temporal and spatial patterns of urban PM_{10} using size years of Finnish monitoring data. Boreal Environment Research 11, 463-479.

Barmpadimos, I., Keller, J., Oderbolz, D., Hueglin, C., Prevot, A.S.H. 2012. One decade of parallel fine ($PM_{2.5}$) and coarse (PM_{10}-$PM_{2.5}$) particulate matter measurements in Europe: trends and variability. Atmospheric Chemistry and Physics 12, 3189-3203.

Cheung, K., Olson, M.R., Shelton, B., Schauer, J.J., Sioutas, C. 2012. Seasonal and spatial variations of individual organic compounds of coarse particulate matter in the Los Angeles Basin. Atmospheric Environment 59, 1-10.

Clements, N., Piedrahita, R., Ortega, J., Peel, L., Hannigan, M.P., Miller, S.L., Milford, J.B. 2012. Characterization and Nonparametric Regression of Rural and Urban Coarse Particulate Matter Mass Concentrations in Northeastern Colorado. Aerosol Science and Technology 46(1), 108-123.

Clements, N., Eav, J., Xie, M., Hannigan, M.P., Miller, S.L., Navidi, W., Peel, J.L., Schauer, J.J., Shafer, M., Milford, J.B., 2013. Concentrations and Source Insights for Trace Elements in Fine and Coarse Particulate Matter in Northeastern Colorado, Atmospheric Environment, *submitted*.

Clements, A.L., Fraser, M.P., Upadhyay, N., Herckes, P., Sunblom, M., Lantz, J., Solomon, P.A. 2013. Characterization of summertime coarse particulate matter in the Desert Southwest-Arizona, USA. Journal of the Air and Waste Management Association 63(7), 764-772.

Elbert, W., Taylor, P.E., Andreae, M.O., Poschl, U. 2007. Contribution of fungi to primary

biogenic aerosols in the atmosphere: wet and dry discharged spores, carbohydrates,

and inorganic ions. Atmospheric Chemistry and Physics 7, 4569-4588.

Falkovich, A.H., Schkolnik, G., Ganor, E., Rudich, Y. 2004. Adsorption of organic compounds

pertinent to urban environments onto mineral dust particles. Journal of Geophysical

Research 109, D02208.

Gueguen, F., Stille, P., Dietze, V., Giere, R. 2012. Chemical and isotopic properties and origins

of coarse airborne particles collected by passive samplers in industrial, urban, and rural

environments. Atmospheric Environment 62, 631-645.

Huffman, J.A., Prenni, A.J., DeMott, P.J., Pohlker, C., Mason, R.H., Robinson, N.H., Frohlich-

Nowoisky, J., Tobo, Y., Despres, V.R., Garcia, E., Gochis, D.J., Harris, E., Muller-

Germann, I., Ruzene, C., Schmer, B., Sinha, B., Day, D.A., Andreae, M.O., Jimenez,

J.L., Gallagher, M., Kreidenweis, S.M., Bertram, A.K., Poschl, U. 2013. High

concentrations of biological aerosol particles and ice nuclei during and after rain.

Atmospheric Chemistry and Physics 13, 6151-6164.

Kumar, A., Sarin, M.M. 2010. Atmospheric water-soluble constituents in fine and coarse mode

aerosols from high-altitude site in western India: Long-range transport and seasonal

variability. Atmospheric Environment 44, 1245-1254.

Kumar, P., Hopke, P.K., Raja, S., Casuccio, G., Lersch, T.L., West, R.R. 2012. Characterization

and heterogeneity of coarse particles across an urban area. Atmospheric Environment

46, 449-459.

Li, R., Wiedinmyer, C., Hannigan, M.P. 2013. Characterization of coarse particulate matter in

the western United States: a comparison between observation and modeling.

Atmospheric Chemistry and Physics 13, 1311-1327.

Li, R., Wiedinmyer, C., Hannigan, M.P. 2013. Contrast and correlations between coarse and

fine particulate matter in the United States. Science of the Total Environment 456-457,

346-358.

Moreno, T., Gibbons, W., Jones, T., Richards, R. 2003. The geology of ambient aerosols:

characterizing urban and rural/coastal silicate $PM_{10-2.5}$ and $PM_{2.5}$ using high-volume

cascade collection and scanning electron microscopy. Atmospheric Environment 37,

4265-4276.

Moreno, N., Alastuey, A., Querol, X., Artinano, B., Guerra, A., Luaces, J.A., Lorente, A., Basora,

J. 2007. Characterization of dust material emitted during harbor operations (HADA

Project). Atmospheric Environment 41, 6331-6343.

Moreno, T., Karanasiou, A., Amato, F., Lucarelli, F., Nava, S., Calzolai, G., Chiari, M., Coz, E.,

Artinano, B., Lumbreras, J., Borge, R., Boldo, E., Linares, C., Alastuey, A., Querol, X.,

Gibbons, W. 2013. Daily and hourly sourcing of metallic and mineral dust in urban air

contaminated by traffic and coal-burning emissions. Atmospheric Environment 68, 33-

44.

Varrica, D., Bardelli, F., Dongarra, G., Tamburo, E. 2013. Speciation of Sb in airborne

particulate matter, vehicle brake linings, and brake pad wear residues. Atmospheric

Environment 64, 18-24.

Williamson, B.J., Rollinson, G., Pirrie, D. 2013. Automated Mineralogical Analysis of PM_{10}: New

Parameters for Assessing PM Toxicity. Environmental Science and Technology 47,

5570-5577.

CHAPTER 8

BIBLIOGRAPHY

Almeida, S.M., Pio, C.A., Freitas, M.C., Reis, M.A., Trancoso, M.A. 2006. Source apportionment of atmospheric urban aerosol based on weekdays/weekend variability: evaluation of road re-suspended dust contribution. Atmospheric Environment 40, 2058-2067.

Amato, F., Viana, M., Richard, A., Furger, M., Prevot, A.S.H., Nava, S., Lucarelli, F., Bukowiecki, N., Alastuey, A., Reche, C., Moreno, T., Pandolfi, M., Pey, J., Querol, X., 2011. Size and time-resolved roadside enrichment of atmospheric particulate pollutants. Atmospheric Chemistry and Physics 11, 2917-2931.

Amato, F., Schaap, M., Denier van der Gon, H.A.C., Pandolfi, M., Alastuey, A., Keuken, M., Querol, X. 2013. Short-term variability of mineral dust, metals, and carbon emissions from road dust resuspension. Atmospheric Environment 74, 134-140.

Antilla, P., Salmi, T. 2006. Characterizing temporal and spatial patterns of urban PM_{10} using size years of Finnish monitoring data. Boreal Environment Research 11, 463-479.

Baduel, C., Voisin, D., Jaffrezo, J.L. 2009. Comparison of analytical methods for Humic Like Substance (HULIS) measurements in atmospheric particles. Atmospheric Chemistry and Physics 9, 5949-5962.

Baduel, C., Voisin, D., Jaffrezo, J.-L. 2010. Seasonal variations of concentrations and optical properties of water soluble HULIS collected in urban environments. Atmospheric Chemistry and Physics 10, 4085-4095.

Barmpadimos, I., Keller, J., Oderbolz, D., Hueglin, C., Prevot, A.S.H. 2012. One decade of parallel fine ($PM_{2.5}$) and coarse (PM_{10}-$PM_{2.5}$) particulate matter measurements in Europe: trends and variability. Atmospheric Chemistry and Physics 12, 3189-3203.

Barnhart, H.X., Haber, M., Song, J. 2002. Overall Concordance Correlation Coefficient for Evaluating Agreement Among Multiple Observers. Biometrics 58, 1020-1027.

275

Belzile, N., Chen, Y.-W., Filella, M., 2011. Human exposure to antimony: I. Sources and intake, Critical Reviews in Environmental Science and Technology 41(14), 1309-1373.

Boreson, J., Dillner, A.M., Peccia, J., 2004. Correlating bioaerosol load with PM2.5 and PM10cf concentrations: A comparison between natural desert and urban-fringe aerosols. Atmospheric Environment 38, 6029-2041.

Bourotte, C., Forti, M.-C., Taniguchi, S., Bicego, M.C., Lotufo, P.A. 2005. A wintertime studyof PAHs in fine and coarse aerosols in Sao Paulo city, Brazil. Atmospheric Environment 39, 3799-3811.

Bowers, R.M., Clements, N., Emerson, J.B., Wiedinmyer, C., Hannigan, M.P., Fierer, N. 2013. Seasonal Variability in Bacterial and Fungal Diversity of the Near-Surface Atmosphere. Environmental Science and Technology, Article ASAP.

Brook, R.D., Bard, R.L., Kaplan, M.J., Yalavarthi, S., Morishita, M., Dvonch, J.T., Wang, L., Yang, H.-Y., Spino, C., Mukherjee, B., Oral, E.A., Sun, Q., Brook, J.R., Harkema, J., Rajagopalan, S. 2013. The effect of acute exposure to coarse particulate matter air pollution in a rural location on circulating endothelial progenitor cells: results from a randomized controlled study. Inhalation Toxicology 25(10), 587-592.

Brunekreef, B., Forsberg, B., 2005. Epidemiological evidence of effects of coarse airborne particles on health. European Respiratory Journal 26, 309–318.

Castillejos, M., Borja-Aburto, V.H., Dockery, D., Gold, D.R., Loomis, D., 2000. Airborne coarse particles and mortality. Inhalation Toxicology 12, 61-72.

CDOT, 2013. Online Transportation Information System, Traffic Data Explorer. Colorado Department of Transportation. Available at http://dtdapps.coloradodot.info/Otis/TrafficData, last accessed March 29, 2013.

Chan, T.L., Lippmann, M. 1980. Experimental Measurements and Empirical Modelling of the Regional Deposition of Inhaled Particles in Humans. *Am. Ind. Hyg. Assoc. J.* 41:399-409.

Chang, H.H., Peng, R.D., and Dominici, F. 2011. Estimating the acute health effects of coarse particulate matter accounting for exposure measurement error. *Biostatistics.* 12(4):637-652.

Charron, A., Harrison, R.M. 2005. Fine ($PM_{2.5}$) and Coarse ($PM_{2.5-10}$) Particulate Matter on A Heavily Trafficked London Highway: Sources and Processes. Environmental Science and Technology 39, 7768-7776.

Chen, F., Williams, R., Svendsen, E., Yeatts, K., Creason, J., Scott, J., Terrell, D., Case, M. 2007. Coarse Particulate Matter Concentrations from Residential Outdoor Sites Associated with the North Carolina Asthma and Children's Environment Studies (NC-ACES). *Atmos. Environ.* 41:1200-1208.

Chen, J., LeBoeuf, E.J., Dai, S., Gu, B. 2003. Fluorescence spectroscopic studies of natural organic matter fractions. Chemosphere 50, 639-647.

Chen, Y., Yang, Q., Krewski, D., Burnett, R.T., Shi, Y., and McGrail, K.M. 2005. The effect of coarse ambient particulate matter on first, second, and overall hospital admissions for respiratory disease among the elderly. *Inhalation Toxicology.* 17:649-655.

Cheng, J.Y.W., Hui, E.L.C., Lau, A.P.S. Bioactive and total endotoxins in atmospheric aerosols in the Pearl River Delta region, China. Atmospheric Environment 47, 3-11.

Cheung, K., Daher, N., Kam, W., Shafer, M.M., Ning, Z., Schauer, J.J., Sioutas, C. 2011. Spatial and temporal variation of chemical composition and mass closure of ambient coarse particulate matter ($PM_{10-2.5}$) in the Los Angeles area. Atmospheric Environment 45, 2651-2662.

Cheung K., Olson, M.R., Shelton, B., Schauer, J.J., Sioutas, C. 2012. Seasonal and spatial variations of individual organic compounds of coarse particulate matter in the Los Angeles Basin. Atmospheric Environment 59, 1-10.

Cheung, K., Shafer, M.M., Schauer, J.J., Sioutas, C., 2012. Historical trends in the mass and chemical species concentrations of coarse particulate matter in the Los Angeles Basin

and relation to sources and air quality regulations. Journal of the Air & Waste Management Association 62, 541-556.

Chow, J.C., Watson, J.G., Fujita, E.M., Zhiqiang, L., Lawson, D.R., Ashbaugh, L.L., 1994. Temporal and spatial variations of $PM_{2.5}$ and PM_{10} aerosol in the Southern California Air Quality Study. Atmospheric Environment 28, 2061-2080.

Clements, N., Piedrahita, R., Ortega, J., Peel, L., Hannigan, M.P., Miller, S.L., Milford, J.B. 2012. Characterization and Nonparametric Regression of Rural and Urban Coarse Particulate Matter Mass Concentrations in Northeastern Colorado. Aerosol Science and Technology 46(1), 108-123.

Clements, N., Eav, J., Xie, M., Hannigan, M.P., Miller, S.L., Navidi, W., Peel, J.L., Schauer, J.J., Shafer, M., Milford, J.B., 2013. Concentrations and Source Insights for Trace Elements in Fine and Coarse Particulate Matter in Northeastern Colorado, Atmospheric Environment, *submitted*.

Clements, N., Milford, J.B., Miller, S.L., Peel, J.L., Hannigan, M.P. 2013. Spatiotemporal and Meteorological Trends of Total and Semivolatile $PM_{10-2.5}$ and $PM_{2.5}$ Mass Concentratons in Northeastern Colorado. *In prep*.

Clements, N., Milford, J.B., Miller, S.L., Navidi, W., Peel, J.L., Hannigan, M.P., 2013. Errors in Coarse Particulate Matter ($PM_{10-2.5}$) Mass Concentrations and Spatiotemporal Characteristics when Using Subtraction Estimation Methods, Journal of the Air and Waste Management Association, *accepted*.

Clements, A.L., Fraser, M.P., Upadhyay, N., Herckes, P., Sunblom, M., Lantz, J., Solomon, P.A. 2013. Characterization of summertime coarse particulate matter in the Desert Southwest-Arizona, USA. Journal of the Air and Waste Management Association 63(7), 764-772.

Coble, P.G. 1996. Characterization of marine and terrestrial DOM in seawater using excitation-emission matrix spectroscopy. Marine Chemistry 51, 325-346.

Countess, R.J., Wolff, G.T., Cadle, S.H., 1980. The Denver winter aerosol: A comprehensive chemical characterization, Journal of the Air Pollution Control Association 30(11), 1194-1200.

Countess, R.J., Cadle, S.H., Groblicki, P.J., Wolff, G.T., 1981. Chemical analysis of size-segregated samples of Denver's ambient particulate, Journal of the Air Pollution Control Association 31(3), 247-252.

Degobbi, C., Hilario, P., Saldiva, N., Rogers, C. 2011. Endotoxin as modifier of particulate matter toxicity: a review of the literature. Aerobiologia 27, 97-105.

Despres, V.R., Huffman, J.A., Burrows, S.M., Hoose, C., Safatov, A.S., Buryak, G., Frohlich-Nowoisky, J., Elbert, W., Andreae, M.O., Poschl, U., Jaenicke, R. 2012. Primary biological aerosol particles in the atmosphere: a review. Tellus B 64, 15598.

Dockery, D.W., Pope, A. III, Xu, X., Spengler, J.D., Ware, J.H., Fay, M.E., Ferris, B.G. Jr., Speizer, F.E. 1993. An Association between Air Pollution and Mortality in Six U.S. Cities. The New England Journal of Medicine 329(24), 1753-1759.

Donahue, N.M., Robinson, A.L., Pandis, S.N. 2009. Atmospheric organic particulate matter: From smoke to secondary organic aerosol. Atmospheric Environment 43, 94-106.

Duarte, R.M.B.O., Pio, C.A., Duarte, A.C. 2005. Spectroscopic study of the water-soluble organic matter isolated from atmospheric aerosols collected under different atmospheric conditions. Analytica Chimica Acta 530, 7-14.

Duarte, R.M.B.O., Santos, E.B.H., Pio, C.A., Duarte, A.C. 2007. Comparison of structural features of water-soluble organic matter from atmospheric aerosols with those of aquatic humic substances. Atmospheric Environment 41, 8100-8113.

Duarte, R.M.B.O., Silva, A.M.S., Duarte, A.C. 2008. Two-Dimensional NMR studies of Water-Soluble Organic Matter in Atmospheric Aerosols. Environmental Science and Technology 42, 8224-8230.

Duce, R.A., Hoffman, G.L., Ray, B.J., Fletcher, I.S., Wallace, G.T., Fasching, J.L., Piotrowicz, S.R., Walsh, P.R., Hoffman, E.J., Miller, J.M., Heffter, J.L, 1976. Trace metals in the marine atmosphere: sources and fluxes, in H.L. Windom and R.A. Duce eds., Marine Pollutant Transfer, D.C. Heath, Lexington, MA, pp. 77-119.

Dungan, R.S., Leytem, A.B. 2009. Airborne Endotoxin Concentrations at a Large Open-Lot Dairy in Southern Idaho. Journal of Environmental Quality 38, 1919-1923.

Dungan, R.S., Leytem, A.B., Bjorneberg, D.B. 2010. Year-long assessment of airborne endotoxin at a concentrated dairy operation. Aerobiologia 26, 141-148.

Dutton, S.J., Williams, D.E., Garcia, J.K., Vedal, S., Hannigan, M.P. 2009. $PM_{2.5}$ characterization for time series studies: Organic molecular marker speciation methods and observations from daily measurements in Denver. Atmospheric Environment 43, 2018-2030.

Dutton, S.J., Schauer, J.J., Vedal, S., Hannigan, M.P. 2009. $PM_{2.5}$ characterization for time series studies: Pointwise uncertainty estimation and bulk speciation methods applied in Denver. Atmospheric Environment 43, 1136-1146.

Dutton, S.J., Rajagopalan, B., Vedal, S., Hannigan, M.P. 2010. Temporal patterns in daily measurements of inorganic and organic speciated $PM_{2.5}$ in Denver. Atmospheric Environment 44, 987-998.

Dutton, S.J., Vedal, S., Piedrahita, R., Milford, J.B., Miller, S.L., Hannigan, M.P. 2010. Source apportionment using positive matrix factorization on daily measurements of inorganic and organic speciated $PM_{2.5}$. Atmospheric Environment 44, 2731-2741.

Eatough, D.J., Long, R.W., Modey, W.K., Eatough, N.L. 2003. Semi-volatile secondary organic aerosol in urban atmospheres: meeting a measurement challenge. Atmospheric Environment 37, 1277-1292.

Edgerton, E.S., Casuccio, G.S., Saylor, R.D., Lersch, T.L., Hartsell, B.E., Jansen, J.J., Hansen, D.A. 2009. Measurements of OC and EC in Coarse Particulate Matter in the

Southeastern United States. Journal of the Air and Waste Management Association 59, 78-90.

EPA, 2004. Speciate Data Browser, Coal Combustion Profiles 3191 and 3192, U.S. Environmental Protection Agency, available at http://cfpub.epa.gov/si/speciate.

EPA, 2009. Integrated Science Assessment for Particulate Matter. EPA/600/R-08/139F. U.S. Environmental Protection Agency, Washington, DC.

Elbert, W., Taylor, P.E., Andreae, M.O., Poschl, U. 2007. Contribution of fungi to primary biogenic aerosols in the atmosphere: wet and dry discharged spores, carbohydrates, and inorganic ions. Atmospheric Chemistry and Physics 7, 4569-4588.

Falkovich, A.H., Schkolnik, G., Ganor, E., Rudich, Y. 2004. Adsorption of organic compounds pertinent to urban environments onto mineral dust particles. Journal of Geophysical Research 109, D02208.

Fast, J., Aiken, A.C., Allan, J., Alexander, L., Campos, T., Canagaratna, M.R., Chapman, E., DeCarlo, P.F., de Foy, B., Gaffney, J., de Gouw, J., Doran, J.C., Emmons, L., Hodzic, A., Herndon, S.C., Huey, G., Jayne, J.T., Jimenez, J.L., Kleinman, L., Kuster, W., Marley, N., Russell, L., Ochoa, C., Onasch, T.B., Pekour, M., Song, C., Ulbrich, I.M., Warneke, C., Welsh-Bon, D., Wiedinmyer, C., Worsnop, D.R., Yu, X.-Y., Zaveri, R. 2009. Evaluating simulated primary anthropogenic and biomass burning organic aerosols during MILAGRO: implications for assessing treatments of secondary organic aerosols. Atmospheric Chemistry and Physics 9, 6191-6215.

Favez, O., Cachier, H., Sciare, J., Le Moullec, Y., 2007. Characterization and contribution to $PM_{2.5}$ of semi-volatile aerosols in Paris (France), Atmospheric Environment 41, 7969-7976.

Feczko, T., Puxbaum, H., Kasper-Giebl, A., Handler, M., Limbeck, A., Gelencser, A., Pio, C., Preunkert, S., Legrand, M. 2007. Determination of water and alkaline extractable

atmospheric humic-like substances with the TU Vienna HULIS analyzer in samples from six background sites in Europe. Journal of Geophysical Research 112, D23S10.

Forster, P., Ramaswamy V., Artaxo P., Berntsen T., Betts R., Fahey D.W., Haywood J., Lean J., Lowe D.C., Myhre G., Nganga J., Prinn R., Raga G., Schulz M., Van Dorland R. 2007. Changes in Atmospheric Constituents and in Radiative Forcing. In: Climate Change 2007: The Physical Science Basis. Contribution of Working Group I to the Fourth Assessment Report of the Intergovernmental Panel on Climate Change [Solomon, S., D. Qin, M. Manning, Z. Chen, M. Marquis, K.B. Averyt, M.Tignor and H.L. Miller (eds.)]. Cambridge University Press, Cambridge, United Kingdom and New York, NY, USA.

Gianini, M., Gehrig, R., Fischer, A., Ulrich, A., Wichser, A., Hueglin, C., 2012. Chemical composition of PM10 in Switzerland: An analysis for 2008/2009 and changes since 1998/1999. Atmospheric Environment 54, 97-106.

Goldman, G.T., Mulholland, J.A., Russell, A.G., Strickland, M.J., Klein, M., Waller, L.A., Tolbert, P.E. 2011. Impact of exposure measurement error in air pollution epidemiology: effect of error type in time-series studies. *Environmental Health*, 10:61.

Graham, B., Mayol-Bracero, O.L., Guyon, P., Roberts, G.C., Decesari, S., Facchini, M.C., Artaxo, P., Maenhaut, W., Koll, P., Andreae M.O. 2002. Water-soluble organic compounds in biomass burning aerosols over Amazonia: 1. Characterization by NMR and GC-MS. Journal of Geophysical Research 107, D20 8047.

Green, D., and Fuller, G.W. 2006. The implications of tapered element oscillating microbalance (TEOM) software configuration on particulate matter measurements in the UK and Europe. *Atmospheric Environment.* 40:5608-5616.

Green, D.C., Fuller, G.W., and Baker, T. 2009. Development and validation of the volatile correction model for PM_{10} – An empirical method for adjusting TEOM measurements for their loss of volatile particulate matter. *Atmospheric Environment.* 43:2132-2141.

Grover, B.D., Kleinman, M., Eatough, N.L., Eatough, D.J., Hopke, P.K., Long, R.W., Wilson, W.E., Meyer, M.B., and Ambs, J.L. 2005. Measurement of Total $PM_{2.5}$ Mass (Nonvolatile Plus Semivolatile) with the Filter Dynamic Measurement System Tapered Element Oscillating Microbalance Monitor. *J. Geophys. Res.* 110, D07S03, doi:10.1029/2004JD004995.

Grover, B.D., Eatough, N.L., Eatough, D.J., Chow, J.C., Watson, J.G., Ambs, J.L., Meyer, M.B., Hopke, P.K., Al-Horr, R., Later, D.W., Wilson, W.E., 2006. Measurement of Both Nonvolatile and Semi-Volatile Fractions of Fine Particulate Matter in Fresno, CA, Aerosol Science and Technology 40, 811-826.

Gueguen, F., Stille, P., Dietze, V., Giere, R. 2012. Chemical and isotopic properties and origins of coarse airborne particles collected by passive samplers in industrial, urban, and rural environments. Atmospheric Environment 62, 631-645.

Haagenson, P.L. 1979. Meteorological and Climatological Factors Affecting Denver Air Quality. Atmospheric Environment 13, 79-85.

Harrison, R.M., Yin, J., Mark, D., Stedman, J., Appleby, R.S., Booker, J., Moorcroft, S. 2001. Studies of the coarse particles (2.5-10 μm) component in UK urban atmospheres. Atmospheric Environment 35, 3667-3679.

Harrison, R.M., Jones, A.M., Gietl, J., Yin, J., Green, D.C., 2012. Estimation of the Contributions of Brake Dust, Tire Wear, and Resuspension to Nonexhaust Traffic Particles Derived from Atmospheric Measurements, Environmental Science and Technology 46, 6523-6529.

Hays, M.D., Cho, S-H, Baldauf, R., Schauer, J.J., Shafer, M., 2011. Particle size distributions of metal and non-metal elements in an urban near-highway environment. Atmospheric Environment 45, 925-934.

Hegde, P., Kawamura, K. 2012. Seasonal variations of water-soluble organic carbon, dicarboxylic acids, ketocarboxylic acids, and α-dicarbonyls in Central Himalayan aerosols. Atmospheric Chemistry and Physics 12, 6645-6665.

Heinrich, J., Pitz, M., Bischof, W., Krug, N., Borm, P.J.A. 2003. Endotoxin in fine ($PM_{2.5}$) and coarse ($PM_{2.5-10}$) particles mass of ambient aerosols. A temporo-spatial analysis. Atmospheric Environment 37, 3659-3667.

Hemann, J.G., Brinkman, G.L., Dutton, S.J., Hannigan, M.P., Milford, J.B., Miller, S.L., 2009. Assessing positive matrix factorization model fit: a new method to estimate uncertainty and bias in factor contributions at the measurement time scale. Atmospheric Chemistry and Physics 9(2), 497-513.

Henry, R.C., Chang, Y.-S., Spiegelman, C.H., 2002. Locating nearby sources of air pollution by nonparametric regression of atmospheric concentration on wind direction, Atmospheric Environment 36, 2237-2244.

Henry, R., Norris, G.A., Vedantham, R., Turner, J.R. 2009. Source Region Identification Using Kernel Smoothing. *Environ. Sci. Technol.* 43:4090-4097.

Hien, P.D., Bac, V.T., Tham, H.C., Nhan, D.D., Vinh, L.D. 2002. Influence of meteorological conditions on $PM_{2.5}$ and $PM_{2.5-10}$ concentrations during the monsoon season in Hanoi, Vietnam. Atmospheric Environment 36, 3473-3484.

Host, S., Larrieu, S., Pascal, L., Blanchard, M., Declercq, C., Fabre, P., Jusot, J.-F., Chardon, B., Le Terte, A., Wagner, V., Prouvost, H., Lefranc, A., 2008. Short-term associations between fine and coarse particles and hospital admissions for cardiorespiratory diseases in six French cities, Occupational Environmental Medicine 65, 544-551.

Huang, X.-F., Yu, J.Z., He, L.-Y., Yuan, Z. 2006. Water-soluble organic carbon and oxalate in aerosols at a coastal urban site in China: Size distribution characteristics, sources, and formation mechanisms. Journal of Geophysical Research 111, D22212.

Huang, Q., McConnell, L.L., Razote, E., Schmidt, W.F., Vinyard, B.T., Torrents, A., Hapeman, C.J., Maghirang, R., Trabue, S.L., Prueger, J., Ro, K.S. 2013. Utilizing single particle Raman microscopy as a non-destructive method to identify sources of PM_{10} from cattle feedlot operations. Atmospheric Environment 66, 17-24.

Hueglin, C., Gehrig, R., Baltensperger, U., Gysel, M., Monn, C., Vonmont, H., 2005. Chemical characterization of PM2.5, PM10 and coarse particles at urban, near-city and rural sites in Switzerland. Atmospheric Environment 39, 637-651.

Huffman, J.A., Sinha, B., Garland, R.M., Snee-Pollmann, A., Gunthe, S.S., Artaxo, P., Martin, S.T., Andreae, M.O., Poschl, U., 2012. Size distributions and temporal variations of biological aerosol particles in the Amazon rainforest characterized by microscopy and real-time UV-APS fluorescence techniques during AMAZE-08, Atmospheric Chemistry and Physics 12, 11997-12019.

Huffman, J.A., Prenni, A.J., DeMott, P.J., Pohlker, C., Mason, R.H., Robinson, N.H., Frohlich-Nowoisky, J., Tobo, Y., Despres, V.R., Garcia, E., Gochis, D.J., Harris, E., Muller-Germann, I., Ruzene, C., Schmer, B., Sinha, B., Day, D.A., Andreae, M.O., Jimenez, J.L., Gallagher, M., Kreidenweis, S.M., Bertram, A.K., Poschl, U. 2013. High concentrations of biological aerosol particles and ice nuclei during and after rain. Atmospheric Chemistry and Physics 13, 6151-6164.

Hwang, I., Hopke, P.K., Pinto, J.P. 2008. Source Apportionment and Spatial Distributions of Coarse Particles During the Regional Air Pollution Study. Environmental Science and Technology 42, 3524-3530.

Iijima, A., Sato, K., Fujitani, Y., Fujimori, E., Saito, Y., Tanabe, K., Ohara, T., Kozawa, K., Furuta, N., 2009. Clarification of the predominant emission sources of antimony in airborne particulate matter and estimation of their effects on the atmosphere of Japan. Environmental Chemistry 6, 122–132.

Iinuma, Y., Kahnt, A., Mutzel, A., Boge, O., Herrmann, H. 2013. Ozone-Driven Secondary
Organic Aerosol Production Chain. Environmental Science & Technology 47, 3639-
3647.

JBS Five Rivers Cattle Feeding. 2013. www.fiveriverscattle.com. Accessed 10/22/2013.

Jia, Y., Bhat, S., Fraser, M.P. 2010. Characterization of saccharides and other organic
compounds in fine particles and the use of saccharides to track primary biologically
derived carbon sources. Atmospheric Environment 44, 724-732.

Jickells, T., Baker, A.R., Cape, J.N., Nemitz, E. 2013. The cycling of organic nitrogen through
the atmosphere. Philosophical Transactions of the Royal Society B 368, 20130115.

Jimenez, J.L., Canagaratna, M.R., Donahue, N.M., Prevot, A.S.H., Zhang, Q., Kroll, J.H.,
DeCarlo, P.F., Allan, J.D., Coe, H., Ng, N.L., Airken, A.C., Docherty, K.S., Ulbrich, I.M.,
Grieshop, A.P., Robinson, A.L., Duplissy, J., Smith, J.D., Wilson, K.R., Lanz, V.A.,
Hueglin, C., Sun, Y.L., Tian, J., Laaksonen, A., Raatikainen, T., Rautiainen, J.,
Vaattovaara, P., Ehn, M., Kulmala, M., Tomlinson, J.M., Collins, D.R., Cubison, M.J.,
Dunlea, E.J., Huffman, J.A., Onasch, T.B., Alfarra, M.R., Williams, P.I., Bower, K.,
Kondo, Y., Schneider, J., Drewnick, F., Borrmann, S., Weimer, S., Demerjian, K.,
Salcedo, D., Cottrell, L., Griffin, R., Takami, A., Miyoshi, T., Hatakeyama, S., Shimono,
A., Sun, J.Y., Zhang, Y.M., Dzepina, K., Kimmel, J.R., Sueper, D., Jayne, J.T., Herndon,
S.C., Trimborn, A.M., Williams, L.R., Wood, E.C., Middlebrook, A.M., Kolb, C.E.,
Baltensperger, U., Worsnop, D.R. 2009. Evolution of Organic Aerosols in the
Atmosphere. Science 326, 1525-1529.

Kan, H., London, S.J., Chen, G., Zhang, Y., Song, G., Zhao, N., Jiang, L., and Chen, B. 2007.
Differentiating the effects of fine and coarse particles on daily mortality in Shanghai,
China. *Environment International*. 33:376-384.

Karanasiou, A.A., Siskos, P.A., Elefheriadis, K., 2009. Assessment of source apportionment by Positive Matrix Factorization analysis on fine and coarse urban aerosol size fractions. Atmospheric Environment 43, 3385-3395.

Kavouras, I.G., Etyemezian, V., Xu, J., DuBois, D.W., Green, M., Pitchford, M., 2007. Assessment of the local windblown component of dust in the western United States, Journal of Geophysical Research 112, D08211.

Kim, D., Ramanathan, V., 2008. Solar radiation budget and radiative forcing due to aerosols and clouds. Journal of Geophysical Research 113, D02203.

Kim, E., Hopke, P.H. 2004. Comparison between Conditional Probability Function and Nonparametric Regression for Fine Particle Source Directions. *Atmos. Environ.*, 38:4667–4673.

Klepper, G., Michaelis, P., Mahlau, G., 1995. Industrial Metabolism: A Case Study of the Economics of Cadmium Control, Kieler Studien 268.

Krivacsy, Z., Gelencser, A., Kiss, G., Meszaros, E., Molnar, A., Hoffer, A., Meszaros, T., Sarvari, Z., Temesi, D., Varga, B., Baltensperger, U., Nyeki, S., Weingartner, E. 2001. Study on the Chemical Character of Water Soluble Organic Compounds in Fine Atmospheric Aerosol at the Jungfraujoch. Journal of Atmospheric Chemistry 39, 235-259.

Kulkarni, P., Chellam, S., Fraser, M., 2006. Lanthanum and lanthanides in atmospheric fine particles and their apportionment to refinery and petrochemical operations in Houston, TX. Atmospheric Environment 40, 508–520.

Kumar, A., Sarin, M.M. 2010. Atmospheric water-soluble constituents in fine and coarse mode aerosols from high-altitude site in western India: Long-range transport and seasonal variability. Atmospheric Environment 44, 1245-1254.

Kumar, P., Hopke, P.K., Raja, S., Casuccio, G., Lersch, T.L., West, R.R. 2012. Characterization and heterogeneity of coarse particles across an urban area. Atmospheric Environment 46, 449-459.

Kwak, J.H., Kim, H., Lee, J., Lee, S. 2013. Characterization of non-exhaust coarse and fine particles from on-road driving and laboratory measurements. Science of the Total Environment 458-460, 273-282.

Lagudu, U.R.K., Raja, S., Hopke, P.K., Chalupa, D.C., Utell, M.J., Casuccio, G., Lersch, T.L., West, R.R. 2011. Heterogeneity of Coarse Particles in an Urban Area. Environmental Science and Technology 45, 3288-3296.

Lee, H.J., Laskin, A., Laskin, J., Nizkorodov, S.A. 2013. Excitation-Emission Spectra and Fluorescence Quantum Yields for Fresh and Ages Biogenic Secondary Organic Aerosols. Environmental Science and Technology 47, 5763-5770.

Lee, T., Yu, X.-Y., Ayres, B., Kreidenweis, S.M., Malm, W.C., and Collett, J.L.Jr. 2008. Observations of fine and coarse particle nitrate at several rural locations in the United States. *Atmospheric Environment.* 42:2720-2732.

Lewis, C.W., Baumgardner, R.E., Stevens, R.K., 1986. Receptor modeling study of Denver winter haze. Environmental Science and Technology 20, 1126-1136.

Li, R., Wiedinmyer, C., Hannigan, M.P. 2013. Characterization of coarse particulate matter in the western United States: a comparison between observation and modeling. Atmospheric Chemistry and Physics 13, 1311-1327.

Li, R., Wiedinmyer, C., Hannigan, M.P. 2013. Contrast and correlations between coarse and fine particulate matter in the United States. Science of the Total Environment 456-457, 346-358.

Lin, L.I.-K., 1989. A Concordance Correlation Coefficient to Evaluate Reproducibility, Biometrics 45(1), 255-268.

Lin, M., Stieb, D.M., and Chen, Y. 2005. Coarse particulate matter and hospitalizations for respiratory infections in children younger than 15 years in Toronto: A case-crossover analysis. *Pediatrics.* 116:e235-e240.

Lin, P., Huang, X.-F., He, L.-Y., Zu, J.Z. 2010. Abundance and size distribution of HULIS in ambient aerosols at a rural site in South China. Journal of Aerosol Science 41, 74-87.

Lin, P., Rincon, A.G., Kalberer, M., Yu, J.Z. 2012. Elemental Composition of HULIS in the Pearl River Delta Region, China: Results Inferred from Positive and Negative Electrospray High Resolution Mass Spectrometric Data. Environmental Science and Technology 46, 7454-7462.

Lipsett, M.J., Tsai, F.C., Roger, L., Woo, M., and Ostro, B.D. 2006. Coarse particles and heart rate variability among older adults with coronary artery disease in the Coachella Valley, California. *Environmental Health Perspectives.* 114:1215-1220.

Liu, Y.-J., Harrison, R.M. 2011. Properties of coarse particles in the atmosphere of the United Kingdom. Atmospheric Environment 45, 3267-3276.

Loo, B.W., Cork, C.P. 1988. Development of High Efficiency Virtual Impactors. *Aerosol Sci. Technol.* 9:167-176.

Lough, G.C., Schauer, J., Park, J.-S., Shafer, M.M., Deminter, J.T., Weinstein, J.P., 2005. Emissions of metals associated with motor vehicle roadways. Environmental Science and Technology 39, 826–836.

Malig, B.J., Ostro, B.D., 2009. Coarse particles and mortality: evidence from a multi-city study in California, Occupational and Environmental Medicine 66(12), 832-839.

Malig, B.J., Green, S., Basu, R., Broadwin, R., 2013. Coarse particles and respiratory emergency department visits in California, American Journal of Epidemiology 178(1), 58-69.

Malm, W.C., Pitchford, M.L., McDade, C., Ashbaugh, L.L. 2007. Coarse particle speciation at selected locations in the rural continental United States. Atmospheric Environment 41, 2225-2239.

Mar, T.F., Norris, G.A., Koenig, J.Q., Larson, T.V., 2000. Associations between air pollution and mortality in Phoenix, 1995-1997. Environmental Health Perspectives 108, 347-353.

Mariani, R.L., de Mello, W.Z. 2007. $PM_{2.5-10}$, $PM_{2.5}$, and associated water-soluble inorganic species at a coastal urban site in the metropolitan region of Rio de Janeiro. Atmospheric Environment 41, 2887-2892.

Marple, V.A., Chien, C.M. 1980. Virtual Impactors: A Theoretical Study. *Environ. Sci. Technol.* 14:976-985.

Marschner, P., Kandeler, E., Marschner, B. 2003. Structure and function of the soil microbial community in a long-term fertilizer experiment. Soil Biology and Biochemistry 35, 453-461.

Mayol-Bracero, O.L., Guyon, P., Graham, B., Roberts, G., Andreae, M.O., Decesari, S., Facchini, M.C., Fuzzi, S., Artaxo, P. 2002. Water-soluble organic compounds in biomass burning aerosols over Amazonia: 2. Apportionment of the chemical composition and importance of the polyacidic fraction. Journal of Geophysical Research 107, D20 8091.

Meister, K., Johansson, C., Forsberg, B., 2012. Estimated short-term effects of coarse particles on daily mortality in Stockholm, Sweden, Environmental Health Perspectives 120, 431-436.

Milford, J.B., Davidson, C.I., 1985. The sizes of particulate trace elements in the atmosphere – a review. Journal of the Air Pollution Control Association 35, 1249-1260.

Milford, J.B., Davidson, C.I., 1987. The sizes of particulate sulfate and nitrate in the atmosphere – a review. Journal of the Air Pollution Control Association 37, 125-134.

Misra, C., Geller, M.D., Shah, P., Sioutas, C., Solomon, P.A. 2001. Development and Evaluation of a Continuous Coarse (PM_{10}-$PM_{2.5}$) Particle Monitor. Journal of the Air and Waste Management Association 51(9), 1309-1317.

Misra, C., Geller, M.D., Sioutas, C., Solomon, P.A. 2003. Development and Evaluation of a PM_{10} Impactor-Inlet for a Continuous Coarse Particle Monitor. Aerosol Science and Technology 37, 271-281.

Moore, K.F., Verma, V., Minguillon, M.C., Sioutas, C. 2010. Inter- and Intra-Community Variability in Continuous Coarse Particulate Matter (PM10-2.5) Concentrations in the Los Angeles Area. Aerosol Science and Technology 44(7), 526-540.

Moreno, T., Gibbons, W., Jones, T., Richards, R. 2003. The geology of ambient aerosols: characterizing urban and rural/coastal silicate $PM_{10-2.5}$ and $PM_{2.5}$ using high-volume cascade collection and scanning electron microscopy. Atmospheric Environment 37, 4265-4276.

Moreno, N., Alastuey, A., Querol, X., Artinano, B., Guerra, A., Luaces, J.A., Lorente, A., Basora, J. 2007. Characterization of dust material emitted during harbor operations (HADA Project). Atmospheric Environment 41, 6331-6343.

Moreno, T., Querol, X., Alastuey, A., Pey, J., Cruz Minguillon, M., Perez, N., Bernabe, R., Blanco, S., Cardenas, B., Gibbons, W., 2008. Lanthanoid geochemistry of urban atmospheric particulate matter. Environmental Science and Technology 42, 6502-6507.

Moreno T., Querol, X., Alastuey, A., Reche, C., Cusack, M., Amato, F., Pandolfi, F., Pey, J., Richard, A., Prevot, A.S.H., Furger, M., Gibbons, W. 2011. Variations in time and space of trace metal aerosol concentrations in urban areas and their surroundings. Atmospheric Chemistry and Physics 11, 9415-9430.

Moreno, T., Karanasiou, A., Amato, F., Lucarelli, F., Nava, S., Calzolai, G., Chiari, M., Coz, E., Artinano, B., Lumbreras, J., Borge, R., Boldo, E., Linares, C., Alastuey, A., Querol, X., Gibbons, W. 2013. Daily and hourly sourcing of metallic and mineral dust in urban air contaminated by traffic and coal-burning emissions. Atmospheric Environment 68, 33-44.

Mueller-Anneling, L., Avol, E., Peters, J.M., Thorne, P.S. 2004. Ambient Endotoxin Concentrations in PM_{10} from Southern California. Environmental Health Perspectives 112, 583-588.

NCDC, 2012. Global Historical Climatology Network – Daily, National Climatic Data Center, http://www.ncdc.noaa.gov/oa/climate/ghcn-daily, accessed Oct. 4, 2012.

Neff, W.D. 1997. The Denver Brown Cloud Studies from the Perspective of Model Assessment Needs and the Role of Meteorology. Journal of the Air and Waste Management Association 47(3), 269-285.

Ohno, T. 2002. Fluorescence Inner-Filtering Correction for Determining the Humification Index of Dissolved Organic Matter. Environmental Science and Technology 36, 742-746.

Ohno, T., Amirbahman, A., Bro, R. 2008. Parallel Factor Analysis of Excitation-Emission Matrix Fluorescence Spectra of Water Soluble Soil Organic Matter as Basis for the Determination of Conditional Metal Binding Parameters. Environmental Science and Technology 42, 186-192.

Ostro, B.D., Broadwin, R., Lipsett, M.J., 2000. Coarse and fine particles and daily mortality in the Coachella Valley, California: A follow-up study. Journal of Exposure Analysis and Environmental Epidemiology 10, 412-419.

Paatero, P., 1998a. User's Guide for Positive Matrix Factorization Program PMF2 and PMF3, Part 1: Tutorial. University of Helsinki, Helsinki, Finland.

Paatero, P., 1998b. User's Guide for Positive Matrix Factorization Program PMF2 and PMF3, Part 2: Reference. University of Helsinki, Helsinki, Finland.

Pacyna, J.M., Pacyna, E.G., Wenche, A., 2009. Changes of emissions and atmospheric deposition of mercury, lead, and cadmium. Atmospheric Environment 43, 117-127.

Pakbin, P., Hudda, N., Cheung, K.L., Moore, K.F., Sioutas, C. 2010. Spatial and Temporal Variability of Coarse ($PM_{10-2.5}$) Particulate Matter Concentrations in the Los Angeles Area. Aerosol Science and Technology 44(7), 514-525.

Pakbin, P., Ning, Z., Shafer, M.M., Schauer, J.J., Sioutas, C. 2011. Seasonal and Spatial Coarse Particle Elemental Concentrations in the Los Angeles Area. Aerosol Science and Technology 45(8), 949-963.

Patterson, E., Gillette, D., 1977. Commonalities in measured size distributions for aerosols having a soil-derived component. Journal of Geophysical Research 82, 2074.

Peng, R.D., Chang, H.H., Bell, M.L., McDermott, A., Zeger, S.L., Samet, J.M., and Dominici, F. 2008. Coarse particulate matter air pollution and hospital admissions for cardiovascular and respiratory diseases among Medicare patients. *JAMA*. 299(18):2172-2179.

Perez, L., Tobias, A., Querol, X., Pey, J., Alastuey, A., Diaz, J., Sunyer, J., 2012. Saharan dust, particulate matter and cause-specific mortality: A case-crossover study in Barcelona (Spain), Environment International 48, 150-155.

Pohlker, C., Wiedemann, K.T., Sinha, B., Shiraiwa, M., Gunthe, S.S., Smith, M., Su, H., Artaxo, P. Chen, Q., Cheng, Y., Elbert, W., Gilles, M.K., Kilcoyne, A.L.D., Moffet, R.C., Weigand, M., Martin, S.T., Poschl, U., Andreae, M.O. 2012. Biogenic Potassium Salt Particles as Seeds for Secondary Organic Aerosol in the Amazon. Science 337, 1075-1078.

Politis, D. N., Romano, J.P, 1994. The stationary bootstrap. Journal of the American Statistics Association 89 (428), 1303-1313.

Polymenakou, P.N., Mandalakis, M., Stephanou, E.G., and Tselepides, A. 2008. Particle size distribution of airborne microorganisms and pathogens during an intense African dust event in the eastern Mediterranean. *Environmental Health Perspectives*. 116:292-296.

Puxbaum, H., Tenze-Kunit, M. 2003. Size distribution and seasonal variation of atmospheric cellulose. Atmospheric Environment 37, 3693-3699.

Qiu, H., Yu, I.T.-S., Tian, L., Wang, X., Tse, L.A., Tam, W., Wang, T.W., 2012. Effects of coarse particulate matter on emergency hospital admissions for respiratory diseases: A time-series analysis in Hong Kong, Environmental Health Perspectives 120, 572-576.

Qiu, H., Yu, I.T.-S. Wang, X., Tian, L., Tse, L.A., and Wong, T.W. 2013. Differential effects of fine and coarse particles on daily emergency cardiovascular hospitalizations in Hong Kong. *Atmospheric Environment*. 64:296-302.

Querol, X., Pey, J., Pandolfi, M., Alastuey, A., Cusack, M., Perez, N., Moreno, T., Viana, M., Mihalopoulos, N., Kallos ,G., Kleanthous, S. 2009. African dust contributions to mean ambient PM_{10} mass-levels across the Mediterranean Basin. Atmospheric Environment 43, 4266-4277.

Ray, A.J., Barsugli, J.J., Averyt, K.B., Wolter, K., Hoerling, M., Doesken, N., Udall, B., Webb, R.S. 2008. Climate Change in Colorado: A Synthesis to Support Water Resources Management and Adaptation - A report for the Colorado Water Conservation Board. CU-NOAA Western Water Assessment.

Reimann, C., De Caritat, P., 2000. Intrinsic flaws of element enrichment factors (EFs) in environmental geochemistry. Environmental Science and Technology 34, 5084–5091.

Santin, C., Yamashita, Y., Otero, X.L., Alvarez, M.A., Jaffe, R. 2009. Characterizing humic substances from estuarine soils and sediments by excitation-emission matrix spectroscopy and parallel factor analysis. Biogeochemistry 96, 131-147.

Schwab, J.J., Felton, H.D., Rattigan, O.V., Demerjian, K.L. 2006. New York State Urban and Rural Measurements of Continuous PM2.5 Mass by FDMS, TEOM, and BAM. *J. Air Waste Manage. Assoc.* 56:372-383.Solomon, P.A., Sioutas, C. (2008). Continuous and Semicontinuous Monitoring Techniques for Particulate Matter Mass and Chemical Components: A Synthesis of Findings from EPA's Particulate Matter Supersites Program and Related Studies. *J. Air Waste Manage. Assoc.* 58:164-195.

Sciare, J., Cachier, H., Sarda-Esteve, R., Yu, T., Wang, X., 2007. Semi-volatile aerosol in Beijing (R.P. China): Characterization and influence on various $PM_{2.5}$ measurements, Journal of Geophysical Research 112, D18202.

Seinfeld, J.H., Spyros, P.N., 2006. Atmospheric Chemistry and Physics - From Air Pollution to Climate Change, 2nd Edition, John Wily & Sons.

Shafer, M.M., Perkins, D.A., Antkiewicz, D.S., Stone, E.A., Quraishi, T.A., Schauer, J.J. 2010. Reactive oxygen species activity and chemical speciation of size-fractionated

atmospheric particulate matter from Lahore, Pakistan: an important role for transition metals. Journal of Environmental Monitoring 12, 704-715.

Sillanpaa, M., Hillamo, R., Saarikoski, S., Frey, A., Pennanen, A., Makkonen, U., Spolnik, Z., Van Grieken, R., Branis, M., Brunekreef, B., Chalbot, M.-C., Kuhlbusch, T., Sunyer, J., Kerminen, V.-M., Kulmala, M., and Salonen, R.O. 2006. Chemical composition and mass closure of particulate matter at six urban sites in Europe. *Atmospheric Environment.* 40:S212-S223.

Simoneit, B.R.T., Elias, V.O., Kobayashi, M., Kawamura, K., Rushdi, A.I., Medeiros, P.M., Rogge, W.F., and Didyk, B.M. 2004. Sugars – dominant water-soluble organic compounds in soils and characterization as tracers in atmospheric particulate matter. *Environmental Science and Technology.* 38:5939-5949.

Solomon, P.A., Sioutas, C. 2008. Continuous and Semicontinuous Monitoring Techniques for Particulate Matter Mass and Chemical Components: A Synthesis of Findings from EPA's Particulate Matter Supersites Program and Related Studies. *J. Air & Waste Manage. Assoc.* 58:164-195.

Stafoggia, M., Samoli, E., Alessandrini, E., Cadum, E., Ostro, B., Berti, G., Faustini, A., Jacquemin, B., Linares, C., Pascal, M., Randi, G., Ranzi, A., Stivanello, E., Forastiere, F., the MED-PARTICLES Study Group, 2013. Short-term associations between fine and coarse particulate matter and hospitalizations in Southern Europe: Results from the MED-PARTICLES project, Environmental Health Perspectives Advance Publication.

Stevens, B., Feingold, G, 2009. Untangling aerosol effects on clouds and precipitation in a buffered system, Nature 461, 607-613.

Stone, E.A., Yoon, S.-C., Schauer, J.J. 2011. Chemical Characterization of Fine and Coarse Particles in Gosan, Korea during Springtime Dust Events. Aerosol and Air Quality Research 11, 31-43.

Sullivan, A.P., Weber, R.J. 2006. Chemical characterization of ambient organic aerosol soluble in water: 2. Isolation of acid, neutral, and basic fractions by modified size-exclusion chromatography. Journal of Geophysical Research 111, D05315.

Taylor, S.R., McLennan, S.M., 1985. The Continental Crust: Its Composition and Evolution. Blackwell, Oxford England.

Tecer, L.H., Alagha, O., Karaca, F., Tuncel, G., Eldes, N., 2008. Particulate matter ($PM_{2.5}$, $PM_{10-2.5}$, and PM_{10}) and children's hospital admissions for asthma and respiratory diseases: A bidirectional case-crossover study, Journal of Toxicology and Environmental Health, Part A: Current Issues 71(8), 512-520.

Thermo Scientific, 2009. TEOM 1405-DF: Dichotomous Ambient Particulate Monitor with FDMS Option. 42-010815 Revision A.003.

Thornburg, J., Rodes, C.E., Lawless, P.A., Williams, R. 2009. Spatial and Temporal Variability of Outdoor Coarse Particulate Matter Mass Concentrations Measured with a New Coarse Particle Sampler During the Detroit Exposure and Aerosol Research Study. *Atmos. Environ.* 43:4251-4258.

Thorpe, A., Harrison, R.M., 2008. Sources and properties of non-exhaust particulate matter from road traffic: a review. Science of the Total Environment 400, 270-282.

Toth, J.J., Johnson, R.H. 1985. Summer Surface Flow Characteristics over Northeast Colorado. Monthly Weather Review 113, 1458-1469.

US Bureau of the Census. 2012. *Annual Estimates of the Resident Population for Counties of Colorado: April 1, 2010 to July 1, 2011.* Prepared by the United States Census Bureau, Population Division. http://www.census.gov/popest/data/counties/totals/2011/tables/CO-EST2011-01-08.csv.

U.S. Census. 2000. United States Census 2000, Urban and Rural Classification. http://www.census.gov/geo/www/ua/ua_2k.html, accessed December 27, 2010.

U.S. Census. 2009a. Table 1. Annual Estimates of the Resident Population for Counties of Colorado: April 1, 2000 to July 1, 2009. 2009 Population Estimates. United States Census Bureau, Population Division. http://www.census.gov/popest/counties/counties.html, accessed December 27, 2010.

U.S. Census. 2009b. Table 4. Annual Estimates of the Resident Population for Incorporated Places in Colorado: April 1, 2000 to July 1, 2009. 2009 Population Estimates. United States Census Bureau, Population Division. http://www.census.gov/popest/cities/SUB-EST2009-states.html, accessed December 27, 2010.

U.S. Census. 2009c. Table 1. Annual Estimates of the Resident Population for Incorporated Places Over 100,000, Ranked by July 1, 2009 Population: April 1, 2000 to July 1, 2009. 2009 Population Estimates. United States Census Bureau, Population Division. http://www.census.gov/popest/cities/SUB-EST2009.html, accessed December 27, 2010.

US Department of Agriculture. 2007. Census of Agriculture: 2007 Census Volume 1, Chapter 2: County Level Data for Colorado.

U.S. Department of Agriculture. 2007. *2007 Census Volume 1, Chapter 2: County Level Data, Table 1. County Summary Highlights: 2007.* Prepared by the United States Department of Agriculture. http://www.agcensus.usda.gov/Publications/2007/Full_Report/Volume_1,_Chapter_2_County_Level/Colorado/.

U.S. EPA. 1995. AP 42 Fifth Edition: Compilation of Air Pollutant Emission Factors, Vol. 1: Stationary Point and Area Sources. U.S. Environmental Protection Agency, Office of Air Quality Planning and Standards, Research Triangle Park, NC.

US EPA. 2004. US EPA Air Quality Criteria for Particulate Matter (Final Report, Oct, 2004). US Environmental Protection Agency, Washington, DC, EPA 600/P-99/002aF-bF.

US EPA. 2006. 40 CFR Part 50: National Ambient Air Quality Standards for Particulate Matter, Vol. 71 No. 200.

US EPA. 2006. 40 CFR Parts 53 and 58: Revisions to Ambient Air Monitoring Regulations; Proposed Rule. Federal Register, Vol. 71, No. 10, Part III.

U.S. EPA. 2009. Integrated Science Assessment for Particulate Matter. EPA/600/R-08/139F. U.S. Environmental Protection Agency, Washington, DC.

U.S. EPA. 2010. http://www.epa.gov/ttn/amtic/files/ambient/criteria/reference-equivalent-methods-list.pdf, accessed December 29, 2010.

U.S. EPA. 2013. National Ambient Air Quality Standards (NAAQS). http://www.epa.gov/air/criteria.html. Accessed November 4, 2013.

Usher, C.R., Michel, A.E., Grassian, V.H. 2003. Reactions on Mineral Dust. Chemical Reviews 103, 4883-4939.

Van Miegroet, H., Boettinger, J.L., Baker, M.A., Nielsen, J., Evens, D., Stum, A. 2005. Soil carbon distribution and quality in a montane rangeland-forest mosaic in northern Utah. Forest Ecology and Management 220, 284-299.

Varrica, D., Bardelli, F., Dongarra, G., Tamburo, E. 2013. Speciation of Sb in airborne particulate matter, vehicle brake linings, and brake pad wear residues. Atmospheric Environment 64, 18-24.

Vedal, S., Hannigan, M.P., Dutton, S.J., Miller, S.L., Milford, J.B., Rabinovitch, N., Kim, S.-Y., Sheppard, L. 2009.The Denver Aerosol Sources and Health (DASH) Study: Overview and Early Findings. *Atmos. Environ.* 43:1666-1673.

Villeneuve, P.J., Burnett, R.T., Shi, Y., Krewski, D., Goldberg, M.S., Hertzman, C., Chen, Y., Brook, J., 2003. A time-series study of air pollution, socioeconomic status, and mortality in Vancouver, Canada. Journal of Exposure Analysis and Environmental Epidemiology 13, 427-435.

Von Schneidemesser, E., Stone, A., Quraishi, t., Shafer, M.M., Schauer, J.J., 2010. Toxic metals in the atmosphere in Lahore, Pakistan. Science of the Total Environment 408, 1640-1648.

Wang, X.-R., Zhang, H.-X., Sun, B.-X., Dai, H.-L., Hang, J.-Q., Eisen, E.A., Wegman, D.H., Olenchock, S.A., Christiani, D.C. 2005. A 20-year follow-up study on chronic respiratory effects of exposure to cotton dust. European Respiratory Journal 26(5), 881-886.

Wang, G., Kawamura, K., Xie, M., Hu, S., Cao, J., An, Z., Waston, J.G., Chow, J.C. 2009. Organic Molecular Compositions and Size Distributions of Chinese Summer and Autumn Aerosols from Nanjing: Characteristic Haze Event Caused by Wheat Straw Burning. Environmental Science and Technology 43, 6493-6499.

Wang, G., Chen, C., Li, J., Zhou, B., Xie, M., Hu, S., Kawamura, K., Chen, Y. 2011. Molecular composition and size distribution of sugars, sugar-alcohols and carboxylic acids in airborne particles during a severe urban haze event caused by wheat straw burning. Atmospheric Environment 45, 2473-2479.

Wang, H., and Shooter, D. 2005. Source apportionment of fine and coarse atmospheric particles in Auckland, New Zealand. *Science of the Total Environment*. 340:189-198.

Wang, M., Ghan, S., Ovchinnikov, M., Liu, X., Easter, R., Kassianov, E., Qian, Y., Morrison, H., 2011. Aerosol indirect effects in a multi-scale aerosol-climate model PNNL-MMF, Atmospheric Chemistry and Physics 11, 5431-5455.

Weishaar, J.L., Aiken, G.R., Bergamaschi, B.A., Fram, M.S., Fujii, R., Mopper, K. 2003. Evaluation of Specific Ultraviolet Absorbance as an Indicator of the Chemical Composition and Reactivity of Dissolved Organic Carbon. Environmental Science and Technology 37, 4702-4708.

Williamson, B.J., Rollinson, G., Pirrie, D. 2013. Automated Mineralogical Analysis of PM_{10}: New Parameters for Assessing PM Toxicity. Environmental Science and Technology 47, 5570-5577.

Wilson, J.G., Kingham, S., Pearce, J., Sturman, A.P., 2005. A review of intraurban variations in particulate air pollution: Implications for epidemiological research, Atmospheric Environment 39, 6444-6462.

Xie, M., Piedrahita, R., Dutton, S.J., Milford, J.B., Hemann, J.G., Peel., J.L., Miller, S.L., Kim, S.-Y., Vedal, S., Sheppard, L., Hannigan, M.P. 2013. Positive matrix factorization of a 32-month series of daily $PM_{2.5}$ speciated data with incorporation of temperature stratification. Atmospheric Environment 65, 11-20.

Yajima, Y., Nishino, H., 1999. Estimation of the autocorrelation function of a stationary time series with missing observations. Sankhya Ser. A 61, 189-207.

Yu, K.N., Cheung, Y.P., Cheung, T., Henry, R.C. 2004. Identifying the Impact of Large Urban Airports on Local Air Quality by Nonparametric Regression. *Atmos. Environ.* 38:4501-4507.

Zanobetti, A., Schwartz, J., 2009. The effect of fine and coarse particulate air pollution on mortality: a national analysis. Environmental Health Perspectives 117, 898-903.

Zaveri, R.A., Shaw, W.J., Cziczo, D.J., Schmid, B., Ferrare, R.A., Alexander, M.L., Alexandrov, M., Alvarez, R.J., Arnott, W.P., Atkinson, D.B., Baidar, S., Banta, R.M., Barnard, J.C., Beranek, J., Berg, L.K., Brechtel, F., Brewer, W.A., Cahill, J.F., Cairns, B., Cappa, C.D., Chand, D., China, S., Comstock, J.M., Dubey, M.K., Easter, R.C., Erickson, M.H., Fast, J.D., Floerchinger, C., Flowers, B.A., Fortner, E., Gaffney, J.S., Gilles, M.K., Gorkowski, K., Gustafson, W.I., Gyawali, M., Hair, J., Hardesty, R.M., Harworth, J.W., Herndon, S., Hiranuma, N., Hostetler, C., Hubbe, J.M., Jayne, J.T., Jeong, H., Jobson, B.T., Kassianov, E.I., Kleinman, L.I., Kluzek, C., Knighton, B., Kolesar, K.R., Kuang, C., Kubatova, A., Langford, A.O., Laskin, A., Laulainen, N., Marchbanks, R.D., Mazzoleni, C., Mei, F., Moffet, R.C., Nelson, D., Obland, M.D., Oetjen, H., Onasch, T.B., Ortega, I., Ottaviani, M., Pekour, M., Prather, K.A., Radney, J.G., Rogers, R.R., Sandberg, S.P., Sedlacek, A., Senff, C.J., Senum, G., Setyan, A., Shilling, J.E., Shrivastava, M., Song, C., Springston, S.R., Subramanian, R., Suski, K., Tomlinson, J., Volkamer, R., Wallace, H.W., Wang, J., Weickmann, A.M., Worsnop, D.R., Yu, X.-Y., Zelenyuk, A., Zhang, Q.

2012. Overview of the 2010 Carbonaceous Aerosols and Radiative Effects Study (CARES). Atmospheric Chemistry and Physics 12, 7647-7687.

Zhang, Q., Anastasio, C., Jimenez-Cruz, M. 2002. Water-soluble organic nitrogen in atmospheric fine particles ($PM_{2.5}$) from northern California. Journal of Geophysical Research 107, D11.

Zhang, X., Liu, Z., Hecobian, A., Zheng, M., Frank, N.H., Edgerton, E.S., Weber, R.J. 2012. Spatial and seasonal variations of fine particle water-soluble organic carbon (WSOC) over the southeastern United States: implications for secondary organic aerosol formation. Atmospheric Chemistry and Physics 12, 6593-6607.

Zhu, K., Zhang, J., Lioy, P.J. 2006. Evaluation and Comparison of Continuous Fine Particulate Matter Monitors for Measurement of Ambient Aerosols. *J. Air and Waste Manage. Assoc.* 57:1499-1506.

Zoller, W.H., Gladney, E.S., Duce, R.A., 1974. Atmospheric concentrations and sources of trace metals at the South Pole, Science 183, 198.